Synthesis and Functionalisation of Cleft Molecules and their Application as Asymmetric Hydrogen Bond Organocatalysts

Natasha Holly Slater

Supervisors: Dr Marc Kimber and Dr Benjamin Buckley

Thesis Abstract

The ability to control chirality in the synthesis of pharmaceuticals, natural and non-natural products is paramount; therefore methodologies that facilitate this control are of immense benefit to society. Towards this end Tröger's base (TB) **1** and its derivatives have been used extensively within the context of molecular recognition because they contain a rigid predictable structure, heteroatoms capable of binding events and *importantly* a chiral cavity (Figure 1). While **1** has proved effective as a chiral cleft molecule, a number of possible carbocyclic analogues have also been investigated as possible surrogates.
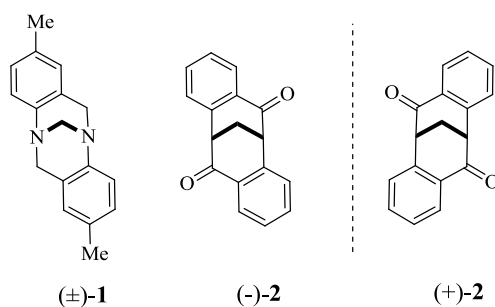
Figure 1: Tröger's Base (TB) 1 and the enantiomers of the carbocyclic cleft analogue 2.

In this work we focus on using the rigid scaffold inherent within the carbocyclic cleft molecule **2** to design and synthesise new ligands for asymmetric catalysis and chiral recognition processes. To date, there has only been one report of derivatives of **2** being used as an asymmetric catalyst where it was employed as a hydrogen bond (H-bond) donor catalyst in a Hetero Diels-Alder reaction (HDA), the enantiomeric excesses (*ees*) of which were modest.

We report the synthesis, geometry and potential asymmetric catalytic properties of a novel family of amino-thiocarbamate functionalised carbocyclic cleft molecules, derived from the stereo selective reduction of the carbocyclic cleft **(±)-2** (Scheme 1).
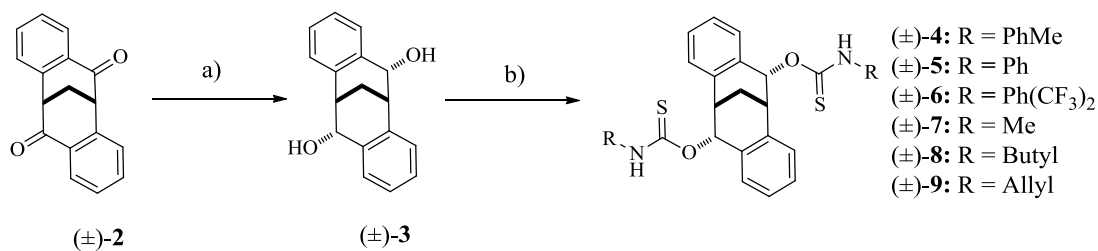
Reagents and conditions: a) NaBH$_4$ (5.0 eq), THF/ MeOH (1:1), rt, 48 h; b) NaH (4.0 eq), R-NCS, THF, rt, 18 h.

Scheme 1: Synthesis of amino-thiocarbamate clefts derived from the reduced carbocyclic molecular cleft (±)-3.

Where possible, X-Ray crystallography was used to fully characterise these molecular clefts and provide important information about the geometry and functional group orientation. Interestingly the crystal structures showed that the nitrogen containing amino-thiocarbamate groups are directed into the cleft cavity thus facilitating binding within the cleft, an important feature when considering molecular recognition and asymmetric catalysis (Figure 2).
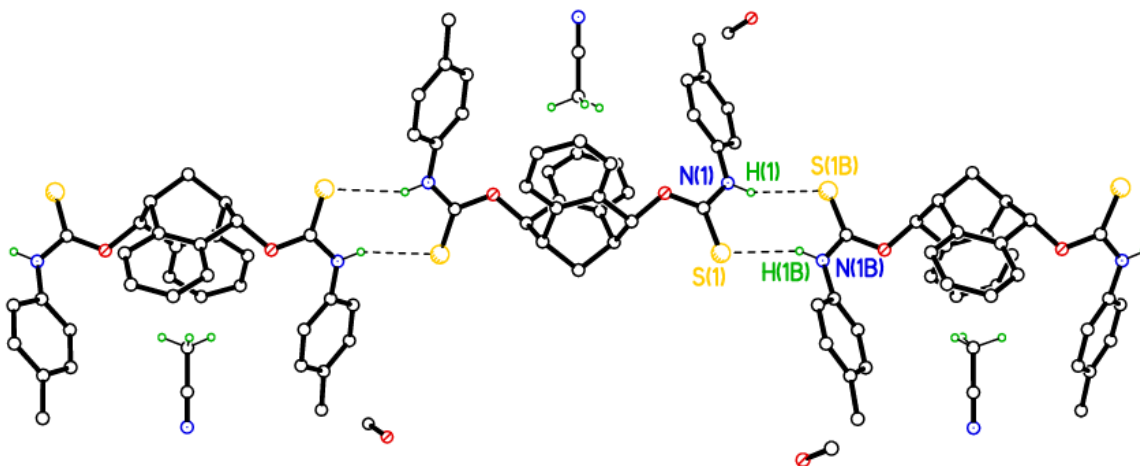
Figure 2: X-Ray of the H-bonded network for (±)-4 showing amino-thiocarbamate groups pointing downwards into the cleft cavity and the C–H$\cdots$π binding of a molecule of AcCN solvent.

The application of these novel amino-thiocarbamate cleft molecules as enantioselective H-bond catalysts was investigated in a series of preliminary catalyst screening reactions. Clefts (+)-**4, 5** and **7** as well as (+)-**2** and (+)-**3** were used in the asymmetric HDA reaction between Rawel diene **10** and benzaldehyde **11** (Scheme 2).
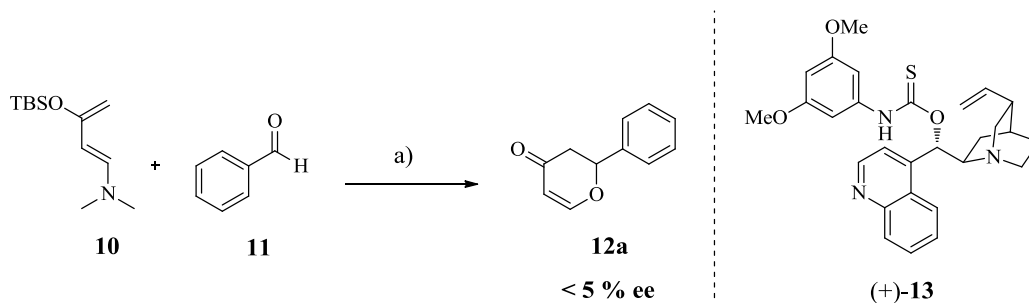
Reagents and Conditions: a) i. catalyst (20 mol %), toluene, -40 $^{\circ}$C, 48 h; ii. CH$_3$COCl, CH$_2$Cl$_2$, -78 $^{\circ}$C, 15 min.

Scheme 2: The Hetero Diels-Alder (HDA) reaction used in catalyst screening reactions.

Whilst application of the novel amino-thiocarbamate catalysts failed to give any enantioselectivity in this HDA reaction, subsequent catalyst screening reactions using the related amino-thiocarbamate substituted cinchonine alkaloid catalysts resulted in a moderate 60 % *ee* when the catalyst **(+)-13** was used.

Novel enantiopure amino-thiocarbamate clefts **(+)-4**, **(+)-5** and **(+)-6** along with the cinchonine alkaloid catalysts **(+)-13 – 17** were also screened for asymmetric catalytic activity in the *N*-bromosuccinimide (NBS) **19** mediated bromolactonisation reaction of alkenoic acid **18** to yield the γ-lactone **20** (Scheme 3).

(+)-14: R = Ph
(+)-15: R = PhMe
(+)-16: R = Ph(CF$_3$)$_2$
(+)-17: (+)-Cinchonine
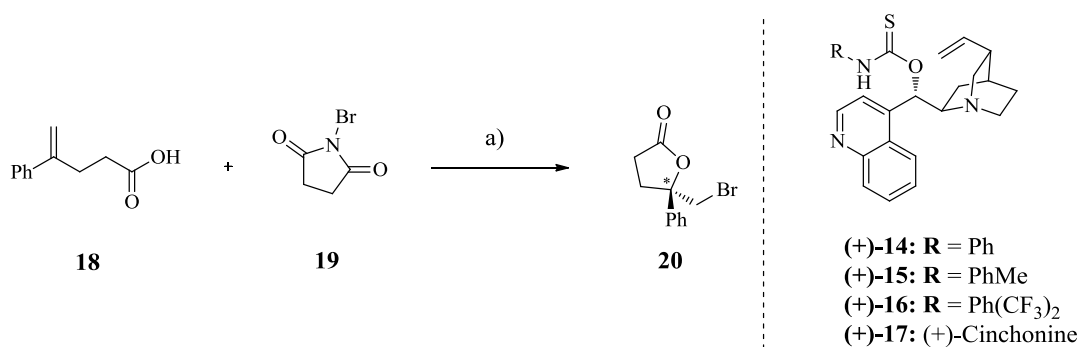
Reagents and conditions: a) Catalyst (10 mol %), NBS (0.12 mmol), CHCl$_3$/PhMe (1:2), -78 $^{\circ}$C, 4h.

Scheme 3: Bromolactonisation reaction of the unsaturated carboxylic acid 18 and NBS, used in catalyst screening reactions.

Preliminary results were encouraging, with catalyst **(+)-4** giving **20** in 20 % *ee*, however more extensive optimisation studies are required.

The synthesis of a mixed chiral cleft **21** derived from **1** and **2** was also investigated with a view towards the assembly of a unique family of rigid chiral cleft molecules with exceptional topology (Figure 3).
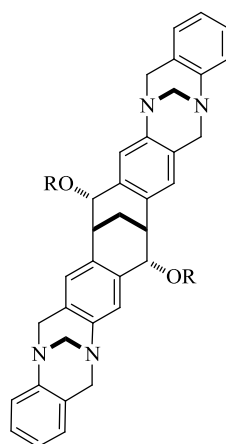
R = H, alkyl, aryl

21

Figure 3: Proposed structure of mixed fused molecular cleft system derived from TB (1) and the carbocyclic molecular cleft (2).

A stepwise approach for the synthesis of precursors which would allow incorporation of the chiral cleft nucleus **2** into a fused system with **1** is reported and provides an excellent starting point for subsequent research. Additionally, the 3-dimensional topology of these molecules may provide templates for future investigations of ligand-receptor interactions implicit in many biological processes.

Acknowledgements

List of Abbreviations

$[\alpha]_D$ – Optical rotation

°C – Degrees centigrade

^{13}C – Carbon-13

^1H – Hydrogen (Proton)

AcCN - Acetonitrile

Atm - Atmospheres

BINAP – 2,2'-Bis(diphenylphosphino)-1,1'Binaphthyl (*organophoshorous compound*)

d – Day(s), Doublet (Spectral)

D – Deuterium

DCC – N, N'-Dicyclohexylcarbodiimide

dba – Dibenzylideneacetone

DMAP – 4-Dimethylaminopyridine

DME – Dimethyl ether

DMSO – Dimethylsulfoxide

dppf – 1,1'Bis(diphenylphosphino)ferrocene

dr – Diastereomeric ratio

ee – Enantiomeric excess

eq – Stoichiometric equivalents

Et – Ethyl

EWG – Electron withdrawing group

g – Gram

H-bond – Hydrogen bond

HDA – Hetero Diels-Alder

h – Hour(s)

i-Pr – *iso*-propyl

IR – Infra red

L –Ligand

m.p. – Melting point

Me – Methyl

min – Minute(s)

mL – Millilitre

mmol – millimole

mol – Mole

MS – Mass Spec

n-Bu – Normal butyl

NMR – Nuclear magnetic resonance

Nuc – Nucleophile

Ph – Phenyl

Pr – Propyl

py – Pyridine

q – Quartet (Spectral)

R – Any atom (not H)

rt – Room Temperature

s – Second(s), Singlet (Spectral)

t – Triplet (Spectral)

TB – Tröger's Base

t-Bu – Tertiary butyl

TEA - Triethylamine

TFA – Trifluoroacetic acid

THF – Tetrahydrofuran

TLC – Thin layer chromatography

TMS - Trimethylsilylacetylene

X – Halogen

Table of Contents

Chapter 1

1.0 Introduction

Chirality lies at the heart of chemistry and biology. The ability to control chirality in the synthesis of pharmaceuticals, natural and non-natural products is paramount; therefore methodologies that facilitate this control are of immense importance.[1] For centuries, chemists have tried to mimic nature's ability to synthesise complex and often chiral molecules. In recent years however, attention has been redirected to designing and synthesising simple molecules capable of performing specific tasks similar to the sophisticated recognition, binding and catalytic processes displayed by enzymes.[2]

1.1 Molecular Clefts

Recognition and binding processes of relatively unfunctionalised molecules often take place on concave surfaces involving non-directional solvophobic effects and van der Waals interactions. Additional interactions such as aromatic stacking and cation π-interactions are feasible if the surface is aromatic.[3] Synthetic molecules with extended concave aromatic surfaces are generally referred to as molecular cleft compounds. The general term cleft refers to molecules that orient a set of functional groups into a V- or U-shaped cavity.[4] Molecular clefts, with their relatively rigid and often chiral concave aromatic surfaces, present themselves as useful structural motifs for the construction of synthetic receptors. Additional functionalisation of these molecular clefts allow for the synthesis of a plethora of related compounds with varying dimensions and functionalities that can offer unique opportunities for the elaboration into supramolecular structures. Improvements in synthetic approaches over recent decades has resulted in the development of a range of molecular cleft compounds with interesting properties, which has in turn inspired investigation into new fields of applications including, but not limited to; receptors,[5] ligands in asymmetric catalysis,[6] drug candidates, new materials for photo and optical applications,[3] and DNA binding molecules.[7]

Molecules featuring convergent functional groups in cleft like shapes have emerged as useful receptors for small molecules. The combination of a well-defined semi-rigid cavity to which tuneable functional groups can be appended in predictable geometries, has allowed for the design of a number of host systems for molecular recognition studies, as well as for the

controlled assembly of complex molecular architectures.[8] These concepts have been well documented, none more so than by the molecular cleft Tröger's Base (TB) **1**.

1.2 Tröger's Base

Tröger's Base (TB) **1** is a small C_2-symmetric molecular cleft shaped molecule consisting of a bicyclic aliphatic unit fused with two aromatic rings (Figure 4).[3] The central methanodiazocine unit projects the aromatic rings in nearly perpendicular fashion making **1** a rather rigid V-shaped molecule. TB **1** possesses a chiral cavity that results from the blocked configuration of the stereogenic nitrogen atoms which are held in position by the chiral methanodiazocine bridge.[9]

(R, R)-1

(±)-1

(S, S)-1
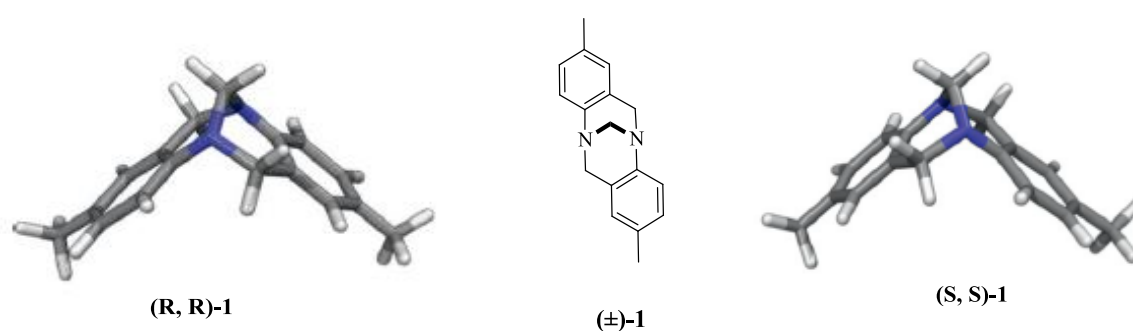
Figure 4: Molecular structure of racemic Tröger's Base (TB) 1 and the MMFF (Merck Molecular Force Field) optimised structures of its enantiomers.[3]

TB **1** was first synthesised in 1887 by Julius Tröger[10] however its correct structure was not established until 1935.[11] In 1944, Prelog and Wieland resolved the two enantiomers of (±)-**1** by chromatographic separation, making **1** one of the first molecules to be resolved on an enantiopure stationary phase.[12] The TB field was reopened in 1985, when Wilcox published the first X-Ray crystallographic study of **1** and described the first potential applications of TB analogues in supramolecular chemistry and in ligand design.[13] Since the beginning of the 21st century synthetic TB chemistry has developed rapidly. A unique set of structural features including C_2-symmetry, rigidity, and a sharply folded geometry with nearly right angles between the planes of the aromatic rings has made derivatives of **1** very attractive for the application in supramolecular chemistry and molecular recognition. Since its first reported synthesis in 1887 over 530 articles detailing its chemistry can be found in the literature, of which approximately 60 % of publications have been made in the last decade.[3]

1.2.1 Synthesis of Tröger's Base and its Analogues

All synthetic methodologies reported for the synthesis of **1** can be considered as variations of the original conditions reported by Tröger, which involved acid catalysed condensation of *p*-toluidine with formaldehyde.[10] To date the most commonly used protocol for the synthesis of **1** and its substituted analogues involve treating a synthetic equivalent of methylene- namely formaldehyde or a precursor such as paraformaldehyde; dimethoxymethane; aqueous formaldehyde; dimethyl sulfoxide[14] and hexamethylene-tetramine, with a suitably substituted aniline derivative in the presence of an acid catalyst. Frequently used acid catalysts include aqueous or alcoholic hydrochloric acid solutions, acetic acid, trifluoroacetic acid (TFA) and methane sulfonic acid. Recently the use of Lewis acids such as $AlCl_3$[15] and $TiCl_4$[16] have also been reported (Scheme 4).[3]
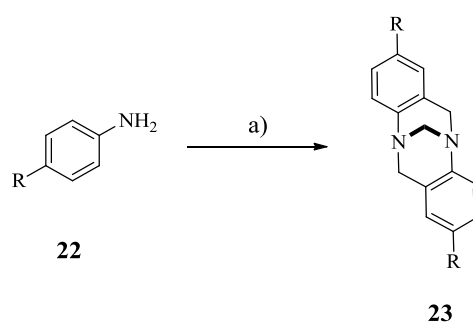
Reagents and Conditions: a) Methylene synthetic equivalent, acid, solvent.

Scheme 4: General method for the synthesis of TB (1) and its analogues.

One of the most common methods uses a combination of paraformaldehyde and trifluoroacetic acid (TFA). Under these reaction conditions a number of symmetrically 2,8-disubstituted TB analogues can be accessed in good to excellent yields (Scheme 5).[17] This procedure was developed by Jensen and Wärnmark in 2001[17] and is considered to be prolific as it allows for the multi-gram synthesis of symmetrical TB analogues bearing both electron-withdrawing and electron-donating substituents. Moreover, it allows for dihalogenated TB derivatives to be synthesised with relative ease, thus providing opportunities for the installation of a range of different functional groups directly onto the TB framework. Prior to this breakthrough it was long believed that to avoid low yielding and sluggish reactions, only electron-donating substituents could be incorporated onto the TB framework.[3]

24: R = H: 78 %
25: R = Br: 63 %
26: R = I: 56 %
27: R = Me, Et, *i*-Pr, *t*-Bu: 86 - 89 %
28: R = MeO, MeS: 64 - 67 %
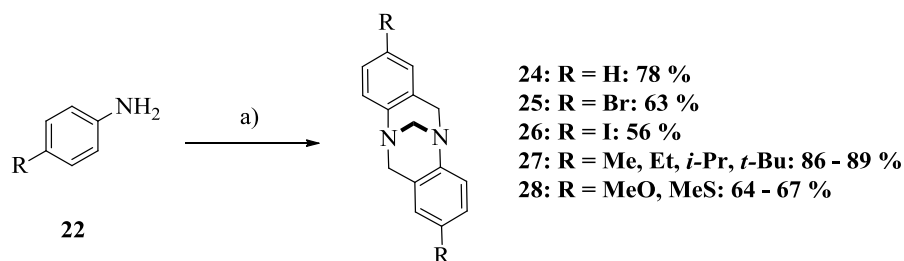
Reagents and Conditions: a) $(CH_2O)_n$, TFA, rt.

Scheme 5: Wärnmark and co-workers procedure for the synthesis of symmetrical TB analogues.

1.2.2   Stepwise Synthesis of Analogues of Tröger's Base

Elegant one-step condensation reactions of simple aniline derivatives to form TB analogues, as mentioned above, are not always applicable. Due to the relatively harsh reaction conditions, the range of accessible analogues is to some extent limited moreover, these direct condensation reactions only give access to symmetric analogues of **1**. To circumvent these limitations alternative methods have been explored for the synthesis of unsymmetrical analogues of **1**. In 1990, Webb and Wilcox reported a stepwise approach which involved the tethering of two differently substituted aniline derivatives through a methylene unit followed by cyclisation with formaldehyde to yield unsymmetrical TB analogues (Scheme 6).[18]
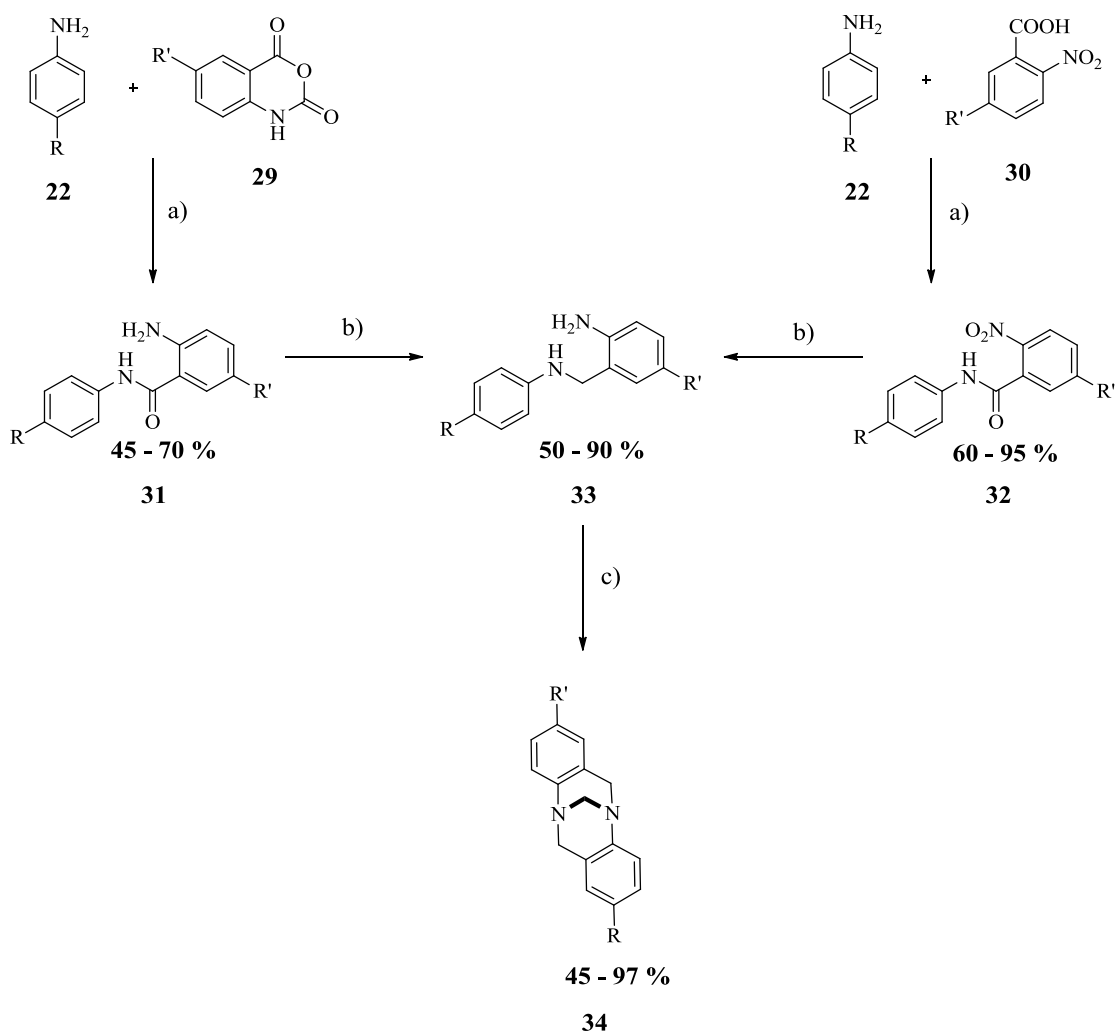
Reagents and Conditions: a) EtOH, reflux; or i) DCC/DMF, ii) benzene/oxalyl chloride, iii) DMF, Py, rt; b) BH$_3$.THF, reflux; or i) Pd, H$_2$, MeOH, ii) LAH, THF, reflux; c) HCHO/HCl, EtOH.

Scheme 6: Webb and Wilcox's stepwise approach for the synthesis of unsymmetrical TB analogues.

A range of substituted anilines **22** were treated with either a derivative of isatoic anhydride **29** (Scheme 6, Route a) or 2-nitrobenzoic acid **30** (Scheme 6, route b). The resulting aminoamides **31** and nitroamides **32** were reduced to the cyclisation precursor **33** before being treated with formaldehyde to afford the corresponding unsymmetrical TB analogues **34** in moderate to excellent overall yields.[18]

In another stepwise approach Becker and co-workers synthesised a highly functionalised TB analogue **38.** Treatment of methyl 4-amino-5-chloro-2-methoxybenzoate **35** with ethyl oxalyl chloride **36** gave the ethyl oxalate 37 in 95 % yield. When a solution of **37** in DMSO was heated to 185–190 $^{\circ}$C for 9 hours the starting material was slowly

consumed. Chromatographic separation of the product mixture gave TB derivative **38** in 16 % yield, as well as a small amount (6 %) of the quinolone derivative **38a** (Scheme 7).[14]
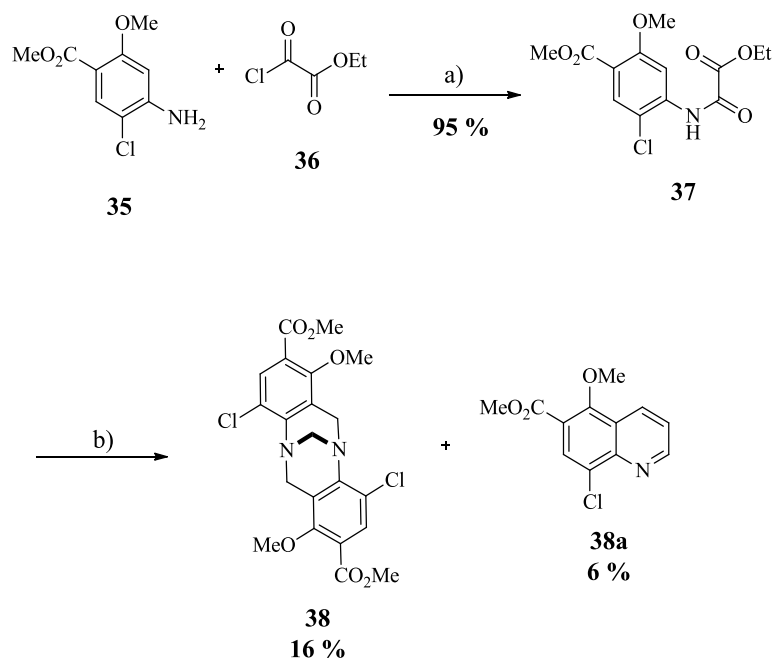
Reagents and Conditions: a) CH$_2$Cl$_2$, pyridine, -78 ^{o}C – rt, 1h; b) DMSO, 185 – 190 ^{o}C, 9 h.

Scheme 7: Becker and co-workers stepwise synthesis of the highly functionalised TB analogue 38.

The group proposed a mechanism reminiscent of the Pummerer reaction for the conversion of **37** to **38** whereby, under the severe reaction conditions DMSO acts as a formaldehyde equivalent. Presumably this mechanism involves nucleophilic removal of the ethyl oxalyl moiety by DMSO with concomitant activation of the sulfoxide as an *O*-acylated species. Accordingly, an *N*-methylthiomethyl aniline could be an intermediate in the formation of both **38** and the unexpected quinolone derivative **38a**, It is well known that activated DMSO can act as an electrophilic source of CH$_2$SCH$_3$ group therefore, the reaction provides a functional equivalent of formaldehyde.

1.2.3   Functionalisation of Tröger's Base

Until the 1980's **1** was mainly used as a model substance for the evaluation of new chiral chromatographic techniques due to the ease in which it can be separated into its enantiomers.[3] In the second half of the 1980s however, interest in functionalised analogues of **1** emerged. In 1985, pioneering work by Wilcox and co-workers confirmed the true structure of **1** by single X-Ray diffraction analysis. During this study the group also reported the

synthesis of several simple yet unprecedented TB analogues which triggered further developments in the derivatisation of TB.[13] The functionalisation of **1** at almost any position on its skeleton is now possible. Figure 5 summarises all the different functionalisation patterns of **1** that have emerged in recent years.[3]

Despite there being significant interest and rapid development in TB chemistry there remains a notable lack of general methodologies for the functionalisation of the TB core. Of the chemistry devoted to the derivatisation of **1** the majority of attention has been centred on the derivatisation of the aromatic rings due to the easy access to halogenated analogues.[3] Herein, this report will focus on methods that facilitate the functionalisation of the aromatic rings in **1**, in particular procedures which enable the synthesis of symmetrically functionalised heterocyclic and nitrogen containing amino and amide analogues.
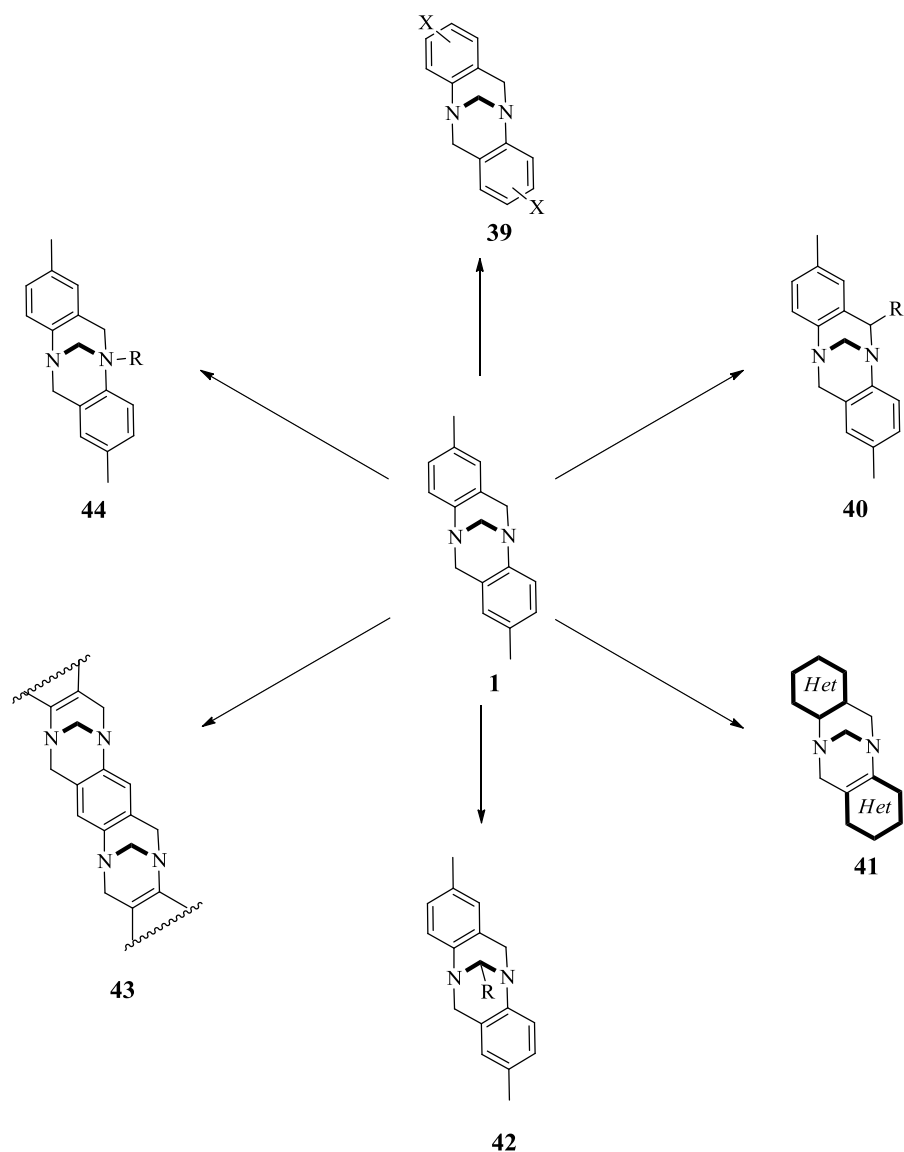
Figure 5: Summary of the functionalisation patterns of the TB framework.

1.2.4   Functionalisation of Tröger's Base at the Aromatic Ring Positions

As previously reported, halogenated analogues of **1** can be accessed with relative ease by treating substituted anilines with paraformaldehyde and trifluoroacetic acid (Scheme 5). In recent years, several reports have emerged demonstrating that transition-metal-catalysed C–C cross-coupling reactions of these halogenated TB molecules gives access to a range of functionalised TB molecules (Scheme 8).[3]
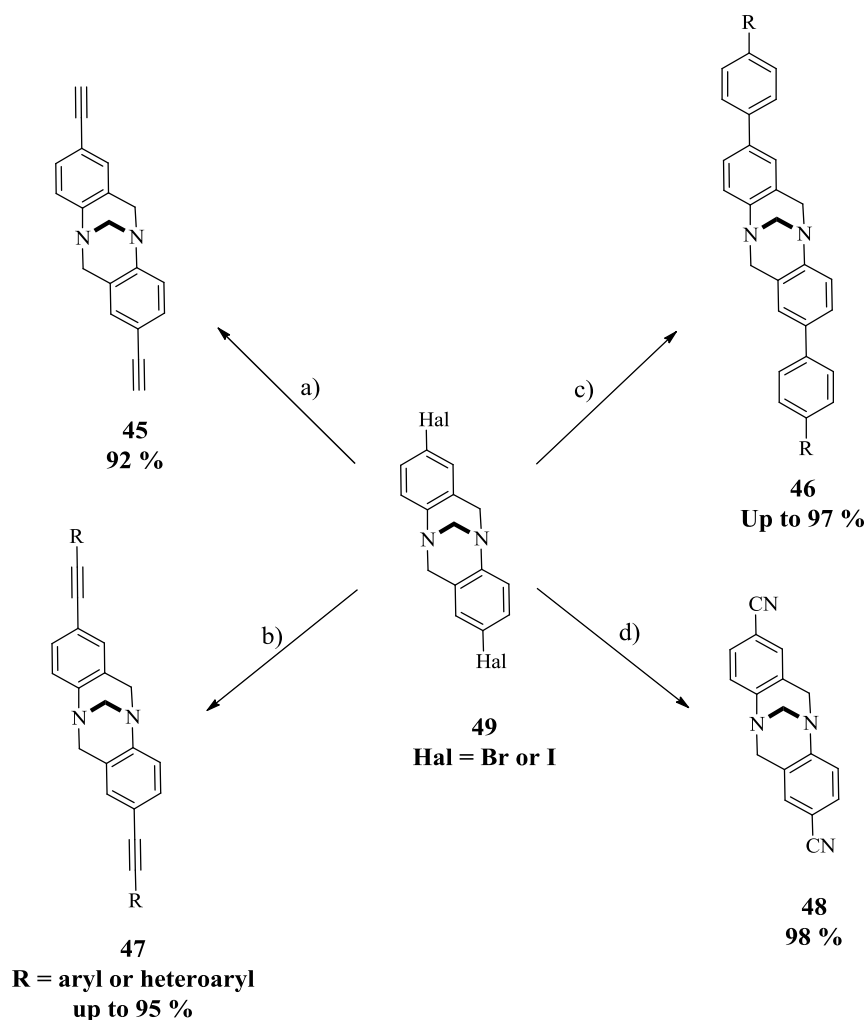
Reagents and Conditions: a) ethynylmagnesium bromide, Pd(PPh$_3$)$_4$; b) Pd(PhCN)$_2$Cl$_2$, P(*t*-Bu)$_3$, CuI, alkyne-R substrate; c) Pd[P(*t*-Bu)$_3$]$_2$, CsF, substituted phenylboronic acid; d) Zn(CN)$_2$, Zn, Pd(Ph$_3$)$_4$, dppf.

Scheme 8: Selected examples of transition-metal catalysed transformations with halogenated-TB analogues.

Corriu-Kumada cross-coupling reactions of halogenated TB's (general structure **49**) with ethynylmagnesium bromide allowed for the introduction of ethynyl groups onto the aromatic rings affording **45** in excellent yields (Scheme 8, Route a).[19] Similarly aryl and heteroaryl substituted alkynyl groups were introduced to give variations of **47** in up to 95 % overall yield, by methods of Sonogashira coupling (Scheme 8, Route b).[20] Lutzen and co-workers reported arylations of halogenated TB analogues by Suzuki-Miyaura coupling with arylboronic acids as coupling partners, which resulted in a range of synthetic analogues related to **46** (Scheme 8, Route c).[21] In addition to classical metal catalysed cross-coupling reactions, C–C bond formation at the aromatic ring position on **1**, has also been achieved by

palladium-catalysed cyanation reactions, which gave **48** in excellent yields (Scheme 8, Route d).[22]

Carbon–heteroatom bond formation through transition-metal-catalysed reactions, starting from dihalogenated analogues of TB has also been reported. Treatment of diiodo-TB **51** under Ullmann conditions allowed for carbon–oxygen bond formation giving the functionalised TB analogue **50** in excellent overall yield (Scheme 9, Route a). Whilst carbon–nitrogen bonds were accessed by either treatment of **51** under Buchwald-Hartwig reaction conditions or copper catalysed amidation,[23] which gave the diamine-substituted TB analogue **52** in 85 % yield (Scheme 9, Route b).[22,24,25]

50   **51**   **52**

R = H or CH$_3$

Reagents and Conditions: a) NaOCH$_3$, CuCl, MeOH/DMF; b) Pd$_2$(dba)$_3$, BINAP, NaO*t*-Bu, benzophenone imine, toluene, THF.

Scheme 9: Selected examples of transition-metal catalysed carbon-heteroatom bond formation in the functionalisation of the TB framework.

Due to the nature and high reactivity of the amino group, it is one of the most important functionalities used for connecting molecular building blocks into more complex architectures. Consequently, the search for new methods for the synthesis of TB analogues containing free amino groups represents an important target, especially from the view of potential applications of TB in supramolecular systems.

The Buchwald-Hartwig approach mentioned above (Scheme 9) is one of the few examples of the direct synthesis of TB systems containing electron-withdrawing amine groups directly attached to the TB framework. This procedure, however, has its limitations, for example it is often met with low reproducibility and requires high catalyst loading therefore, the need for a more reliable procedure was highly desirable. In 2012 Sturala and Cibulka reported a novel

method for the synthesis of the symmetrical diamine-substituted TB analogues **52** and **56** (Scheme 10).[26]

Reagents and Conditions: a) (CH$_2$O)n, TFA, -15 ^{o}C – rt; b) KNO$_3$ (2.2 eq), H$_2$SO$_4$; c) H$_2$/Pd, K$_2$CO$_3$, MeOH; d) Zn(dust), AcOH, reflux.

Scheme 10: General reaction scheme for the synthesis of amine-substituted TB analogues.

This procedure involves the regioselective nitration of the dihalogenated or tetra-halogenated TB intermediates **54** with potassium nitrate (2.2 eq) in sulphuric acid. The resulting nitro groups and halogen atoms are then simultaneously reduced by hydrogenation (Scheme 10, Route c) to give the diamine derivative **52** with no additional substituents. Alternatively, chemoselective reduction of the nitro groups, without loss of the halogen substituents was achieved by treatment of **54** with zinc dust and acetic acid, resulting in the halogenated-diamine-substituted TB analogue **56** (Scheme 10, Route d).

Many more examples detailing preparative routes to functionalised TB analogues starting from ring di-substituted halogenated TBs can be found in the literature. In addition alternative routes involving the direct halogenation of the aromatic rings have also been reported and thus provide a route to the desymmetrisation of TB,[27] details of which are beyond the context of this report.

1.2.5 Heterocyclic Tröger's Base Analogues

The combination of the unique structural architecture of **1** and the acceptor and donor properties offered by aromatic heterocycles yield interesting structures that have been shown to be beneficial in many fields of applications such as medicinal chemistry. This has led to a number of groups focusing on developing protocols for the synthesis of aromatic heterocyclic analogues of **1**. Since 1991, numerous heterocyclic TB analogues have been synthesised through a one-step condensation reaction in which the aromatic heterocyclic molecule is directly fused onto the aromatic rings of **1**. For example, Yashima and co-workers synthesised the first aromatic heterocyclic polyaromatic TB analogue **58**, by acid induced condensation of 5-amino-1, 10-phenanthroline **57** and formaldehyde in an alcoholic hydrochloric acid solution (Scheme 11).[28]

57

58
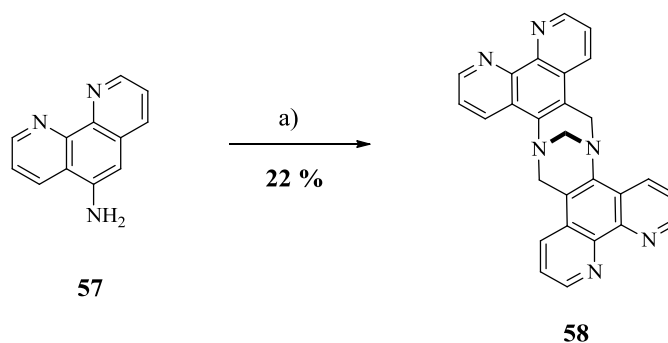
Reagents and Conditions: a) HCHO, HCl (*aq*), EtOH.

Scheme 11: Yashima and co-workers synthesis of the first heterocyclic polyaromatic TB analogue containing phenanthroline.

The intercalating ability of heterocyclic polyaromatics with DNA promoted further preparative and binding studies involving TB analogues incorporating the heterocyclic phenanthroline and acridine functional groups. Since Yashima's publication at least 35 other example of these heterocyclic derivatives can be found in the literature.[3] To date all of the synthetic approaches developed have been individually optimised to produce high yields therefore, an additional study to provide an appropriate general synthetic methodology for their synthesis is required. The π-deficient properties of many heterocycles may account for the lack of generalised procedures for the synthesis of these heterocyclic TB analogues by a one-step condensation reaction.

In 1997, Goswani and Ghosh reported an alternative pathway to access heterocyclic TB analogues, which involved introducing the heterocyclic functional group after the

condensation-step, which forms the TB core, has taken place. This procedure eliminates the issues associated with π-deficient heterocycles and one-step condensation reactions. Using this approach the group synthesised aminopyridine analogues including the H-bond receptor TB analogue **62** (Scheme 12).[5,29]
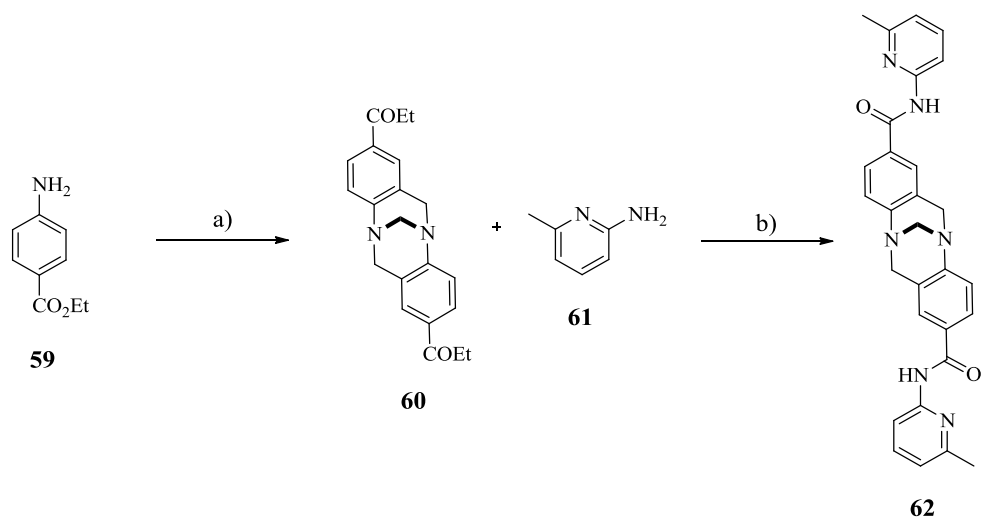
Reagents and Conditions: a) (CH$_2$)$_6$N$_4$, TFA, 60 ^{o}C; b) LiOH, THF, DCC.

Scheme 12: Alternative synthesis of aromatic heterocyclic TB analogues.

1.3 Cleft Molecules Structural Analogues to Tröger's Base

Despite the spectacular success of **1** limitations of this framework in supramolecular chemistry has led to the synthesis of a number of molecular cleft molecules bearing a chiral cavity reminiscent to that found in **1**. These include a methylene bridged diketone carbocyclic cleft **2**,[30] an ether-bridged carbocyclic cleft **63**, an amine-bridged diazocine cleft **64**,[31] and an unbridged dithiocine cleft **65**[32] (Figure 6).
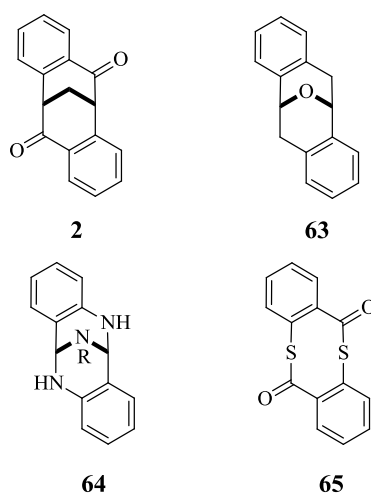
Figure 6: Molecular clefts closely related to TB (1).

These molecular cleft frameworks differ from **1** in the atoms involved in the formation of the bridgehead structure which contribute to differences in the dimension of the cleft molecules. Table 1 summarises the interplanar 'cleft' angle (θ) between the planes defined by the two aromatic rings in the different cleft molecules.[8]

Table 1: Interplanar 'cleft' angle (θ) between planes defined by aromatic rings in cleft molecules analogues to TB.

Entry	Cleft Molecule	Bridge Type	Interplanar 'cleft' angle (θ) ($^{\circ}$)[a]
1	**2**	Methylene	92.9
2	**63**	Ether	93
3	**64**	Substituted amine	77.9, 76.6[b]

[a] Data obtained from crystalline racemates.
[b] Two types of molecule in unit cell.

To date, only a few of these cleft molecules have been thoroughly evaluated for incorporation into supramolecular systems, however each may be expected to have substantially different properties. Of these reported analogues of **1** the carbocyclic cleft **2** has received much attention, with a number of functionalised derivatives being reported in the literature. This molecular cleft has been shown to display a number of advantages over **1**, both in its synthesis and derivatisation.

In the prominent history of **1** there has been a lack of general methodologies to functionalise the TB core resulting in restricted access to its analogues.[3] The molecular cleft **2**, however, presents readily modifiable carbonyl groups at the periphery of the cleft core, allowing for additional opportunities for functionalisation. The development of high yielding methods for functionalisation and resolution of its enantiomers coupled with additional opportunities to introduce recognition and binding groups through the reactive carbonyl groups are particularly attractive features of this system compared with **1**. In this report the chirality, cleft dimensions and chemistry of the carbocyclic molecular cleft **2** are explored with emphasis on methods for the functionalisation of both the aromatic rings and the cleft ring atoms. Applications of functionalised derivatives of the enantiopure cleft **2** as asymmetric H-bond organocatalysts will also be discussed in some detail.

1.4   Carbocyclic Molecular Cleft

The carbocyclic molecular cleft dibenzobicyclo[*b,f*][3.3.1] nona-5a,6a-dione **2** may be regarded as a carbocyclic analogue of **1** in which each of the tertiary nitrogen atoms have been removed.[33] The two aromatic rings are held rigidly in essentially the same relative orientation to one another as in **1** by a methylene bridge (Figure 7).

Me

N   N

Me

(±)-**1**

O

O

(±)-**2**

O

O

$\theta = 92.9^\circ$
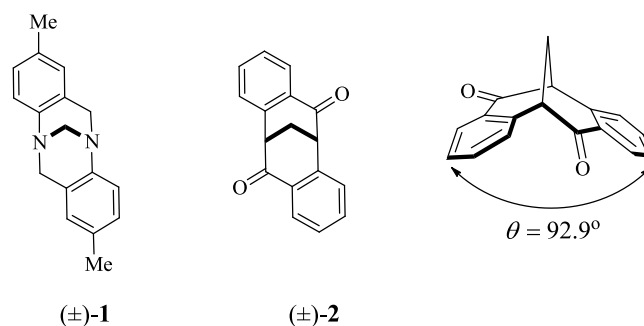
Figure 7: TB (±)-1 and the carbocyclic molecular cleft (±)-2

The methylene bridge in **(±)-2** leads to similar asymmetry to that displayed by **(±)-1** and provides a complementary building block for the incorporation into the design of molecular clefts and related supramolecular structures. In addition to the unique properties offered by its C_2-symmetry, ridged and sharply folded geometry, the V-shaped cleft also contains carbonyl groups which are readily modified. In contrast to **1** which has been widely utilised in the development of a variety of molecular cleft type structures, there are relatively few supramolecular compounds that have incorporated **2** into their structures. However, increased interest and improved synthetic approaches have resulted in the synthesis of several derivatives of **2** which have been shown to display interesting properties. This has consequently inspired investigation into their applications in a number of new fields such as ligands in asymmetric catalysis,[6] achiral spacers in chiral stationary phases[34] and as enantioselective transporters of chiral molecules.[35]

1.4.1   Synthesis of the Racemic and Enantiopure Carbocyclic Cleft 2

The molecular cleft **2** was first reported in 1960 by Setter and Reischi[36] but was not fully characterised and resolved until 1975 by Tatemitsu and co-workers whom reported the synthesis of a range of optically active derivatives of **2** with the same absolute configuration as the (-)-enantiomer.[30] The various methodologies reported for the synthesis of **2** are indeed variations of the original conditions reported by Tatemitsu. Modification of Tatemitsu and co-workers original method starting from commercially available starting materials, has led

to a reliable procedure which gives access to both racemic and enantiopure **2** in good overall yields and enantioselective (*ee*) values. Regrettably due to the early nature of Tatemistu's original publication there are some inconsistencies in the reporting of yields, where possible yields and *ee* values have been reported (Scheme 13).[30]
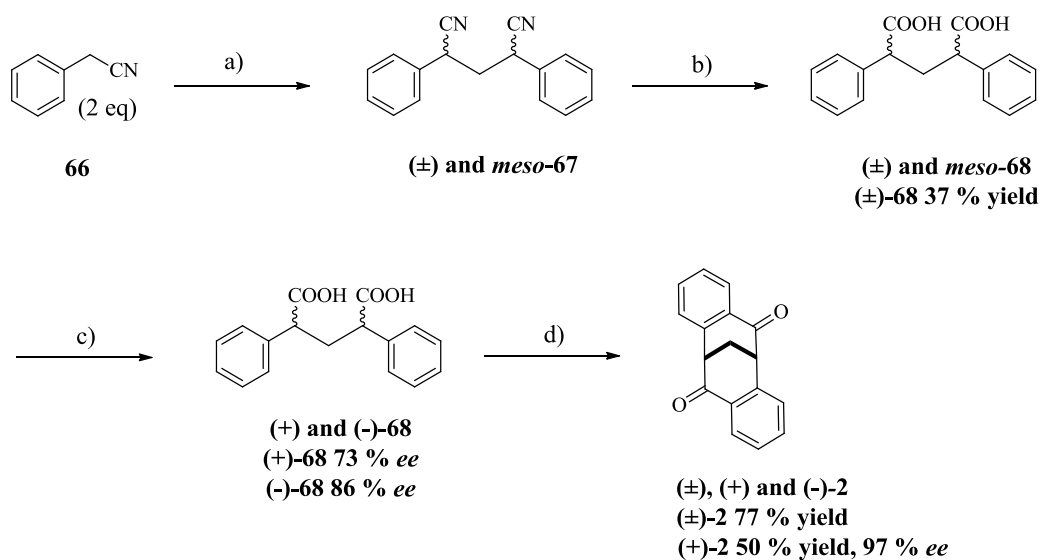
Reagents and Conditions: a) CH$_2$I$_2$, NaOH, 145 $^{\circ}$C, 2 h; b) EtOH, KOH, H$_2$O, reflux, 16 h; c) i. (±)-**68** from recrystallization in toluene, ii. Enantiomer separation; quinine / EtOH; d) *conc.*H$_2$SO$_4$, 85 $^{\circ}$C, 2h.
Scheme 13: Tatemitsu's procedure for the synthesis of racemic and enantiopure carbocyclic molecular cleft 2.

Repeated recrystallization of the *meso* and (±)-2, 4-diphenylpentanedioic acids **68** from hot toluene gave the pure racemate (±)**-68**. Subsequent quinine resolution allowed for the separation of the enantiomers to give the optically pure diacids **(+)-68** and **(-)-68**. The next step which involves a double acid mediated Friedel-Crafts acylation reaction is the most important step in the synthesis of **2** and generates the bicyclic ring system.[30] Both racemic and enantiomeric forms of **68** can be cyclised under the same dehydrative cyclisation reaction conditions by treatment with concentrated sulphuric acid to give the respective carbocyclic cleft **2** in moderate to good yields (Scheme 14).
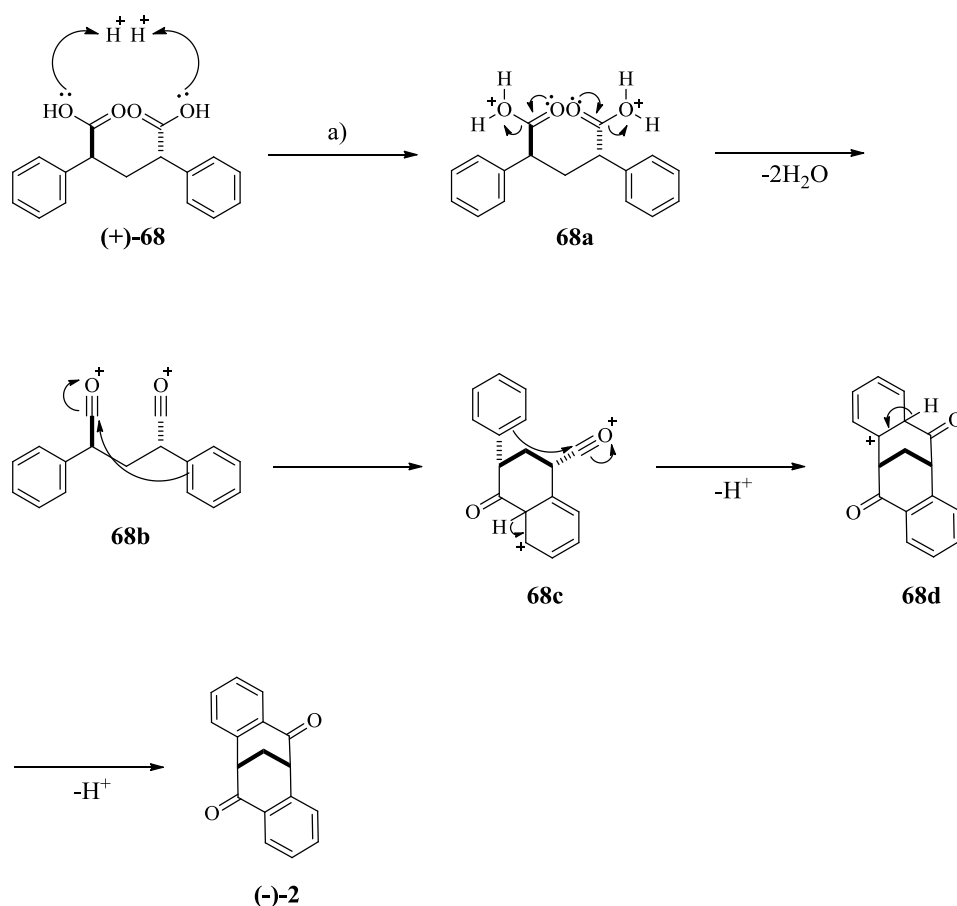
Reagents and Conditions: a) *conc.*H_2SO_4, 85 °C, 2h.

Scheme 14: Mechanism for the acid mediated Friedel-Crafts acylation reaction to for the bicyclic ring system in 2.

It is this final cyclisation step which has the largest implication on the ability to introduce different functional groups onto the rigid cleft framework.[8] As will be discussed, it has been shown that strong deactivating groups on the aromatic rings of the precursors can prevent this cyclisation step from occurring. In some cases it has therefore been necessary to explore alternative reaction pathways to allow for the functionalisation of the cleft framework in **2**. In fact, the majority of methods reported for the functionalisation of **2** focuses on post-synthetic modification of the molecular cleft via the introduction of functional groups directly onto the carbocyclic framework.

1.4.2 Synthesis of derivatives of the Carbocyclic Molecular Cleft 2

Of the chemistry devoted to the derivatisation of **1**, most has been centred on the functionalisation its aromatic rings due to the easy access of halogenated analogues.[19,17] In contrast, the presence of the carbonyl groups on the periphery of the cleft in **2** provides a

handle whereby a range of functional groups can be introduced into the system, providing access to a range of new chiral molecular clefts that contain complementary, yet unique features compared with **1**. For example, the halogenated dibromo- carbocyclic cleft **(±)-72** (Scheme 15) can be synthesised with relative ease, thus allowing entry into aryl and alkynyl-substituted cleft derivatives through metal-catalysed cross-coupling reactions. In addition the carbonyl groups can be readily transformed into hydroxyls **3** (Scheme 19) or oximes **97** (Scheme 22) by reduction with lithium aluminium hydride and hydroxylamine, respectively. Herein methods for the functionalisation of **2** at both the aromatic ring positions and carbonyl groups are discussed.

1.4.3 Functionalisation of the Carbocyclic Cleft at the Aromatic Ring Positions

Much of the work detailing the derivatisation of the molecular cleft **2** has been pioneered by the Harding group in Australia whom have published a number of articles devoted to the synthesis and chemistry of **2**. In 1998, Harding and co-workers introduced a protocol for the synthesis of racemic dibromo- and dimethyl carbocyclic clefts, **(±)-72** and **(±)-73**, respectively (Scheme 15).[33]

69a: R = Br
69b: R = CH$_3$

(±)- and *meso*
70

(±)- and *meso*
71

(±)-72: R = Br   17 % yield
(±)-73: R = CH$_3$ 18 % yield
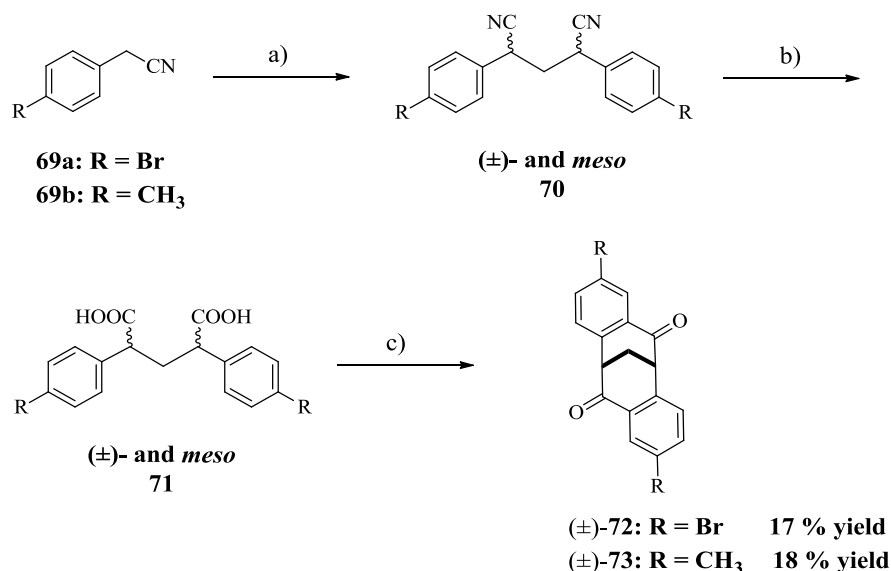
Reagents and Conditions: a) CH$_2$I$_2$, NaOH, 145 $^{\circ}$C, 2h; b) EtOH, KOH, H$_2$O, reflux, 16 h; c) *conc.*H$_2$SO$_4$, 85 $^{\circ}$C, 2 h.

Scheme 15: Harding and co-workers synthesis of racemic dibromo (±)-72 and dimethyl-(±)-73 functionalised carbocyclic clefts.

These clefts were synthesised from commercially available substituted benzyl nitriles (**69a** and **69b**) in a three-step procedure, reminiscent of the route taken by Tatemitsu for the synthesis of the parent unsubstituted molecular cleft **2**.

1.4.3.1 Carbon-Carbon Bond Formation

The introduction of halogens onto the cleft framework was particularly desirable as they provided an excellent handle for subsequent modification of the cleft through metal-catalysed cross-coupling reactions. It was the Harding group again, whom reported the preparation of a range of aryl derivatives starting from the dibromo cleft (±)-**72**, thus highlighting the potential of **2** as a building block for the construction of new supramolecular hosts (Table 2).[8]

Table 2: Metal-catalysed cross-coupling reactions of (±)-72 for the synthesis of functionalised derivatives of 2.

(±)-**72**   (±)-**74-77**
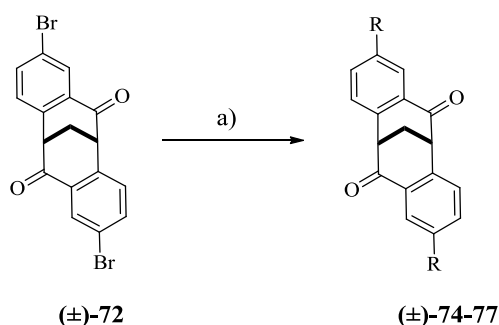
Reagents and Conditions: a) $RB(OH)_2$, $PdCl_2(PPh_3)_2$, Na_2CO_3, $DME:H_2O$ (5:1), 80 °C, 16 h, N_2.

Entry	Cleft (±)	R	Yield (%)
1	**74**	Ph	96
2	**75**	*o*-MeOPh	97
3	**76**	*p*-MeOPh	93
4 [a]	**77**	—C≡CH	75

[a] *Reaction Conditions:* a) i. TMS-acetylene, $PdCl_2(PPh_3)_2$, CuI, TEA, 60 °C, N_2, 3 days, ii. KOH, MeOH, 3 h.

Treatment of racemic (±)-**72** with phenyl, *ortho-* and *para*-methoxyphenylboronic acids under palladium-mediated Suzuki cross-coupling reaction conditions generated the corresponding racemic bisaryl carbocyclic clefts (±)-**74**, **75** and **76** respectively in > 90 % yield (Table 2, entries 1–3). Similarly treatment of (±)-**72** with trimethylsilylacetylene (TMS)

in the presence of PdCl$_2$(PPh$_3$)$_2$, copper iodide and triethylamine (TEA), followed by deprotection afforded the bisacetylene derivative (±)-77 in 75 % yield (Table 2, entry 4).[8]

In 2006, Harding and co-workers reported procedures for the further elaboration of (±)-2, in the synthesis and characterisation of ditopic symmetrical bis(pyridyl) ligands. During a course of studies aimed towards the assembly of chiral metallomacrocycles of nanoscale dimensions the group successfully synthesised new molecular clefts presenting pyridyl, ethynylpyridyl and *para*-(4'-pyridyl)phenyl groups; (±)-78 (L1), (±)-79 (L2) and (±)- 80 (L3) respectively (Figure 8).[37]
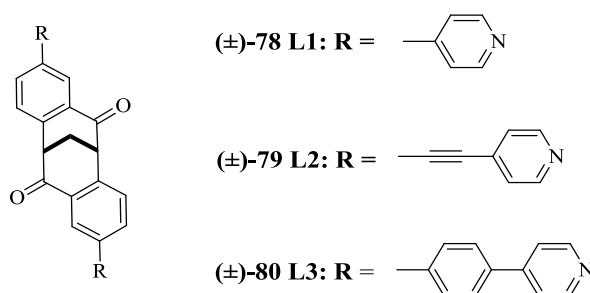
Figure 8: Ligands (±)-78 (L1), (±)-79 (L2) and (±)-80 (L3) derived from the molecular cleft (±)-2.

Ligand **L1** (±)-78 was prepared by the direct coupling of the dibromo cleft (±)-72 with (4 pyridyl)boronic acid pinacol easter under the catalysis of PdCl$_2$(PPh$_3$)$_2$ (Scheme 16, route a). The synthesis of **L2** starting from (±)-72 was first attempted using the protocol previously mentioned for the synthesis of (±)-77 (Table 2, entry 4), thus (±)-72 was treated under standard Sonogashira conditions with 4-ethynylpyridine hydrochloride, PdCl$_2$(PPh$_3$)$_2$ and CuI in neat TEA. However, these conditions afforded only the homo-coupled product (4, 4'-dipyridyl)butadiene **81** (Scheme 16, route b).

L1

(±)-78

a) | **78 %**

b)

or iii

81

Br

O

O

Br

(±)-72

c) i *or* c) ii

20 %

d) | **83 %**

L2

(±)-79

Br

O

O

N

(±)-82
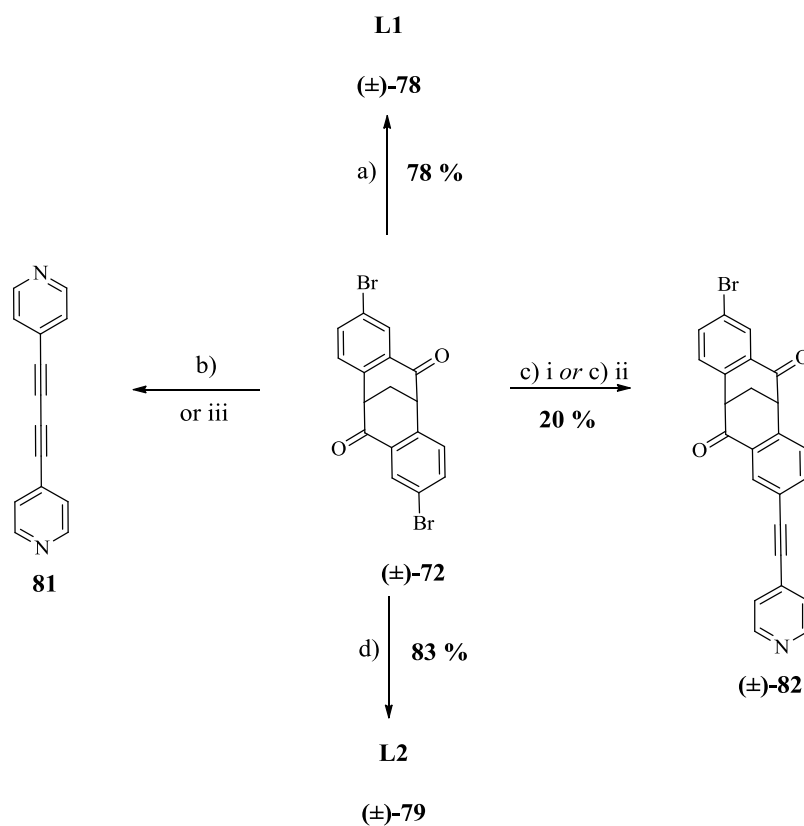
Reagents and Conditions: a) PdCl$_2$(PPh$_3$)$_2$, Na$_2$CO$_3$, (4-pyridyl)boronic acid pinacol ester, DME-H$_2$O, 85 ^{o}C, 3 days, N$_2$; b). PdCl$_2$(PPh$_3$)$_2$, CuI, Et$_3$N; c) i. Pd(PPh$_3$)$_4$, CuI, Et$_3$N, THF, c) ii. Pd(PPh$_3$)$_4$, CuI, Et$_3$N, MeCN; d). Pd(PPh$_3$)$_4$, CuI, Et$_3$N, DMF, rt, 2h.

Scheme 16: Synthesis of ligands L1 and L2.

Similarly, use of the more active palladium catalyst Pd(PPh$_3$)$_4$ under comparable reaction conditions led to the synthesis of the mono-coupled product **(±)-82** (Scheme 16, route c). More in-depth studies into the synthesis of the target ligand **L2** led the group to identify Pd(PPh$_3$)$_4$-CuI as the most efficient catalytic system. In addition, it was discovered that the solvent choice was critical in mediating the cross-coupling reactions. For instance, THF and acetonitrile resulted in the formation of the mono-coupled cleft **(±)-82** in 30 and 43 % respectively, while the use of DMF led to the synthesis of the desired ligand **L2 (±)-79** in 83 % yield (Scheme 16, route d).[37]

Ligand **L3** which contains two new bisaryl bonds was in theory accessible via a number of different routes, however evaluation of several different methodologies led the group to report only one successful procedure for its synthesis.[37] Coupling of **(±)-72** and (4-hydroxyphenyl)boronic acid pinacol ester under PdCl$_2$(PPh$_3$)$_2$ catalysed Suzuki reaction conditions gave the soluble bisphenol cleft **(±)-83** in 58 % yield. This was then treated with

21

triflic anhydride and pyridine to afford the corresponding bistriflate cleft (±)-**84**.This intermediate was reacted under Pd(PPh$_3$)$_4$ catalysed Suzuki reaction conditions to give the target cleft **L3** in 68 % overall yield following recrystallization from methanol and trifluoroacetic acid (Scheme 17).[37]
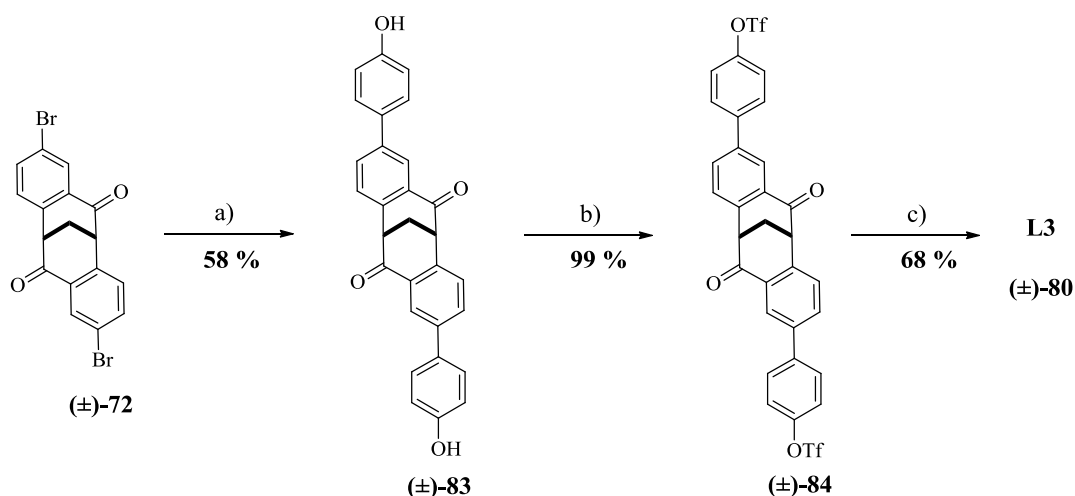
Reagents and Conditions: a) 4-(hydroxylphenyl)boronic acid pinacol ester, PdCl$_2$(PPh$_3$)$_2$, Na$_2$CO$_3$, DME-H$_2$O; b) TF$_2$O, pyridine, CH$_2$Cl$_2$; c) (4-pyridyl)boronic acid pinacol ester, Pd(PPh$_3$)$_4$, Na$_2$CO$_3$, DMF-H$_2$O.

Scheme 17: Synthesis s of L3.

Extensive X-Ray crystallographic analyses were undertaken to provide a measurement of the 'cleft' angle (*θ)* in order to determine the likely outcome of metal complexation and self-assembly studies. Table 3 summarises the interplanar 'cleft' angle (*θ*) between the two planes defined by the benzene rings in each of the ligands.[37] These results were consistent with the notion that the dimensions of the cleft can be controlled by the nature of the substituents on the aromatic rings.

In addition to synthetic work and X-Ray analysis, the group also performed some novel preliminary metal complexation studies with palladium (II) using the racemic ligand **L1**. Initial studies confirmed that under appropriate conditions ditopic symmetrical bis(pyridyl) ligands such as **L1**, **L2,** and **L3** can be used in the assembly of chiral [2+2] metallomarcrocycles. The group are currently investigating whether these functionalised clefts can be incorporated into the design of chiral metallomarcrocycles of nanoscale dimensions.

Table 3: Interplanar 'cleft' angle (θ) in clefts L1, L2 and L3.
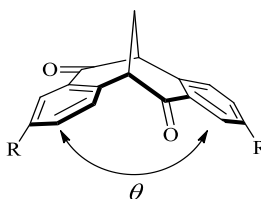
Entry	Ligand	Interplanar 'cleft' angle (θ) ($^\circ$) [a]
1	**L1**	97.80(3)
2	**L2**	102.47(8)
3	**L3**	103.30(4), 109.80(4)[b]

[a] All data were obtained on crystalline racemates.
[b] The asymmetric unit contains two independent molecules.

1.4.3.2 Carbon-Nitrogen Bond Formation

Like in the derivatisation of **1**, introduction of the amino group onto the framework of **2** was considered to be highly desirable as it facilitates the introduction of H-bond donor and acceptor groups onto the cleft framework. The general procedure for synthesis of **2** and its halogenated analogues shown in Schemes 13 and 15 was, however, not applicable to substrates containing nitro groups, as the strong electron-withdrawing properties of the nitro substituents prevented the final ring closure step from occurring.

In 2000 Harding and co-workers reported a procedure which involved the direct nitration of (±)-**2**, thus treatment of (±)-**2** with sulphuric acid and potassium nitrate led to regioselective nitration of the aromatic rings yielding the dinitro cleft (±)-**85** in 75 % yield. Subsequent selective reduction of (±)-**85** with refluxing iron in acetic acid gave the diamine cleft (±)-**86** in 93 % yield (Scheme 18).[8]
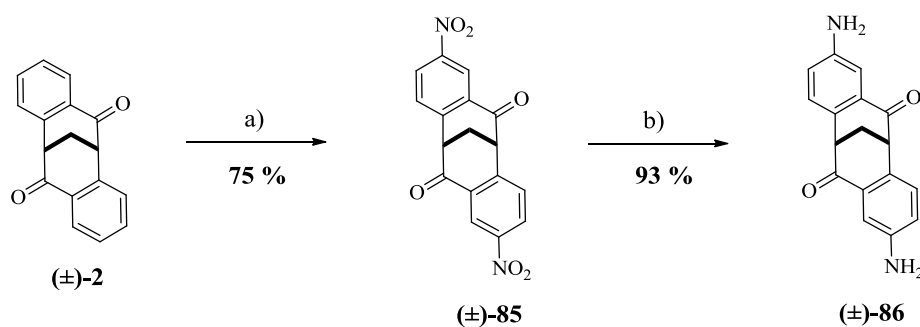
Reagents and Conditions: a) H_2SO_4, KNO_3, 0 °C, 30 min, rt, 16 h; b) Fe, AcOH, EtOH, N_2, reflux, 6h.

Scheme 18: Direct functionalisation of the cleft framework (±)-2 by regioselective nitration.

Similarly nitration of the dimethyl cleft **(±)-73** afforded exclusively the dimethyl-dinitro cleft **(±)-87** in 61 % overall yield (Figure 9).[8]
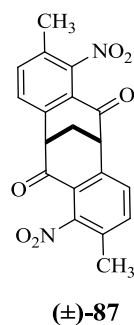
Figure 9: Harding and co-workers dimethyl-dinitro cleft (±)-87.

As in previous studies Harding and co-workers used X-Ray crystallographic data of the substituted clefts to show that there is a moderate degree of flexibility in the dimensions of the cleft in terms of the interplanar 'cleft' angle (θ) between the two aromatic rings depending on the nature of the R substituents (Table 4). Like the results in Table 3 these measurements demonstrate how the cleft dimensions may be fine-tuned or exploited in the design of biomimetic systems through substitution of the aryl rings, thus further exemplifying the versatility of this molecular cleft framework.

Table 4: Interplanar 'cleft' angle (θ) between planes defined by aromatic rings in ring functionalised cleft molecules.
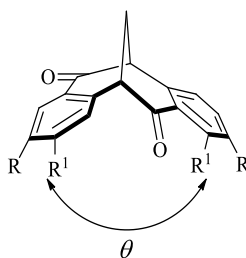
Entry	Cleft ($\pm$)	R	R^1	Interplanar 'cleft' angle (θ) (^{o})[a]
1	**72**	Br	H	91.4
2	**73**	CH$_3$	H	104.3, 101.7[b]
3	**74**	Ph	H	100.4
4	**76**	*p*-MeOPh	H	99.7
5	**85**	NO$_2$	H	83.9
6	**87**	CH$_3$	NO$_2$	102.7

[a] All data were obtained on crystalline racemates.
[b] Two types of molecules in unit cell.

1.4.4 Functionalisation of the Carbocyclic Cleft by Reaction of the Carbonyl Groups

The carbonyl groups at the periphery of the carbocyclic ring system in **2** are clear targets for functionalisation. Amenable to post-synthetic modification they offer additional opportunities to introduce recognition features onto the cleft. In recent years several groups have manipulated the chemistry surrounding these carbonyl groups to give a comprehensive list of ring mono- and disubstituted carbocyclic cleft derivatives.

Significant advances in the functionalisation of **2** have been developed by the Harding group however; it was Tatemitsu whom first described the functionalisation of **2** at the carbonyl positions. In the same paper that detailed the synthesis, resolution and chiroptical properties of **2**, Tatemitsu and co-workers reported the preparation of several ring substituted molecular clefts starting from the reduced form of the enantioenriched carbocyclic cleft **(-)-3** (79.8 % *ee*).[30] Stereoselective reduction of the carbonyl groups, by hydride attack at the least hindered face of the cleft, afforded the corresponding diol **(-)-3**, which was further

functionalised as esters **(-)-88** and **(-)-89** for characterisation (Scheme 19).[30] No yields were reported in the literature for this synthesis.
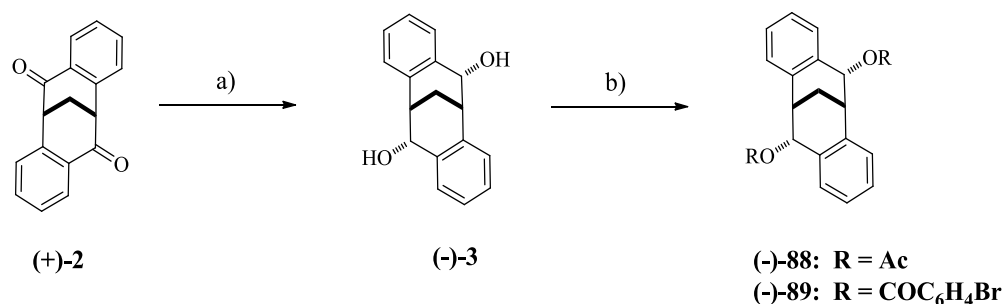
Reagents and Conditions: a) LiAlH$_4$, THF, 0 ^{o}C, 1 h; b) R = Ac, pyridine, acetic anhydride, 90 ^{o}C, 5.5 h; R = COC$_6$H$_4$Br, pyridine, *p*-bromobenzoyl chloride, 60 ^{o}C, 20 h.

Scheme 19: Tatemitsu and co-workers synthesis of reduced molecular cleft (-)-3 and the diester substituted clefts (-)-88 and (-)-89.

The reduced molecular cleft **(-)-3** was obtained either by catalytic hydrogenation over platinum oxide catalyst or by reduction with lithium aluminium hydride in THF.[30] An excess of sodium borohydride in a solution of THF and methanol at room temperature has also been shown to be an effective reducing agent giving the reduced cleft in good yields.[38,39] Extensive NMR studies of the reduced cleft **(-)-3** showed that the hydroxyl groups are pseudo-axial meaning that both groups are directed into the chiral cavity of the cleft, a feature that has since captured the interest of a number of research groups.

A decade later in 1985, members of the Tatemistu research group in Japan published a paper detailing the synthesis of a range of optically active crown ethers and dipodands prepared from enantiomerically pure **(-)-2** and **(-)-3** clefts. The effectiveness of these compounds as enantioselective transporters of chiral molecules through bulk liquid membranes was also assessed and provided valuable information about the enantiomeric selectivity of molecular clefts containing the carbocyclic cleft framework.[38]

Treatment of **(-)-3** with sodium hydride in the presence of the respective substituted para-toluene / bis-toluene sulfonate gave access to crown ethers **(-)-90** and **(+)-91** and the open chained polyether **(-)-92**. Table 5 summarises the reaction conditions used by the group to synthesise compounds **(-)-90, (+)-91** and **(-)-92**.

Table 5: Summary of the reaction conditions used for the synthesis of crown ethers and dipodands prepared from (-)-3.[38]
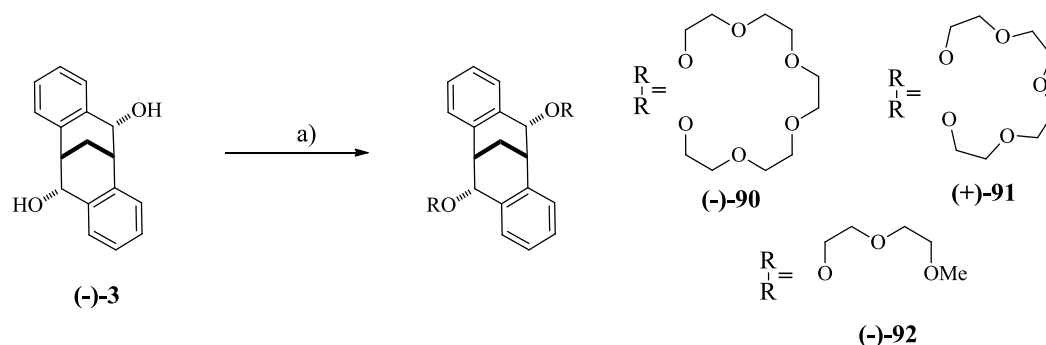
Entry	Crown ether	Reagents and conditions a)	Mp (^{o}C)	Yield (%)
1	(-)–90	3,6,9,12-tetraoxatetradecane-1,14-diyl bis-toluene-p-sulphonate (pentaethyleneglycol ditosylate), NaH, THF, reflux, N$_2$, 24 h	116-117	16
2	(+)–91	3,6,9-trioxaundecane-1,12-diyl bistoluene-p-sulphonate (tetra-ethyleneglycolditosylate), NaH, THF	72–74	11
3	(-)–92	6-methoxy-3-oxapentan-1-yl toluene-p-sulphonate, NaH, DMF, 45 ^{o}C, 24 h	Oil	86

In addition to novel crown ethers derived from chiral (-)-3, the group also reported for the first time the synthesis of (+)-94 which possesses hydroxymethyl groups at the periphery of the cleft. (Scheme 20).[38]
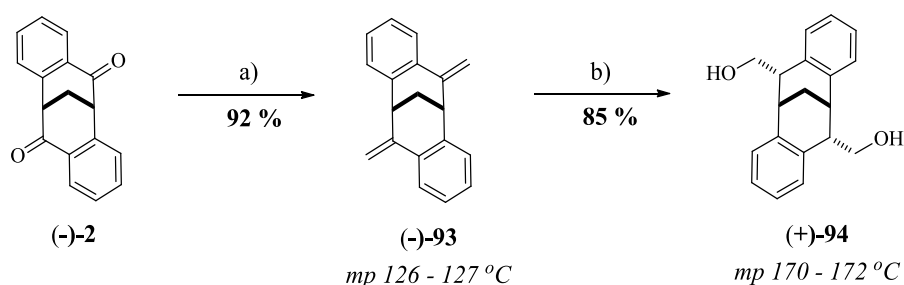
Reagents and Conditions: a) Wittig condensation; methyltriphenylphosphonium bromide, KOtBu, THF; b) i. Diborane, THF; ii. 30 % H$_2$O$_2$, THF, 3M NaOH.

Scheme 20: Synthesis of dihydroxymethyl diol (+)-94 by Wittig Condensation.

The bisalkene (-)-93 was accessed in 92 % yield by Wittig condensation of (-)-2 with methyltriphenylphosphonium bromide and potassium *tert*-butoxide in THF. Subsequent treatment of (-)-93 with diborane in THF followed by oxidation with 30 % hydrogen peroxide in THF gave (+)-94 in 85 % yield (Scheme 20). Subsequent reaction of the hydroxymethyl groups with pentaethylene glycol ditosylate and tetraethylene glycol ditosylate in the presence of a mixture of sodium hydride-THF gave crown ethers (+)-95 and (+)-96 in 12 % and 4 % yields, respectively (Scheme 21).[38]
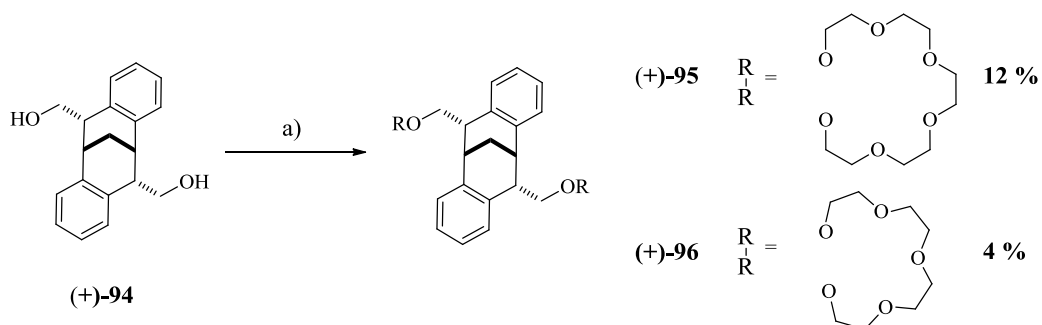
Reagents and Conditions: a) i. pentaethylene glycol ditosylate (NaH-THF); ii. tetraethylene glycol ditosylate, NaH-THF .

Scheme 21: Synthesis of crown ethers (+)-95 and (+)-96.

The group explored the enantiomer recognition properties of these crown ethers by measuring the transportation of chiral molecules through bulk liquid membranes. Chloroform solutions of the ligand to be tested were separated from an inner aqueous phase (0.1 M HCl) and an outer phase (0.08 M HCl), which contained $LiPF_6$ and the racemic guests; (±)-1,2-diphenylethylamine hydrochloride (**A**) and methyl-(±)-phenylglycinate hydrochloride (**B**). Transportation of the racemic guests was monitored by ultraviolet spectroscopy, and the *ee* of the transported guest molecule was monitored by circular dichroism (CD). Table 6 shows the enantiomer recognition behaviour of these crown ethers towards the racemic guests (±)-1,2-diphenylethylamine hydrochloride (**A**) and methyl-(±)-phenylglycinate hydrochloride (**B**).[38]

Table 6: Differential transport of enantiomeric molecules through bulk liquid membranes by application of the enantiopure crown ethers and open-chain polyether.

Entry	Host	Guest	Time (h)	Transport (%)	Configuration of dominant enantiomer	Optical purity (%)
1	(-)-90	A	3.5	14	*S*	74
2	(+)-91	A	4	17	*S*	38
3	(-)-92	A	1.5	11	*S*	84
4	(+)-95	A	3	14	*S*	32
5	(+)-96	A	2.5	15	*S*	80
6	(-)-90	B	48	14	-	0
7	(+)-91	B	22	26	*R*	23
8	(-)-92	B	72	15	*S*	8
9	(+)-95	B	36	12	-	0

All the crown ethers showed enantiomeric selectivity towards primary ammonium salts with the nature of the R substituent strongly affecting the degree of selectivity. In general the crown ethers were more selective and more rapid at transporting (±)-1,2-diphenylethylamine hydrochloride (**A**) than methyl-(±)-phenylglycinate hydrochloride (**B**). Optimal transport properties were exhibited by dipodand **(-)-92** which produced 84 % optically pure 1, 2-diphenylethylamine hydrochloride (**A**) (Table 6, entry 3). Since this publication, there have been no subsequent reports of further reaction of the alkenes in **(-)-93** or of the hydroxyl groups in **(-)-94**. Further elaboration of these molecular clefts is expected, due to the high reactivity of the respective functional groups. Perhaps more significantly, since this report which was published over 25 years ago, there have been no additional reports examining the enantiomer recognition / selectivity of functionalised derivatives of the enantiopure molecular cleft **2**.

In 2002 Harding and co-workers reported the synthesis of a dioxime derivative (±)-**97**. Treatment of (±)-**2** with excess hydroxylamine hydrochloride and sodium hydroxide in refluxing ethanol, followed by an acidic workup gave the racemic dioxime cleft (±)-**97** in 52 % yield (Scheme 22).[40]
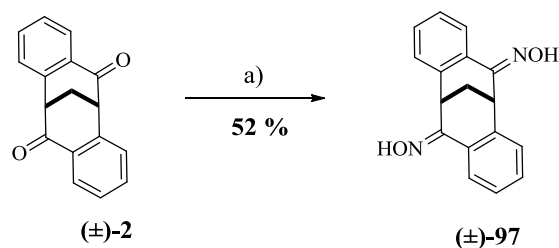
Reagents and Conditions: a) NH₂OH.HCl, NaOH, EtOH, H₂O, reflux, 24 h.

Scheme 22: Harding and co-workers synthesis of the dioxime cleft (±)-97.

Synthesis of **(±)-97** was important as it demonstrated that despite being relatively hindered the carbonyl groups on the cleft framework are susceptible to attack by larger nucleophiles, thus opening up the potential for the installation of other functionalities by nucleophilic addition. X-Ray crystallographic data showed that the hydroxyl groups in **(±)-97** are orientated into the cavity of the cleft (Figure 10);[40] a desirable characteristic when considering the relative binding properties of the cleft cavity.
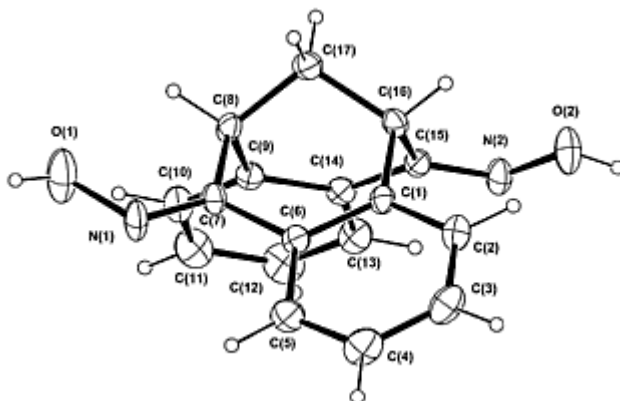
Figure 10: X-Ray crystal structure of (±)-97 showing the orientation of hydroxyl groups into the cavity of the cleft.[40]

In 2004, a group in Sweden detailed for the first time synthetic routes for the introduction of amine functionalities onto the cleft at the carbonyl positions.[34] Prior to this publication, direct nitration of the aromatic rings to give **(±)-85** followed by iron reduction to give **(±)-86** was the only example detailing the installation of the amine group onto the carbocyclic cleft framework **2** (Scheme 18).

Due to its C_2-symmetric, ridged and conformationally restrained framework, the carbocyclic molecular cleft **2** was selected by the group as a chiral selector unit in an investigation to explore the effects of chiral spacer length in chiral stationary phases in liquid

chromatography. For the first time the application of functionalised derivatives of **2** formed the focal point of the study rather than purely derivatisation and characterisation. As part of their investigation the group reported synthetic routes to three novel nitrogen containing molecular clefts derived from **(+)-2**. Amine functionalities were introduced by reaction of the enantiopure cleft **(+)-2** with benzyl amine to produce *bis*-benzyl imine **(+)-98** in 49 % yield, followed by reduction using sodium borohydride to give the *bis*-benzyl amine **(+)-99** in 75 % yield. The diamine **(-)-86a** was then obtained in 85 % yield following removal of the benzyl groups by hydrogenolysis (Scheme 23).[34]
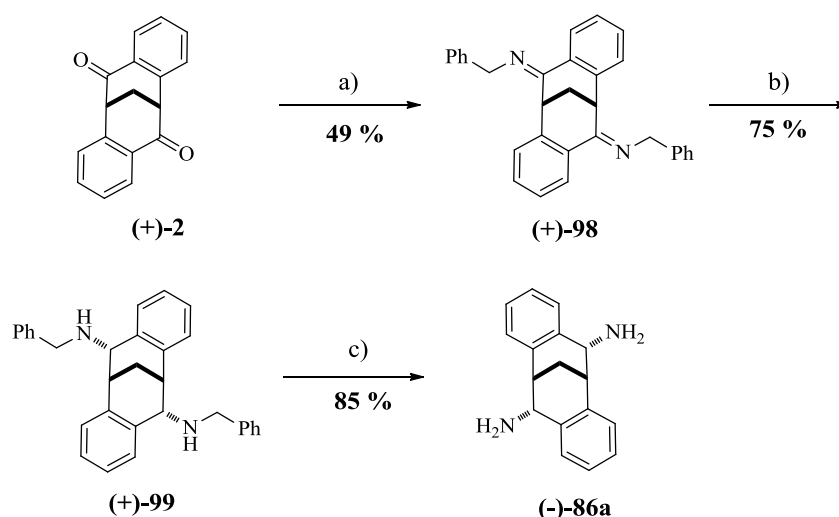
Reagents and Conditions: a) BnNH$_2$, 4Å Molecular Sieves, toluene, reflux, 48 h; b) NaBH$_4$, MeOH:THF (1:1), rt, 18 h; c) H$_2$, Pd/C (10 %), EtOH, 4 Atm, 50 $^{\circ}$C, 48 h.

Scheme 23: Synthesis of enantiopure diamine cleft (-)-86a.

The amine groups in **86a** allowed for further derivatisation of the molecular cleft thus, reaction of **(+)-86a** and 3-butenoyl chloride, obtained from vinylacetic acid and oxalyl chloride, resulted in a 75 % yield of **(+)-100** (Scheme 24, route b). In addition reaction of the **(-)-86a** enantiomer with 10-undecenoyl chloride gave **(-)-101** in 85 % (Scheme 24, route a).[34]
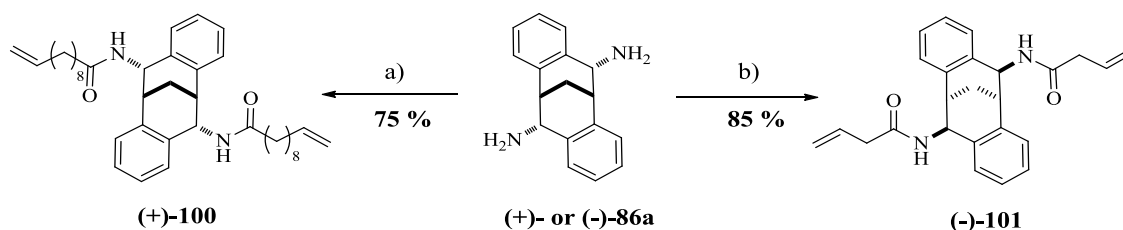
Reagents and Conditions: a) Et$_2$O, 10-undecenoyl chloride, 4-tert-butylcatechol, 0 $^{\circ}$C, 1.5 h; b) Na$_2$CO$_3$ (5 %), Et$_2$O, 3-butyl chloride, 4-tert-butylcatechol, 0 $^{\circ}$C, 1.5 h

Scheme 24: Synthesis of chiral selectors (+)-100 and (-)-101 from pure enantiomers of 86a.

Following synthesis and characterisation the enantiopure amine functionalised clefts (+)-**100** and (-)-**101**, were used as chiral selectors in liquid chromatography studies. These cleft molecules were cross-linked and immobilised to vinyl-silica by hydrosilylation reactions involving a multifunctional hydrosilane. Their selectivity was evaluated by chromatographic separation of a series of racemic test substances, details of which are beyond the depth of this report.[34]

A few years later in 2007, a group headed by Friberg reported the synthesis of a range of substituted molecular clefts derived from (-)-**2**, including several C$_2$-symmetrical diols (-)-**102–105**, a hydroxyketone (+)-**106** and an amino-alcohol (+)-**110** (Scheme 25, 26 and 27).[6]
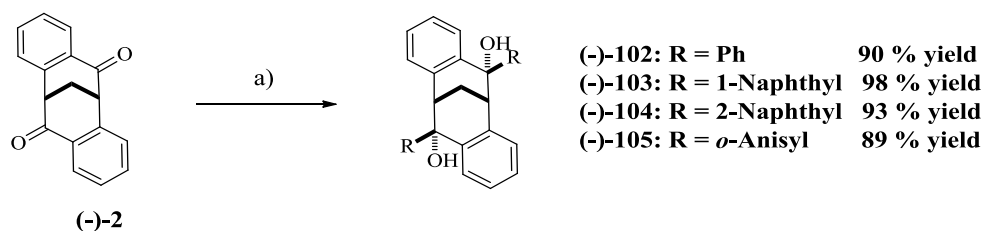
Reagents and Conditions: a) RMgX or *o*-AnLi in THF, rt, 2 h.

Scheme 25: Synthesis of C$_2$-symmetric diols prepared from (-)-2 by addition of excess Grignard or lithium reagents.

The C$_2$-symmetric diols (-)-**102-105** were prepared in high yields and > 99 % *ee* by treating (-)-**2** with an excess of the corresponding Grignard or lithium reagent (Scheme 25). While the hydroxyketone (+)-**106** was obtained in high yield by addition of 1.2 eq of 1-naphthyl magnesium bromide (Scheme 26, route a) to (+)-**2**. Compound (-)-**108** was obtained by methylation of (+)-**106** followed by addition of the second naphthyl substituent (Scheme 26).[6]
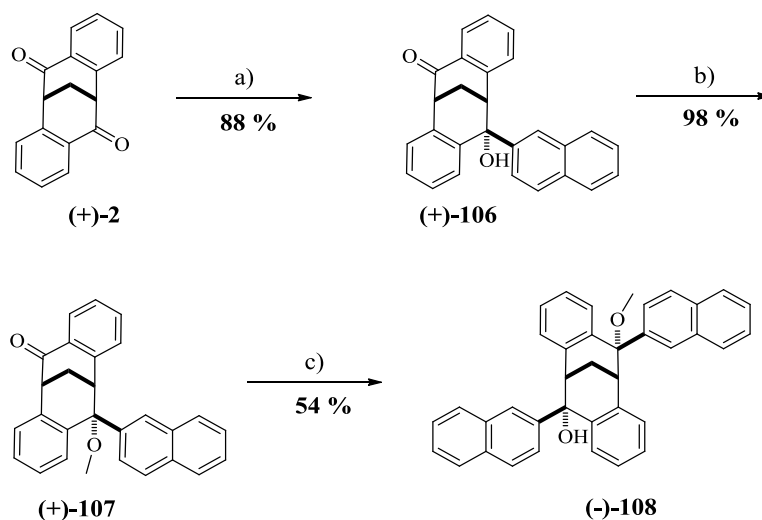
Reagents and Conditions: a) 1-naphthylMgBr, THF, rt, 1 h; b) MeI, NaH, THF, 0 °C;

c) 1-naphthylMgBr, THF, rt, 5 h.

Scheme 26: Synthesis of hydroxyketone (+)-106 and naphyl-substituted molecular cleft (-)-108.

The amino-alcohol cleft **(+)-109** was synthesized via formation of the corresponding benzylimine derivative, followed by the reduction with sodium borohydride in methanol (Scheme 27).[6]
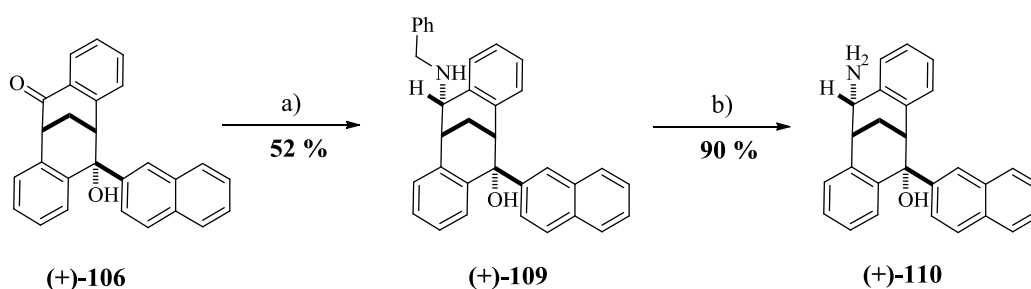
Reagents and conditions: a) i. BnNH$_2$, 4 Å MS, toluene, reflux, 22 h, ii. NaBH$_4$, MeOH, reflux, 5 h;

b) Pd/C (5 %), HCOOH, MeOH, rt, 5 h.

Scheme 27: Synthesis of amino-alcohol clefts (+)-109 and (+)-110 from the hydroxyketone cleft (+)-106.

Catalytic hydrogenation of **(+)-109** using palladium on carbon and molecular hydrogen resulted in irreproducible yields of the target compound due to hydrogenolysis of **(+)-110** during the course of the reduction. This was circumvented by the use of formic acid and palladium on carbon in a transfer hydrogenation reaction, which resulted in a high yield of **(+)-110** (Scheme 27).[6] These reaction conditions are similar to those reported for the synthesis of the diamine cleft **(-)-86a** (Scheme 23).[34]

These functionalised cleft structures are reminiscent of previously synthesised TB derivatives, which were used to explore the effect of functional group positioning in a series of host-guest studies which relied on the positioning of functional groups in a predictable geometry.[3] Thus, the possibility of utilising these chiral clefts for substrate-organisation in combination with H-bond activation for enantioselective catalysis was investigated for the first time. The enantiopure functionalised clefts **(-)-102 –105** and **(+)-106 - 110**, as well as, the previously synthesised amines **(+)-99** and **(-)-86a** were utilised in the HDA of benzaldehyde and an aminodiene, details of which will be discussed in detail in Chapter 3.

Most recently, in 2010, the Kimber group at Loughborough University disclosed a convenient method for the selective functionalisation of **2**, detailing for the first time the synthesis of clefts incorporating heterocyclic groups.[39] In theory these heterocyclic groups presented both Brønsted acid and base binding sites capable of metal binding and molecular recognition processes. During a research programme aimed at utilising the molecular cleft **3** in catalysis and molecular recognition processes the group devised methods for the simple diesterification and mono- dialkylation of **3** with 2-, 3- and 4- pyridyl subunits (Scheme 28).

Reagents and conditions: a) NaBH$_4$, THF/MeOH, rt, 48 h; b) 2-,3-,or 4-pyridyl acid chloride, DMAP, pyridine, 50 ^{o}C, 16 h.

Scheme 28: Diesterification of (±)-3 to give dipyridyl-ester derivatives (±)-111a-d.

Following stereoselective reduction of (±)-**2** with sodium borohydride, diesterification of the resulting reduced cleft (±)-**3** was achieved by reaction with either 2-, 3-, or 4-pyridyl acid chloride hydrochloride salts, pyridine and catalytic amounts of DMAP at 50 °C for 16 h. This repeatedly gave the respective dipyridyl esters **111a-d** in moderate to good yields.[39]

Dietherification of (±)-**3** to give the dialkylated products was, however, not achieved quite so readily. Treatment of (±)-**3** with 2-, 3- and 4-bromomethylpyridyl hydrobromide salts as the alkylating reagents and using sodium hydride as the base unexpectedly gave the monoalkylated products (±)-**113a-c** in good to excellent yields (Scheme 29, route b). Although, this result was initially disappointing, it provided the group with a facile entry into the monoalkylated products. The group eventually achieved dialkylation of (±)-**3** by using an adapted method reported by Ley and Heaney,[41] which involved treatment of (±)-**3** with the desired 2-bromomethylpyridyl hydrobromide salt (2.2 eq) in DMSO and an excess of potassium *tert*-butoxide (4.4 eq). This gave the dialkylated products (±)-**112a-c** in good to excellent yields (Scheme 29, route a).[39]

(±)-**112**		(±)-**3**		(±)-**113**
		R =		
(±)-**112a** 87 %				(±)-**113a** 87 %
(±)-**112b** 79 %				(±)-**113b** 88 %
(±)-**112c** 94 %				(±)-**113c** 92 %

Reagents and conditions: a). 2-,3- or 4-bromomethylpyridyl hydrobromide salt (2.2 eq), DMSO, KO*t*Bu (4.4 eq), rt, 18 h; b). 2-,3- or 4-bromomethylpyridyl hydrobromide salt, NaH (3.0 eq), THF, rt 18 h.

Scheme 29: Dietherification of (±)-3 to give mono- (±)-113a-c and dialkylated (±)-112a-c molecular cleft as reported by the Kimber group.

X-Ray analysis of these pyridyl substituted clefts revealed some important characteristics in terms of the clefts recognition and binding properties. It was shown that the

pyridyl substituents were directed into the cleft cavity thus creating a chiral environment potentially capable of metal binding. Moreover, X-Ray analysis showed that the clefts were filled with either solvent molecules or the external surfaces of other cleft molecules via C–H···π interactions, thus demonstrating their ability to take up molecules with the appropriate shape and chirality (Figure 11).[39]

Figure 11: Molecular structure of (+)-112b / CH$_2$Cl$_2$ showing pyridyl groups pointing 'downwards' into the clefts and the C–H···π binding of CH$_2$Cl$_2$ solvate.

Recently the group have performed a series of binding studies in order to evaluate the molecular recognition and binding abilities of these molecular clefts. The uptake and binding of specific target molecules has been evidenced by a series of inclusion complexes with an excess of phenyl boronic acid. The 4-pyridyl cleft **(±)-112b** was shown to self-assemble into the *bis*-boroxine in the presence of excess phenyl boronic acid.[42] The X-Ray crystal structure shown in Figure 12 clearly shows the pyridyl stabilised boroxines as well as CH$_2$Cl$_2$ solvent molecules within the cavity of the cleft bound by C–H···π interactions. These results are particularly important as they provide proof of principle in terms of the ability of these clefts to be used for the specific binding and uptake of target molecules. The group are yet to optimise these binding properties to determine how they can be perfected for catalysis however it will no doubt be the focal point in subsequent research projects.[42]

Figure 12: X-Ray crystal structure of the 4-pyridyl cleft (+)-112c and phenyl boronic acid complex.

1.5   Application of Functionalised Carbocyclic Cleft Derivatives

Despite the recent interest in the carbocyclic cleft **2**, applications of its functionalised derivatives remain elusive compared to those of **1**. The essential properties of **2** – the chiral, rigid, and aromatic cavity, together with the synthetic entries that have recently been made available are bound to inspire new applications of its analogues, however to date no real ground breaking application of molecules containing this skeleton have been reported. Aside from the disubstituted bis-pyridines which were used to direct stereoselective metal self-assembly processes[37] and the chiral crown ethers which were used as effective enantioselective transporters of chiral molecules,[38] as mentioned previously, there has only been one other example reporting the effective application of functionalised clefts incorporating the carbocyclic cleft molecular framework. This involved them being used as enantioselective H-bonding catalysts in an asymmetric HDA reaction.[6] To date this is the only example where the chirality associated with the molecular cleft **2** has been manipulated and used catalytically to induce enantioselectivity in an organic transformation.

1.6 Objectives

The aim of this research project was to develop new easily synthesizable organic based catalysts for asymmetric synthesis. We aimed to utilise the rigid scaffold inherent within the chiral carbocyclic cleft shaped nucleus **2** to design and synthesise a novel family of cleft molecules which present highly tuneable chiral environments for use in asymmetric catalysis and molecular recognition. The main target was to develop a system capable of directing H-bond interactions into a chiral environment with the overall goal of producing highly active, enantioselective organocatalysts and use these in the synthesis of biologically active compounds. This approach is extremely attractive as the cleft molecule **2** can be modified with relative ease, thus altering the steric and electronic properties of the catalyst, a process which can be vital for activity and selectivity.

There was an emphasis on achieving symmetrical functionalisation of the molecular cleft at the prochiral carbonyl positions at the periphery of the cleft framework. Similarly the installation of functional groups capable of H-bonding was deemed imperative, to achieve a system which exhibits a high degree of chirality and bonding donor and acceptor recognition sites. Initially the priority was to develop and optimise procedures for the synthesis of the desired target using the racemic bicycle (±)-**2**. Once a reliable synthetic methodology had been established the objective was then to synthesise the chiral analogues in no less than 90 % *ee*. The bulk of this report is dedicated to the synthesis, functionalisation and characterisation of novel cleft molecules derived from **2**, which is reported in Chapter 2.

The secondary aim of this research project, which is reported in Chapter 3, was to evaluate these novel functionalised molecular clefts for asymmetric catalytic activity, with an emphasis on achieving good to excellent *ee* values Previous studies have demonstrated that functionalised derivatives of **2** can be used as H-bonding catalysts in an asymmetric HDA reaction, resulting in moderate *ee* values. As a result the asymmetric HDA reaction between Rawel diene **10** and benzaldehyde **11** was selected as the test reaction for screening the novel clefts for enantioselectivity. In addition, we aimed to explore the application of these catalysts in the *N*-bromosuccinimide (NBS) **19** mediated bromolactonisation reaction of unsaturated carboxylic acids, comparing their activity to related cinchonine alkaloid catalysts.

The final aim of this project was to synthesise a mixed fused ring system containing both the chelating nitrogen functionality from **1** as well as the carbonyl functionality from **2**.

Thus the objective was to synthesis a mixed chiral cleft derived from **1** and **2**, with a view towards the assembly of a unique family of rigid chiral clefts molecules with exceptional topology. Such a molecule would contain a true chiral cavity, with the potential to directly assemble substrates within the chiral environment. Chapter 4 details the synthetic approaches taken in the attempted synthesis of this proposed mixed fused molecular cleft system.

Chapter 2

2.0   Results and Discussion

Synthesising symmetrically functionalised chiral cleft molecules remains a challenge to the synthetic chemist. In recent years this endeavour has become even more appealing because of the increased interest in developing organic molecules for the use in asymmetric organocatalysis. Consequently, several approaches for the installation of different functional groups capable of chiral recognition and binding have been developed and reported with emphasis on installing functional groups capable of H-bonding. Between the different alternatives that exist for the functionalisation of the carbocyclic molecular cleft **2**, there is only one example in the literature that reports the application of functionalised cleft molecules related to **2** in asymmetric catalysis.[6] In view of the potential significance of these cleft derivatives as asymmetric catalysts, we aimed to synthesise a range of functionalised molecular clefts based around the carbocyclic molecular cleft **2** (Figure 13).

(-)-**2**   (+)-**2**
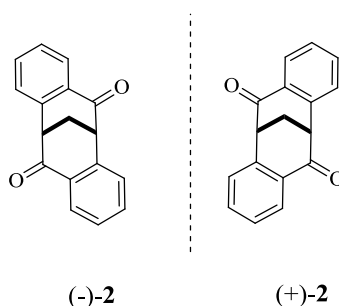
Figure 13: The enantiomers of the carbocyclic molecular cleft 2.

With this in mind, literature procedures were followed and extended in an attempt to synthesise a range of novel bifunctional catalysts derived from the bicycle **2**. Herein, the synthesis and characterisation of functionalised derivatives of **2** containing the versatile amino-thiocarbamate group is reported. Synthesis of the desired target molecules were explored and optimised using the racemic bicycle (±)**-2** and where possible chiral host-guest interactions were translated into the realm of catalytic asymmetric synthesis using the novel enantiopure amino-thiocarbamate clefts (Chapter 3).

2.1   Synthesis of Carbocyclic Cleft

Initially the focus was to synthesise **2** as a racemic mixture and as its pure enantiomers to give the core framework for derivatisation. The racemic bicycle (±)**-2** was

accessed according to the procedure initially reported by Tatemitsu.[30] The carbocyclic cleft (±)-2 was therefore synthesised via a three-step synthetic pathway starting from commercially available phenylacetonitrile 66 (Scheme 30).
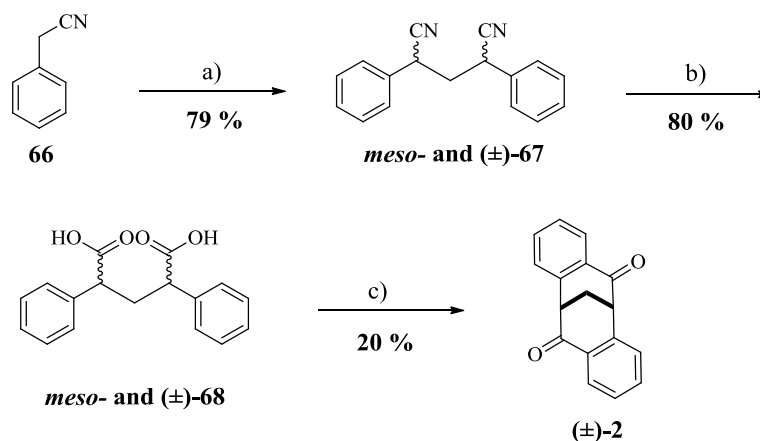
Reagents and conditions: a) CH_2I_2, NaOH, 145 °C, 2 h; b). EtOH, KOH, H_2O, reflux, 16 h; c) *conc.* H_2SO_4, 145 °C, 2 h.

Scheme 30: Synthesis of the racemic carbocyclic cleft (±)-2.

Two equivalents of 66 were condensed at 145 °C for 2 h with diiodomethane in the presence of stoichiometric amounts of finely powdered sodium hydroxide to give crude *meso* and (±)-2,4-diphenylglutanitrile 67. Under these reaction conditions crude *meso-* and (±)-67 were repeatedly isolated as dark orange / brown oils with a yield in excess of 70 %. In the synthesis of (±)-2 product diastereoisomers were not separated but used directly in the next step. Hydrolysis of crude *meso-* and (±)-67 in refluxing ethanolic potassium hydroxide for 16h gave crude *meso-* and (±)-2,4-diphenylpentanedioic acids 68 as an orange / brown oil in 80 % yield. A two-fold intramolecular sulphuric acid-mediated Friedel-Crafts acylation reaction gave (±)-2 in an average 20 % overall yield. Given that *meso-* 68 cannot cyclise to form the bicycle 2 due to geometric constraints the maximum obtainable yield for this step is 50 %. Despite these limitations, attempts to optimise the chemistry at this stage of the synthesis served as a point of interest during the repeated synthesis of (±)-2.

Resolution of enantiomers was achieved by classic recrystallization and separation of the diastereomeric mixture of 68. Crude *meso* and (±)-68 were recrystallized from hot toluene three times to remove the unwanted *meso* compound. Repeated recrystallization gave the pure racemic diacids (±)-68 as an off-white solid in an average yield of 40 %. The pure

racemic mixture was then separated by quinine salt resolution which gave enantiomerically enriched (+) and (-)-**68** in 35 % and 18 % yields, respectively (Scheme 31).[30,34]
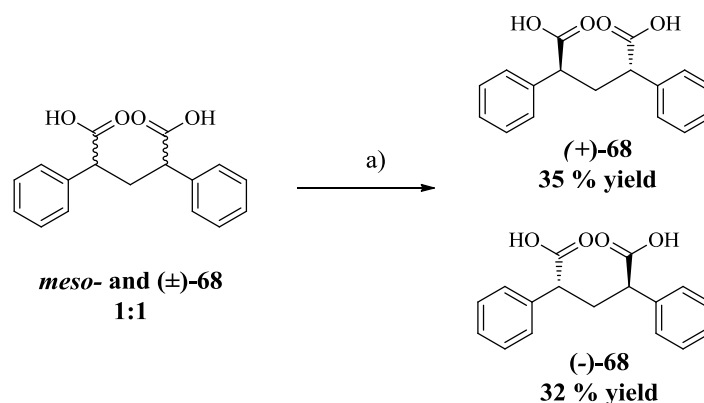
Reagents and conditions: a) i. (±)-68 from recrystallization in toluene; ii. Enantiomer separation; quinine, EtOH, rt, 18 h.

Scheme 31: Quinine resolution of enantiomers of 68.

Treatment of both the (+) and (-)-**68** enantiomers with an excess of concentrated sulphuric acid at 145 °C for 2 h gave enantiomerically enriched (-) and (+)-**2** respectively, via the previously mentioned double-acid mediated Friedel-Crafts acylation reaction. The absolute configuration of the bicycle (+) and (-) enantiomers were determined by chiral HPLC analysis which confirmed that enantiomerically pure (-) or (+)-**2** were isolated with good to excellent *ee.* Repeated slow recrystallization of the clefts from hot methanol improved the *ee* of isolated products from 69 to > 90 % *ee*. Table 7 summarises the isolated yields and *ee* values of the racemic and enantiomerically pure clefts.

Table 7: Summary of the isolated yields, ees and melting points of racemic and enantiomerically pure carbocyclic molecular clefts 2 following recrystallization.

Entry	Stereochemistry of 2	Yield (%)	*ee* (%)[a]	Melting point (°C)	*Lit.* Melting point (°C)[30]
1	(±)	20	< 5	146.1 – 146.6	147.7 – 147.8
2	(+)	42	> 99	189.7 – 194.1	194.0 -194.5
3	(-)	58	> 99	191.6 – 193.3	No data reported

[a] Determined by HPLC analysis on Chiralcel OD-H column, 98:2 hexane :2-propanol, 0.6 mL min^{-1}, 220 nm detector.

Under almost identical reaction conditions, ring disubstituted derivatives of **2** can be synthesised. By using an appropriately *para*-substituted phenylacetonitrile precursor, the cleft may be functionalised at the aromatic ring positions. However, the harsh hydrolysis and acylation reaction conditions required for cleft formation limits the range of substituents which can be introduced onto the cleft framework via this procedure. With this in mind and following a literature procedure first reported by Harding and co-workers in 1998,[33] the racemic dimethyl cleft (±)-**73** was synthesised and isolated in 14 % overall yield, starting from commercially available methylphenylacetonitrile **69b** (Scheme 32).
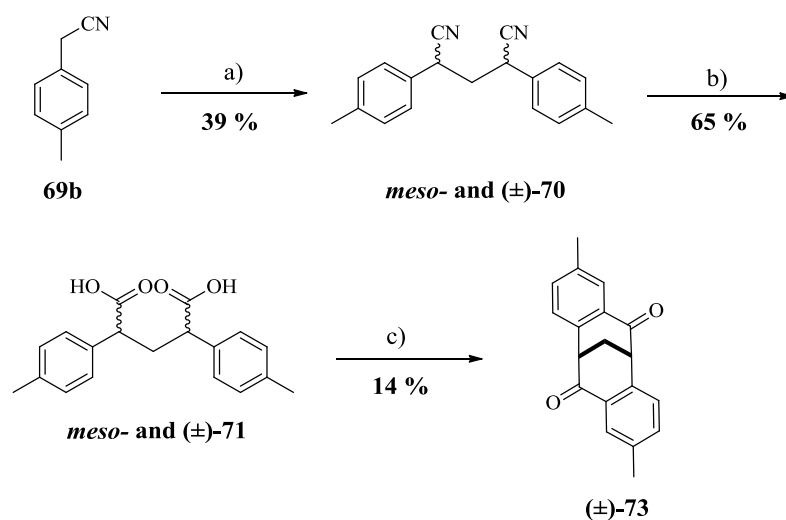
Reagents and conditions: a) CH_2I_2, NaOH, 165 $^{\circ}$C, 45 min; b) EtOH, KOH, H_2O, 80 $^{\circ}$C, 18 h; c) *conc.* H_2SO_4, 100 $^{\circ}$C, 45 min.

Scheme 32: Synthesis of racemic dimethyl cleft (±)-73.

^{1}H and ^{13}C spectral analysis of the isolated product (±)-**73** was consisted with literature values. Further derivatisation of this molecular cleft was not explored in this research project however; the relative ease in which this cleft can be accessed presents opportunities for further development.

2.2 Functionalisation of the Carbocyclic Molecular Cleft

As previously disclosed, the parent carbocyclic cleft **2** is amendable to post-synthetic modification both at the aromatic rings and at the bridge ketones. Coupling of **2** with a number of different functional groups gives promising binding entities in which several recognition features may be orientated into the concave region of the molecular cleft. Based on previous work carried out by Tatemitsu,[30] Harding[4,8,33] and the Kimber group[39] which

focused on achieving functionalisation of the molecular cleft framework **2**, we decided to look at developing viable synthetic routes for the synthesis of novel functionalised cleft derivatives.

Recent reports on the synthesis and use of a new class of bifunctional catalyst incorporating the amino-thiocarbamate functional group led us to focus on installing this functionality onto our chiral carbocyclic cleft in order to access a new family of potentially useful bifunctional asymmetric catalysts.[43] Details of their accessibility will be discussed below, as well as other methodologies used to introduce several different potentially useful functional groups onto the cleft framework. Some literature procedures were followed exactly in order to gain access to readily modifiable substrates, whereas others were extended to give novel derivatives of **2**.

2.2.1 Stereoselective Reduction of the Carbonyl Groups

The stereoselective reduction of both carbonyl groups has previously been reported as being one of the most attractive characteristics of **2** as it allows for a large range of functional groups to be introduced onto the cleft framework at these positions. Previous work has shown that hydride attacks exclusively from the convex face of the cleft to give a single diastereomer in which the resulting hydroxyl groups are pseudo-axial.[30] The conformation of this reduced cleft in which the hydroxyl moieties are both orientated into the cavity of the cleft provides a promising binding environment for a range of substrate molecules (Figure 14).

3
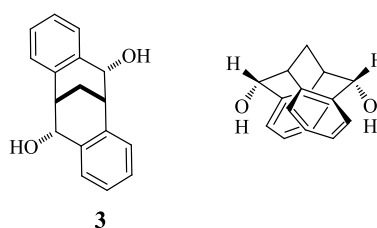
Figure 14: Structure of the reduced carbocyclic cleft 3 showing the orientation of hydroxyl groups into the cleft cavity.

The susceptibility of these bridge carbonyls to undergo attack by a variety of nucleophiles is a key consideration of our research and plays a pivotal role in the extent to which **2** can be functionalised. As previously mentioned, there have been several different methods reported in the literature for the reduction of **2**.[30,39] In this investigation reduction of the carbonyl groups on **2** was achieved by using an excess of sodium borohydride (5.0 eq) in

a 1:1 mixture of THF and methanol at room temperature for 48 h, a methodology which had previously been used by the Kimber group to access (±)-**3** (Scheme 33).[39]

(±), (+) and (-)-2   (±), (+) and (-)-3
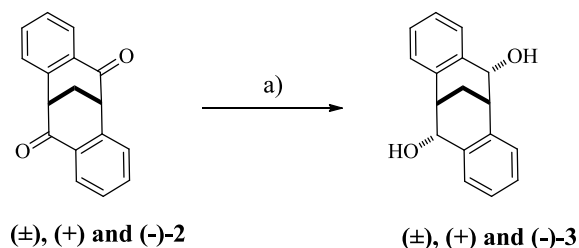
Reagents and conditions: a) NaBH$_4$ (5.0 eq), THF/MeOH (1:1), rt, 48 h.

Scheme 33: General reaction conditions for the stereoselective reduction of the carbonyl groups on 2 to give the reduced cleft 3.

Under these reaction conditions both the racemic and enantiopure carbocyclic clefts were successfully reduced to give the corresponding reduced cleft **3** in excess of 70 % yield. HPLC analysis was used to confirm the absolute configuration of the enantiomers of **3** which were shown to be consistent with the absolute configuration of the starting material **2**. Table 8 summarises the yields and *ee* values of the reduced molecular clefts.

Table 8: Summary of the yields and *ee* values of racemic and enantiopure 3.

Entry	Configuration of 3	Yield (%)	*ee* (%)	Melting point (°C)	*Lit*. Melting point (°C)[30]
1	(±)	79	< 5	236.6 – 238.6	225.0
2	(+)	81	> 99	186.2 – 188.2	179.7 – 189.4
3	(-)	72	> 99	184.3 – 185.8	187.9– 188.3

[a] Determined by HPLC analysis on Chiralcel OD-H column, 95:5 hexane : 2-propanol, 0.6 mL min^{-1}, 220 nm detector.

The highest optical purity of **(-)-3** reported by Tatemitsu was 79.8 % *ee*.[30] By comparison these results offer a much higher level of enantiopurity.

2.2.2 Synthesis of Dichloride Carbocyclic Molecular Cleft (±)-114

During Tatemitsu and co-workers exploration into the relationship between structure and optical activity they successfully constructed a library of functionalised carbocyclic cleft molecules derived from the enantiopure dissymmetric diol **(-)-3**.[30] Of particular interest to

this research project in terms of accessing functionalised derivatives of the molecular cleft **2**, was the groups reported synthesis of the dichloride cleft **114**. We envisaged that **114** would provide a handle in which several different functionalities could be installed onto the cleft framework due to the leaving group ability of the chlorine atoms. Based on an adapted literature procedure, treatment of **(±)-3** with an excess of thionyl chloride (45.0 eq), neat under reflux for 24 h gave **(±)-3** in 83 % yield (Scheme 34).
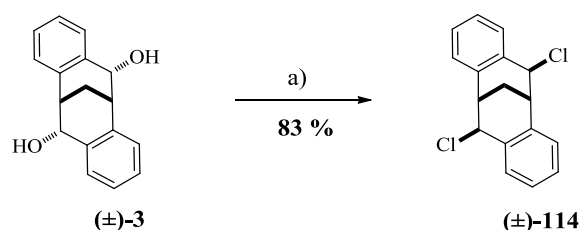
Reagents and conditions: a) SOCl$_2$ (45.0 eq), reflux, 24 h.

Scheme 34: Synthesis of dichloride cleft (±)-114.

A crystal suitable for X-Ray crystallography was isolated and submitted for analysis (Figure 15) (See Appendix 7.1 for crystal data).
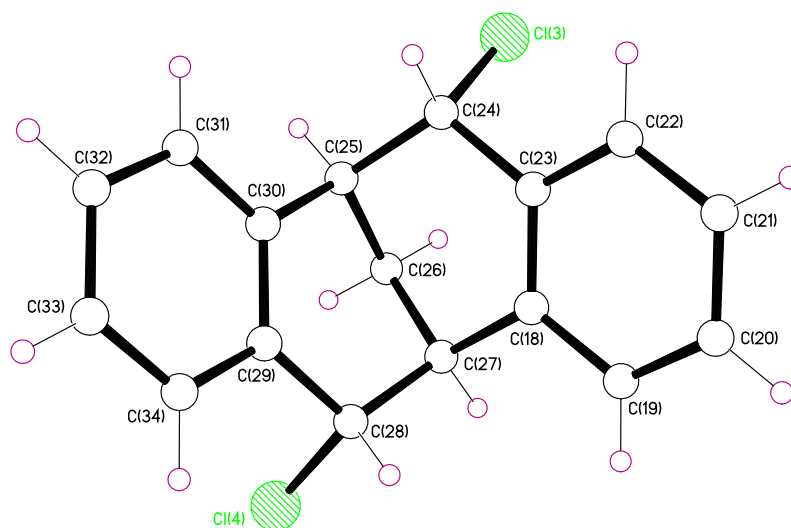
Figure 15: X-Ray crystal structure of (±)-114.

Analysis of the X-Ray crystal structure of **(±)-114** indicates that both chloride atoms are in the pseudo-equatorial position, thus pointing outwards from the chiral cavity. Inversion of the stereochemistry at the reaction centre is characteristic of an S$_N$2 displacement reaction therefore, this arrangement was expected given that installation of the chloride atoms results

from S_N2 displacement of the hydroxyl groups on (±)-**3**. Confirmation of the two pseudo-equatorial chloride atoms in the product (±)-**114** is indicative of two pseudo-axial hydroxyl groups in the starting material (±)-**3**. This supports the structure proposed for **3**, in which we assumed both hydroxyl groups were directed into the cavity of the cleft based on previous reports made in the literature. This product provides no information about the relative facial accessibilities of the bridge carbonyls in **2**, in contrast to the reduced diol **3**, however it does provide supporting evidence to suggest that a nucleophile approaching the electrophilic carbonyl carbons on the cleft will attack from the methanodiazocine bridge side.

Given the reactivity and potential leaving group ability of the chlorine atom, it was proposed that (±)-**114** would allow for the installation of a variety of functional groups with relative ease. Utilisation and functionalisation of (±)-**114** currently remains an unexplored area for our group; however confirmation of the synthetic procedure provides scope for subsequent exploration.

2.2.3   Attempted Synthesis of Pyridine Functionalised Carbocyclic Cleft Derivatives

During a series of preliminary experiments aimed at installing nitrogen containing groups, namely pyridine, directly onto the molecular cleft (±)-**2** we unexpectedly gained access to both the mono-hydroxylated cleft (±)-**123** and diphenyl cleft (±)-**102** (Scheme 35).

(±)-123   **(±)-2**   **(±)-102**
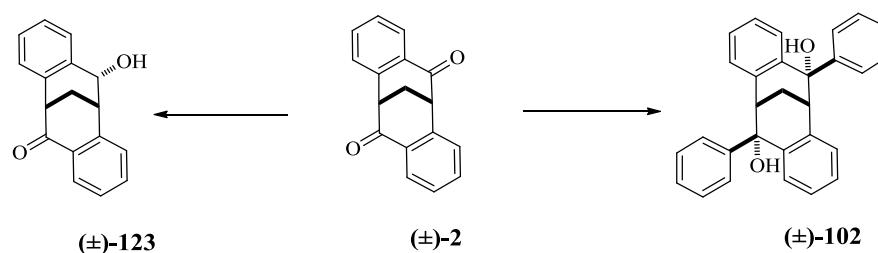
Scheme 35: General pathway for synthesis of (±)-123 and (±)-102 during attempted synthesis of pyridine functionalised clefts.

At the time our work was focused on developing a methodology for the installation of the pyridine group onto the carbocyclic cleft framework, starting from (±)-**2**. Although the Kimber group has previously reported the installation of the pyridyl functional group onto the cleft by diesterification and dietherification to give the dipyridyl esters (±)-**111a-d** and the dialkylated pryridyls (±)-**112a-c** respectively,[39] installation of the pyridine ring directly onto the cleft has yet to be reported. Moreover, we proposed that *m*-CPBA mediated oxidation of

the pyridine groups could give access to highly useful pyridine N-oxide functionalised clefts (Scheme 36).
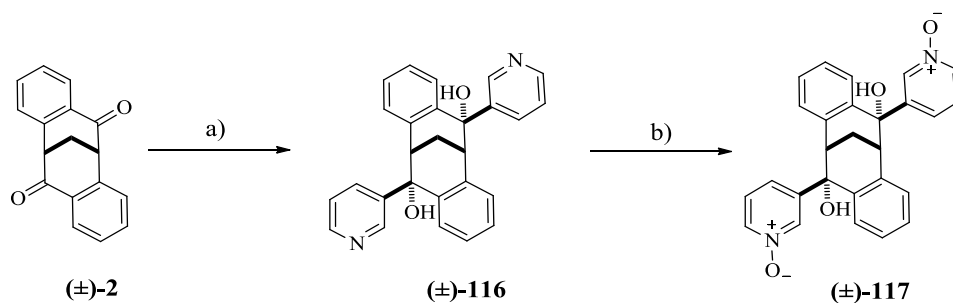
Reagents and Conditions: a) heteroaryl Grignard reagent; b) *m*-CPBA oxidation.

Scheme 36: Proposed synthetic route to the pyridine N-oxide functionalised cleft (±)-117.

During the attempted synthesis of the bis-functionalised 3-substituted-pyridyl cleft **(±)-116** by in-situ Grignard addition the diphenyl molecular cleft **(±)-102** was isolated in 99 % yield (Scheme 37).
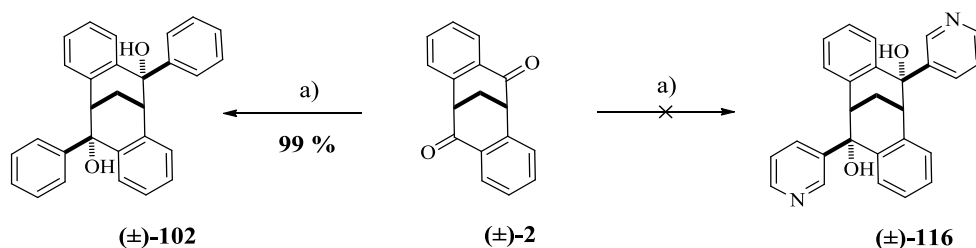
Reagents and Conditions: a) i.3-bromopyridine, PhMgBr (1:1), THF, -40 $^{\circ}$C, 0.5 h; ii. THF, -40 $^{\circ}$C, 1 h, rt, 1 h.

Scheme 37: General scheme for the attempted synthesis of (±)-116.

2.2.3.1 In-situ Synthesis of Hetero-aryl Grignard Reagent

The synthesis of the heterocyclic Grignard reagent **122** was attempted by using an adapted literature procedure initially reported by Knochel and co-workers.[44] According to seminal work reported by the group, a variety of functionalised heterocyclic Grignard reagents can be prepared by using an iodine- or bromine-magnesium exchange reaction for example chloro-4-iodopyridine **118** reacts with *i*-PrMgBr at -40 $^{\circ}$C within 30 min to furnish the magnesium species **119**. The latter species then adds to hexanal, leading to the alcohol **120** in 85 % yield (Scheme 38).[44]

48
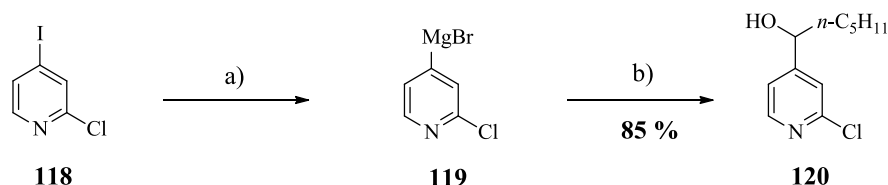
Reagents and Conditions: a) *i*-PrMgBr, -40 °C, 0.5 h, b). *n*-C$_5$H$_{11}$CHO.

Scheme 38: Knochel and co-workers synthesis of the heterocyclic Grignard reagent 119 by an iodine-magnesium exchange reaction.

With this in mind generation of the heterocyclic Grignard reagent 1**22** was attempted by treating commercially available 3-bromopyridine **121** with phenylmagnesium bromide (PhMgBr) at -40 °C for approximately 30 min (Scheme 39).
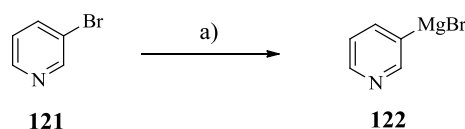
Reagents and Conditions: a) PhMgBr (1:1), THF, -40 °C, 30 min.

Scheme 39: Attempted preparation of heteroaryl Grignard reagent 122 by a bromine-magnesium exchange reaction.

Formation of the Grignard reagent **122** was assumed complete after this time and was added to a solution of (±)-**2** in THF. The reaction was stirred at -40 °C for 1 h, then allowed to reach room temperature over 1 h. Following extraction into ethyl acetate analysis of the isolated product did not indicate formation of the desired cleft (±)-**116** instead the diphenyl cleft (±)-**102** was prepared in excellent yield (Scheme 40).
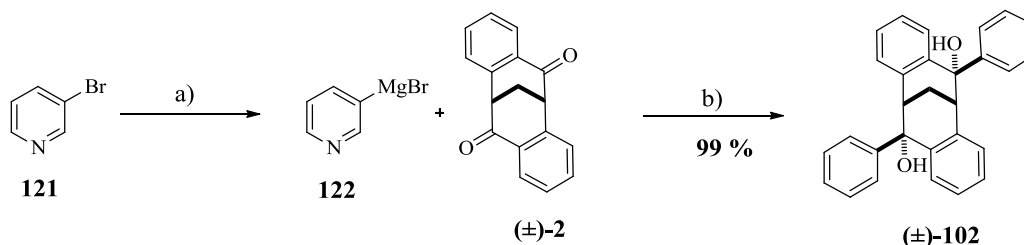
Reagents and conditions: a). PhMgBr (1:1), THF, -40 °C, 30 min; b)THF, -40 °C, 1 h, rt, 1 h.

Scheme 40: Synthesis of diphenyl cleft (±)-102 during the attempted synthesis of (±)-116.

A crystal suitable for X-Ray crystallography was isolated from the purified product and submitted for analysis and the absolute structure of (±)-**102** was reliably determined (Figure 16, see Appendix 7.3 for crystal data).
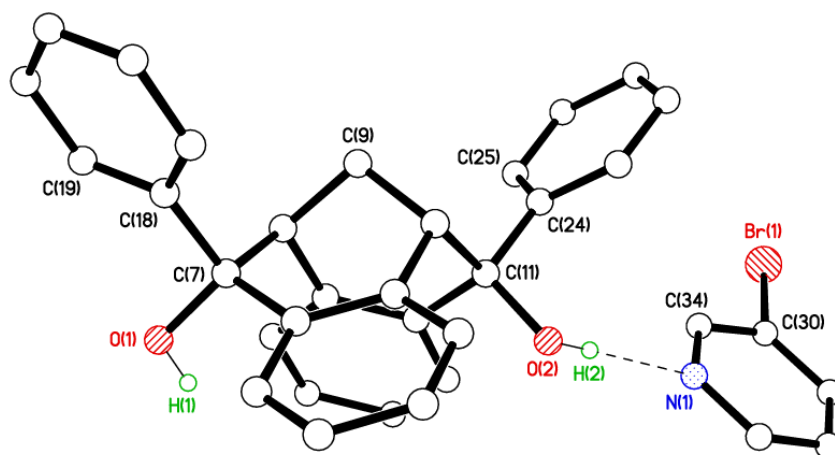
Figure 16: X-Ray crystal structure of diphenyl cleft (±)-102 H-bonded to a molecule of 3-bromopyridine 121.

The X-Ray crystal structure of **(±)-102**, illustrates the rigid cleft shape of the molecule and the position of the two appending phenyl units which are orientated away from the interior of the cleft. The hydroxyl groups are both directed into the cleft cavity thus creating an environment which exhibits the potential to bind substrates via H-bonding within a chiral pocket. This concept has previously been manipulated by Friberg and co-workers whom reported the application of enantiopure **(-)-102** as an asymmetric H–bonding catalyst.[6] Interestingly, the crystal selected for analysis demonstrated the H-bonding abilities of these appending hydroxyl groups. As shown in Figure 16, one of the hydroxyl groups forms an O–H⋯N-H H-bond to a molecule of 3-bromopyridine (Table 9).

Table 9: H-bond geometry between (±)-102 and a molecule of 3-bromopyridine 121.

Entry	Donor	Hydrogen	Acceptor	D—H/Å	H⋯A/Å	D⋯A/Å	D—H⋯A/°
1	O(2)	H(2)	N(1)	0.84	2.07	2.905(3)	174.7

The complex between **(±)-102** and 3-bromopyridine **121** is significant as it demonstrates how these molecules interact with guest species. These clefts have the potential to form H-bond interactions with H-bond acceptor groups via one of several different modes of binding. These include; through a single H-bond, through double H-bond interactions, cooperative H-bonding or through C–H⋯π H-bond interactions. These H-bonding models are further discussed in Chapter 3. Figure 16, clearly shows binding through a single H-bond interaction

which may be attributed to the relative cleft dimensions and distance between H-bonding groups.

2.2.4 Synthesis of Diphenyl Carbocyclic Cleft (±)-102

Formation of (±)-102 in the above reaction is likely to have occurred, because the bromine-magnesium exchange between 3-bromopyridine 121 and PhMgBr did not produce the target pyridyl Grignard reagent 122 (Scheme 39). This could be due to the electronic nature of the heterocycle influencing the rate of the halogen-magnesium exchange reaction. Consequently an excess of PhMgBr was available to react with the carbonyl groups on (±)-2 resulting in the formation of (±)-102 rather than the target compound (±)-116 (Scheme 37). The reaction of PhMgBr directly with (±)-2 to give (±)-102 was in fact reported by Friberg and co-workers. A general procedure involving the reaction of (-)-2 directly with an excess of Grignard or organolithium reagent in dry THF at room temperature for 2 h was reported by the group to give access to several C_2-symmetric diols (See Scheme 25, Chapter 1).[6] Using these reaction conditions we were able to synthesis the diphenyl cleft (±)-102 in 96 % yield (Scheme 41).
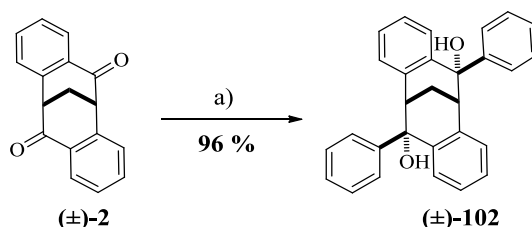
Reagents and conditions: a) PhMgBr, THF, 0 °C- rt, 16 h.

Scheme 41: Synthesis of diphenyl cleft (±)-102 using the procedure reported by Friberg and co-workers.

Not only did this procedure allow us to reliably synthesise (±)-102 it also helped us to explain why it was isolated as the major product during the attempted synthesis of (±)-116 via the procedure mentioned above. The availability of (±)-102 was important during our own investigation into the use of functionalised derivatives of the carbocyclic cleft as asymmetric H-bond catalysts in the HDA reaction (Chapter 3).

2.2.5 Synthesis of the mono-hydroxylated Carbocyclic Cleft (±)-123

In a subsequent attempt to synthesis the substituted dipyridyl molecular cleft (±)-116 the mono-hydroxylated molecular cleft (±)-123 was unexpectedly isolated (Scheme 42).
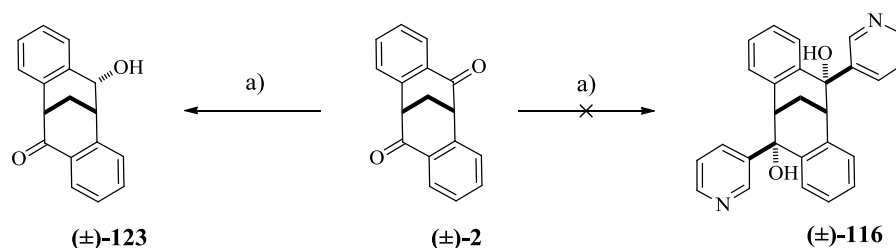
Reagents and Conditions: a) i. *i*-PrMgBr, LiCl (1:1), THF, rt, 1 h, ii. (±)-**2**, THF, rt, 18 h.

Scheme 42: Summary of reaction outcomes during the attempted synthesis of (±)-116.

Due to the failed attempt at synthesising the reactive pyridyl Grignard reagent **122** via a bromine-magnesium exchange reaction between 3-bromopyridine **121** and PhMgBr (Scheme 39), an alternative method to access reactive pyridyl Grignard reagents was explored. While halogen-metal exchange reactions are among the most common methods for the preparation of organometallic reagents such as **122**, limitations occur due to the low reactivity of organo-magnesium reagents which means that sometimes competing reactions can occur. In recent years Knochel and co-workers have discovered that the use of salt additives can increase both the rate and efficiency of this type of reaction. After some optimisation it was found that the most effective reagent can be generated from isopropylmagnesium chloride (*i*-PrMgCl) and 1.0 eq of lithium chloride to give the new reagent *i*-PrMgCl.LiCl. Using this reagent the group demonstrated that it is possible to convert a variety of functionalised and highly sensitive substrates to their corresponding functionalised organometallic reagent, including both aryl- and heteroaryl magnesium derivatives.[45]

With this in mind we attempted to synthesise the heteroaryl magnesium reagent **124** by first generating the reactive salt *i*-PrMgCl.LiCl by addition of a solution of *i*-PrMgCl in THF to LiCl (1:1). The resulting *i*-PrMgCl.LiCl solution was then added slowly over a period of 30 min to the stirred solution of 3-bromopyridine **121**. The resulting reaction mixture was then stirred at room temperature for 1 h. Formation of the heterocyclic Grignard reagent **124** was assumed complete upon an observed colour change (Scheme 43).
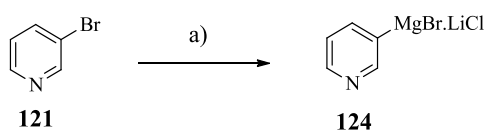
Reagents and conditions: a). *i*-PrMgBr, LiCl (1:1), THF, rt, 1 h.

Scheme 43: Attempted in-situ synthesis of hetero-aryl Grignard reagent 124.

52

Unfortunately when (±)-2 was treated with a solution of 124 at room temperature for 18 h in THF, the target molecular cleft (±)-116 was not generated, instead the mono-hydroxylated cleft (±)-123 was isolated in 13 % yield (Scheme 44).
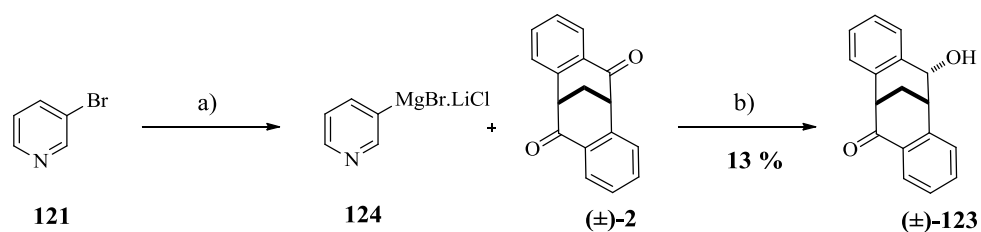
Reagents and conditions: a) *i*-PrMgBr, LiCl (1:1), THF, rt, 1 h; b) THF, rt, 18 h.
Scheme 44: Synthesis of mono-hydroxyated cleft (±)-123.

A viable explanation for this outcome is that formation of the pyridyl magnesium reagent 124 was incomplete, meaning that when (±)-2 in THF was added to the solution of 124, unreacted *i*-PrMgCl was able to react with the electrophilic carbonyls on (±)-2. However, due to the bulky nature of the isopropyl group it is possible that attack by the nucleophilic carbon on *i*-PrMgCl was blocked by steric restraints. Instead it is possible that a hydride from *i*-PrMgCl attacked one of the carbonyl groups on (±)-2 to give the reduced product (±)-123. This mechanism is completely speculative; it does not explain why only one of the carbonyl groups was reduced, moreover it can be expected that a more general set of reaction conditions can be used to access the mono-hydroxylated derivative (±)-123, for instance by using fewer equivalents of sodium borohydride in the reduction of (±)-2. Although this procedure gave access to the novel carbocyclic cleft (±)-123, further exploration into the repeatability of this procedure was not carried out as it was not considered to be of any significance to this particular project

Proton NMR spectroscopy was used to characterise (±)-123. A break in the symmetry of the molecule was evidenced by two singlet peaks occurring at δ 3.84 and 3.62 ppm representing the two C–H groups of the cleft carbocycle. Similarly the bridge head CH_2 protons, which normally occur as a single triplet peak in the region of δ 2.36 ppm in the C_2-symmetrical diol (±)-3, was split into two doublet of triplets at δ 2.76 and 2.52 ppm. Moreover, the carbon NMR spectra of (±)-123 showed a carbonyl peak at δ 197.26 ppm and a C–H peak at δ 70.09 ppm correlating to the reduction of only one of the carbonyl groups on the cleft framework.

A crystal suitable for X-Ray crystallography was isolated and submitted for analysis. Full characterisation of the crystal structure confirmed formation of the mono-hydroxylated product **(±)-123** thus providing further evidence to support the NMR spectral data (Figure 17, see Appendix 7.2 for crystal data).
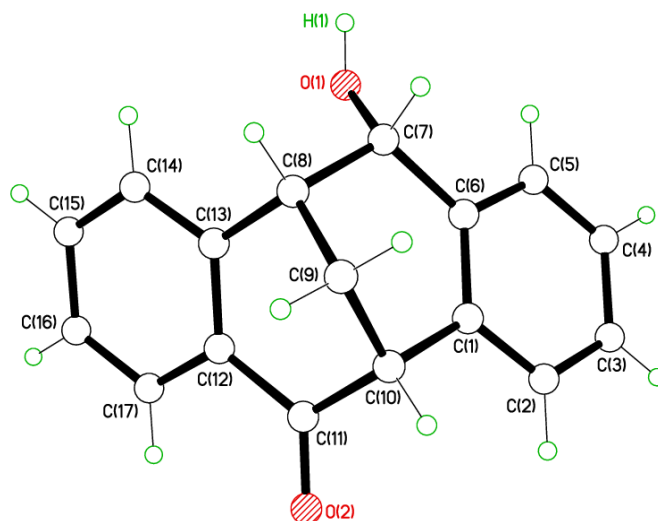
Figure 17: X-Ray crystal structure of mono-hydroxylated molecular cleft (±)-123.

The crystal structure of **(±)-123** was found to contain one molecule in the asymmetric unit. Like in **(±)-3**, the reduced hydroxyl group was directed into the cavity of the cleft. In addition, packing plots revealed that groups of symmetry related molecules formed six-membered H-bonded chair shaped rings via the OH groups (Figure 18, Table 10).

Table 10 summarises the H-bond geometry of these complexes.

Entry	Donor	Hydrogen	Acceptor	D—H/Å	H⋯A/Å	D⋯A/Å	D—H⋯A/°
1	O(1)	H(1)	O(1)[i]	0.84	1.80	2.6401(12)	175.5
Symmetry operations for equivalent atoms: (i) y−1/3,−x+y+1/3,−z+1/3							
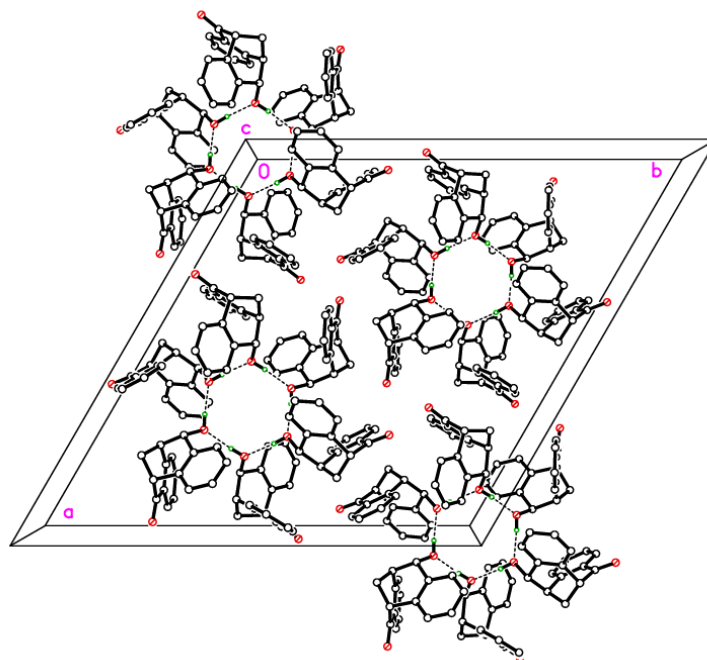
Figure 18: The H-bond network in the crystal structure of (±)-123. Symmetry related molecules form six-membered H-bonded rings via the OH groups.

2.3   Amino-thiocarbamate Functionalised Carbocyclic Clefts

The installation of a sulphur Lewis base group (a thiocarbamate) and an amine H-bond donor group onto the rigid carbocyclic cleft framework to give an amino-thiocarbamate bifunctional cleft catalyst was investigated for the first time (Scheme 45).

125   **3**   **126**
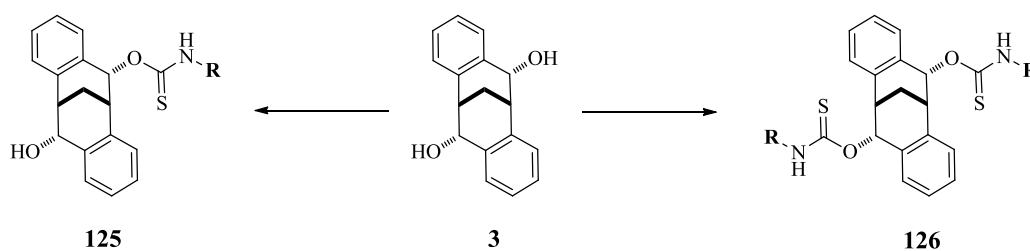
Scheme 45: General structure of the novel amino-thiocarbamate clefts accessible from the reduced carbocyclic cleft 3.

The overall aim was to develop this type of system and produce highly active, enantioselective organocatalysts that can be used to catalyse a range of asymmetric organic transformations. This approach is extremely attractive as these types of catalysts can be easily prepared over one-step starting from **3**. Moreover, the range of commercially available isothiocyanates as coupling partners to **3** is large and varied therefore these catalysts can be

easily modified, thus altering the steric and electronic properties of the clefts, a process which can be vital for activity and selectivity.

Herein the synthesis, characterisation and complex X-Ray structures of functionalised carbocyclic cleft derivatives containing this versatile amino-thiocarbamate group are reported. Synthesis of these novel amino-thiocarbamate cleft molecules was explored and optimised using racemic (±)-3 and where possible chiral host-guest interactions were translated into the realm of catalytic asymmetric synthesis using the enantiomerically enriched amino-thiocarbamate clefts, which shall be explored in detail Chapter 4.

2.3.1   Catalyst Design Rationale

In recent years it has been reported that molecules capable of selectively binding substrate molecules within a chiral pocket, are excellent mediators for enantioselective synthesis due to their ability to form highly ordered transition states (Figure 19).[46,47]
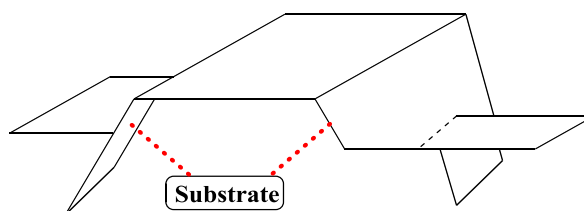
Figure 19: Schematic representation of substrate binding within a chiral pocket to form a highly order transition states.

Substrate activation by non-covalent interactions such as small-molecule chiral H-bond donors has emerged as an important paradigm for enantioselective catalysis and therefore for the preparation of valuable chiral molecules.[46] Indeed asymmetric reactions controlled by chiral H-bond catalysts are reminiscent of enzyme catalysed reactions found in nature where chirality transfer from enzymes allows for the synthesis of enantiomerically pure biological compounds.[48] In an attempt to mimic nature, organic chemists have designed chiral catalysts that exploit H-bonds to promote highly enantioselective transformations.

Inspired by the number of elegant reports emerging from the use of amino-thiocarbamate catalysts as asymmetric controllers in enantioselective reactions, which provide access to a number of valuable molecules with practical levels of enantioselectivity[43,49,50] (See Chapter 4), we decided to explore the possibility of installing this functionality onto our chiral cleft framework. We proposed that introduction of the

amino-thiocarbamate group at the carbonyl positions would create a chiral pocket whereby two amino-thiocarbamate groups are directed into the cavity of the molecular cleft creating an enantioenriched environment for the binding of target substrates (Figure 20).
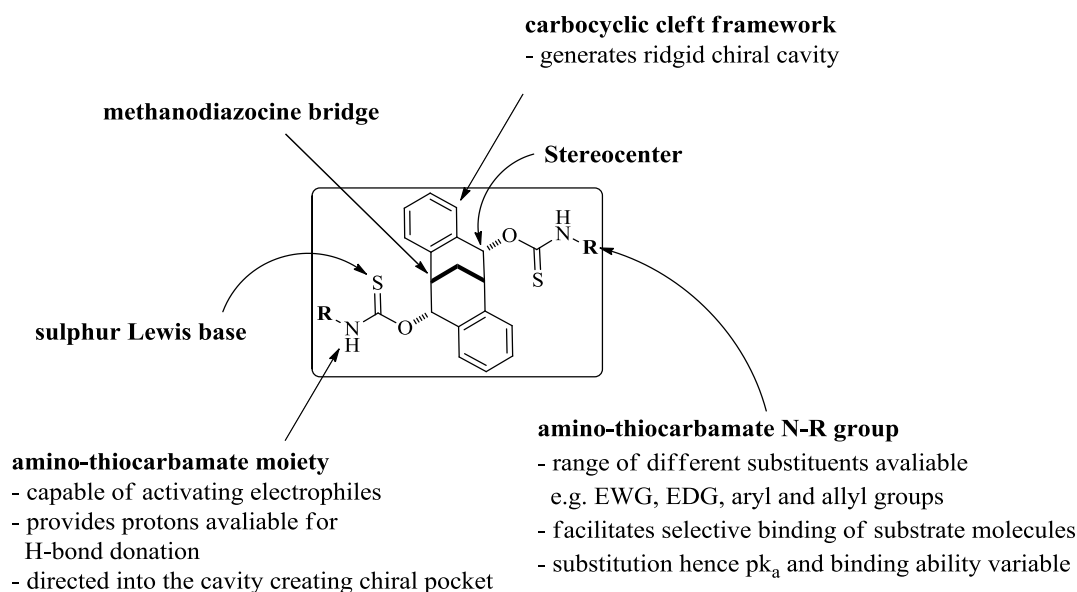
Figure 20: Design rationale for amino-thiocarbamate-substituted carbocyclic cleft catalysts.

This catalyst design displays two potential modes of binding through H-bond interactions these include through C–H···π interactions originating from the aromatic rings on the cleft nucleus and secondly through the potential thiocarbamate N–H H-bond donor groups. In fact the thiocarbamate N–H groups offer two separate modes of binding / activation: single H-bond donation (**A**) and double H-bond donation (**B**) (Figure 21).
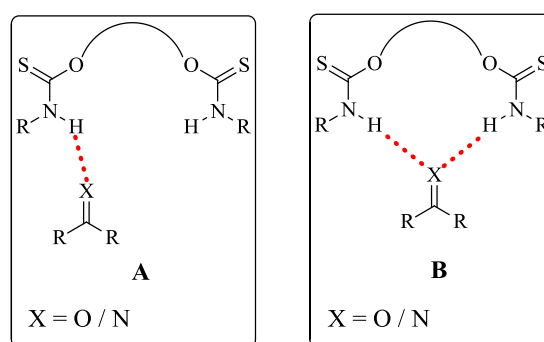
Figure 21: Modes of bonding / electrophile activation by H-bonding: (A) single H-bond donation and (B) double H-bond donation.

In addition to binding to target molecules to generate rigid catalyst-substrate transition states, this catalyst design presents two complementary modes of substrate activation facilitated by

the amino-thiocarbamate groups. Firstly the N–H group can be used to activate electrophiles such as carbonyl compounds and imines towards nucleophilic attack via H-bonding to their lone pairs of electrons which in turn, decreases the energy gap between the lowest unoccupied molecular orbital (LUMO) of the electrophile and the highest occupied molecular orbital (HOMO) of the nucleophile, thus facilitating the reaction between the two reacting partners. Secondly, the sulphur Lewis base can be used to activate a Lewis acid such as a halogen atom for halolactonisation reactions.[49] The idea that Lewis base activated systems could be effective in the activation of heteroatoms for electrophilic lactonisation reactions was initially proposed by Denmark and co-workers.[51] It has been further exemplified using the sulphur Lewis base system **127** (Figure 22) by Yeung's group for halogen activation for bromolactonisation reactions (See Chapter 4).[43]

127
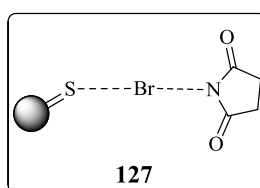
Figure 22: Proposed Lewis acid activation of halogens for lactonisation reactions.

2.3.2   Asymmetric Induction Potential of Functionalised Cleft Catalysts

The chiral cavity in these cleft molecules results from the blocked configuration of the stereogenic amino-thiocarbamate groups which are held in position by the methylene bridge (Figure 20). The binding of substrates in this chiral pocket within the catalyst in such a way that favours one trajectory of the reaction more than the other, thus producing an excess of one enantiomer is the mechanism in which we envisioned these molecules could undertake to be efficient asymmetric catalysts (Figure 23).

Top face hindered

chiral pocket

X

R¹ R²

Bottom face more accessible
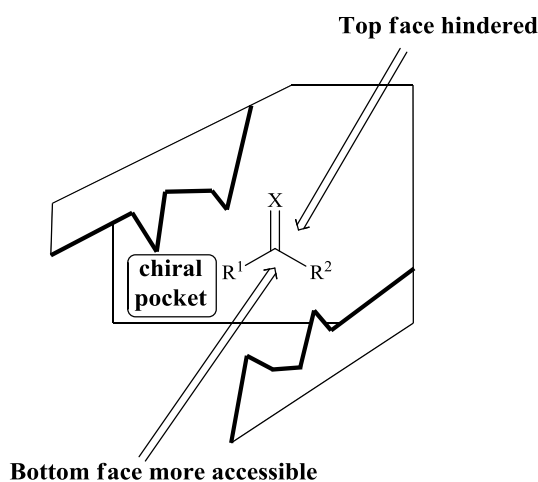
Figure 23: Schematic model illustrating possible asymmetric induction by inclusion in chiral pocket generated by the molecular cleft framework.

2.3.3 Synthesis of Amino-thiocarbamate Functionalised Carbocyclic Clefts

Using a procedure initially reported by Yeung and co-workers for the synthesis of amino-thiocarbamate derived cinchona alkaloid catalysts,[43] treatment of (±)-**3** with a substituted isothiocyanate in the presence of sodium hydride in anhydrous THF at room temperature for 18 h allowed for the synthesis of a range of symmetrically functionalised amino-thiocarbamate cleft derivatives. Under these reaction conditions we were able to isolate purify and characterise a range of racemic disubstituted aryl amino-thiocarbamate clefts including the *p*-tolyl amino-thiocarbamate cleft (±)-**4**, the phenyl amino-thiocarbamate (±)-**5**, and the electron deficient 3,5-*bis*(trifluoromethyl)phenyl amino-thiocarbamate cleft (±)-**6**. In addition to aryl substituted amino-thiocarbamate clefts we also successfully synthesised several allyl functionalised amino-thiocarbamate clefts including the methyl amino-thiocarbamate (±)-**7**, the bulky butyl amino-thiocarbamate (±)-**8** and the allyl amino-thiocarbamate (±)-**9** (Scheme 46). The presence of the alkene group on (±)-**9** lends itself for subsequent functionalisation; the potential for polymerisation is particular attractive.

(±)-**4:** R = PhMe   **70 %**
(±)-**5:** R = Ph   **57 %**
(±)-**6:** R = Ph(CF₃)₂   **44 %**
(±)-**7:** R = Me   **75 %**
(±)-**8:** R = Butyl   **20 %**
(±)-**9:** R = Allyl   **68 %**

(±)-**3**
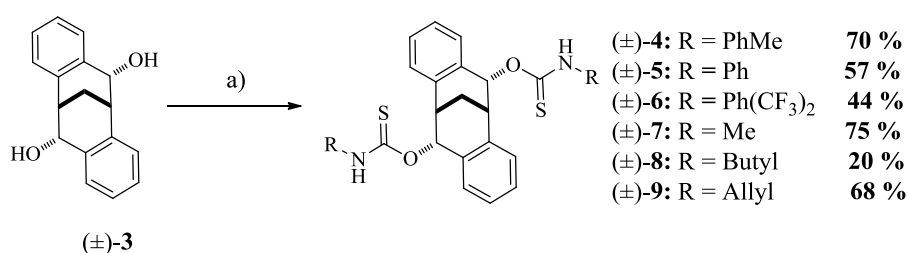
Reagents and Conditions: a) R-NCS, NaH (4.0 eq), THF, rt, 18 h.

Scheme 46: Synthesis of C₂-symmetrical amino-thiocarbamate cleft derivatives.

The isolated compounds were purified by silica column chromatography and recrystallized when necessary from acetonitrile to give the functionalised clefts in moderate yields. By reducing the number of equivalents of sodium hydride and coupling with stoichiometric amounts of the desired isothiocyanate, we were able to isolate the mono-substituted *p*-tolyl amino-thiocarbamate molecular cleft **(±)-128** in 68 % yield (Scheme 47).

(±)-3   (±)-128
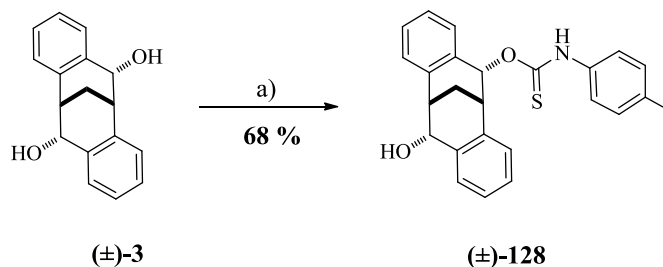
Reagents and Conditions a) NaH (1.0 eq), PhMeNCS (1.0 eq), THF, rt, 18 h.
Scheme 47: Synthesis of mono *p*-tolyl amino-thiocarbamate cleft (±)-128.

Although yields were moderate reaction conditions were mild and the degree of functionalisation could be controlled with relative ease allowing for the selective synthesis of mono and disubstituted clefts.

2.3.3.1 Synthesis of Enantiopure Amino-thiocarbamate Functionalised Carbocyclic Clefts

Once the novel racemic amino-thiocarbamate molecular clefts had been fully characterised, we used the reaction conditions reported above to synthesise the corresponding enantiopure amino-thiocarbamate clefts. The enantiopure molecular cleft **3** with > 96 % *ee* was used in the synthesis of chiral amino-thiocarbamate clefts. It was assumed that the enantiopurity of the precursor **3** was translated with neglible loss of *ee* into the product amino-thiocarbamate functionalised clefts. Where possible the optical activity (α_D) of the synthesised chiral clefts were measured and recorded. The yield, *ee* of the parent diol **3** (assumed *ee* of amino-thiocarbamate clefts) and the optical activity (α_D) of the synthesised chiral molecular clefts are summarised in Table 11.

Table 11: Summary of the *ee* values of the precursor cleft 3, yield (%) and optical activity (α_D) of the amino-thiocarbamate clefts.

(+)/(-)-3   (+)/(-)
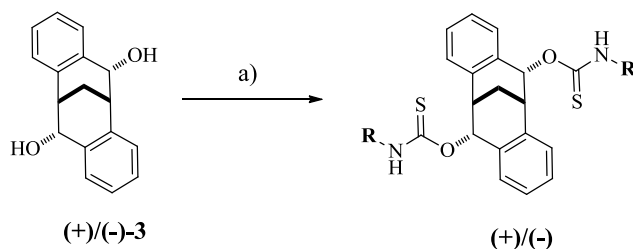
Reagents and conditions: a) NaH (4.0 eq), RNCS, THF, rt, 18 h.

Entry	Cleft	R	Enantiomer configuration	Yield (%)	$\alpha_D{}^a$	*ee* of (+)/(-)-3[b]
1	**4**	PhMe	(-)	10	-152.8	99.6
2	**4**	PhMe	(+)	12	174.3	91.8
3	**5**	Ph	(-)	56	-156.0	99.6
4	**5**	Ph	(+)	6	156.8	91.8
5	**6**	Ph(CF$_3$)$_2$	(-)	35	-145.6	99.6
6	**6**	Ph(CF$_3$)$_2$	(+)	41	127.6	91.8
7	**7**	Me	(+)	56	10.4	91.8
8	**8**	Butyl	(+)	49	4.58	91.8

[a] *c*. 1.0, CHCl$_3$.

[b] *ee* values of isolated amino-thiocarbamate cleft assumed to be same as precursor **3** determined by HPLC.

^{1}H NMR and ^{13}C NMR spectroscopy, MS, IR, melting point analysis, and where possible X-Ray crystallography was used to fully characterise the isolated compounds. Details with regards to the characterisation of these complex molecules shall now be discussed.

2.4 Characterising the Amino-thiocarbamate Carbocyclic Clefts

In general characterisation of the functionalised molecular clefts was met with some difficulty due to the often broad nature of the NMR spectra. Where possible complex NMR experiments were performed, however, access to these services was limited throughout this project therefore the data collected may necessitate review and more in-depth analysis.

2.4.1 NMR Spectral Analysis

Before the NMR spectra of the novel amino-thiocarbamate clefts could be assigned it was important that the structure of the precursor diol **3** was fully understood to allow for a direct comparison between the starting material and isolated product to be made. Table 12 summarises the characteristic peaks in the ^{1}H NMR spectrum of **(±)-3**.

Table 12: Summary of ^{1}H NMR spectra of (±)-3.

(±)-3
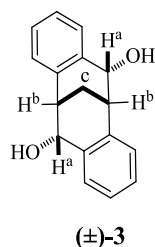
Entry	Protons	Group	Chemical shift δ (ppm)[a]	Splitting pattern	J coupling (Hz)
1	a	C–H	5.09	dd	5.6, 12.0
2	b	C–H	3.37	dt	2.4
3	c	CH_2	2.46	t	3.2
4	Aromatics	Ar–H	7.59	d	7.2
			7.31 – 7.21	m	N/A

[a] Peaks integrate to two hydrogens.

It was anticipated that the triplet peak at δ 2.46 ppm corresponding to the methylene CH_2 bridgehead protons (c) (Table 12, entry 3) and the doublet of triplets at δ 3.37 ppm relating to the C–H protons (b) at the apex of the cleft (Table 12, entry 2) would remain almost constant in the spectra of the functionalised clefts unless the C_2 symmetry of the molecule was broken, therefore these peaks provided a reliable reference point when assigning the spectra of the amino-thiocarbamate functionalised clefts.

Whilst the ^{1}H NMR spectrum of the C_2 symmetric diol **(±)-3** was relatively straight forward to assign, with sharp peaks, distinct splitting patterns and clear integrations the spectra obtained for the novel amino-thiocarbamate clefts were significantly more complex. The spectra obtained for and amino-thiocarbamate clefts were very broad making it difficult to assign the spectrum with confidence. A possible explanation for the broadness of the peaks, in particular in the aromatic region results from the potential existence of more than

one species in the sample. It is possible that there is a degree of rotational exchange in the molecules therefore each of the cleft molecules potentially exists as a mixture of rotatomers. Given the limited understanding of the orientation and flexibility of the appending amino-thiocarbamate groups it is only possible to surmise that rotation about the single C–O bonds gives rise to conformational isomers thus resulting in broadening of the NMR peaks (Figure 24).

(±)-4
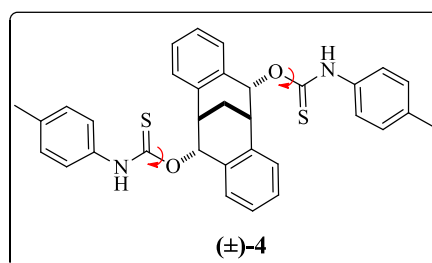
Figure 24: Proposed rotational exchange of the amino-thiocarbamate groups attached to the cleft framework giving rise to conformational isomers and broadening of the ^{1}H NMR spectra.

The ^{1}H NMR spectrum and ^{1}H-^{1}H COSY of the mono-*p*-tolyl amino-thiocarbamate cleft (±)-127 provided some important information which allowed for some discrepancies in the spectra of the disubstituted clefts to be understood (See Appendix 7.19 for COSY). For example, the COSY of (±)-127 showed that proton $\mathbf{H^a}$ had unexpectedly shifted to the aromatic region of the spectra, appearing as a multiplet at δ 6.93 – 6.92 ppm (Figure 25).

(±)-127
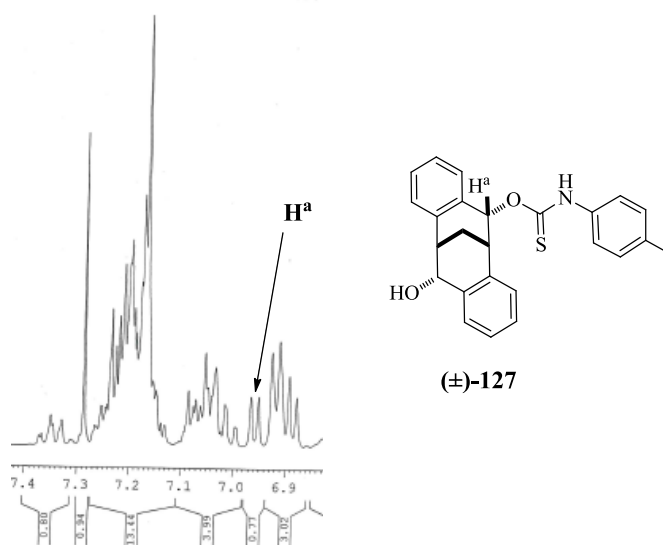
Figure 25: Aromatic region of ^{1}H NMR spectra of (±)-127 showing the $\mathbf{H^a}$ proton in the aromatic region as identified by HMQC couplings.

Selective irradiation of the multiplet at δ 6.93 – 6.92 ppm allowed couplings from this proton to be followed to neighbouring mulitplets which lead to this peak being assigned to the **H^a** proton. This proton was assumed 'missing' on initial inspection of the spectrum of (±)-**127**. It is not fully understood at this stage why this proton shift in the NMR spectra occurs however, these observations proved to be useful in the assignment of the ^{1}H NMR spectra of the disubstituted clefts where peaks corresponding to these C–H protons appeared to be 'missing'. In most cases the broad nature of proton spectrum meant that these peaks where masked by the aromatic protons thus preventing them from being formally identified however it was assumed that they were present in this region unless their presence was evidenced elsewhere in the spectra.

In an attempt to simplify the NMR spectra and gain a more comprehensive understanding of the structure of the amino-thiocarbamate clefts, more in-depth spectral analysis was required thus where possible variable temperature NMR experiments were performed. In addition HMQC and COSY were used to assist in the assignment of the ^{1}H and ^{13}C NMR spectra. VT NMR experiments were performed on clefts (±)-**4 - 7**, thus ^{1}H NMR spectra of the clefts were acquired at several different temperatures starting from +25 ^{o}C (which was taken as room temperature) all the way down to -40 ^{o}C at 10 ^{o}C intervals. Unfortunately, these experiments provided no additional information consequently it remained a challenge to fully assign the spectra with confidence. As a result the NMR spectrums of the clefts were assigned as a mixture of rotamers. The VT-NMR experiments proved the complex nature of these systems. It can be expected that more in-depth analysis would allow for a better understanding of these cleft structures. Where possible elemental analysis and X-Ray crystallography was used to fully characterise and determine the absolute structure of the isolated clefts.

2.4.2 X-Ray Crystallographic Analysis

Crystals suitable for analysis were obtained for racemic clefts (±)-**4**, **5**, **6** and **7**, and enantiopure (+)-**4**, for which the absolute structure was reliably determined. Due to small crystal dimensions three data sets (+)-**4**, (±)-**6** and (±)-**7** were collected using the synchrotron radiation at the Advanced Light Source (ALS).

2.4.2.1 X-Ray Crystal Structure of Phenyl Amino-thiocarbamate Cleft (±)-5

The crystal structure of the racemic phenyl-amino-thiocarbamate cleft **(±)-5** shown in Figure 26, illustrates the rigid cleft framework and the position of the two appending phenyl-amino-thiocarbamate units which are orientated towards the interior of the cleft. Interestingly the sulphur and thiocarbamate N–H groups are pointing outwards away from the cleft cavity such that only the aromatic phenyl groups are directed inwards towards the cleft.
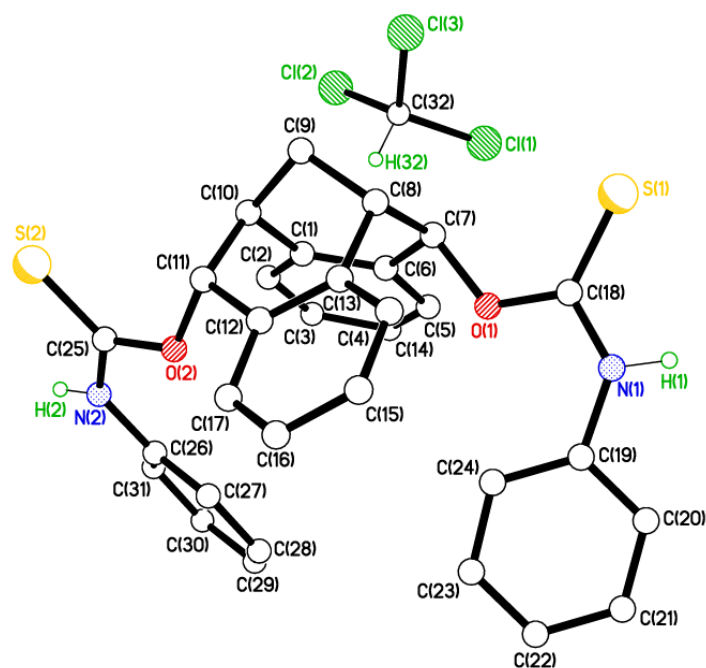
Figure 26: X-Ray crystal structure of racemic phenyl-amino-thiocarbamate cleft (±)-5.

The crystal structure of **(±)-5** was found to contain one crystallographically independent molecule of **(±)-5** and one disordered molecule of chloroform. The chloroform solvate molecule resides outside the cleft and is bound via a weak C–H···π interaction with the C(1) > C(6) ring; H···ring centroid = 2.42 Å (Figure 27).
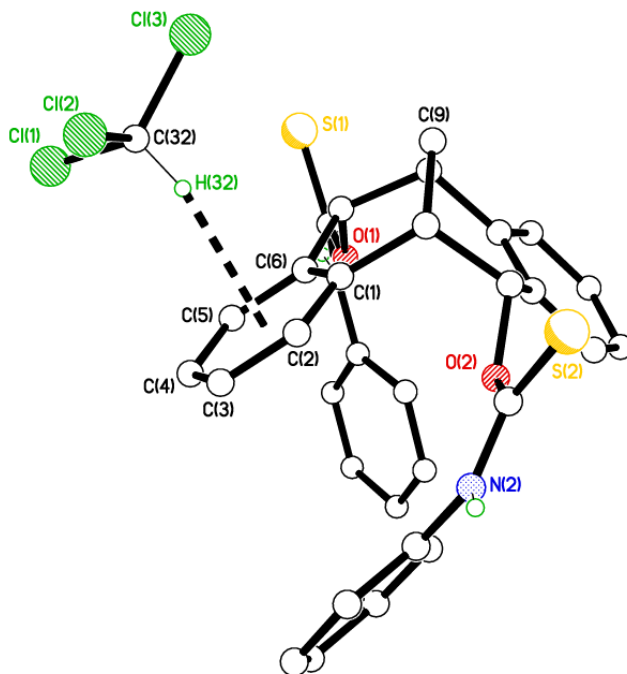
Figure 27: Chloroform solvate molecule bound to (±)-5 via C–H···π H-bonding interactions. Minor chloroform disorder omitted for clarity.

Molecules of **(±)-5** were shown to interact with each other according to the packing plot shown in Figure 28.
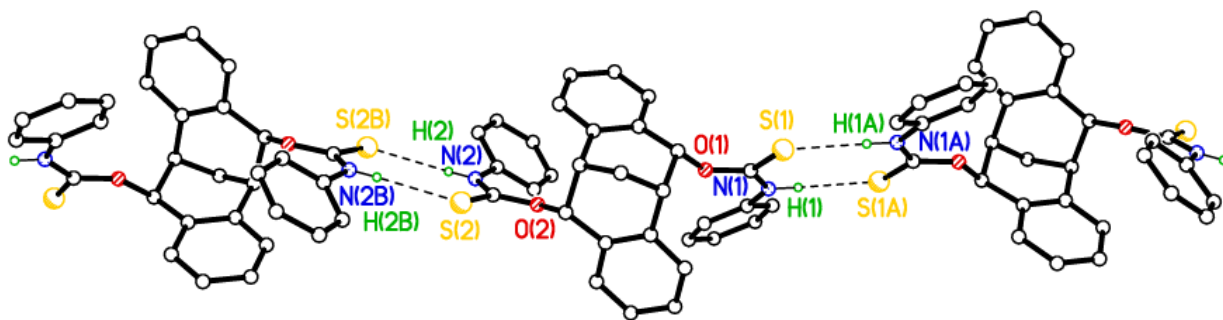
Figure 28: The H-bonded network in the crystal structure of (±)-5.

Thus, molecules of **(±)-5** are linked together in an oligomeric H-bonded network with amino-thiocarbamate groups forming pairs of centro-symmetric N–H···S H-bond interactions to neighbouring molecules (Table 13).

Table 13: H-bond geometry for H-bonded network in crystal structure of (±)-5.

Entry	Donor	Hydrogen	Acceptor	D—H/Å	H···A/Å	D···A/Å	D—H···A/°
1	N(1)	H(1)	S(1)^{i}	0.88 (2)	2.50 (2)	3.3623 (14)	167 (2)
2	N(2)	H(2)	S(2)^{ii}	0.82 (2)	2.55 (2)	3.3610 (12)	170 (2)

Symmetry codes: (i) -*x*+1, -*y*+1, -*z*; (ii) -*x*, -*y*, -*z*+1.

2.4.2.2 X-Ray Crystal Structure of *p*-tolyl Amino-thiocarbamate Cleft (+)-4

Due to small crystal dimensions this data set was also collected using synchrotron radiation at the ALS. The X-Ray crystal structure of the (+) enantiomer of the *p*-tolyl-amino-thiocarbamate cleft **(+)-4**, shows that the substituted amino-thiocarbamate groups are also directed into the cavity of the cleft bicycle with the thiocarbamate sulphur and N–H groups pointing outwards away from the centre of the cavity (Figure 29).
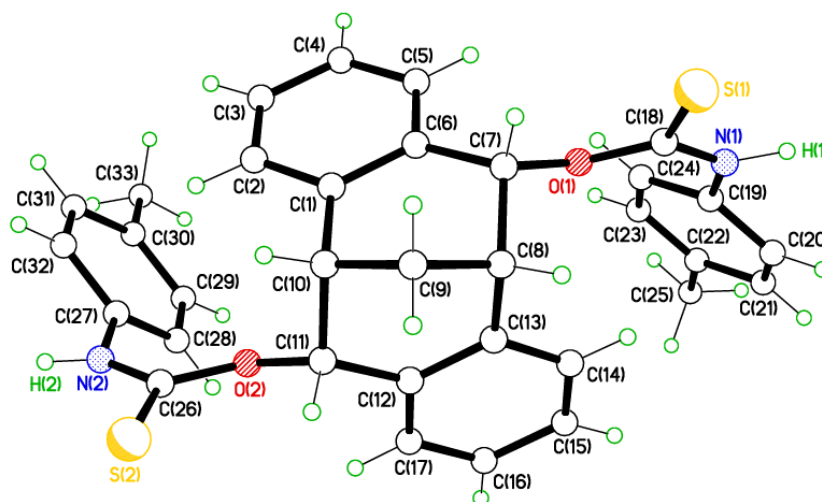
Figure 29: X-Ray crystal structure of (+)-4.

Molecules of **(+)-4** were bound to each other by a very similar H-bonding network as displayed in the crystal structure of **(±)-5** (Figure 28). Thus molecules are linked together via pairs of centro-symmetric N–H···S H-bonds forming chains of molecules (Figure 30, Table 14).
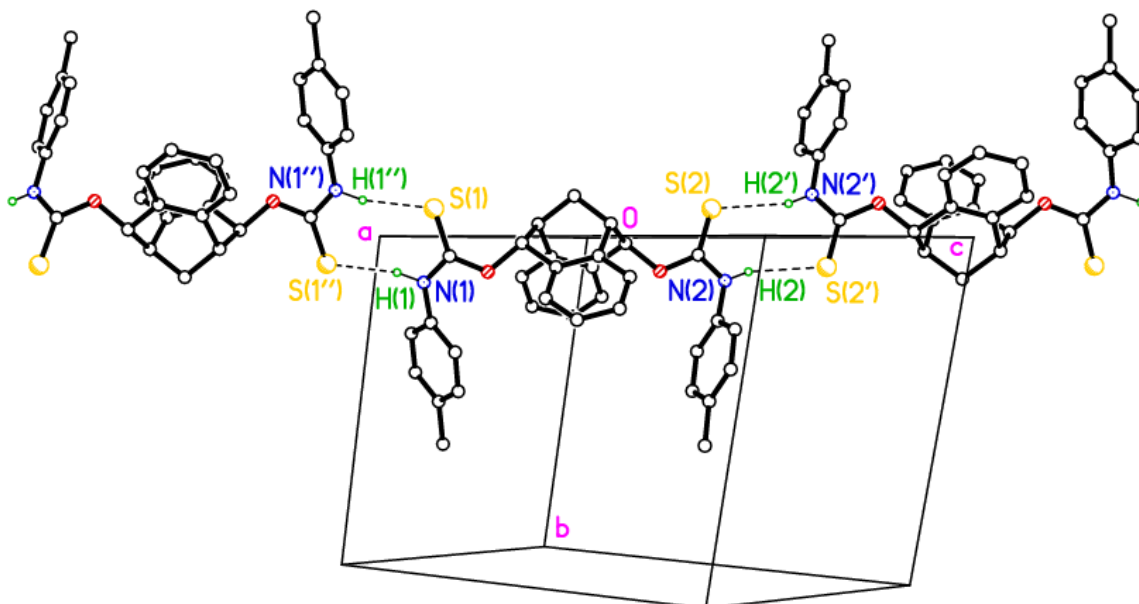
Entry	Donor	Hydrogen	Acceptor	D—H/Å	H···A/Å	D···A/Å	D—H···A/°
1	N(1)	H(1)	S(1)[i]	0.89 (3)	2.43 (3)	3.3029 (17)	166 (2)
2	N(2)	H(2)	S(2)[ii]	0.88 (3)	2.45 (3)	3.3189 (16)	166 (2)

Symmetry codes: (i) -*x*+2, -*y*, -*z*; (ii) -*x*, -*y*, -*z*+1.

Figure 30: The H-bond network between molecules of (+)-4. Table 14 summaries the H-bond geometry displayed by this H-bonding network.

The packing plot in Figure 31 illustrates how these chains of H-bonded molecules interact with each other to form stacks of molecules within a unit cell. The terminal tolyl group containing C(33) from one chain penetrates into the cavity of a molecule in the next chain 'above / below' such that the tolyl group containing C(25) (See Figure 29 for atom numbering) lies between the molecules.

This is not the first time that this packing pattern, which is illustrated schematically in Figure 32, has been observed for functionalised cleft molecules derived from the carbocyclic cleft **2**.
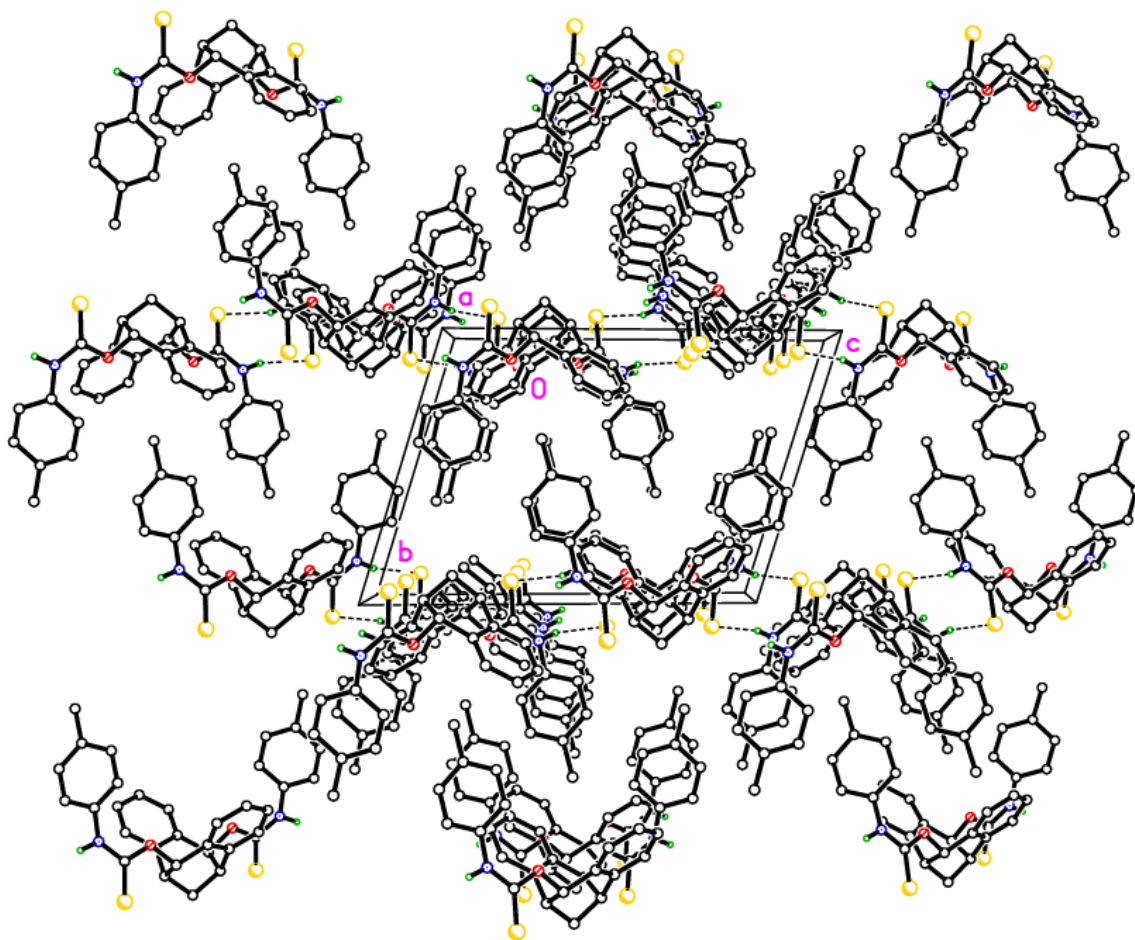
Figure 31: Packing plot and H-bond network in (+)-4.

A
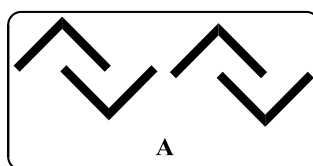
Figure 32: Motif for the 'above/below' molecular cleft packing pattern (A) displayed by molecules of (+)-4.

Interestingly analogous cleft molecules reported to exhibit this 'above/below' packing pattern (**A**) have also been shown to display very similar interplanar dihedral /"cleft" angles (θ) between the two planes defined by the cleft aromatic rings. The correlation between the size of the cleft and the type of packing pattern, suggests that the cleft size is perhaps influenced not only by the nature of the appending functional groups but also by the way in which the molecules interact with each other. Table 15 summarises the interplanar dihedral / "cleft"

angles (θ) of functionalised cleft derivatives of **2**, which have been reported to have the same 'above / below' type packing motif (**A**) as the amino-thiocarbamate cleft **(+)-4**.

Table 15: Interplanar dihedral / 'cleft' angle (θ) between the planes defined by aromatic rings in functionalised cleft molecules derived from 2. These cleft molecules have also been reported to display the same 'above/below' packing motif (A) as the amino-thiocarbamate cleft (+)-4.

Entry	Cleft	Interplanar dihedral / 'cleft' angle ($\theta)$ (degrees)
1	(±)-**85**	96.09
2	(±)-**72**	91.42
3	(+)-**4**	86.95

2.4.2.3 X-Ray Crystal Structure of 3,5- Bis(trifluoromethyl) phenyl Amino-thiocarbamate Cleft (±)-6

Single crystals of **(±)-6** suitable for X-Ray diffraction analysis were obtained by recrystallization from light petroleum and dichloromethane. Due to small crystal dimensions, this data set was collected using synchrotron radiation at the ALS.

In the crystal structure of **(±)-6**, the fluorine atoms which make up the CF_3 groups were modelled as split over two sets of positions with one of the $C_6H_3CF_3$ groups (modelled with atoms C(54) > C(57), C(60) and F(13) > F(15)) showing the potential to be more disordered than the others (Figure 33, b). As a result restraints were used on geometry and displacement parameters (See Appendix 7.6). Like the other *N*-aryl functionalised amino-thiocarbamate clefts **(+)-4** and **(±)-5**, the Ph(CF$_3$)$_2$ substituted amino-thiocarbamate groups are directed into the cleft cavity with the thiocarbamate sulphur and N–H groups directed away from the interior of the cleft (Figure 33).

a)
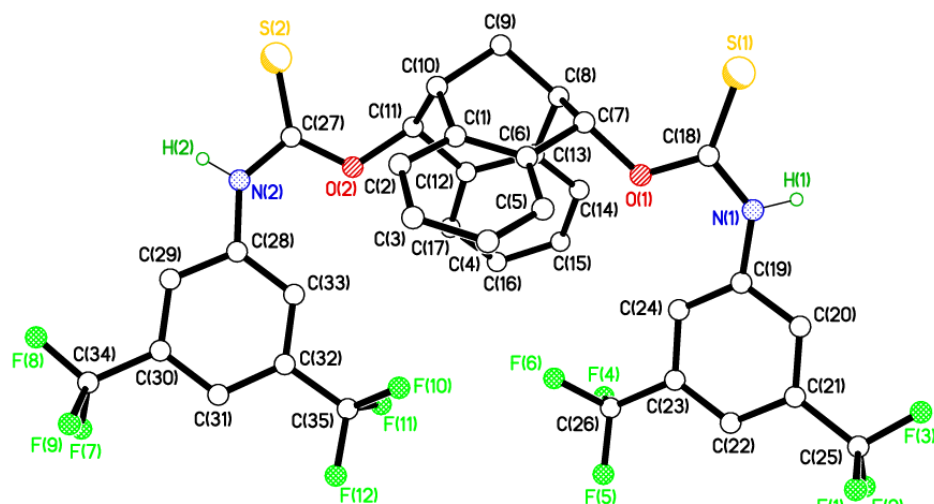
b)
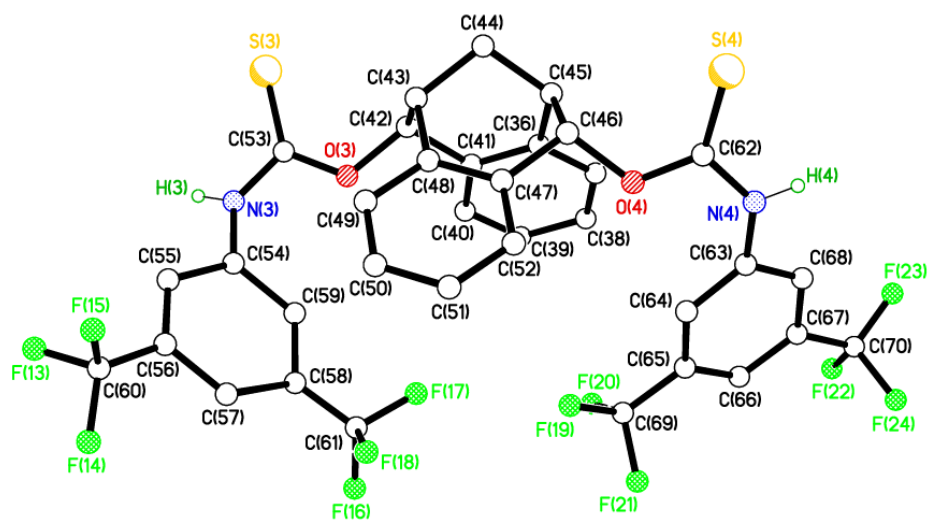
Figure 33: The X-Ray crystal structure of (±)-6, with the appending fluoroaryl groups model as split over two sets of positions (a and b).

It would appear from X-Ray packing plots that the bulky pendant fluorinated aromatic groups block the cleft cavity preventing any interactions between the π-systems of neighbouring cleft molecules. As a result the only interactions observed in the H-bond network of **(±)-6** are between one of the thiocarbamate N–H groups and the sulphur atom of a neighbouring molecule resulting in a 2-dimentional H-bonded sheet (Figure 34).
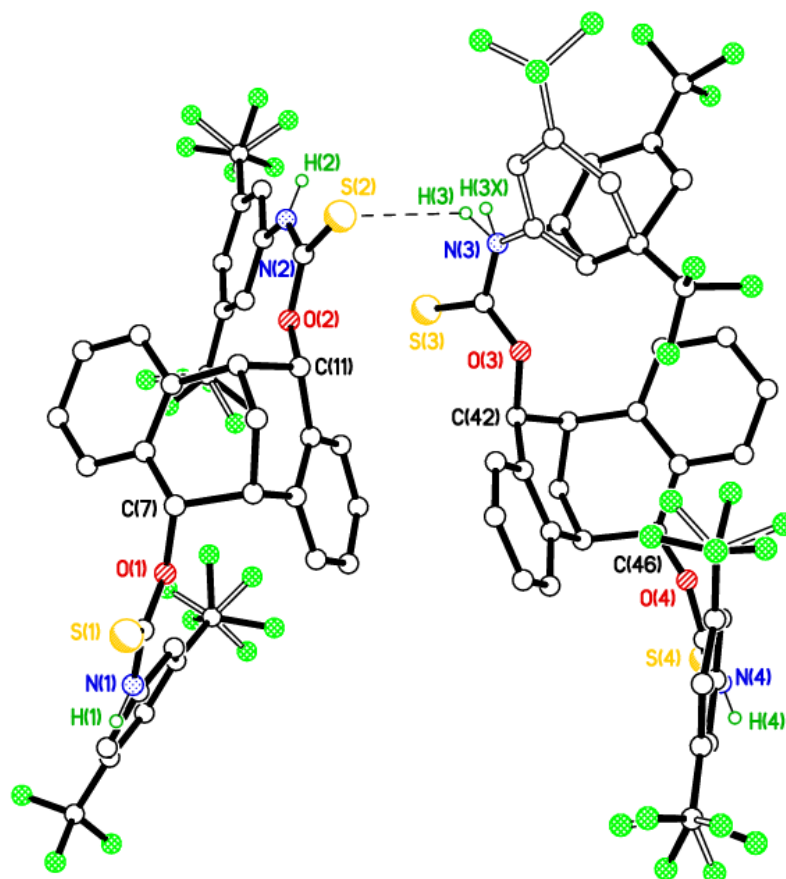
Figure 34: H-bond network between molecules of (±)-6 in the asymmetric unit, and the two sets of positions taken up by the disordered $C_6H_3CF_3$ unit.

The length of the H-bonds between the sulphur and N–H groups in the asymmetric unit (Table 16) are very similar to the length of H-bonds shown in (+)-4 and (±)-5 and the methyl-amino-thiocarbamate cleft (±)-7, however the overall packing pattern displayed by this molecule is considerably more complex due to the fluoroaryl groups.

Table 16: H-bond geometry displayed by H-bonded molecules of (±)-6.

Entry	Donor	Hydrogen	Acceptor	D—H/Å	H···A/Å	D···A/Å	D—H···A/°
1	N(1)	H(1)	S(3)[i]	0.84 (2)	2.61 (4)	3.369 (5)	151 (6)
2	N(2)	H(2)	S(2)[ii]	0.85 (2)	2.96 (6)	3.560 (6)	130 (6)
3	N(3)	H(3X)	S(1)[iii]	0.88	2.51	3.351 (6)	160
4	N(4)	H(4)	S(3)[iv]	0.83 (2)	2.65 (4)	3.436 (6)	157 (7)

Symmetry codes: (i) x, $y+1$, z; (ii) $-x+1$, $-y+1$, $-z+2$; (iii) x, $y-1$, z; (iv) $-x+1/2$, $y+1/2$, $-z+3/2$.

2.4.2.4 X-Ray Crystal Structure of Methyl Amino-thiocarbamate (±)-7

Due to small crystal dimensions this data set was also collected using synchrotron radiation at the ALS. Like the *p*- tolyl, phenyl and fluoroaryl substituted amino-thiocarbamate groups in (+)-4, (±)-5 and (±)-6 respectively, the appending methyl-thiocarbamate groups are directed into the cavity of the cleft (Figure 35).
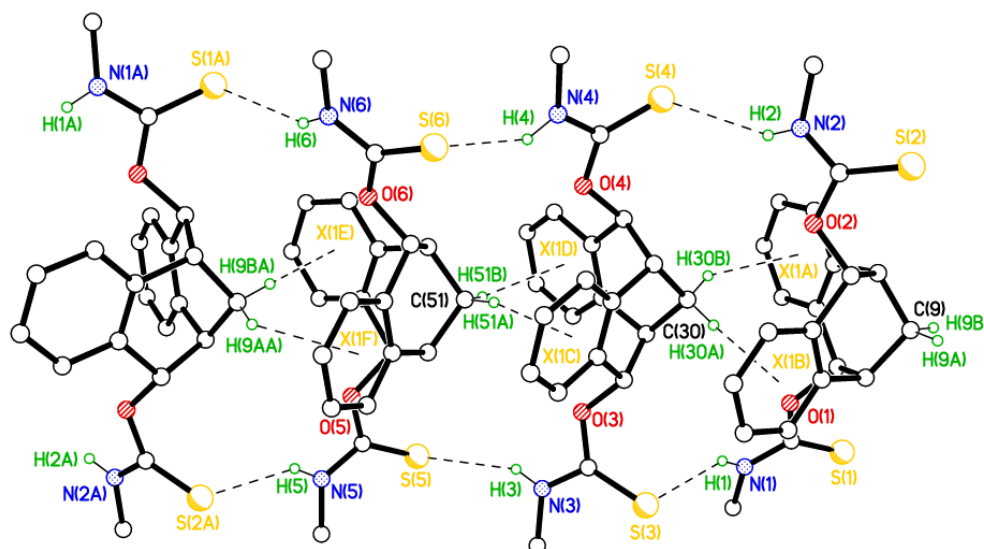
Entry	Donor	Hydrogen	Acceptor	D—H/Å	H···A/Å	D···A/Å	D—H···A/°
1	N(1)	H(1)	S(3)	0.84 (3)	2.58 (3)	3.310 (2)	145 (3)
2	N(2)	H(2)	S(4)	0.80 (3)	2.74 (3)	3.257 (2)	151 (2)
3	N(3)	H(3)	S(5)	0.80 (2)	2.70 (2)	3.4072 (18)	148 (2)
4	N(4)	H(4)	S(6)	0.90 (3)	2.62 (3)	3.3255 (19)	135 (2)
5	N(5)	H(5)	S(2)[i]	0.82 (3)	2.61 (3)	3.3221 (17)	147 (2)
6	N(6)	H(6)	S(1)[i]	0.82 (3)	2.73 (3)	3.457 (2)	149 (2)

Symmetry code: (i) $x+1$, $-y+1/2$, $z+1/2$.

Figure 35: X-Ray crystal structure of (±)-7 and the H-bond network displayed by H-bonded molecules within the unit cell. Table 17 summaries the H-bond geometry displayed by this H-bonding network.

However, unlike the N-aryl substituted thiocarbamate clefts mentioned previously, the thiocarbamate N–H groups in (±)-7 are shown to be directed into the cavity of the cleft, presumably the less bulky methyl groups facilitate this orientation. This removes the ability of the thiocarbamate N–H groups to form centro-symmetric H-bonds with neighbouring clefts, as demonstrated by the clefts (+)-4 and (±)-5 (Figures 28 and 30), which appears to

influence the way in which molecules of (±)-7 interact with each other. The packing pattern displayed by (±)-7 showed that molecules are linked via N–H⋯S H-bonds into chains / ladders, thus the apex of one molecule is accommodated in the cleft of the other to form columns of apex-to-base stacked molecules (**B**), like a stack of party hats. The two hydrogens in the CH_2 at the bridgehead of the cleft at C(9); C(30) and C(51) (Figure 35) make up pairs of C–H⋯π interactions with the cleft of the molecule 'above' (Table 17). The apex-to-apex (or bridgehead- to- bridgehead) separation, illustrated schematically in Figure 36, provides a crude measure of the contact between stacked molecules.
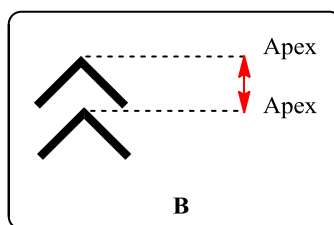
Figure 36: The apex-to-apex packing motif (B) for the molecular packing displayed by molecules of (±)-7.

Table 18 summarises the H-bond geometry of this stacking pattern and thus provides a crude measure of the contact between the stacked cleft molecules.

Table 18: The geometry of the C–H⋯π H-bond interactions between stacked molecules of (±)-7 (See Figure 35 for numbering).

Entry	Hydrogen	Acceptor	H⋯A/Å
1	H(30B)	X(1A)	2.52
2	H(30A)	X(1B)	2.63
3	H(51A)	X(1C)	2.59
4	H(51B)	X(1D)	2.57
5	H(9BA)	X(1E)	2.87
6	H(9AA)	X(1F)	2.60

In addition to this molecular stacking pattern, this cleft presents a highly unusual cooperative packing system, where each group of three molecules is H-bonded to the next group of three molecules but with a 180° rotation between one group and the next (Figure 37).
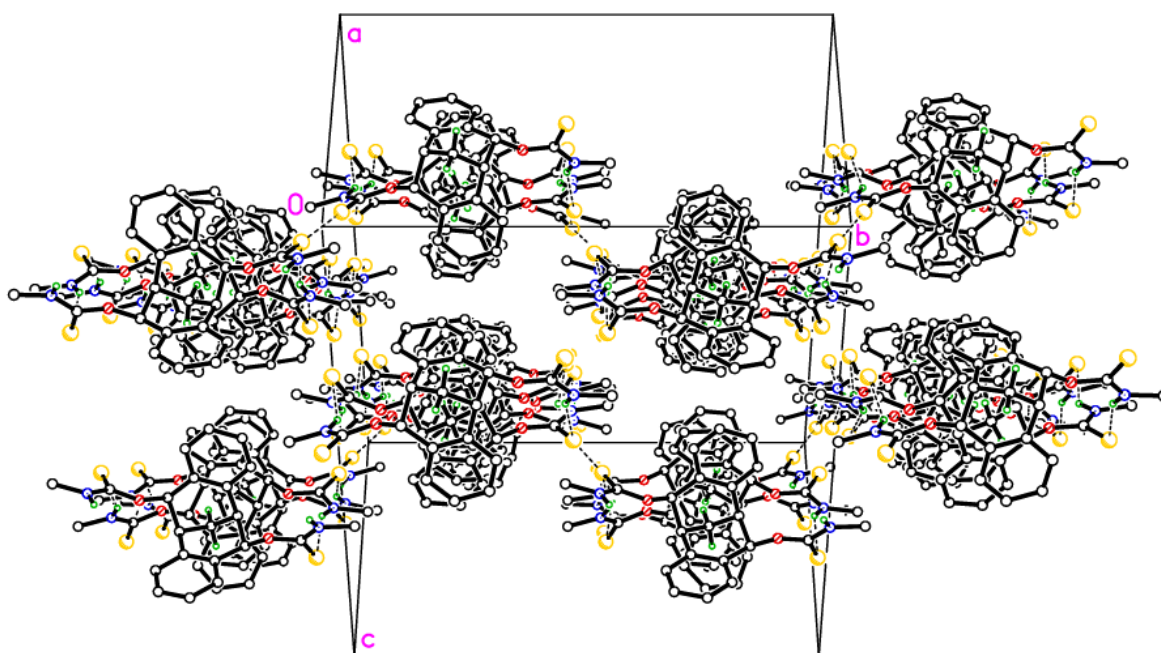
Figure 37: Packing plot and H-bond network displayed by molecules of (±)-7.

X-Ray crystallographic analysis of **(+)-4**, **(±)-5**, **(±)-6**, and **(±)-7** clearly highlights the rigid cleft shape of all the molecules and indicates that the complexing substituted amino-thiocarbamate groups are all directed into the cleft cavity. With the exception of **(±)-7**, the amine and sulfur groups are orientated away from the cleft cavity allowing them to form centro-symmetric H-bonds with neighbouring cleft molecules. Where the amine groups are directed into the cleft cavity, molecules interact to form a unique 'apex-cleft base' style packing pattern (**B**) (Figures 35 and 36). In addition, apart from **(±)-6** where bulky pendant fluorinated aromatic groups block the cleft preventing any interactions with the π-systems, the clefts are filled with external surfaces of other cleft molecules via C–H···π interactions demonstrating their ability to take up molecules with the appropriate shape.

2.5 Uptake and Binding Properties of Carbocyclic Cleft Molecules

Of particular interest to this research project, in relation to the up-take and binding of molecules within the cleft cavity, was the X-Ray crystal structure of **(±)-4**. Essentially the molecular structure of **(±)-4** is exactly the same as the (+)-enantiomer (Figure 29) with complexing *p*-tolyl-amino-thiocarbamate groups pointing into the cavity of the cleft bicycle and both the N–H and sulfur groups of the appending amino-thiocarbamate groups pointing

away from the interior of the cavity. Like in **(+)-4**, this arrangement of functional groups allowed molecules to form chains linked by pairs of centro-symmetric N–H···S H-bonds (Figure 38, Table 19).
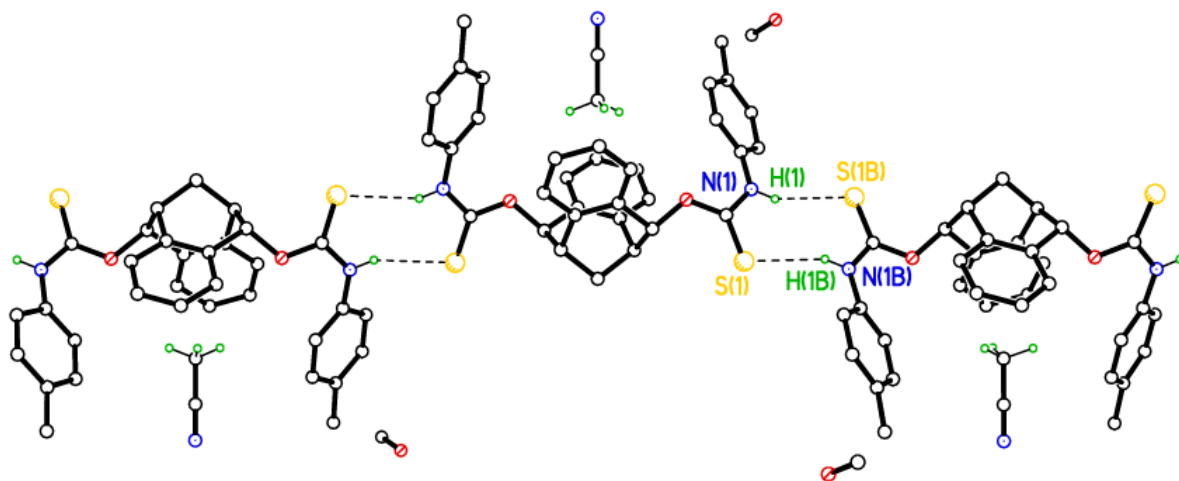
Entry	Donor	Hydrogen	Acceptor	D—H/Å	H···A/Å	D···A/Å	D—H···A/^{o}
1	N(1)	H(1)	S(1)^i	0.816 (8)	2.602 (18)	3.3611 (10)	155.4 (15)

Symmetry code: (i) −x+5/2,−y+1/2,−z−1/2.

Figure 38: The H-bonding network and geometry displayed by cleft clefts in the crystal structure of (±)-4. Table 19 summaries the H-bond geometry displayed by this H-bonding network.

Unlike the crystal structure of **(+)-4** which was found to contain crystallographically independent molecules with no solvent of crystallisation, the crystal structure of the racemic compound **(±)-4** contained solvate molecules of methanol which lie disordered over a two-fold axis exo to the cleft molecules. Moreover, an acetonitrile solvate molecule bound via a pair of C–H···π interactions resides in the cleft cavity (Figure 39).
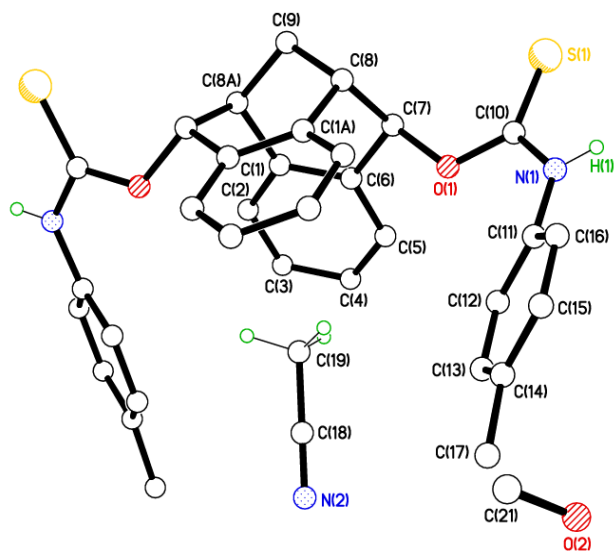
Figure 39: X-Ray crystal structure of racemic cleft (±)-4 showing the C–H···π binding of a solvate molecule of acetonitrile within the cleft cavity.

Interestingly, because the cleft cavity is occupied with solvent molecules bound to the cleft by moderate C–H···π interactions, neighbouring H-bonded chains made up of molecules of (±)-4 are unable to interact as they did in (+)-4 where the terminal *p*-tolyl group from one chain penetrates into the cavity of the molecule in the next chain forming an 'above / below' type packing pattern (**A**) (Figure 32). Instead chains of H-bond molecules arrange into groups of six molecules which interact to form rings with the internal clefts filled with acetonitrile solvate molecules (Figure 40).
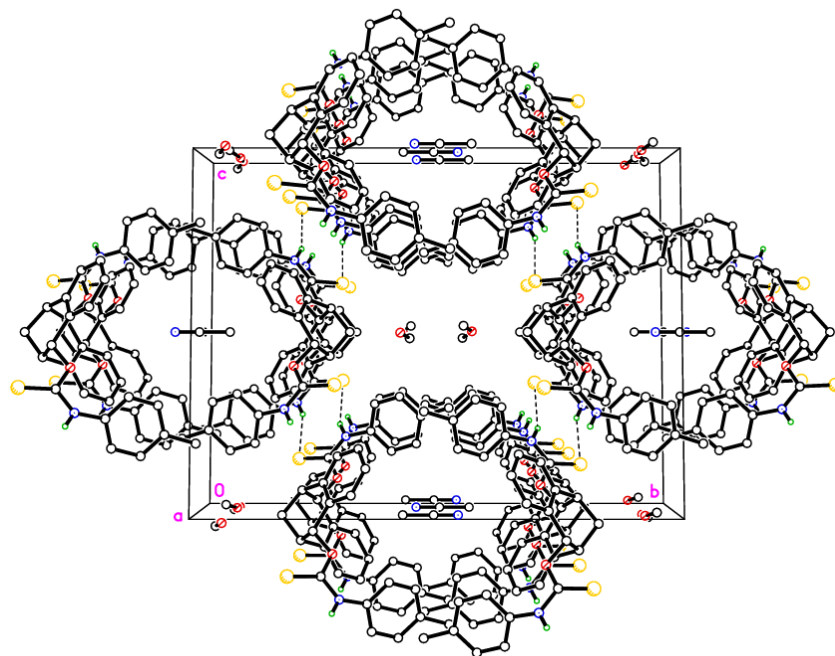
Figure 40: Packing plot and H-bond network displayed by (±)-4.

The crystal structure of **(±)-4** provided evidence of the ability of these novel amino-thiocarbamate clefts to bind guest molecules with complementary size and binding features. Interestingly, binding within the cleft cavity was facilitated by C–H$^{...}\pi$ H-bond interactions originating from the core carbocyclic cleft framework, and not by H-bonds involving the thiocarbamate groups. To determine whether the amino-thiocarbamate groups contribute to the binding of solvate molecules within the cleft cavity additional inclusion complexes involving the unfunctionalised carbocyclic cleft are required for comparison.

2.6 Dimensions of Functionalised Carbocyclic Cleft Molecules

The dihedral angle formed by the least square planes of the two opposing aromatic rings immediately attached to the bridgehead superstructure provides a simple measure of the interplanar 'cleft' angle (θ). X-Ray crystal structures of a range of functionalised TB systems have shown that there is a moderate degree of flexibility in the bicyclic ring system with the dihedral angle (θ) between the two aryl rings depending on the nature of the ring substituents. Similarly, previous X-Ray crystal analysis of functionalised cleft molecules derived from 2 have also provided evidence to suggest that functionalisation of the ring system affects the geometry of the cleft in terms of 'cleft' angle (θ). Table 20 summarises the variation in 'cleft' angle (θ) as the amino-thiocarbamate *N*-substituents were varied. For comparison the dihedral 'cleft' angle (θ) displayed by a range of functionalised cleft molecules derived from the carbocyclic cleft molecule **2** are also reported. In addition, the dihedral 'cleft' angle (θ) of the

78

pyridine substituted carbocyclic clefts (±)-**111a**, (±)-**111b** and (±)-**112c** are reported for the first time.

Table 20: Summary of the interplanar 'cleft' angles (θ) displayed by functionalised carbocyclic cleft molecules derived from 2.

Entry	Compound	Interplanar 'cleft' angle θ (^{o})
1	(±)-**4**	86.9
2	(+)-**4**	87.4
3	(±)-**6**	83.3
4	(±)-**7**	83.4
6	(±)-**5**	79.4
7	(±)-**111a**[39]	73.3
8	(±)-**111b**[39]	89.3
9	(±)-**113c**[39]	87.7
10	(±)-**72**[33]	91.4
11	(±)-**2**[30]	92.9
12	(±)-**73**[33]	104.3
13	**1**[52]	74.0
14	**L1** (±)-**78**[37]	97.8
15	**L2** (±)-**79**[37]	102.5
16	**L3**[a] (±)-**80**[37]	103.3, 109.8[a]
17	(±)-**74**[8]	100.4
18	(±)-**76**[8]	99.7
19	(±)-**85**[8]	83.1
20	(±)-**87**[8]	102.7

Overall, Table 20 shows that there is a moderate degree of flexibility in the dimensions of the cleft with 'cleft' angles between 83.4^o and 109.8^o being observed. In general there is little discrimination between the cleft angles of the amino-thiocarbamate clefts (Table 20, entries 1–6) and the pyridyl carbocyclic clefts (Table 20, entries 7–9). Similarly, despite the difference in electronic nature and size of the different amino-thiocarbamate substituents there is only a very small variation in the bond angles (79.4 – 87.4^o). Although the methyl groups in (±)-**7** are much smaller than the bulky fluoroaryl

groups in (±)-**6**, both clefts have almost identical dihedral 'cleft' angles of 83.3° and 83.4° respectively (Table 20, entries 3 and 4). This suggests that there may be other permitting factors which affect the cleft dimensions. For instance, it is possible that the cleft size is influenced by the way in which the molecules pack together, which is related to functional group orientation and interaction.

When functionalisation of the molecular cleft **2** occurs at the aromatic ring positions there is a significant increase in the 'cleft' angle (θ) as the electronic properties of the substituents change from electron-withdrawing groups to electron-donating groups. For example, bond angles vary from 83.1° when the aromatic rings are substituted with electron-withdrawing nitro groups (Table 20, entry 19) to 104.3° when these groups are replaced with electron-donating methyl groups (Table 20, entry 12). However, the cleft angles displayed by the amino-thiocarbamate clefts (±)-**6** and (±)-**7** (Table 20, entries 3 and 4), where the fluoroaryl groups are highly electron-deficient in comparison to the methyl groups, there is no change in the interplanar 'cleft' angles. This implies that the electronic nature of the substituents at the periphery of the cleft has little or no effect on the overall cleft dimensions, whereas a change to the electronic nature of the aromatic rings has a significant impact on the size and dimensions of the cleft. It is therefore reasonable to assume that derivatisation of the clefts at the aromatic ring positions would allow more control over the cleft dimensions and hence potential binding properties of these molecules. Further comparison between clefts substituted at the aromatic ring positions with the novel amino-thiocarbamate and pyridyl clefts showed that in all cases, functionalisation of the aromatic rings on the cleft bicycle results in notably larger 'cleft' angles compared to clefts that have functional groups attached directly to the core of the cleft framework. The effect of 'cleft' angle on the binding properties of these cleft molecules is yet to be explored however, it is reasonable to assume that the dimensions of the cleft molecules will play an important role in the selective binding of substrate molecules, allowing only molecules of complementary size to be bound within the cleft cavity.

The next Chapter is devoted to the exploration of the application of these novel amino-thiocarbamate clefts as asymmetric H-bond catalysts in both the hetero Diels Alder (HDA) reaction and the NBS mediated bromolactonisation reaction of unsaturated carboxylic acids.

Chapter 3

3.0 Catalysis

Important biological molecules such as DNA and proteins and therefore many pharmaceutical drugs are chiral – that is, they are non-superimposable on their mirror image (the pair of asymmetric molecules are known as enantiomers), therefore any chemical reaction that can selectively synthesize one enantiomeric form of a chiral compound is potentially very useful. In recent years a tremendous effort has been put into the development of methods for the selective synthesis of single pure enantiomers for uses such as pharmaceuticals, flavours, fragrances, insect pheromones and other compounds of biological relevance.[53] The demand for chiral compounds, often as single enantiomers, has escalated sharply in recent years, driven particularly by the demands made by the pharmaceutical industry where chirality plays a major role.[48]

Single enantiomer drug sales display continuous growth worldwide with many of the top selling drugs being marketed as single enantiomers. The single enantiomer form of a drug is therapeutically more effective and has been shown to have fewer side effects; consequently regulatory agencies across the world have introduced guidelines and polices which provide incentive for investment in single enantiomer drugs.[53] As a result the chiral drug industry constitutes approximately one third of all drug sales worldwide with the majority of newly introduced drugs being chiral.[54] The growing economic importance of chiral compounds has spurred major research efforts from many academic and industrial labs which has led to the rapid development of enantioselective synthetic methodologies. Such aproaches have now reached a high degree of diversity and complexity.[1] These advances have been facilitated by an increase in the availability of separation techniques as well as analytical assays for the precise determination of the enantiopurity of chiral compounds. The development of chiral stationary phases (CSP), gas chromatography (GC) and liquid chromatography (LC) amongst other analytical techniques has opened up a new dimension in the area of separation technologies and therefore the synthesis of enantiomerically pure compounds.[53]

3.1 Asymmetric Catalysis

Asymmetric catalysis is one of the most important strategies for the synthesis of enantiopure compounds. The presentation of the Nobel Prize for ligand chemistry in 2001 to William S. Knowles and Ryoji Noyori (for their work on chiral catalysed hydrogenation

reactions) and Barry. K. Sharpless (for his work on chiral ligand catalysed oxidation reactions) recognized the enormous significance attached to chiral catalysts in asymmetric synthesis. Building on their seminal work, the area of asymmetric catalytic enantioselective reactions now covers a range of reaction mechanisms and conditions.[55,56] In contrast to the vast literature on Lewis-acid and metal-catalysed processes there are fewer asymmetric transformations catalysed by organic molecules. Only in the past 10 years has the potential of catalysing reactions with small organic molecules started to be uncovered, prior to this the use of metal catalysts or metal-ligand catalysts dominated the research scene.[46,57]

3.1.1 Asymmetric Organocatalysis

Organocatalysis is an emerging area in asymmetric synthesis and offers a mild practical and generally simple method of making small functionalised molecules with high enantiopurity.[1] Moreover, nature provides us with an array of enantiopure organic compounds from which to develop organic catalysts, these include α-amino acids, α-hydroxy acids, nucleic acids, and carbohydrates. One of the most attractive aspects of organocatalysis is that the biomimetic use of multiple, relatively weak catalyst-substrate interactions as opposed to single, strong Lewis- acid / Lewis base attractions facilitates the design of so called bifunctional catalysts: catalysts which possess complementary functionality capable of activating two components of a chemical reaction simultaneously.[58] The rapid growth of organocatalysts over the last decade has been fuelled by the development of a small number of generic activation modes which include, but are not limited to; secondary amine catalysis via enamines (**A**), secondary amine catalysis via iminium ions (**B**) and hydrogen bonding (H-Bonding) catalysis (**C**) (Figure 41).[57]
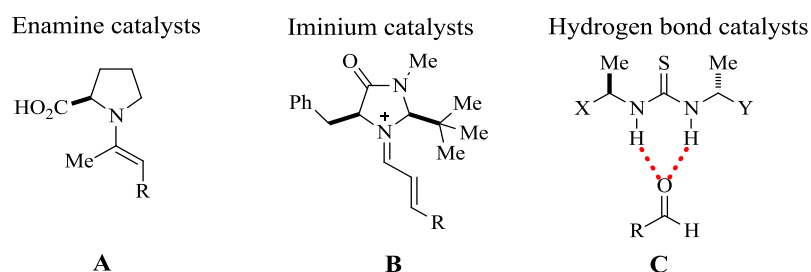
Figure 41: Generic activation modes in organocatalysis.

In comparison with transition metal catalysed processes, organic based catalysts have several advantages in not only ease of product purification, greater ease of handling, and reduced toxicity, but also in their inherent stability to air and moisture. Moreover, they are

often cheaper than their transition metal counterparts. Attractive features of H-bonding catalysts, in particular, include their stability, ease of preparation, low toxicity and potential to catalyse a range of novel transformations. The research presented herein describes H-bonding catalysis both with respect to catalyst development and to the application of these catalysts in the synthesis of enantiomerically pure molecules. This catalytic strategy has potential as a general paradigm for the application of our functionalised cleft molecules which display H-bond donor functional groups which are potentially capable of facilitating H-bonding within a chiral environment and therefore present the potential to be used as enantioselective H-bonding catalysts.

3.2 Hydrogen Bonding (H-Bonding) Catalysts

A crucial function of H-bonds in nature is transition state stabilization during enzyme catalysis. Synthetic chemists have applied this mode of activation to asymmetric catalysis where H-bond donors are used in small chiral molecules to activate electrophiles and to impart facial selectivity during catalysis.[46] Recent developments in this field have been rapid resulting in a plethora of structurally distinct catalysts including both dual and bifunctional catalyst systems. An important component of such catalysts is structural rigidity and the display of H-bond donating functional groups. Molecules that have been reported to be effective as H-bonding catalysts include phosphoric acids **129**,[59] diols **130**,[60] guanidiniums **131**,[61] ureas **132a**[62,63] and thioureas **132b** [62,63] (Figure 42).

Ar = 1= naphthyl

129   **130**

131   **132a** = O
                           132b = S
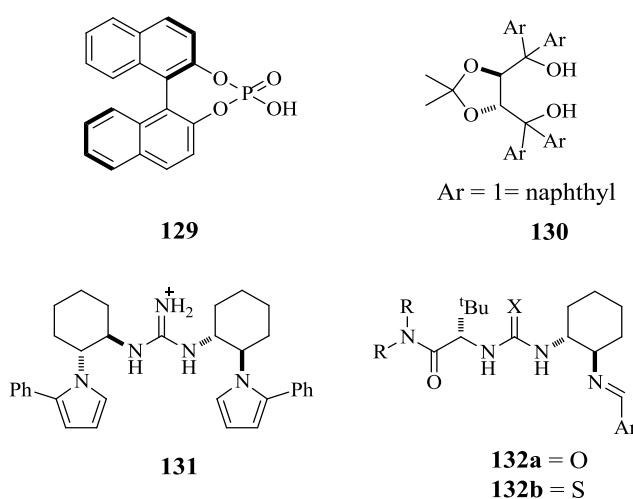
Figure 42: Representative H-bonding catalysts.

Species capable of simultaneously donating two H-bonds, such as ureas **131a**, thioureas **132b**, as well as guanidinium ions **131**, have emerged as a class of privileged

catalyst structures, finding applications in such mechanistically diverse transformations as 1,2-additions, acyl transfer, 1,4-addition, and cycloaddition reactions. More recently, efficient strategies for obtaining high *ee* values using only a single H-bond have been reported. Chiral diols such as TADDOL **130**[60] and BAMOL derivatives[64] as well as phosphoric acids **129** have been shown to be effective as single H-bond donors (via cooperative catalysis) capable of highly enantioselective catalysis.

3.2.1 Mechanistic Considerations

The activation mode by which these catalysts operate is reminiscent of Lewis acid catalysis. The mechanism of H-bond activation occurs via the donation of H-bonds to an electrophilic substrate such as carbonyl compounds or imines. In the activation of carbonyl groups for example, the lone pairs of electrons on the carbonyl oxygen atom can be considered as hard Lewis base sites. Coordination of these lone pairs to Lewis acids or H-bond donor groups lowers the electron density at the oxygen atom and the energy of the energetic potential of the lowest unoccupied molecular orbital (LUMO), the C=O π^* orbital (Scheme 48).[57,65]
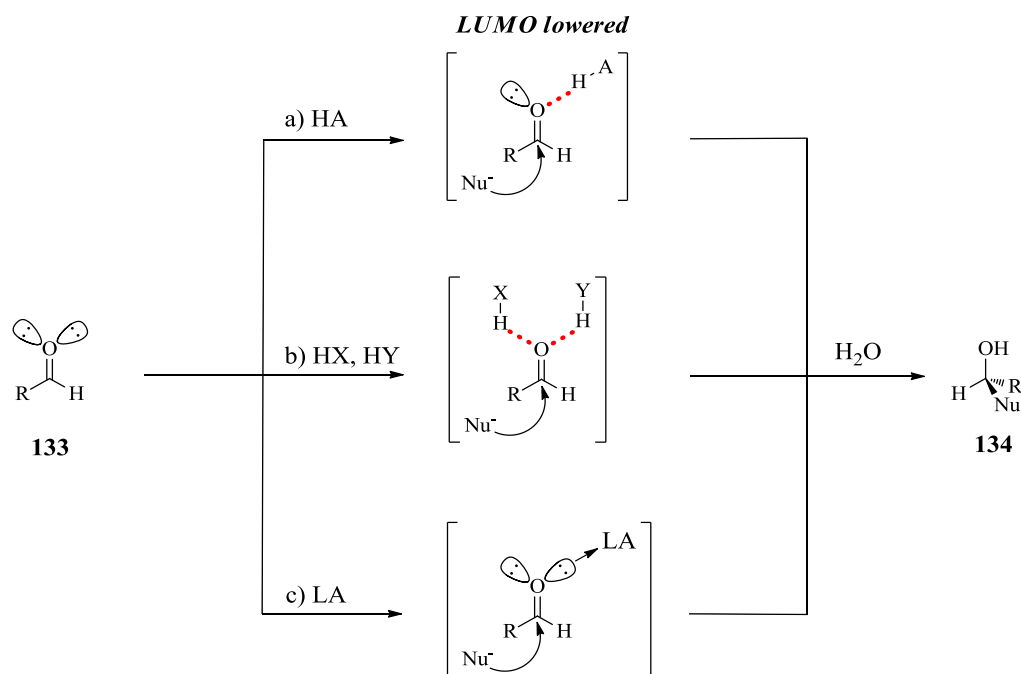
Scheme 48: General modes of carbonyl activation by coordination: a) single H-bond (HA), b) double H-bond (HX, HY) and c) Lewis acid (LA).

This electronic redistribution, in turn, decreases the energy gap between the LUMO of the electrophile and the highest occupied molecular orbital (HOMO) of the nucleophile, thus

facilitating the reaction between the two reacting partners. After bond formation occurs, the H-bond donor can then dissociate from the product to allow for catalyst turnover

In terms of promoting enantioselective transformations these types of catalysts stabilise the transition state in a 'chiral pocket' via weak H-bond interactions (See Chapter 2, Figure 23 for model of chiral pocket and asymmetric induction). This mechanism of asymmetric induction involves a substrate molecule which has a prochiral face becoming temporarily bound to the catalyst. Essentially, the substrate molecule is 'fixed' within an asymmetric environment or 'chiral pocket' within the catalyst. The prochiral substrate molecule is bound to the catalyst in such a way that favours one trajectory of the reaction more than the other. Therefore, when the substrate molecule reacts a new chiral centre is enantioselectively introduced into the molecule thus producing an excess of one enantiomer. The most efficient catalyst systems are those which can completely block the other trajectory of the reaction. This concept of transition state stabilisation within a 'chiral pocket' has become the basis of rational design and optimisation of asymmetric organocatalysts.[58]

3.2.2 H-Bonding Catalysts in the Enantioselective Hetero-Diels Alder (HDA) Reaction

The enantioselective hetero Diels-Alder (HDA) reaction between electron-rich dienes and aldehydes represents one of the most widely used methods for the construction of optically active 6-membered oxygen containing heterocycles. In 1982, the HDA reaction was extended to unactivated aldehydes and heterodienophiles by Danishefsky and co-workers.[66] Since then the reaction has been the subject of intensive investigations in the field of asymmetric synthesis, mainly because of the ease with which the dihydropyranone products can be elaborated to numerous pyran containing natural products.

The first H-bond mediated enantioselective [4 + 2] cycloaddition Diels-Alder (DA) reaction was reported in 2000 by Göbel and co-workers.[67] The group used axially chiral amidinium host molecules such as **138** to direct the enantioselective DA reaction between dienes such as **135** and a diketone dienophile **136** (Scheme 49).
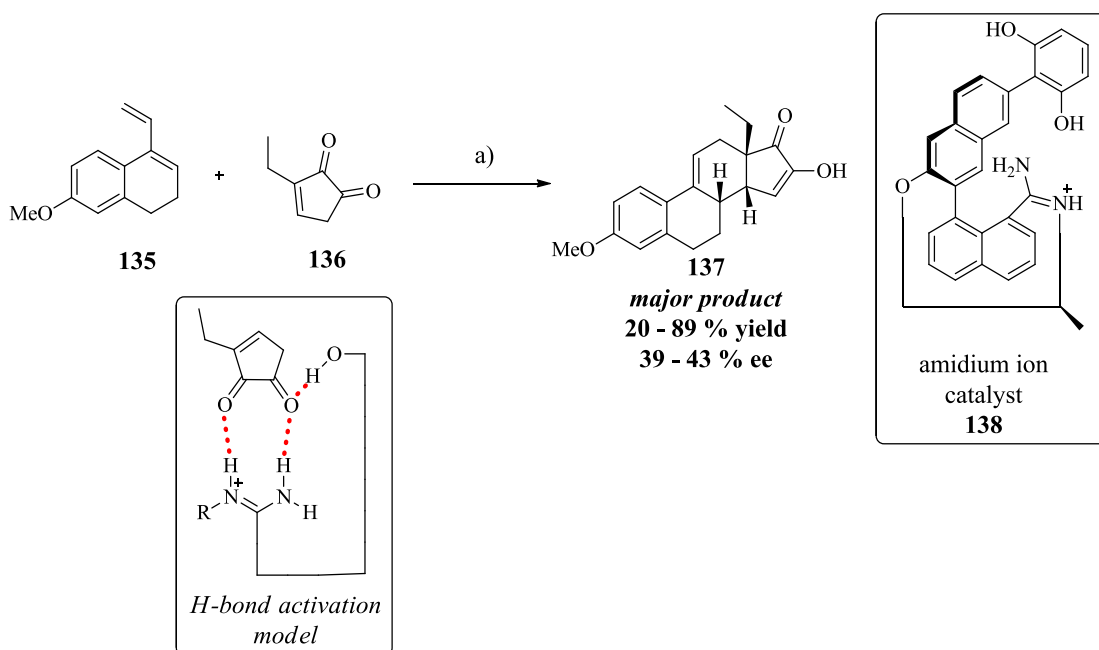
Reagents and conditions: a) Catalyst **138** (10–100 mol %), CH$_2$Cl$_2$, 4–5 ^{o}C.

Scheme 49: Chiral amidinium catalysts used in the first H-bond mediated enantioselective DA reaction as reported by Göbel and co-workers.

Although the enantioselectivites were only modest (up to 43 % ee with a stoichiometric amount of amidinium salt **138**), the reaction rates were accelerated by more than 100-fold in the presence of catalytic amounts of the amidinium ion **138.**

In the pursuit to identify more reactive dienes for the DA reaction, Rawel and co-workers developed the reactive diene; 1-amino-3-siloxybutadiene **10** (Rawel diene), which is readily prepared on a large scale from acetyl-acetaldehyde dimethyl acetal.[68] Rawel diene **10** is sufficiently activated to allow the HDA reaction to proceed under mild, strictly thermal conditions, and therefore does not require the assistance of a Lewis acid catalyst. Aldehydes can be converted to dihydropyranones through a HDA reaction with the subsequent unmasking effected by acetyl chloride (Scheme 50).[69]

TBS = *tert*-butyldimethylsilyl
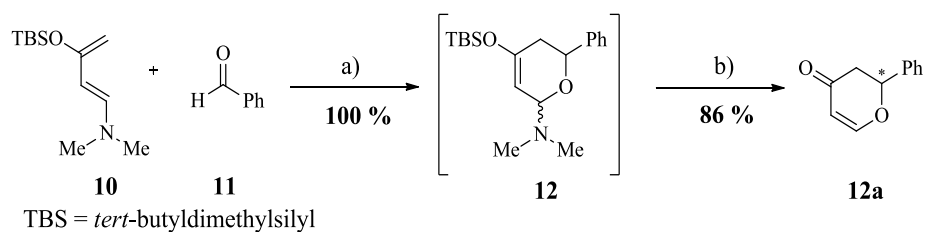
Reagents and conditions: a) CDCl$_3$, rt, 2 h; b) AcCl, CHCl$_2$, -78 $^{\circ}$C, 30 min.

Scheme 50: HDA reaction of Rawel diene 10 with benzaldehyde 11 under strictly thermal conditions.

In recent years, it has been reported that catalysts capable of H-bonding to the carbonyl of the aldehyde can have a dramatic effect on the rate of this cycloaddition reaction. Moreover, chiral H-bond donors have been reported to impart facial selectivity in the HDA reaction thus controlling the direction of nucleophilic attack, as a result the synthesis of dihydropyranone products with excellent *ee* values have been reported.[46,60]

3.2.2.1 Single H-bond Catalysed Enantioselective HDA Reactions

In 2002, Rawel and Huang showed that solvents capable of donating a H-bond increased the rate of HDA reactions involving the highly activated diene **10** and various aldehydes and ketones, by nearly three orders of magnitude.[70] Soon thereafter the Rawel group developed a catalytic, highly enantioselective version of the HDA reaction. The group identified the TADDOL (α,α,α',α'-tetraaryl-1,3-dioxolan-4,5-dimethanol) class of chiral alcohols as efficient catalysts for the asymmetric HDA reaction.[71] The group reported that in the presence of (*R,R*)-1 naphthyl TADDOL **139** (0.2 eq) the reactive diene **10** reacted with a variety of aromatic, aliphatic and α,β-unsaturated aldehydes, which upon acetyl chloride mediated removal of the TBS and dimethylamino groups, gave the corresponding dihydropyranones in good overall yields and *ee* values (Scheme 51).[71]
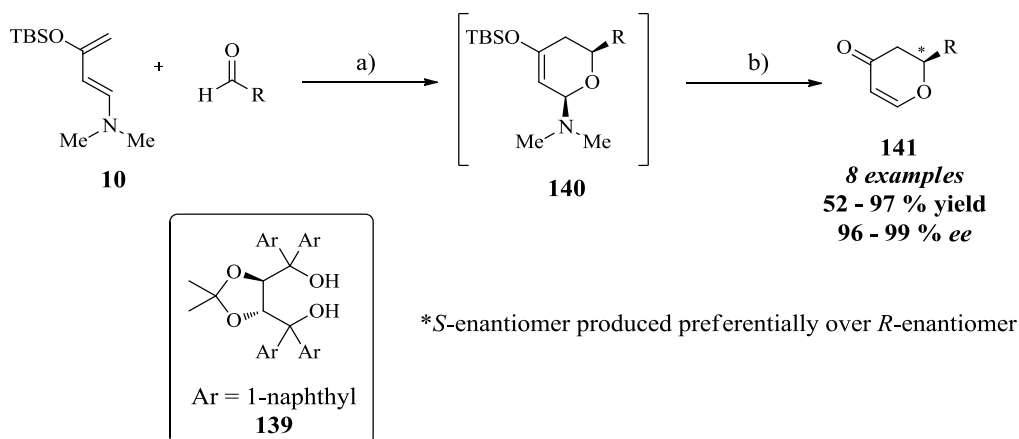
Reagents and conditions: a) TADDOL **139** (0.2 eq), toluene, -40 °C or -78 °C, 24 h or 48 h; b) CH$_3$COCl, CH$_2$Cl$_2$ / toluene, -78 °C, 15 min.

Scheme 51: TADDOL catalysed asymmetric HDA reaction as reported by Rawel and co-workers.

The mode of activation was hypothesized to involve a single H-bond from a hydroxyl group on the TADDOL catalyst to the aldehyde. It was thought that this H-bond could be enhanced by intramolecular H-bonding between the two hydroxyl groups (cooperative catalysis) (Figure 43).

A
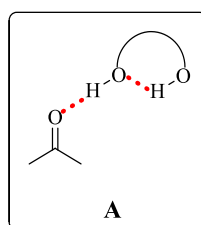
Figure 43: Cooperative catalysis - Single H-bond activation enhanced by intramolecular H-bonding. Proposed mode of activation in the TADDOL catalysed HDA reaction.

In 2004, Ding and co-workers reported the X-Ray crystal structure of a TADDOL-DMF complex which helped identify important structural features of the TADDOL catalyst and provided evidence to support the proposed mechanism of cooperative catalysis. The X-Ray crystal structure showed intramolecular H-bonding between the two hydroxyl groups and an intermolecular H-bond to the oxygen of DMF. (Figure 44).[72,73]
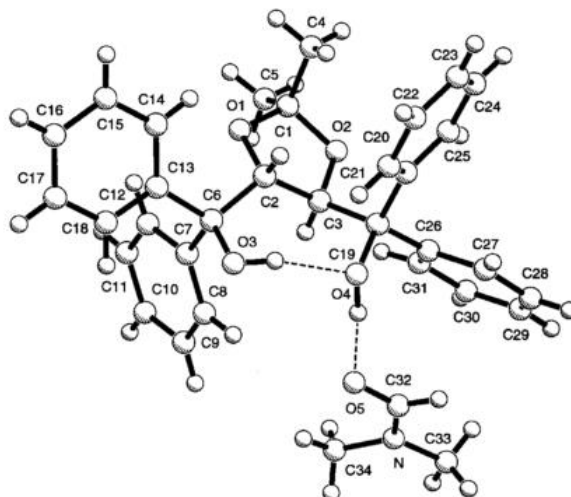
Figure 44: Ding and co-workers X-Ray crystal structure of a TADDOL-DMF complex.

As a direct result of the intramolecular H-bond between the two hydroxyl groups the proton not engaged in H-bonding is both acidified and orientationally defined. The "free" TADDOL hydroxyl proton is therefore able to engage in a single H-bond with the acceptor, in this instance, the oxygen of the DMF molecule and in the HDA reaction, the oxygen of the aldehyde. Additional, computational investigations of the mode of activation of TADDOL in the DA reaction and asymmetric HDA confirmed that cooperative catalysis is favourable [74]

Further investigations by Rawel and co-workers led to the development of the BAMOL (1,1'-biaryl-2,2'-demthanol) derivative catalysts **142a** and **142b** (Figure 45).[64]
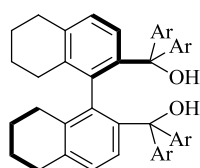
142a Ar = 4-F-3,5-Me$_2$C$_6$H$_2$
142b Ar = 4-F-3,5-Et$_2$C$_6$H$_2$

Figure 45: Rawel and co-workers chiral H-bonding BAMOL catalyst.

In general, the BAMOL catalysts created a more varied chiral environment around the reactive site in comparison to the TADDOL catalyst **139**, leading to enhanced selectivity. This complex was found to catalyse the HDA reaction of **10** with a variety of aliphatic, vinylic and aromatic aldehydes in moderate to excellent yields and *ee* values (Scheme 52).[64]
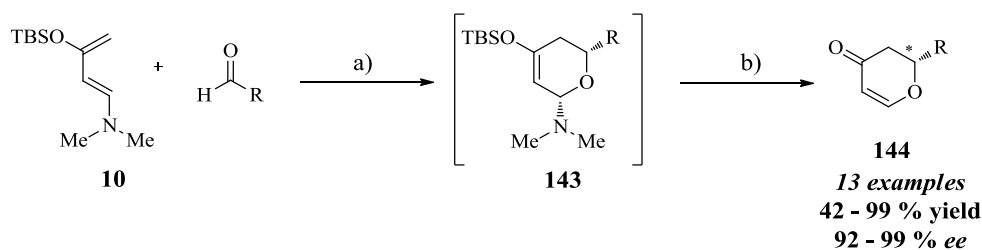
Reagents and conditions: a) BAMOL **142a** or **142b** (20 mol %), toluene, -40 °C or -80 °C, 24 h or 48 h; b) CH₃COCl, CH₂Cl₂/toluene, -78 °C, 30 min.

Scheme 52: BAMOL catalysed asymmetric HDA reaction.

Like with the TADDOL catalyst **139**, an X-Ray crystal structure of a BAMOL-benzaldehyde complex revealed an intramolecular H-bond between the two hydroxyl groups of the catalyst and an intermolecular H-bond between the oxygen in benzaldehyde (Figure 46).[64]
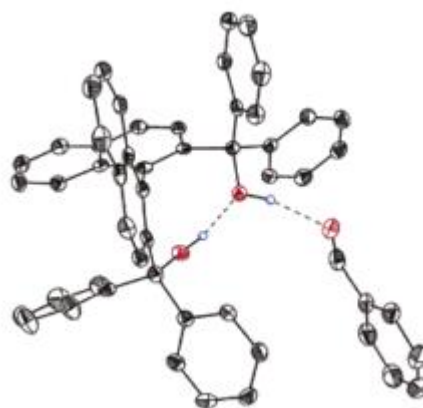
Figure 46: X-Ray crystal structure of an inclusion complex between a BAMOL derived catalyst and benzaldehyde reported by Rawel and co-workers.

This complex therefore suggested that carbonyl activation was through a single H-bond enhanced by intramolecular H-bonding (cooperative catalysis (**A**)) as was postulated for the TADDOL catalyst.

Since this pioneering work by Rawel and co-workers, various H-bonding organocatalysts have been developed for the asymmetric catalysis of the HDA reaction. However, because the organisation of the catalyst-substrate complex by intramolecular H-bonds is most likely the key for high enantioselectivity, examples of monodentate alcohol catalysts which activate electrophiles by single H-bond donation (**B**) remain elusive (Figure 47).[6]
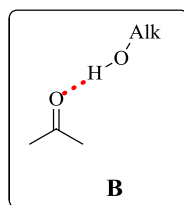
Figure 47: Single H-bond activation (B).

In 2007 Friberg and co-workers reported the first example of an asymmetric HDA reaction of benzaldehyde and Rawel diene **10** catalysed by single H-bond activation (**B**). During a study aimed at investigating the possibility of utilising chiral cleft molecules derived from the carbocyclic molecular cleft **2** as enantioselective H-bond catalysis, Friberg and co-workers revealed that chiral alcohols derived from this molecular cleft were capable of catalysing the HDA reaction, giving dihydropyranone products in up to 52 % *ee*.[6]

3.2.3   Carbocyclic Cleft Catalysed Enantioselective HDA Reaction

As mentioned in Chapter 1 (and above), Friberg and co-workers reported the synthesis of a family of chiral H-bonding clefts including C_2-symmetric diols **(-)-102–105**, a hydroxyketone **(+)-106** and an amino alcohol **(+)-110** all derived from the carbocyclic molecular cleft **(-)-2**. In addition, the previously synthesised amines **(-)-86a** and **(+)-99** were also included in this catalysis investigation (Figure 48).[6]

(-)-102: R = Ph
(-)-103: R = 1-Naphthyl
(-)-104: R = 2-Naphthyl
(-)-105: R = *o*-Anisyl

(+)-106

(+)-110

(-)-108

(+)-99

(-)-86a
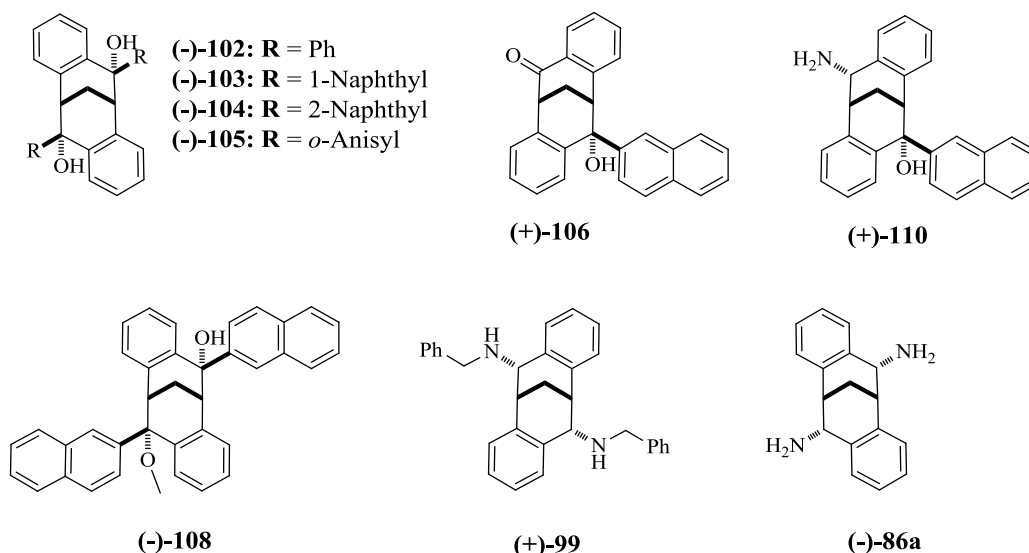
Figure 48: H-bond cleft catalysts screened in the enantioselective HDA reaction.

The HDA reaction between benzaldehyde **11** and Rawel diene **10** was selected as the test reaction in this organocatalytic study. The reactions were performed in toluene at -40 $^{\circ}$C for

48 h. At this temperature the background reaction was negligible. Treatment of the cyclisation adduct **12** with acetyl chloride gave the desired dihydro-4-pyrone **12a** in moderate yields and *ee* values (Table 21).[6]

Table 21: Summary of the results reported by Friberg and co-workers for the screening of H-bond cleft catalysts in the HDA reaction.
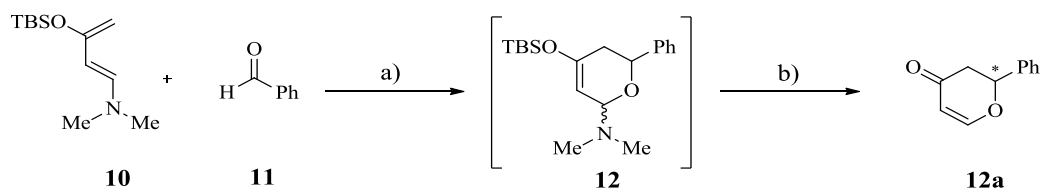
Reagents and conditions: a) catalyst (20 mol %), toluene, -40 °C, 48 h; b) CH₃COCl, CH₂Cl₂,-78 °C, 15 min.

Entry	Catalyst	*ee* (%)[a]	Configuration[b]	Yield (%)[c]
1	(+)-**2**	0	-	20
2	(+)-**1**	0	-	14
3	(-)-**102**	38	(*S*)	41
4	(-)-**103**	48	(*S*)	50
5	(-)-**104**	10	(*S*)	9
6	(-)-**105**	0	-	24
7	(+)-**106**	52	(*R*)	41
8	(-)-**108**	50	(*R*)	40
9	(+)-**110**	38	(*R*)	29
12	(+)-**99**	0	-	7
13	(-)-**86a**	0	-	21

[a] Determined by HPLC analysis on Chiralcel OD-H column.
[b] Determined by the order of elution on the Chiralcel OD-H column.
[c] Isolated yields.

Evaluation of the results obtained from the initial catalyst screening reactions, as summarised in Table 21, led the group to make the following observations: (a) H-bonding was not an absolute requirement for catalysis, the cleft itself had a catalytic effect, although the enantioselectivites were lost (Table 21, entries 1 and 2). It can, therefore, be assumed that H-bonds are necessary in this system for stereocontrol; (b) the monodentate alcohols (+)-**106** and (-)-**108** (Table 21, entries 7 and 9) afforded yields and *ee* values that essentially did not

differ from the results obtained for the diols **(-)-102** and **(-)-103** (Table 21, entries 3 and 4). Thus, catalysis most likely occurs by single H-bond activation (**B**) (Figure 47); (c) intramolecular H-bonding is likely to account for the lack of *ee* in the application of **(-)-105** (Table 21, entry 6). Intramolecular H-bonding between the hydroxyl group and the methoxy oxygen disturbs H-bond donation to the substrate aldehyde, as a result co-ordination of benzaldehyde resulted in both its *Re-* and *Si-* face being exposed equally to **10** resulting in a complete loss of *ee*; (d) amine H-bonding in this system was not efficient at catalysing the HDA reaction (Table 21, entries 12 and 13).

The group used a combination of X-Ray crystallography and computational studies to propose a viable model for the mode of activation by these cleft compounds.[6] Previously reported X-Ray crystal structures of inclusion complexes between the hydroxyketone cleft molecule **(±)-145** (Figure 49) and DMSO revealed some important interactions between the host and guest molecules.
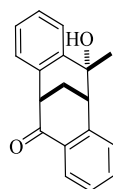
(±)-145

Figure 49: Hydroxyketone cleft used in recognition and binding studies.

The X-Ray crystal structure of the **(±)-145** and DMSO adduct showed a single H-bond between a sulphoxide oxygen non-bonding pair and the hydrogen of the hydroxyl group. This allowed the DMSO sulphur atom to position itself almost centrally within the V-shaped cavity of the cleft (Figure 50).[75]
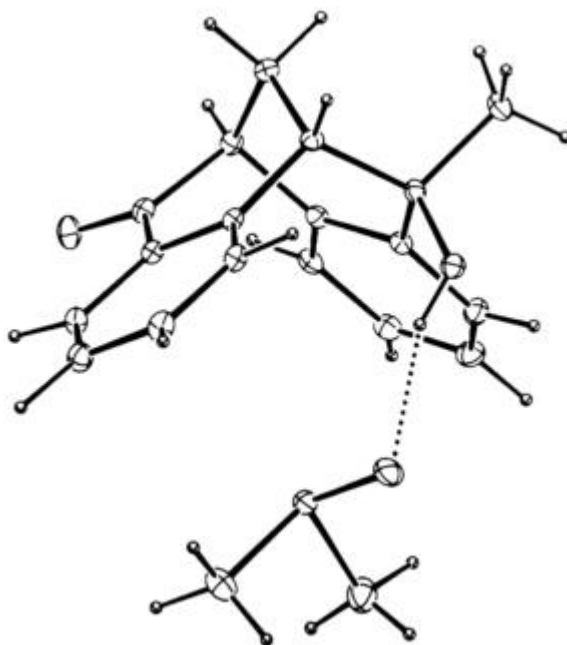
Figure 50: Crystal structure of the (±)-145 and DMSO adduct showing the H-bonded interaction between host and guest.

With this is mind, Friberg and co-workers proposed that similar interactions and substrate orientation, between their cleft molecules and benzaldehyde, would lead to a suitably rigid catalyst-substrate complex to facilitate the enantioselective HDA reaction.

In an attempt to evaluate the viability of this proposed mode of catalyst-substrate binding, the group undertook a molecular mechanistic computational investigation. This involved placing benzaldehyde **11** in the cavity of **(+)-106** and then performing a procedure to minimise the energy of the complex. This gave three low energy arrangements $R1$, $R2$ and S with steric energies of 234.34, 236.11 and 236.08 kJ mol^{-1}, respectively (Figure 51). It was assumed that the diene **10** could only attack the carbonyl of benzaldehyde **11** from the exposed face, that is, the *Re*-face of $R1$ and $R2$ and the *Si*-face of S. The Boltzman factor was used to calculate the population distribution at -40 ^{o}C which corresponded to 55 % *ee* of the product, when the above assumptions were made. This theoretical value compared well with the experimental value of 52 % *ee* (Table 21, entry 7) therefore, it was reasonable for the group to assume that benzaldehyde behaves similar to DMSO in coordinating to the cavity of clefts such as **(+)-106** and **(±)-145.**
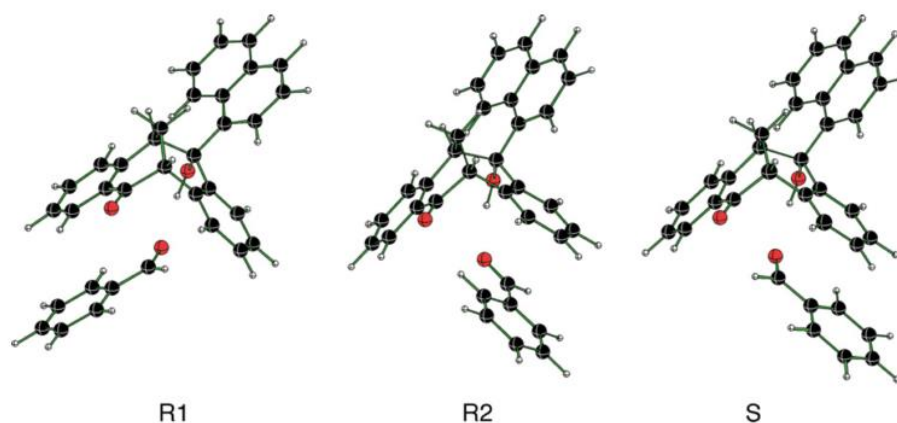
Figure 51: Computational models of the three low energy arrangements *R*1, *R*2 and *S* of the energy minimised complex between benzaldehyde 11 and the hydroxyketone cleft (±)-145.

The group was, however, doubtful that other cleft catalysts would coordinate to benzaldehyde in the same manner. As a result they surmised that there are likely to be several different modes of coordination depending on the exact structure of the catalyst.[6]

Overall the group reported the first successful application of chiral cleft molecules based on the carbocyclic cleft framework **2** as asymmetric organocatalysts. Up to 52 % *ee* was obtained in the HDA reaction between benzaldehyde **11** and diene **10** when the monodentate alcohol **(+)-106** was used (Table 21, entry 7). Transition state structure organisation could be envisaged by coordination of the substrate in the cleft in combination with H-bond for enantioselective catalysis. Despite the modest enantioselectivites obtained, substrates other than benzaldehyde may fit better in the cavity of the catalysts. In addition, although the amine derivatives **(-)-86a** and **(+)-99** were inferior in this reaction, they may be useful as organocatalysts in other organic transformations.[6]

The successful application of these chiral cleft molecules in the enantioselective HDA reaction inspired us to explore the potential of our novel amino-thiocarbamate clefts as H-bond donor catalysts in the HDA reaction. Although a more in-depth understanding and representative model for the exact mode of activation is still required, and only modest enantioselectivites were observed this report highlighted the capability of molecules containing this cleft framework to direct stereocontrol in organic synthesis. Herein we report the application of a novel class of chiral carbocyclic cleft molecules bearing the amino-thiocarbamate functionality as H-bonding catalysts in the HDA reaction between diene **10** and benzaldehyde **11**. As well as looking at the reactivity of these cleft molecules in the HDA

reaction we also explored the application of the related H-bond donor amino-thiocarbamate functionalised cinchona alkaloid catalysts.

3.3 Results and Discussion

In order to catalyse the HDA reaction and achieve enantiocontrol in the nucleophilic attack of activated aldehydes, there are a few requirements that must be met. First, the catalyst must be able to activate the carbonyl group of the aldehyde by means of H-bond donation; therefore the catalyst must present functional groups capable of H-bond donation. Secondly, the catalyst system must be able to provide enantiofacial discrimination of the *Re-* and *Si-* faces of the π-system in the aldehyde by protecting one face from nucleophilic attack. Directional functionality which facilitates the formation of a substrate-catalyst complex within a chiral environment is a prerequisite. The essential properties of the core carbocyclic cleft framework– the chiral, rigid and aromatic cavity, together with the plethora of synthetic entries which allow for readily tuneable H-bond donor groups to be readily incorporated onto the cleft framework make this molecule an ideal candidate for asymmetric catalysis.

In Chapter 2, the synthesis of a novel family of H-bond donor molecules which have a unique design, featuring two amino-thiocarbamate groups attached to the ridged carbocyclic cleft framework was reported. These cleft molecules present two H-bond donating N–H groups which can in theory be independently tuned by changing the electronic nature of the R substituents (Figure 52).
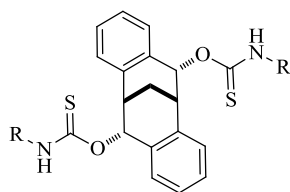
Figure 52: General structure of the amino-thiocarbamate cleft H-bond catalysts.

Enantiopure cleft molecules were synthesised according to the procedures outlined in Chapter 2. Catalyst availability and time restraints meant only the enantiopure clefts (+)**-4**, (+)**-5** and (+)**-7** were screened in the HDA reaction. In addition (+)**-3** and (+)**-2** were also included in this investigation (Figure 53).
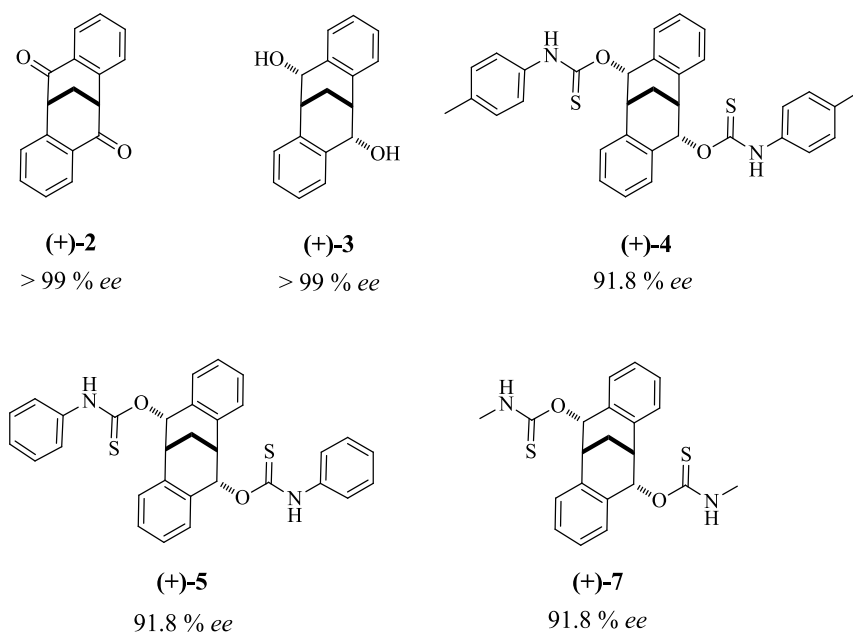
Figure 53: H-bond cleft catalysts screened in the HDA reaction.

3.3.1 Synthesis of Rawel Diene 10

The substrate, aminodiene **10** (Rawel diene) was synthesised over two steps in a one-pot reaction according to the procedure reported by Rawel and co-workers.[76] Commercially available vinylogous amide; *trans*-4-(dimethyl) amino-3-buten-2-one **146** was treated with NaHMDS (sodium hexamethyldisilazide) in THF at -78 °C for 1 h, followed by silylation with TBSCl (tertbutyldimethylsilylchloride) at room temperature for 1.5 h. Bulb-to-bulb distillation (150.3 °C, 110 mbar) of the crude mixture gave the target diene **10** as a light-yellow oil in 86 % yield (Scheme 53).
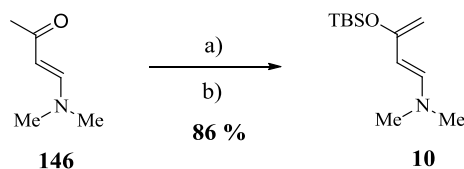
Reagents and conditions: a) NaHMDS (1.0 M in THF), THF, -78 °C, 1 h, N$_2$; b) TBSCl, -78 °C to rt, 1.5 h.

Scheme 53: Synthesis of Rawel diene 10, substrate to the HDA reaction.

3.3.2 Control Experiment- Uncatalysed HDA Reaction

Initially we explored the racemic HDA reaction of diene **10** with benzaldehyde **11**, using reaction conditions reported by Rawel and co-workers.[69]As expected, the reaction

proceeded smoothly at room temperature going to completion in less than an hour, as monitored by TLC. Decomposition of the Diels-Alder adduct **12** with acetyl chloride yielded the target dihydropyranone product **12a** in 82 % yield and < 5 % *ee*, as determined by chiral HPLC analysis with Daicel Chiralcel OD-H (Scheme 54, Appendix 7.16).
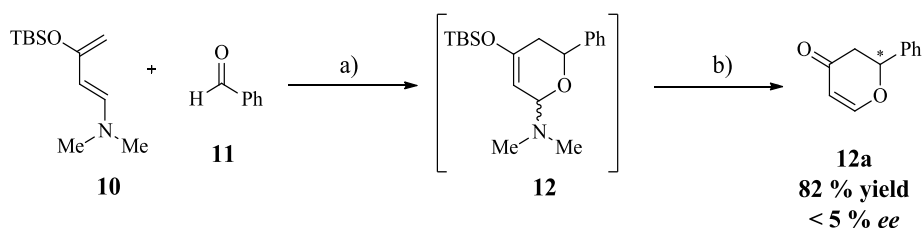
Reagents and conditions: a) CDCl$_3$, rt, 1 h; b) AcCl, CHCl$_3$, -78 $^{\circ}$C, 30 min.

Scheme 54: Control experiment, uncatalysed HDA reaction of diene 10 and benzaldehyde 11.

These results, as well as, ^{1}H NMR spectroscopic data were consisted with the literature; therefore this material was used as a reference standard for *ee* determination of the products from the asymmetric reactions.

3.3.3 Catalyst Screening

Friberg and co-workers general procedure for the asymmetric HDA reaction using 20 mol % catalyst (0.1 mmol), diene **10** (0.5 mmol) and benzaldehyde **11** (1.0 mmol) in toluene at -40 $^{\circ}$C for 48 h, followed by the removal of the TBS and dimethylamino groups with acetyl chloride at -78 $^{\circ}$C was applied to the novel amino-thiocarbamate cleft catalysts **(+)-4**, **(+)-5** and **(+)-7**, as well as **(+)-2** and **(+)-3**.[6] The structure of the isolated products were confirmed by ^{1}H and ^{13}C NMR spectroscopy and the *ee* determined by chiral HPLC analysis. The results from this investigation are summarised in Table 22.

Overall, the yields of the isolated product **12a** were consistent with those reported by Friberg and co-workers during their catalyst screening reactions (Table 21),[6] indicating that these cleft molecules had a catalytic effect on the HDA reaction. However, the amino-thiocarbamate cleft molecules, as well as, the unfunctionalised clefts **(+)-2** and **(+)-3** gave disappointing results in terms of *ee*. In fact, like the amine derived clefts **(-)-86a** and **(+)-99** (Table 21, entries 13 and 12), these clefts failed to direct any enantioselectivity in the HDA reaction. These results support the notion that amine H-bonding is not efficient in catalysing the HDA reaction.[6] Until an inclusion complex of one of the enantiopure amino-thiocarbamate clefts with benzaldehyde can be accessed the mode of catalyst-substrate

binding remains unknown, as a result we can only make assumptions about these interactions in an attempt to explain the complete loss of enantioselectivity when these clefts were used as H-bonding catalysts.

Table 22: Results from the application of H-bond cleft catalysts in the HDA reaction.
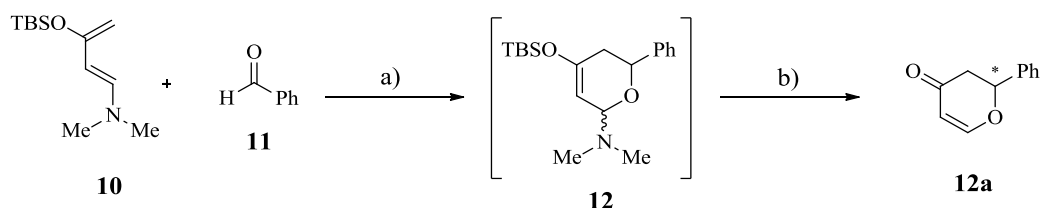
Reagents and conditions: a) catalyst (20 mol %), toluene, -40 °C, 48 h; b) CH₃COCl, CH₂Cl₂, -78 °C, 15 min.

Entry	Catalyst	*ee* (%)[a]	Yield (%)[b]
1	-	<5	5
2	(+)-**2**	<5	14
3	(+)-**3**	<5	30
4	(+)-**3**[c]	<5	47
5	(+)-**4**	<5	49
6	(+)-**5**	<5	31
7	(+)-**7**	<5	30

[a] Determined by HPLC analysis on Chiralcel OD-H column, 85:15 hexane, 2-propanol, 0.6 mL min⁻¹, 214 nm detector.
[b] Isolated yields.
[c] Stoichiometric amounts of catalyst used.

The disappointing results reported above may be a result of unproductive self-associative interactions between cleft molecules. These interactions could essentially prevent substrate organisation and H-bond activation of the benzaldehyde substrate. As discussed in Chapter 2, X-Ray crystallographic analysis of the amino-thiocarbamate cleft structures, showed that the amine N–H and sulphur groups in clefts (+)-**4** and (±)-**5** are pointing away from the chiral cavity of the cleft lending themselves to form strong-centrosymmetric N–H···S H-bonds with each other (Figure 54).

a)
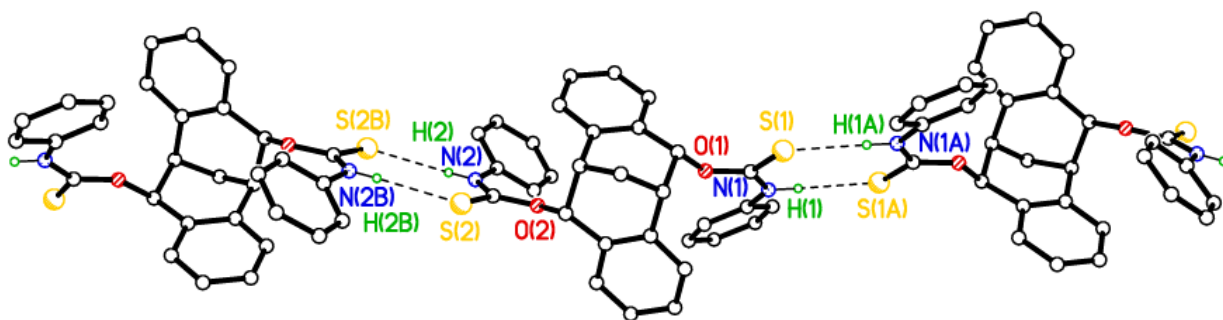
b)
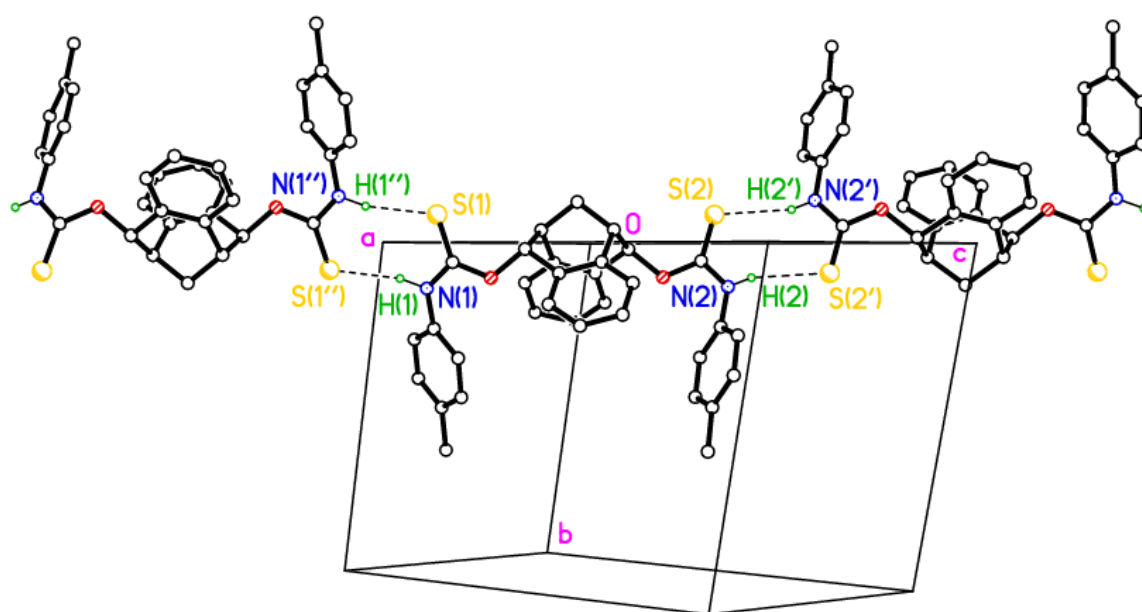
Figure 54: a) The H-bond network in the crystal structure of (±)-5. b) The H-bonding network in the crystal structure of (+)-4. In both examples, the amine and sulphur groups are pointing away from the cavity of the clefts resulting in pairs of centrosymmetric N–H···S H-bonds.

On the other hand, in the example of (±)-**7**, the X-Ray crystal structure showed that the H-bonding N–H groups are pointing into the cleft cavity. With this orientation of the H-bonding donor groups, it would be expected that H-bond interactions between the cleft and substrate would facilitate binding of **10** within the cavity of the cleft, therefore within a chiral environment. However, X-Ray crystal structures of this cleft indicate that the molecules are linked via N–H···S H-bonds into chains / ladders, where the apex of one molecule is accommodated in the cleft of another to form columns of apex-to-base stacked molecules

(Figure 55). Like in the above examples, these interactions between cleft molecules may prevent substrate-organisation and therefore hinder the ability of the cleft to direct any stereocontrol in the HDA reaction.
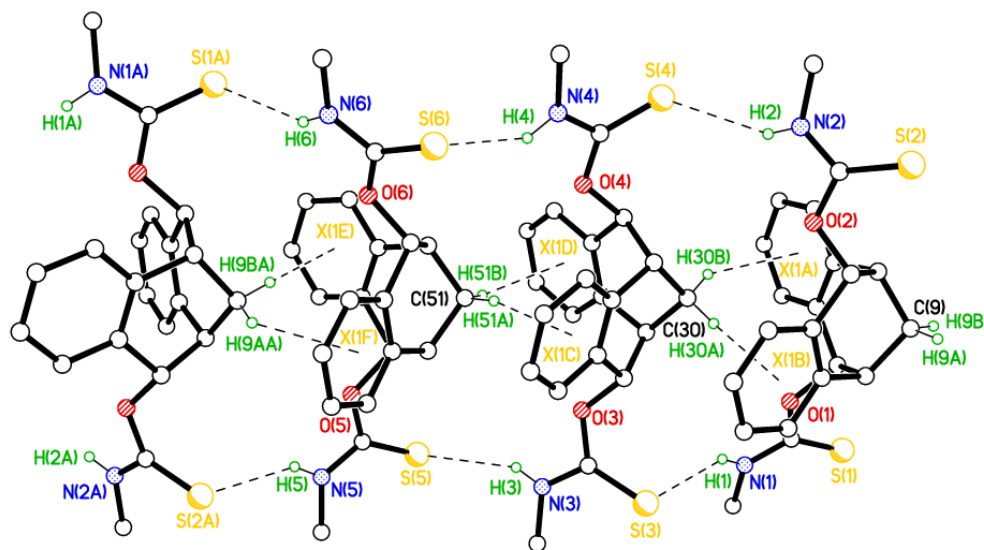
Figure 55: H-bond network displayed by molecules of (±)-7.

Although these clefts failed to induce any enantioselectivity in the HDA reaction they did have a notable catalytic effect. Under the same reaction conditions, the yields of the catalysed reactions were considerably higher than those observed for the uncatalysed reaction and the reaction with catalytic amounts of **(+)-2**, which has no ability to H-bond (Table 22, entries 1 and 2). With this in mind it is possible to assume that these clefts activated **10** by means of H-bond donation however, because the H-bond donor N–H groups are pointing outwards from the chiral cavity, in **(+)-4** and **(+)-5**, benzaldehyde would reside outside the chiral cleft cavity, resulting in both the *Re-* and *Si-* faces of the π-system of the carbonyl group being exposed to nucleophilic attack by the diene **11** (Figure 56).
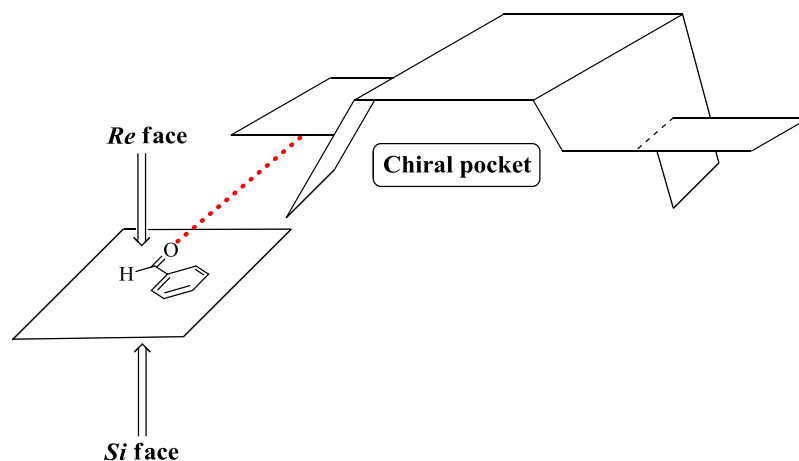
Figure 56: Model illustrating how binding outside the chiral cavity generated by the molecular cleft results in no discrimination between the *Re*- and *Si*- face of benzaldehyde.

Although both amine groups in **(+)-7** are directed into the cleft cavity they are too far apart to facilitate intramolecular co-operative H-bonding (Figure 57).
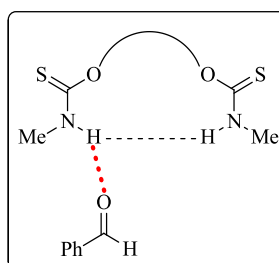
Figure 57: The H-bond amine groups in (+)-7 are too far apart to facilitate co-operative H-bond activation of benzaldehyde

Similarly, the two N-H H-bond donor groups in **(+)-7** may be too far apart for double H-bond activation (**B**) (Figure 21) to be a viable mode of activation. It is possible that the clefts activate the carbonyl group in **11** by single H-bond activation however; this may place the benzaldehyde molecule at distances that are too far remote for the chiral cleft to have any stereocontrol. In fact, the X-Ray crystal structure we obtained for the related diphenyl cleft **(±)-102** H-bonded to a molecule of 3-bromopyridine (Chapter 2), demonstrates the binding of guest molecules *exo-* to the cleft cavity, which supports this theory (Figure 58).
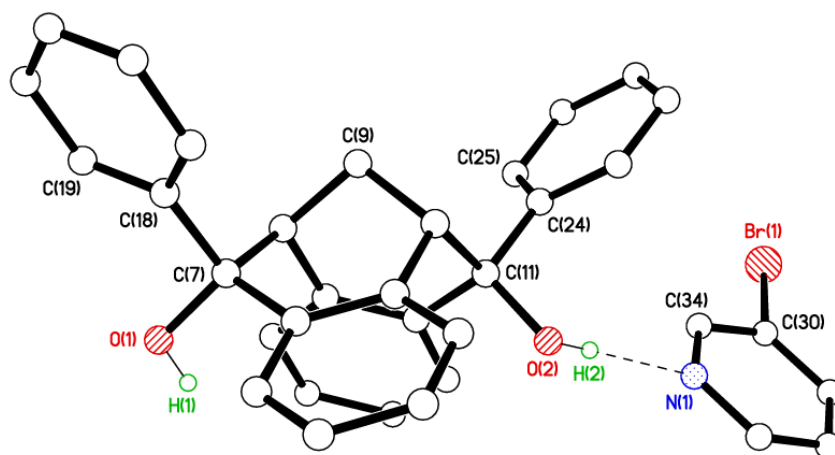
Figure 58: X-Ray crystal structure of diphenyl cleft (±)-102 H-bonded to a molecule of 3-bromopyridine 121. The guest molecule 121 is situated *exo-* to the cleft cavity.

An alternative explanation to the lack of enantioselectivity observed in these reactions involves consideration of the inclusion complexes obtained for cleft **(±)-4** and a molecule of acetonitrile, as well as, the relatively new X-Ray crystal structures obtained by the Kimber group during a series of binding studies, of inclusion complexes involving the 4-pyridyl cleft **(±)-112b** and phenyl boronic acid (Chapter 1).

In both examples, guest molecules are bound to the functionalised cleft molecules via a pair of C–H···π interactions, which position the guest molecules almost centrally within the cleft cavity (Figure 59). Without additional evidence to support this we can only speculate that similar interactions exist between the amino-thiocarbamate clefts and **11**. The positioning of **11** almost central within the cleft cavity would achieve a suitably rigid catalyst-substrate complex which should in theory facilitate the enantioselective HDA reaction.

However, the lack of *ee* observed when the amino-thiocarbamate clefts were applied as asymmetric catalyst in this HDA reaction may be because the H-bond donor groups capable of activating **11** towards nucleophilic attack, in **(+)-4** and **(+)-5** are pointing away from the interior of the cleft cavity. Consequently, molecules of **11** bound by C–H···π within the chiral cleft cavity will not be sufficiently activated for attack by **10**. Meanwhile, molecules of **11** bound to the cleft by single N–H H-bonds which lay external to the cleft cavity are activated towards nucleophilic attack and therefore, react more readily with **10** resulting in a HDA reaction that lacks any enantioselectivity. Whilst this model cannot be ruled out we are yet to access a cleft-benzaldehyde complex to support this theory.

103

a)
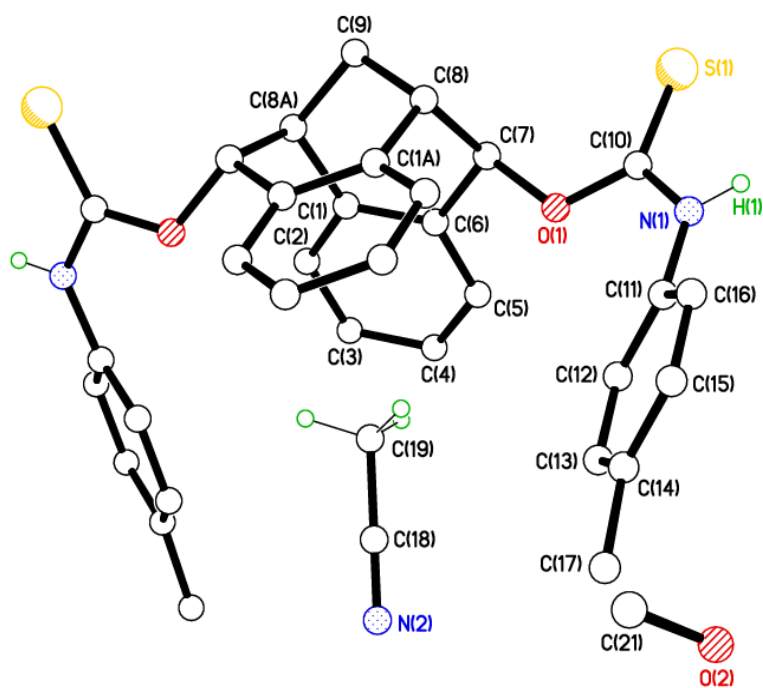
b)
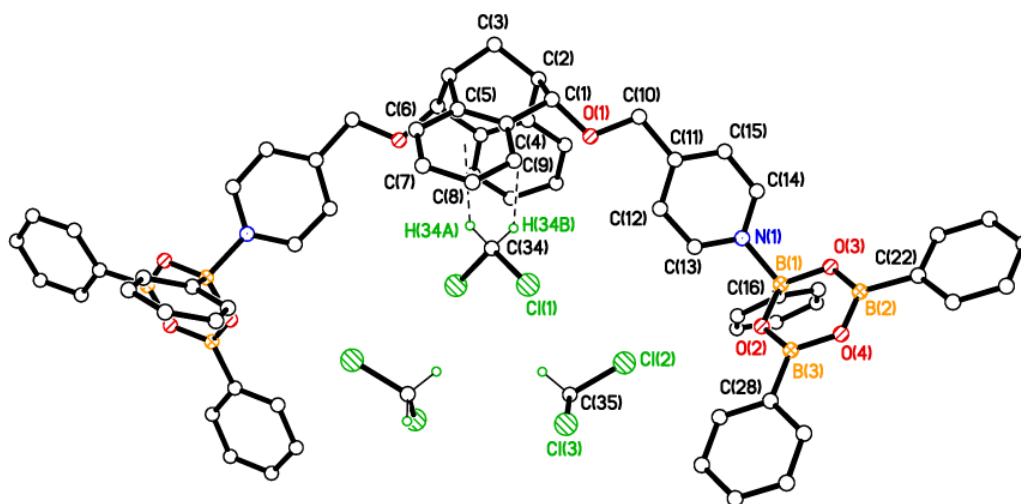
Figure 59: a) The X-Ray crystal structure of (±)-4 showing the C–H···π binding of a solvate molecule of acetonitrile within the cleft cavity; b) The X-Ray crystal structure of (+)-112b / CH₂Cl₂ showing the C–H···π binding of CH₂Cl₂ solvate molecules within the cleft cavity.

The relative stereochemical arrangement of the catalyst functional groups in a manner, that is conducive for the nucleophile / electrophile activation is an important

consideration in the catalyst design and may go a long way in explaining why the cleft catalysts did not have any stereochemical control in the HDA reaction. Although these results were disappointing in terms of the application of these cleft derivatives as enantioselective organocatalysts they performed well at catalysing the HDA reaction. More in-depth studies involving optimisation of reaction conditions and complex binding experiments can be expected to provide a better understanding of this catalyst system. In addition the structure of the cleft can be easily modified by varying the substituents, which could be used for tailoring the system for the recognition of specific substrates and / or to improve the interaction with various aldehydes to facilitate the HDA reaction. Whilst the performances of these amino-thiocarbamate cleft derivatives as enantioselective organocatalysts were inferior in this reaction, they may be useful in other organocatalytic reactions. These initial results as well as the possibility to use these clefts in other reactions lend itself to be the focus of subsequent research projects.

In light of the poor efficiency afforded by the amino-thiocarbamate clefts catalysts, we began to search for an alternative strategy to achieve efficient asymmetric catalysis of the HDA reaction. Here in, the application of cinchona alkaloid derived bifunctional catalysts incorporating the amino-thiocarbamate H-bond donor functional group as asymmetric catalysts in the HDA reaction between **10** and **11** is reported.

3.4 Bifunctional H-Bond Donor Catalysts

The development of chiral catalysts capable of simultaneous activation of a nucleophile and an electrophile is an active area of investigation.[77] Much of the pioneering research in this field has involved Lewis acids equipped with additional Brønsted or Lewis basic functionality. In recent years, dual activation strategies involving H-bonding for electrophile activation have been reported. Progress in this area has been accomplished through the discovery of new applications for existing, naturally occurring catalysts, as well as through the design and synthesis of novel bifunctional entities based on known H-bond donor motifs

3.4.1 Cinchona Alkaloid Catalysts

Cinchona alkaloid derivatives modified to include H-bonding components have emerged in the last couple of years as readily accessible, robust and tuneable bifunctional organocatalysts for a range of synthetically useful transformations. The naturally occurring

cinchona alkaloids are an ideal choice as chiral inducers because they are; abundantly provided by nature, commercially available at relatively moderate prices, readily modified structurally for diverse catalytic applications and readily obtainable in diastereomeric pairs, allowing access to either enantiomeric products. Consequently, the synthetic potential of this class of catalyst has been quickly recognised and exploited by several research groups. The key to their success is an ability to interact with both the nucleophilic and electrophilic reaction components simultaneously and to control their encounter in a well-defined chiral environment (Figure 60).[47]

C-9 stereocentre
- synthetic route makes both diastereomers avaliable

quinuclidine tertiary amine ring
- variable absolute configuration at C-8

nucleophile activation

electrophile activation

(+)-146
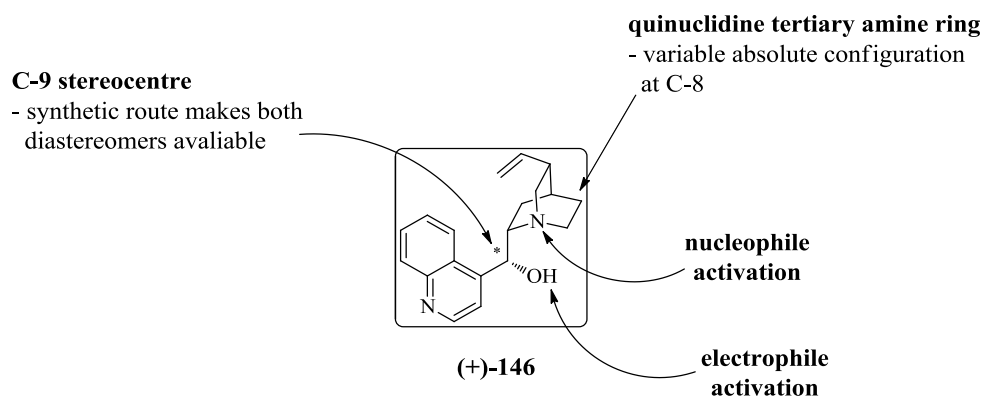
Figure 60: Structural features of cinchona alkaloid derivatives which make them an attractive class of asymmetric organocatalysts.

Investigations into the potential mechanism of asymmetric catalysis by cinchona alkaloids using computational methods has shown that the mode of catalysis involves both the quinuclidine nitrogen to activate the nucleophile via general base catalysis and the hydroxyl group at the C-9 position to activate the electrophile via H-bond interactions.[77] Essentially, the two functional groups provide specific enzyme-like interactions that pre-organise and orientate the reactants in an optimum position for reaction. The highly structured transition state, generated by these catalysts is stabilised by a network of H-bonds and accounts for their ability to direct the stereochemical outcome of the reaction.

3.4.1.1 Amino-thiocarbamate Functionalised Cinchona Alkaloid Catalysts

Derivatisation of the cinchonine framework by substituting the C-9–OH group with other H-bond donating groups has been investigated by several research groups, the rationale being to combine the catalytic and H-bond donating ability of these groups with that of the cinchona framework. The stereochemistry of bulky groups at C-9 also have the potential to direct the rigidity and conformational stability of the transition-state intermediates and hence,

106

the stereochemical outcome.[47] With this in mind, we proposed that the family of amino-thiocarbamate cinchona alkaloid derived catalyst, first synthesised in 2010 by Yeung and co-workers,[43] could be used to catalyse the asymmetric HDA reaction between benzaldehyde **11** and Rawel diene **10**. It was thought that the HDA reagents could be activated via a network of H-bonds originating from the H-bond donor amino-thiocarbamate groups at the C-9 position, within the 'chiral pocket' generated by the cinchona framework, thus creating a ridged transition state capable of directing the stereochemical outcome of the reaction (Figure 61).

C-9 stereocentre

quinuclidine tertiary amine ring
- potential to activate Rawel's diene **10**
- located in close proximity to the amino-thiocarbamate group

amino-thiocarbamte moiety
- capable of activating the electrophilic carbonyl group in **11**
- provides protons avaliable for H-bond donation

amino-thiocarbamate N-aryl group
- relatively unhindered (facilitates selective substrate binding orientation)
- substitution (hence pk_a and binding ability) variable

Figure 61: Design rationale for amino-thiocarbamate-substituted cinchona alkaloid catalysts and their application as asymmetric catalysts in the HDA reaction.

Yeung and co-workers had reported that these catalysts could be accessed over one-step starting from commercially available (+)-cinchonine (+)**-146**. Treatment of (+)**-146** with sodium borohydride in the presence of a substituted isothiocyanate at room temperature led to the synthesis of 6 novel amino-thiocarbamate cinchona catalysts with R substituents ranging from electron withdrawing groups (R = $Ph(CF_3)_2$) to sterically bulky *t*-butyl groups.[43] The relative ease in which this family of catalysts could be accessed made them particularly attractive to our group.

3.4.2   Cinchona Alkaloid Catalysed HDA Reaction

Using the reaction conditions reported by Yeung and co-workers, we successfully synthesised the amino-thiocarbamate derived cinchona alkaloid catalysts (+)**-13**, (+)**-147**,

(+)-148 and a novel catalyst incorporating the *p*-tolyl substituted amino-thiocarbamate group **(+)-149** (Scheme 55).

(+)-**13:** R = Ph(OMe)$_2$ **71 %**
(+)-**147:** R = Ph   **64 %**
(+)-**148:** R = Ph(CF$_3$)$_2$ **16 %**
(+)-**149:** R = PhMe   **67 %**

(+)-**146**
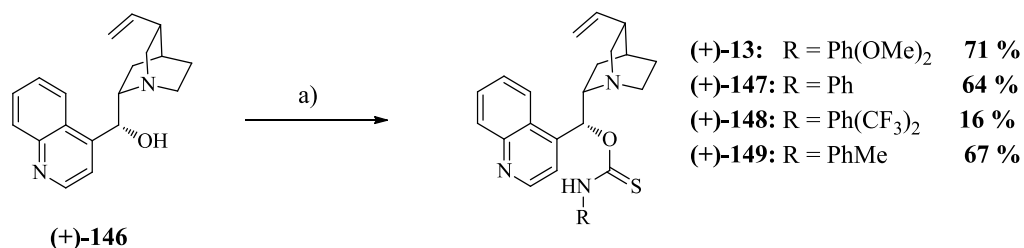
Reagents and conditions: a) NaH, RNCS, THF, rt, 18 h.
Scheme 55: Synthesis of amino-thiocarbamate cinchona alkaloid catalysts.

Following synthesis and characterisation, these catalysts were then examined as for catalytic activity in the HDA reaction between **10** and **11**. Using the general procedure reported by Friberg and co-workers the cycloaddition reactions were carried out in toluene at -40 °C for 48h, in the presence of the indicated catalyst, followed by acetyl chloride removal of the TBS and dimethylamino groups.[6] Catalysts (+)-**13**, (+)-**147** and (+)-**149** as well as (+)-**146** were included in this investigation. Table 23 summarises the results of these catalyst screening reaction.

When the unfunctionalised cinchonine framework (+)-**146** was used in catalytic amounts (20 mol %) the cycloaddition product **12a** was afforded in 67 % yield, although no enantioselectivity was observed (Table 23, entry 2). At this temperature the uncatalysed HDA reaction affords a significantly lower yield (Table 23, entry 1), thus indicating that the cinchonine core alone has a catalytic effect on the HDA reaction. Presumably this catalytic affect is the outcome of H-bonding between the hydroxyl group at C-9 on cinchonine and the carbonyl group of benzaldehyde. This H-bonding potentially lowers the energy of the LUMO in **11** therefore, activating it for nucleophilic attack by the diene **10**. A direct comparison between the catalytic activity of (+)-**146** (Table 23, entry 1) and the amino-thiocarbamate cinchonine derivatives (+)-**13**, (+)-**147** and (+)-**149** (Table 23, entries 3–9) indicate that the amino-thiocarbamate moiety facilitates the enantioselective cyclisation reaction. This suggests that the cinchonine core and the amino-thiocarbamate groups at the stereogenic C-9 position work cooperatively to catalyse the enantioselective HDA reaction, reinforcing the bifunctional nature of this family of catalysts.

Table 23: Results from the application of the amino-thiocarbamate cinchona alkaloid catalysts in the HDA reaction.
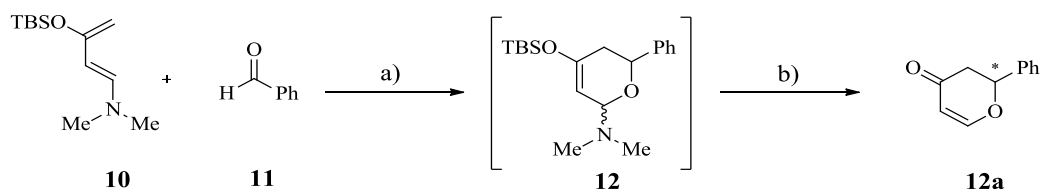
Reagents and conditions: a) catalyst (20 mol %), toluene, 48 h; b) CH₃COCl, CH₂Cl₂, -78 °C, 15 min.

Entry	Catalyst	Temperature (°C)	*ee* (%)[a]	Yield (%)[b]
1	-	-40	<5	5
2	(+)-146	-40	<5	67
3	(+)-13	-40	22	53
4	(+)-13[c]	-40	60	74
5	(+)-13	-78	31	40
6	(+)-13	0	21	12
7	(+)-147	-40	<5	44
8	(+)-149	-40	14	84
9	(+)-149[c]	-40	28	55

[a] Determined by HPLC analysis on Chiralcel OD-H column.
[b] Isolated yields.
[c] Catalyst used in stoichiometric amounts.

The electronic character of the amino-thiocarbamate *N*-aryl substituent was found to play a crucial role in the enantioselectivity. Catalyst (+)-13 containing two electron-rich methoxy groups afforded the highest *ee* of 22 % (Table 23, entry 3). Replacing the methoxy groups with a methyl group in the *para* position in (+)-149 gave excellent yields however, there was a noticeable reduction in the enantioselectivity compared to (+)-13 (Table 23, entry 8). Reducing the electron density of the aromatic substituent further in (+)-147 led to complete loss of *ee* (Table 23, entry 7). Mechanistically, these observations suggest that the acidity of the amino-thiocarbamate NH may be important to the enantioselectivity. This could be attributed to the strength of the H-bond interaction between N–H and the carbonyl group in 11. These observations are consistent with those reported by Yeung's group in their application of these catalysts in the asymmetric bromolactonisation of unsaturated carboxylic acids.[43]

To probe the effect of these molecules further both catalysts (+)-**13** and (+)-**149** were used in stoichiometric amounts. Under these conditions a notable difference in the isolated yields and enantioselectivites were observed (Table 23, entries 4 and 9). Whilst stoichiometric amounts of (+)-**149** led to a decrease in the isolated yield (55 % compared to 84 %) the enantioselectivity of the reaction increased to 28 % *ee* (Table 23, entries 8 and 9). Stoichiometric amounts of (+)-**13** resulted in an increase in the yield of **12a** from 53 % to 74, moreover the *ee* of the cycloadduct **12a** increased to 60 % (Table 23, entries 3 and 4). These results suggest that when the amino-thiocarbamate catalysts are used in catalytic amounts (20 mol %) at -40 $^{\circ}$C there are potentially two competing pathways; the catalysed reaction vs the uncatalysed reaction (Scheme 56).
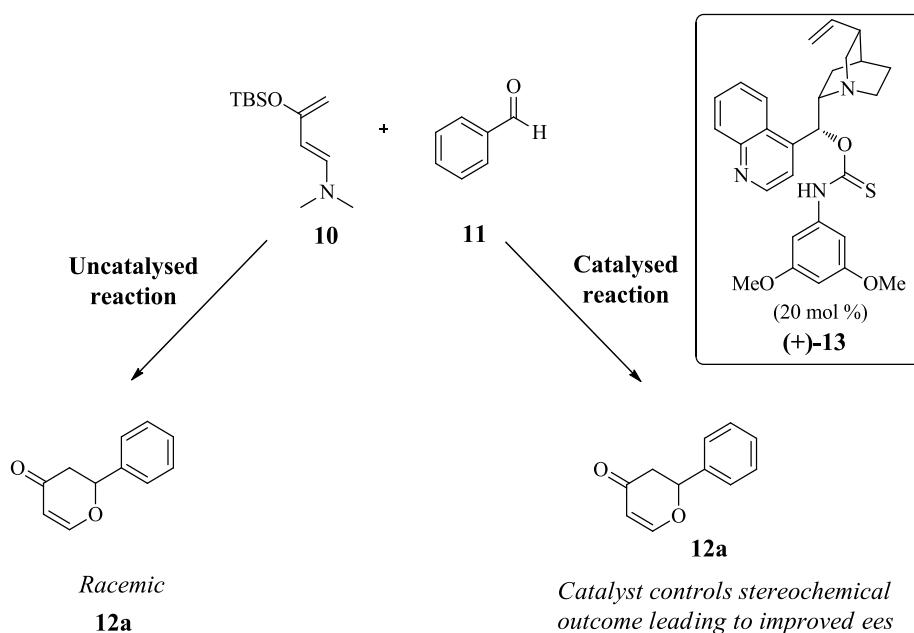
Scheme 56: Competing pathways in the catalysed HDA reaction at -40 $^{\circ}$C.

This is supported by a change in the *ee* of **12a** when the reaction was performed at different temperatures. Using the best catalyst (+)-**13** (20 mol %) the HDA reaction was carried out at both -78 $^{\circ}$C and 0 $^{\circ}$C (Table 23, entries 5 and 6). Whilst the reduction in *ee* at 0 $^{\circ}$C is negligible when compared to the results observed at -40 $^{\circ}$C, when the reaction was performed at -78 $^{\circ}$C there was a more noticeable increase in *ee*, from 22 % to 31 % (Table 23, entries 3 and 5). This implies that the uncatalysed reaction is inhibited at lower temperatures whilst the catalysed reaction proceeds readily at these temperatures. At -78 $^{\circ}$C it would appear that the competition between the two alternative pathways is significantly reduced; only substrate

molecules activated by the catalyst undergo the cycloaddition reaction, resulting in the formation of **12a** in higher *ee*.

Whilst these results are not conclusive they are encouraging in terms of the ability of these molecules to be used as asymmetric catalysts in the HDA reaction. More in-depth studies are required to understand the mode in which these catalysts activate the substrate molecules in particularly how they affect the stereochemical outcome of the cycloaddition reaction. In addition, substrates other than benzaldehyde may be expected to provide a better fit into this catalyst system leading to better yields and higher *ee* values. Assumptions have been made with regards to the involvement of the amino-thiocarbamate moiety in terms of H-bond activation of **11** however; the role of the quinuclidine tertiary amine ring is not yet understood. Potentially it acts in a bifunctional manner with the amino-thiocarbamate group whereby both functional groups simultaneously activate **10** and **11**. Alternatively, it locks **11** in a 'chiral pocket' within the catalyst framework and acts by blocking either the *Re-* or *Si-*face of the carbonyl group meaning nucleophilic attack is only permitted from one side. Catalyst-substrate binding studies such as X-Ray crystallographic analysis of complexes between the catalyst and HDA reactants can be expected to provide valuable information regarding this catalyst system.

During these preliminary studies, the reaction yields ranged from moderate to excellent, while the *ee* values were significantly affected by the nature of the *N*-aryl substituents, as well as by changes in the reaction temperature. Overall, we noticed several important phenomena that may help us understand important aspects of these molecules and how they function as enantioselective organocatalysts in the HDA reaction: (1) the cinchonine core has a catalytic effect on the HDA reaction, however the amino-thiocarbamate functional group is required for any enantioselectivity to be observed; (2) having an electron-rich aromatic system attached to the amino-thiocarbamate group appears to be important. A possible consequence is a reduction in the acidity of the N–H group may be beneficial to the enantioselectivity of the reaction; (3) the uncatalysed reaction pathway competes with the catalysed reaction at -40 $^{\circ}$C thus variation of other reaction parameters including temperature, reaction time, solvent and additives may help improve the enantioselectivity without loss of efficiency.

3.5 Asymmetric Bromolactonisation Reactions

In addition to exploring the catalytic properties of the novel amino-thiocarbamate clefts in the HDA reaction, we performed a series of preliminary experiments in an attempt to evaluate their ability to act as asymmetric H-bond catalysts in the bromolactonisation reaction of unsaturated carboxylic acids. Inspired by the number of elegant reports emerging for the use of organocatalysts incorporating the amino-thiocarbamate functional group in enantioselective bromolactonisation reactions, which give access to a range of valuable halolactones with a practical level of enantioselectivity, the bromolactonisation reaction between 4-phenyl-4-pentenoic acid **18** and *N*-bromosuccinimide (NBS) **19** was selected as a second test reaction for the application of these catalysts (Scheme 57).
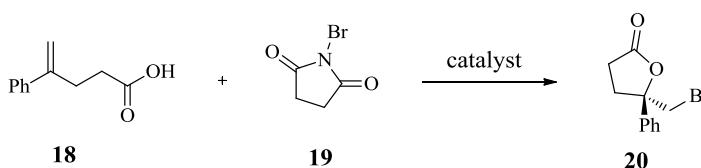
Scheme 57: General reaction scheme for the bromolactonisation reaction of the unsaturated carboxylic acid 18 and NBS 19 to give the γ-lactone 20.

3.5.1 Halolactonisation Reactions

Electrophilic halolactonisation reactions give access to biologically relevant molecules whether directly as bioactive natural products or as valuable synthetic intermediates they are therefore, an important class of organic transformation. Halolactonisation reactions, involve intramolecular nucleophilic species attacking the carbon-carbon double bond of an alkene which is activated by electrophilic halogenated reagents to give cyclic compounds (Scheme 58).[78]
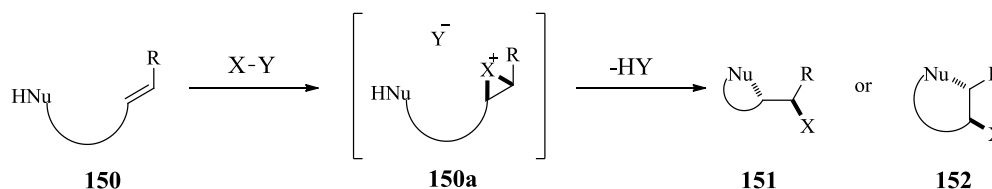
Scheme 58: General reaction scheme for the halolactonisation of functionalised alkenes.

Haloethers, halohydrins, dihalides, haloamines and halolactams are just some of the products which can be accessed through these cyclisation reactions. In fact of the several thousand known halogenated natural product architectures the majority possess domains that

are the result of at least one electrophilic halocyclisation reaction. In addition to the obvious importance and utility of the products of these transformations, exploration into the effects of substrate structure and subsequent interactions with catalysts, has led to synthetically useful improvements in cyclisation selectivity. However, the development of catalytic enantioselective halocyclisation methods remains a formidable task and presents a unique challenge and opportunity for various paradigms of catalysis. As a result, the design of new chiral catalysts for asymmetric halocyclisation reactions is a topic of increasing interest in synthetic organic chemistry and is currently a highly active field of research.

Mechanistic studies initiated by Brown and co-workers identified a serious obstacle in the development of catalytic enantioselective iodination and bromination methods, specifically, the susceptibility of iodonium and bromonium ions to undergo degenerate halogen exchange with alkenes (Scheme 59).[78,79]
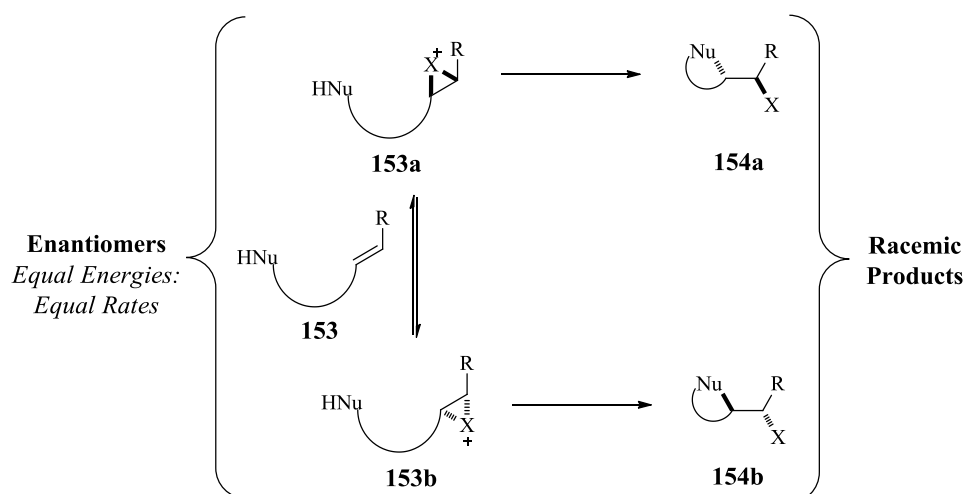
Scheme 59: The racemisation of halonium ions by degenerate exchange.

The predicament invoked by this halonium transfer is that this process racemizes the halonium ions, **153a** and **153b**, at rates that can compete with nucleophilic capture. This means that delivery of a halonium equivalent to only one face of the double bond could be inefficient in terms of enantiocontrol since the resultant halonium ion intermediate could, prior to cyclization, rapidly transfer its halogen atom to an unreacted alkene and thereby erode any initial facial selectivity.[78] The majority of recent research in this field has been focused on developing synthetic strategies which have the potential to prevent this or other racemisation processes. For instance, the development of chiral catalysts that remain bound to the halonium ion until newly created stereocenters are irreversibly set, thus maintaining a

chiral environment, regardless of exchange, has proven to be an effective strategy. It is this concept that we sought to manipulate by application of the amino-thiocarbamate cleft catalysts.

3.5.2 Asymmetric Bromolactonisation Reactions

Stereoselective, electrophile-promoted nucleophilic addition reactions to alkenes are efficient methods for the preparation of a multitude of stereo-defined synthetically relevant acyclic and heterocyclic structures. Despite the significance of these transformations, catalytic enantioselective variants are, with few exceptions outside of transition-metal initiated processes, limited due to the lack of suitable enantioselective organocatalysts.

In 2007, Denmark and co-workers reported the use of sulfur Lewis base catalysts in the activation of a phenylselenium group for electrophilic lactonisation (Scheme 60).[51]
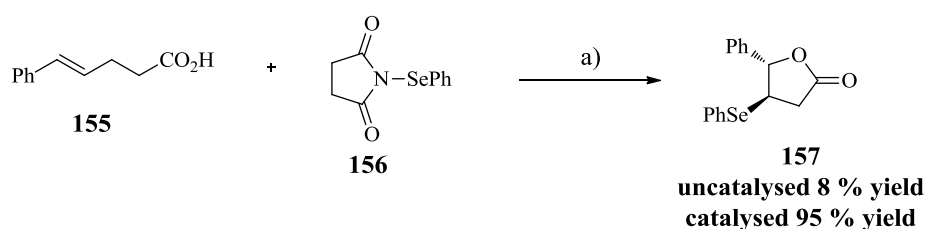
Reagents and conditions: a) Lewis base catalyst: $(Me_2N)_3P=Se$ (0.10 eq), CH_2Cl_2, 23 ^{o}C, 3h.

Scheme 60: Denmark and co-workers Lewis base catalysed selenolactonisation reaction.

The group suggested that if a chiral Lewis base was used, the reaction pathway would occur in a chiral environment and therefore allow for enantiotopic face selection in the lactonisation reaction. This seminal work has led to the development of several catalytic systems capable of directing the stereochemical outcome of a range of lactonisation reactions.

The first of these enantioselective halolactonisation reactions was reported less than 5 years ago in 2010 by Tang and co-workers.[80] The group reported that modified Cinchona alkaloids such as cinchonidine urea (+)-**160** are capable of catalysing the NBS-induced enantioselective bromolactonisation of 1,3-enynes **158** via conjugate opening of achiral bromonium ions. Under these reaction conditions 6- and 7- membered-ring lactones with pendant allenes bearing axial chirality were accessed in up to 92 % *ee* (Scheme 61).
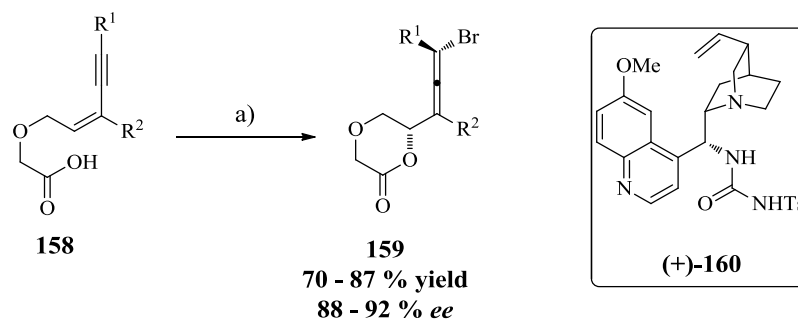
Reagents and conditions: a) (+)-**160** (20 mol %), NBS (1.2 eq), ClCH₂CH₂Cl, rt, 0.5 – 10 h.

Scheme 61: Tang and co-workers enantioselective bromolactonisation of conjugated (Z)-enynes.

More recently in 2012, Fujioka's group disclosed the C_3-symmetric chiral organocatalyst **163**, which is capable of producing enantioenriched bromolactones in the presence of the brominating reagent 1,3-dibromo-5,5-dimethylhydantoin (DBDMH) (Scheme 62).[81]
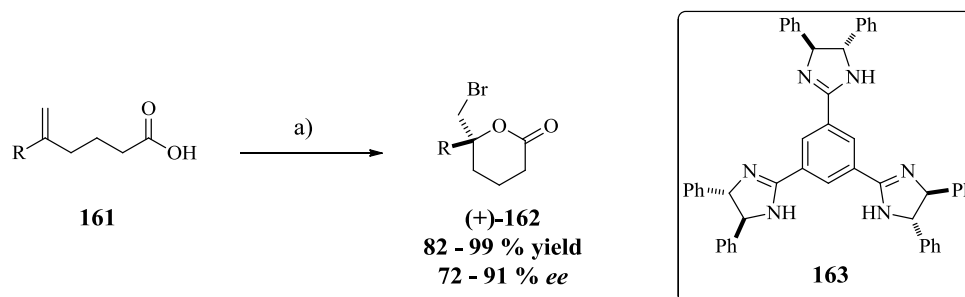
Reagents and conditions: a) cat **163** (10 mol %), DBDMH (1.0 eq), PhMe, -40 °C, 4–46 h.

Scheme 62: Fuijoka and co-workers enantioselective bromolactonisation reaction using the C_3-symmetric chiral organocatalyst 163.

3.5.3 Amino-thiocarbamate Catalysts in Asymmetric Bromolactonisation Reactions

Of particular interest to this research project is the work reported by Yeung and co-workers whom in 2010 published an organocatalytic approach for the synthesis 5-membered-ring bromolactones using the previously mentioned bifunctional chiral amino-thiocarbamate catalyst (+)-**13**. The scope of this reaction and catalyst system was evidenced by the synthesis of 22 examples of γ-lactones in excellent yields and *ee* values, starting from a range of 1,1-disubstituted alkenoic acids **164** (Scheme 63, a). To demonstrate the synthetic utility of this methodology, the optimised protocol was applied to the 1,2-disubstituted alkene substrate **166** to give the δ-lactone **167** in good yield and *ee* (Scheme 63, b).[43]

115

a)

164

a)

165
67 - 99 % yield
28 - 93 % ee

(+)-13

b)

166

a)

167
80 % yield
80 % ee
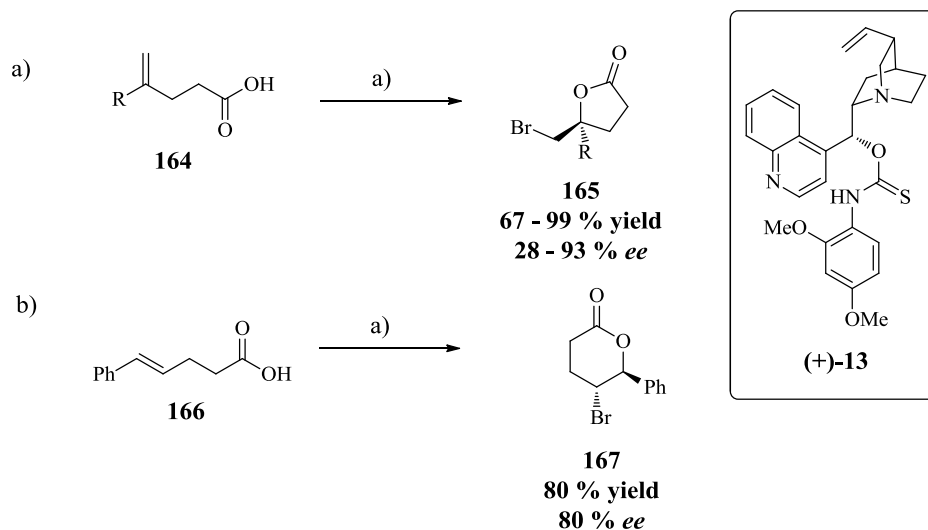
Reagents and conditions: a) **(+)-13** (10 mol %), NsNH$_2$ (50 mol %), CHCl$_3$/PhMe (1:2), -78 $^\circ$C , 20 – 126 h.

Scheme 63: Yeung and co-workers reported asymmetric bromolactonisation reactions catalysed by an amino-thiocarbamate cinchonine catalyst (+)-13.

Soon thereafter the same group reported the efficient and enantioselective bromolactonisation of a range of 1,2-disubstituted alkenoic acids using an amino-thiocarbamate catalyst **(+)-170** derived from (+)-quinidine. This catalyst led to the formation of γ-lactones containing two chiral centres with excellent yields (up to 99 %) and *ee* values (up to 95 % *ee*) (Scheme 64).[50]

168

a)

169
44 - 99 % yield
61 - 95 % ee

(+)-170
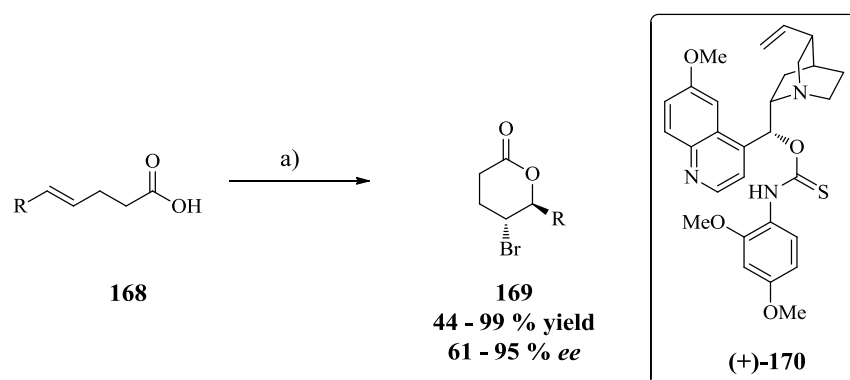
Reagents and conditions: a) **(+)-170** (10 mol %), NBS, CHCl$_3$/PhMe (1:2), -30 $^\circ$C to -78 $^\circ$C, 14-80 h.

Scheme 64: Enantioselective bromolactonisation of 1,2-disubstituted alkenoic acids using amino-thiocarbamate catalyst (+)-170.

Further elaboration of this catalyst system led Yeung and co-workers to develop the enantioselective organocatalytic bromoaminocyclisation reaction using the amino-thiocarbamate catalyst **(+)-173**. This catalyst was used in the facile and efficient

116

enantioselective bromoaminocyclisation of a range of unsaturated sulphonamides **171**, which gave a range of enantioenriched pyrrolidines **172** with up to 99 % yield and 99 % *ee* (Scheme 65).[49]
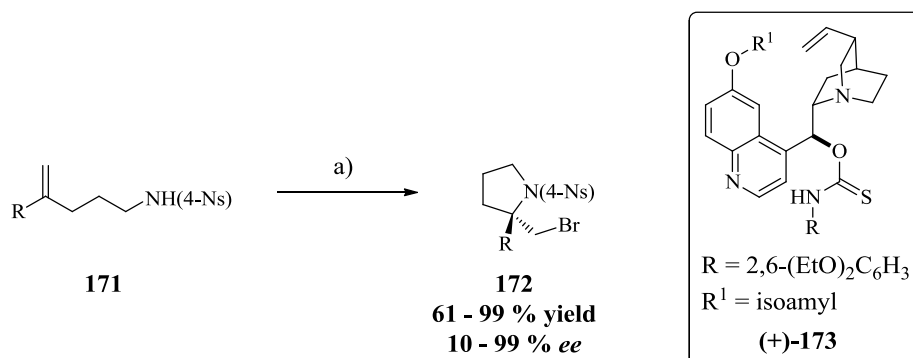
Reagents and conditions: a) (+)-**173** (10 mol %), NBS, -62 °C, 3–6 days.

Scheme 65: Asymmetric bromoaminocyclisation of unsaturated sulfonamiodes using an amino-thiocarbamate catalyst.

To gain an understanding into how these amino-thiocarbamate catalysts activate the reagents and induce enantioselectivity in the bromolactonisation reactions, Yeung and co-workers examined several catalyst analogues of the cinchonine derived amino-thiocarbamate (+)-**13**. The group discovered that replacing the S and / or N–H with O, or N–H with N–Me in catalyst was ineffective in offering appreciable *ee* in the bromolactonisation of **18**. Replacing the thiocarbamate group with the well-known double H-bond catalyst, thiourea led to a complete loss of enantioselectivity. Based on these observations the group proposed that either pure Lewis-base or H-bond activation of NBS is unlikely to be the sole origin of enantioselectivity in the bromolactonisation reaction. Taking into account the importance of both the N–H and sulphur of the amino-thiocarbamate group towards enantioselectivity, an intermediate involving dual activation of NBS was proposed (Figure 62).[43]

117

174
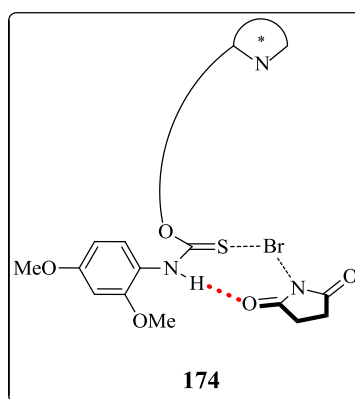
Figure 62: Proposed mechanism of dual activation of NBS by amino-thiocarbamate catalysts.

This mechanism was extended to account for the enantioselectivites observed. Thus a ridged transition state which prevents the problematic olefin-olefin halogen exchange racemization was proposed (Figure 63).[43]

175
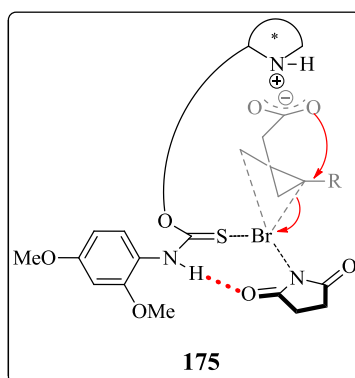
Figure 63: Proposed transition state structure and mechanism of the enantioselective bromolactonisation reaction.

In this model, the quinuclidine component interacts with the nucleophilic carboxylic acid, and the electron rich 2,4-dimethyoxyphenyl ring acts as a steric screening group, as well as, controlling the acidity of the thiocarbamate N–H group. With this proposed arrangement of substrates within the chiral 'pocket' defined by the (+)-cinchonine framework, intramolecular nucleophilic attack by the deprotonated carboxylic acid allows asymmetric delivery of the bromine from NBS, thus yielding enantioenriched lactones.[43]

3.6 Results and Discussion

By analogy to the work by Yeung and co-workers where the use of an amino-thiocarbamate catalyst activated a bromine electrophile for enantioselective bromolactonisation,[43] we reasoned that the novel amino-thiocarbamate clefts could be utilised

in a similar manner to give good efficiency and *ee* values in the bromolactonisation of simple unsaturated carboxylic acids such as **18**. Herein, the results from a series of preliminary reactions are reported.

3.6.1 Synthesis of Unsaturated Alkenoic Acid 18

The unsaturated carboxylic acid **18** was synthesised over four-steps starting from commercially available dimethyl malonate **176** according to a procedure reported by Yeung and co-workers (Scheme 66).[43]
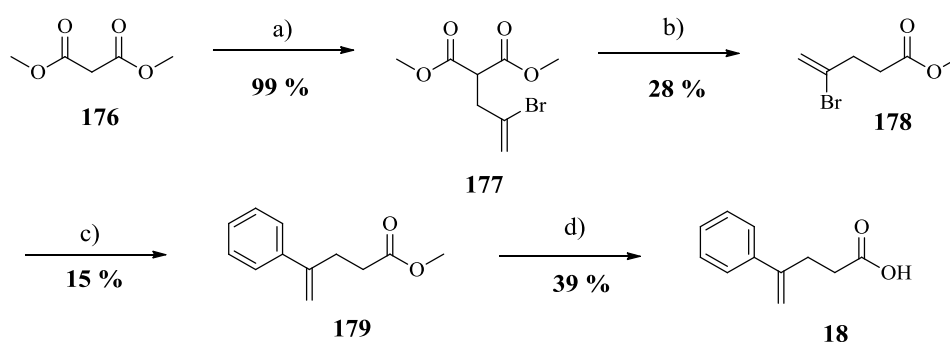
Reagents and conditions: a). NaH, THF, TBAI, 2,3-dibromopropene, reflux, 19 h; b). LiCl, DMSO, 140 °C, 48 h; c). phenyl boronic acid, Pd(PPh$_3$)$_4$, Na$_2$CO$_3$, dioxane/H$_2$O, 100 °C, 16 h; d). LiOH.H$_2$O, THF, 25 °C, 12 h.

Scheme 66: Synthesis of the unsaturated carboxylic acid 4-phenyl-4-pentenoic acid 18.

Treatment of dimethyl malonoate **176** with sodium hydride in the presence of 2,3-dibromopropene and TBAI (tetrabutylammonium iodide) gave **177** in 99 % crude yield. Decarboxylation of **177** with lithium chloride yielded the intermediate methyl 4-bromopent-4-enoate **178** which was treated with phenylboronic acid under Suzuki reaction conditions to give the ester **179** in 15 % yield. Subsequent hydrolysis of ester **179** with lithium hydroxide monohydrate in THF at room temperature over night gave the target alkenoic acid **18** in 39 % yield.

3.6.2 Catalyst Screening Reactions

Yeung and co-workers procedure (no additives) for the asymmetric bromolactonisation reaction was followed. As a result, alkenoic acid **18**, NBS **19** and 10 mol % of the investigational amino-thiocarbamate catalysts, **(+)-4**, **(+)-5** or **(+)-6**, were stirred in a solution of chloroform / toluene (1:2) at -78 °C for 4 h. The amino-thiocarbamate cinchonine catalysts **(+)-13**, **(+)-147**, **(+)-148** and **(+)-149**, and well as, the unfunctionalised

(+)-cinchonine framework (+)-**146** were also included in this investigation. The structure of the isolated γ-lactone **20** was confirmed by ^{1}H and ^{13}C NMR spectroscopy and the *ee* values determined by chiral HPLC. The results from this investigation are summarised in Table 24.

Table 24: Summary of the results from the screening of amino-thiocarbamate functionalised catalysts in the asymmetric bromolactonisation reaction.
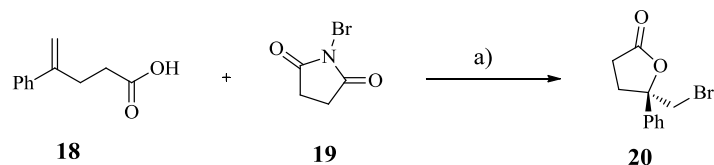
Reagents and conditions: a) Catalyst (10 mol %), NBS (0.12 mmol), CHCl$_3$/PhMe (1:2), -78 ^{o}C, 4h.

Entry	Catalyst	*ee* (%)[a]	Literature *ee* (%)[43]	Yield (%)[b]
1	**-**	<5	-	64
2	(+)-**4**	20	-	75
3	(+)-**5**	9	-	25
4	(+)-**6**	<5	-	54
5	(+)-**13**	14	50	82
6	(+)-**146**	<5	<5	46
7	(+)-**147**	23	37	57
8	(+)-**148**	-19	-29	56
9	(+)-**149**	24	-	50

[a] Determination by HPLC analysis on Chiralcel OD-H column.

[b] Isolated yield following prep-plate TLC.

Amino-thiocarbamate clefts (+)-**4**, (+)-**5** and (+)-**6** led to moderate yields and poor *ee* values when used in the bromolactonisation reaction of **18** (Table 24, entries 2–4). Interestingly, when the (+)-cinchonine derived amino-thiocarbamate catalysts (+)-**13**, (+)-**147**, (+)-**148** and (+)-**149** (Table 24, entries 5, 7-9) were used in this investigation they produced *ee* values which were not consistent with the literature values. This questions a) the repeatability of Yeung's procedure and results and b) the reliability of our experimental set up. Nevertheless these results produced some interesting observations with regards to the

relationship between the electron density of the *N*–aryl substituent and the enantioselectivity of the bromolactonisation reaction.

At a glance the amino-thiocarbamate clefts did not offer an improvement in the yield of the bromolactonisation product **20**, resulting in uniformly moderate yields, which were not significantly different from the 64 % yield, observed in the uncatalysed reaction (Table 24, entry 1). The amino-thiocarbamate cleft **(+)-4** gave γ-lactone **20** with the highest *ee* at 20 % (Table 24, entry 2). Interestingly, a decrease in the electron density of the *N*-aryl substituent, and hence increased acidity of the thiocarbamate N–H led to a reduction in the *ee*. When the *p*-tolyl group in **(+)-4** was replaced with a phenyl group **(+)-5**, there was a noticeable decrease in the *ee* from 20 % to 9 % (Table 24, entries 2 and 3). Similarly, when the highly electron deficient 3,5-bis(trifluoromethyl) phenyl amino-thiocarbamate cleft **(+)-6** was used in catalytic amounts, there was a complete loss of enantioselectivity (Table 24, entry 4). This reduction in *ee* as the electron density of the aromatic amino-thiocarbamate substituent decreased is consistent with the observations disclosed by Yeung and co-workers in the initial cinchonine alkaloid amino-thiocarbamate catalyst screening reactions. Moreover, these results are consistent with the observations we made during the application of these catalysts in the HDA reaction.

3.6.2.1 Proposed Mechanism

Given the relative orientation of the appending amino-thiocarbamate groups and H-bond N-H donors, as determined by the X-Ray crystal structures of these cleft compounds, and the results observed in the catalyst screening reactions (Table 24), it is likely that interactions between NBS and the catalysts led to the bromolactonisation reaction between NBS and **18** occurring outside of the chiral environment generated by the cleft catalysts. With this in mind, as well as, consideration of the mechanism and transition state structure proposed by Yeung and co-workers for the dual activation of NBS, it is reasonable to assume that each molecule of catalyst is potentially capable of activating two molecules of NBS (Figure 64).

180
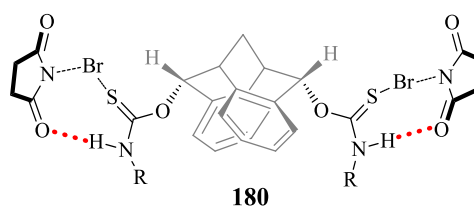
Figure 64: Proposed activation of NBS by amino-thiocarbamate functionalised cleft catalysts.

In this model, the Lewis basic sulphur atom of the amino-thiocarbamate group co-ordinates to the bromine atom in NBS. This enhances the electrophilicity at the bromine atom through net repolarisation of the electron density of the resultant Lewis acid-base adduct. The electrophilicity of the bromine atom is enhanced further, by H-bonding between the thiocarbamate N-H group and the carbonyl of the succinimide (Figure 65).

181
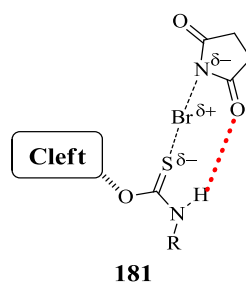
Figure 65: A schematic diagram illustrating the potential dual activation of NBS by the amino-thiocarbamate cleft catalysts.

Simultaneous nucleophilic attack of the electrophilic bromine by the alkene double bond and protonation of the succinimide by the carboxylic acid in **18** forms the fully ionised bromonium cation intermediate **181a** (Scheme 67).

181   **181a**
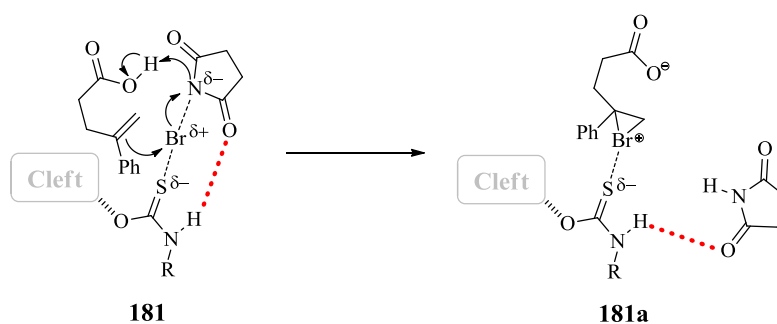
Scheme 67: Nucleophilic attack of the activated bromine atom by the alkene double bond in 18, and the deprotonation of the appending carboxylic acid.

Since the formation of the bromonium ion is the enantio-determining step, the ideal enantioselective bromolactonisation reaction would selectively form the bromonium ion at either the *Si-* or *Re-* face of the alkene. It is reasonable to suggest that the bulky functional groups attached to the amino-thiocarbamate groups may have contributed to some facial selectivity in this step by acting as steric screening groups. However, because activation of NBS was not facilitated within the chiral environment generated by the cleft, olefin-to-olefin

halonium exchange was possible meaning that the stereochemistry of the bromonium ion was not set before intramolecular nucleophilic attack by the pendant deprotonated carboxylic acid, resulting in formation of the 5-membered bromolactone **20** either as the racemic product (Table 24, entry 4) or with low *ee* values (Table 24, entries 2 and 3) (Scheme 68).
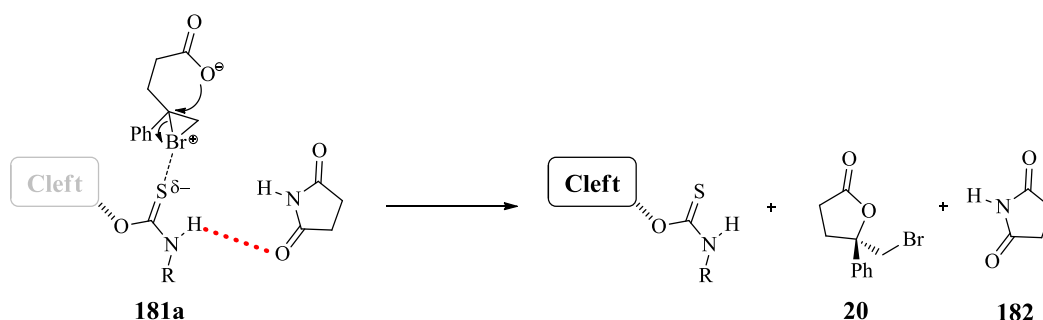
Scheme 68: Intramolecular nucleophilic attack to give the bromolactonisation product 20.

Both the five- and six-membered rings could be formed in this bromolactonisation reaction; however the five-membered ring is formed preferentially as predicted by Baldwin's rule for ring closure (Scheme 69). Formation of the 5-membered ring lactone **20** was confirmed by ^{1}H NMR spectroscopic analysis of the isolated products.
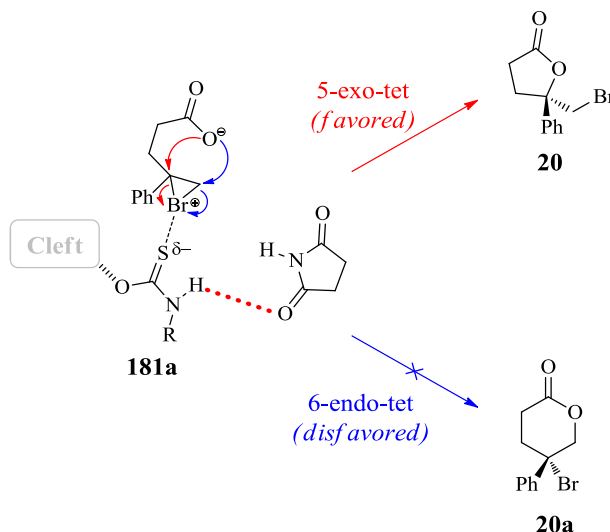
Scheme 69: Formation of the 5-membered ring lactone as predicted by Baldwin's rule.

It is highly unlikely that the dimensions of the clefts coupled with the orientation of functional groups would facilitate bifunctional activation of NBS and **18** to give a transition state similar to that proposed by Yeung and co-workers (Figure 63). Even if the cleft catalysts facilitated the binding and activation of NBS within the chiral cleft cavities, the 'free'

123

thiocarbamate N-H would not be electrophilic enough to interact efficiently with the deprotonated carboxylic acid like the quinuclidine component of the cinchonine amino-thiocarbamate catalysts did.

It is reasonable to assume that the biggest contributing factors in terms of how the amino-thiocarbamate clefts interact with the bromolactonisation substrates are the dimensions of the cleft cavity and relative orientation of functional groups. Incorporation of molecules within the chiral cavity of the cleft can be considered to be highly restricted by its dimensions and steric accessibility.

3.7   Optimisation of Cleft Catalysts

In terms of improving the enantioselectivites of both the asymmetric HDA and bromolactonisation reactions there are several reaction parameters which can be varied systematically including solvent systems, reaction time and temperature as well as the use of additives. In addition the installation of other functional groups onto the molecular cleft framework which present different recognition and binding groups is a possibility.

Due to the limitations observed in the application of the C_2-symmetric amino-thiocarbamate clefts in the HDA and bromolactonisation reactions, it is reasonable to suggest that unsymmetrical clefts may offer a more efficient mode of activation. The ability to bind reagents within the chiral cavity of the cleft such that the reaction pathway occurs within a chiral environment is considered vital for asymmetric induction. In addition complementary binding entities which facilitate independent electrophile and nucleophile activation have been shown to be effective in introducing enantioselectivity into a reaction.

With this in mind we proposed a synthetic methodology to access a second generation catalyst system related to the amino-thiocarbamate cleft catalysts, consisting of an amino-thiocarbamate group and a terminal triazole group (Scheme 70). We envisaged that this catalyst system would serve to optimise the selectivity observed in the asymmetric transformations, in particular the bromolactonisation reaction of **18**. It is possible that this bifunctional catalyst could be utilised in a similar way to the (+)-cinchonine derived catalysts in the asymmetric bromolactonisation reactions.
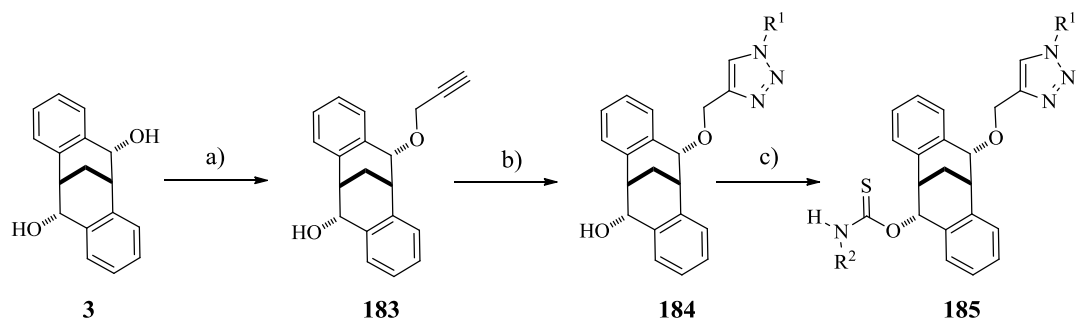
Reagents and conditions: a) propargyl bromide, base; b) R^1-N_3, click conditions; c) NaH, THF, R^2NCS.

Scheme 70: Proposed synthesis of a bifunctional amino-thiocarbamate-triazole cleft catalyst.

The proposed reaction pathway consists of three-steps starting from the readily accessible enantiopure reduced cleft **(-)/(+)-3**. Treatment of **(-)/(+)-3** with a strong base in the presence of sub-stoichiometric amounts of propargyl bromide would afford the mono-functionalised cleft **183**. Subsequent treatment of **183** under standard click-reaction conditions could give access to the triazole functionalised cleft **184**. The final step involves introducing the amino-thiocarbamate group onto the cleft system, thus treatment of **184** with sodium hydride in the presence of substituted isothiocyanates could potentially yield the target bifunctional catalyst **185**. Unfortunately, time restraints prevented full exploration into the proposed synthesis of cleft catalyst **185**, however initial preliminary experiments gave access to the intermediate **183**. Small scale treatment of **(±)-3** with sodium hydride in the presence of propargyl bromide in DMF at room temperature for 16 h gave the mono-allyl functionalised cleft **(±)-183** in 24 % yield (Scheme 71).
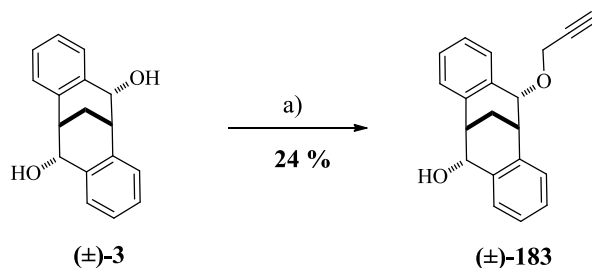
Reagents and conditions: a) NaH, propargyl bromide, DMF, 0 °C – rt, 18 h.

Scheme 71: Synthesis of mono-functionalised cleft intermediate (±)-183.

The synthesis of clefts incorporating two different functional groups therefore presenting bifunctional activity could serve as a starting point for subsequent research projects. In addition, the ease in which functional groups can be introduced onto the aromatic rings of the

carbocyclic cleft framework offers additional opportunities for catalyst derivatisation. Alternatively replacing the amino-thiocarbamate groups with other H-bond donor groups such as the well-known double H-bond catalyst thiourea may give improved activity.

Chapter 4

4.0 Fused Cleft Systems

Chiral molecular recognition via structurally well-defined intermolecular non-covalent interactions, underpins several areas of asymmetric catalysis, receptor-ligand interactions and chemical sensing.[82] Within the area of synthetic chemistry, chiral molecular recognition is dependent upon the ability to design and synthesise appropriate receptors with predictable geometries and binding sites. Towards this end TB **1** and its derivatives have been used extensively within the area of molecular recognition because they contain; a rigid predictable structure, heteroatoms capable of binding events and most importantly a chiral cavity.[39]

Additional interactions such as aromatic stacking and cation π-interactions are made feasible by extended concave aromatic surfaces. In this context attention has been drawn to the synthesis of fused analogues of **1**. A fused TB analogue is a TB that contains more than one methanodiazocine unit and has an aromatic ring fused to two such units (Figure 66).
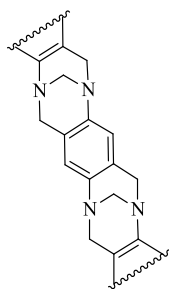
186

Figure 66: General structure of a fused TB system.

"Bis", "tris" and "oligo" fused TB analogues therefore refer to molecules containing 2, 3 or more methanodiazocine units, respectively. [3]

4.1 Synthesis of Fused TB Derivatives

The first example of a bis-TB skeleton was reported by Pardo and co-workers in 2001. The group synthesised bis-TB analogues starting from the unsymmetrical TB **187** following a synthetic pathway similar to the procedure reported by Wilcox and co-workers for the synthesis of unsymmetrical TB analogues.[83] In this line of research, mono-TB **187** was

extended stepwise to the fused bis-TB analogue **191** in the forms of *syn* **191a** and *anti* **191b** diastereomers (Scheme 72).[9]
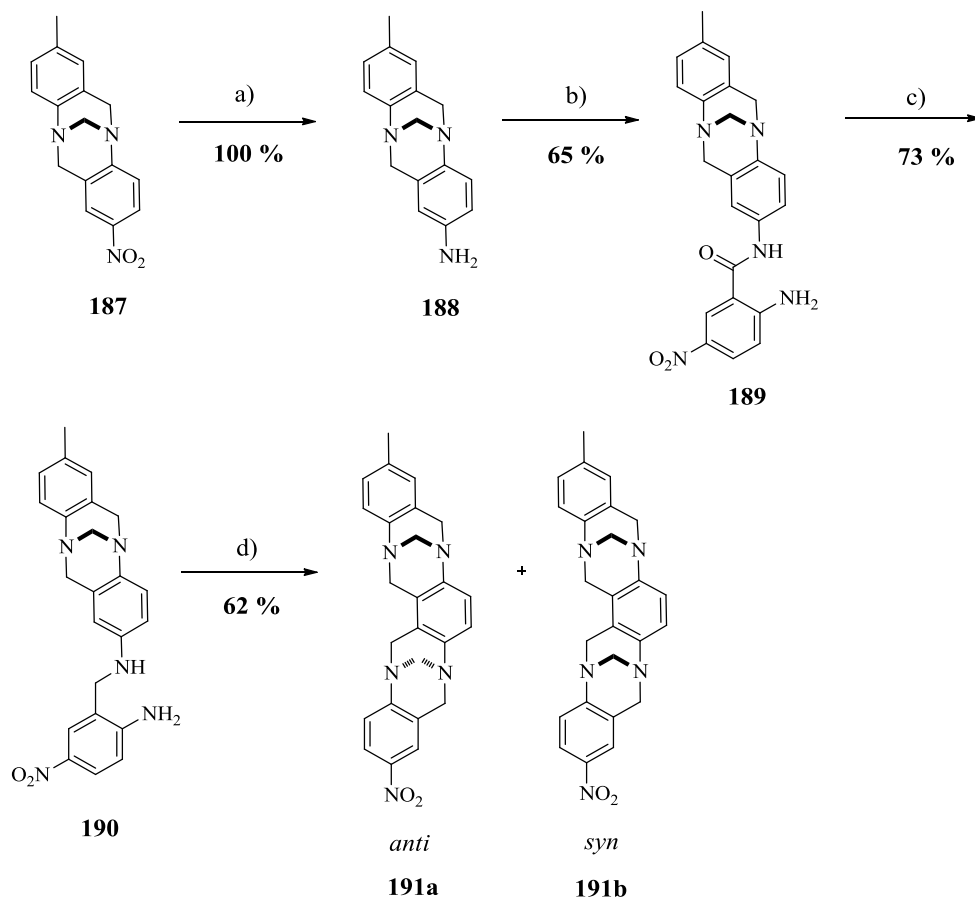
Reagents and conditions: a) H_2/Pd 10 % (C), $CHCl_3$/EtOH, rt, 3 h; b) 6-nitroisatoic anhydride, THF, reflux, 3 h, c) BH_3.THF, reflux, 1 h; d) 37 % aqueous CH_2O, 95 % EtOH, 36 % HCl, 90 °C, 24 h.
Scheme 72: Pardo and co-workers step-wise synthesis of unsymmetrical fused TB derivatives.

Whilst there have been a number of reports detailing the synthesis and application of bis,[9] tri[84, 85] and oligo[86] fused TB analogues, a mixed fused ring system containing both **1** and another carbocyclic cleft fused to the same aromatic ring remains a novel concept. Although the chiral cavity present in both **1** and **2** have been individually utilised for chiral recognition and catalysis purposes, a mixed chiral cleft derived from both cleft systems has yet to be explored (Figure 67).

21
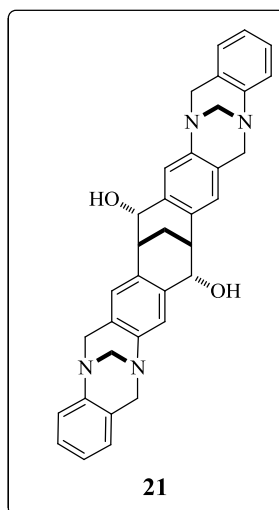
Figure 67: General structure proposed for a fused molecular cleft containing TB 1 and the carbocyclic cleft 2.

Such a chimera would be expected to display unique topology as illustrated by **192a** and **192b** in Figure 68. In addition, this combined molecular cleft would contain a true chiral cavity with the potential to directly assemble substrates within a chiral environment via hydroxyl functionality on the central carbocyclic cleft, as well as, the peripheral nitrogen atoms contained within the flanking TBs, thus allowing for the direct engineering of highly specific chiral environments within the cavities.
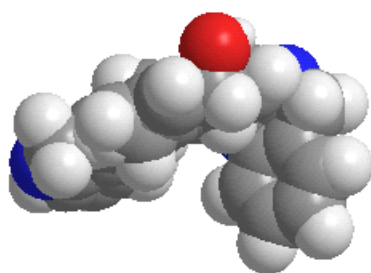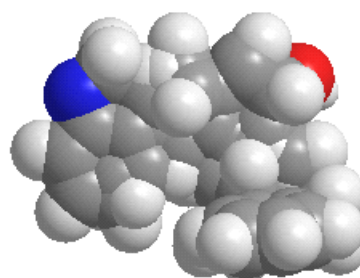
192a: Side view   **192b: Bottom view**

Figure 68: Three-dimensional space filling model of 21.

In this chapter, preliminary reactions into the synthesis of this unique family of rigid chiral cleft molecules were explored for the first time. Whilst the total synthesis of this extended molecular cleft was not achieved, procedures for the synthesis of novel intermediates were developed and thus provide an excellent starting point for future development. Here in a series of preliminary experiments aimed at developing a synthetic

pathway to a mixed fused cleft system incorporating both **1** and **2** is reported. In addition an overview of the potential applications of this fused cleft system is reviewed.

4.2   Proposed Synthesis of a Mixed Fused Cleft System

Based on Pardo and co-workers synthetic pathway to the bis-TB analogue **191**,[9] we proposed a 3-stepped method for the synthesis of (±)-**21**, starting from the diamine cleft (±)-**86** (Scheme 73).
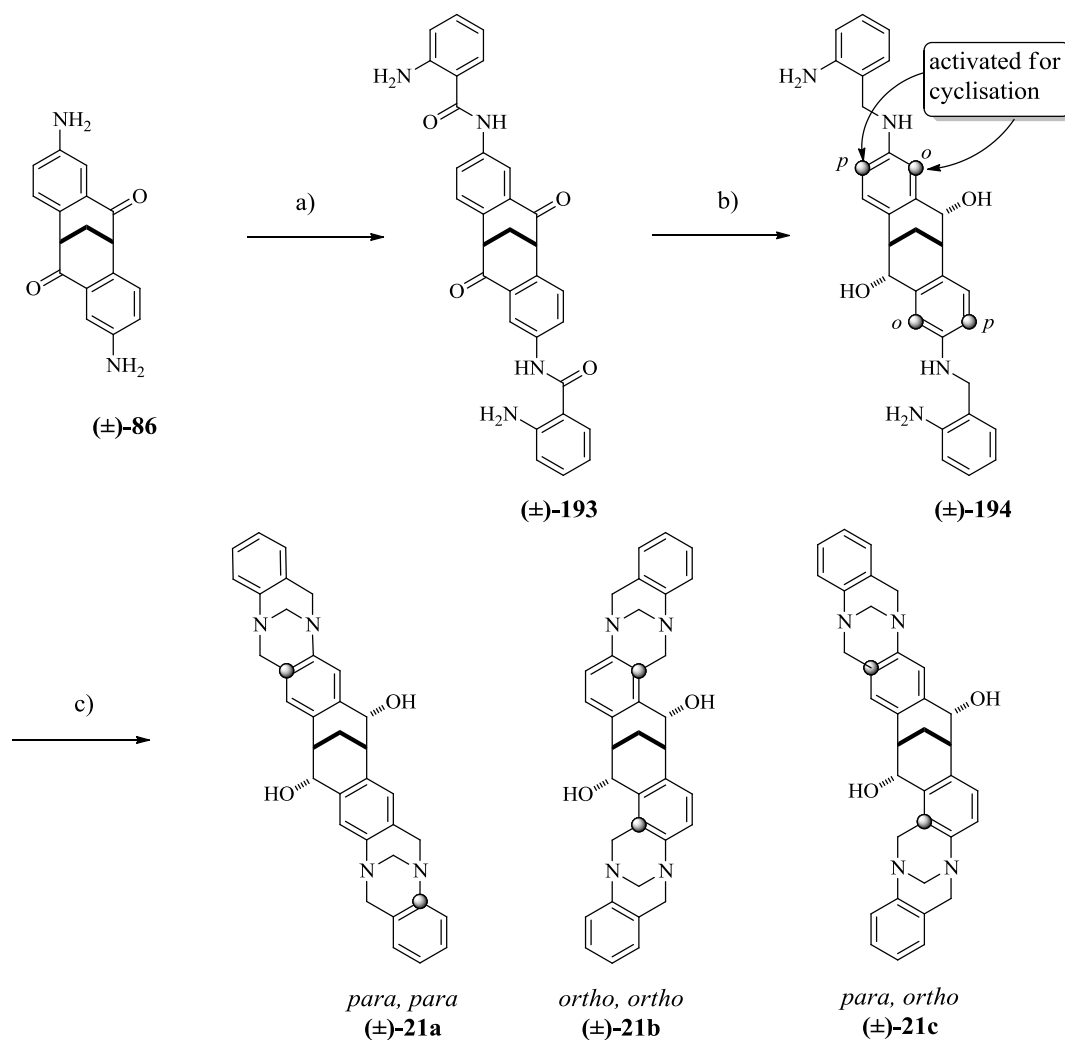
Reagents and conditions: a) Isatoic anhydride, EtOH or DMF, reflux; b) Reduction: LiAlH$_4$ or BH$_3$.THF, reflux; c) HCHO/H$^+$.

Scheme 73: Proposed synthetic route to the fused cleft (±)-21.

As mentioned in Chapter 1, the diamine cleft substrate (±)-**86** can be synthesised using a procedure developed by Harding and co-workers. This involves the regioselective nitration of (±)-**2** followed by chemoselective reduction of the nitro groups to give (±)-**85** (Scheme 74).[8]
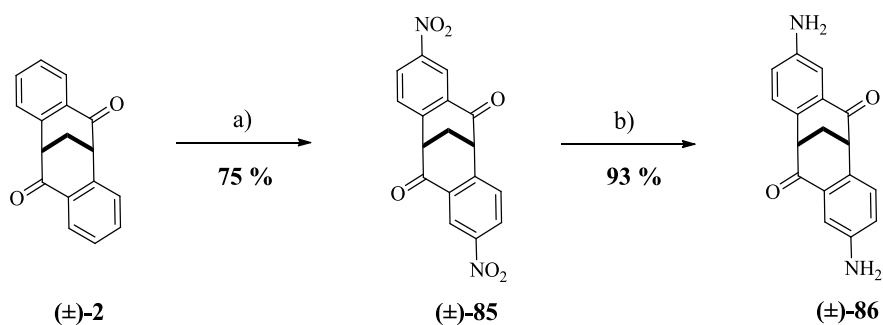
Reagents and conditions: a). H_2SO_4, KNO_3, 0 °C, 30 min, rt, 16 h; b). Fe, AcOH, EtOH, N_2, reflux, 6 h.

Scheme 74: Harding and co-workers synthesis of the diamine cleft (±)-86.

We proposed that the precursor **(±)-86** could be converted into the substrate for cyclisation **(±)-194**, by condensation with isatoic anhydride followed by reduction, using a similar approached used by Wilcox and co-workers in the synthesis of unsymmetrical TB analogues.[83] Cyclisation of the amine **(±)-194** will then be accomplished by treatment with formaldehyde in the presence of acid. It is important to note at this point that product distribution from this cyclisation is not trivial and may produce up to nine distinct products, not including enantiomers. Firstly, cyclisation can occur at either position flanking the amine potentially yielding three isomers; **(±)-21a** (*para, para*), **21b** (*ortho, ortho*) and **21c** (*para, ortho*) (Scheme 73). Secondly, each of these three will potentially yield up to three products, for example **(±)-21a** (*para, para*) will generate three regioisomers **(±)-21a(i)**: *syn, syn, anti*; **(±)-21a(ii)**: *anti, syn, anti*; and **(±)-21a(iii)** *syn, syn, syn*, respectively (Figure 69).

syn, syn, anti
(±)-21a(i)*:*

anti, syn, anti
(±)-21a(ii)

syn, syn, syn
(±)-21a(iii)
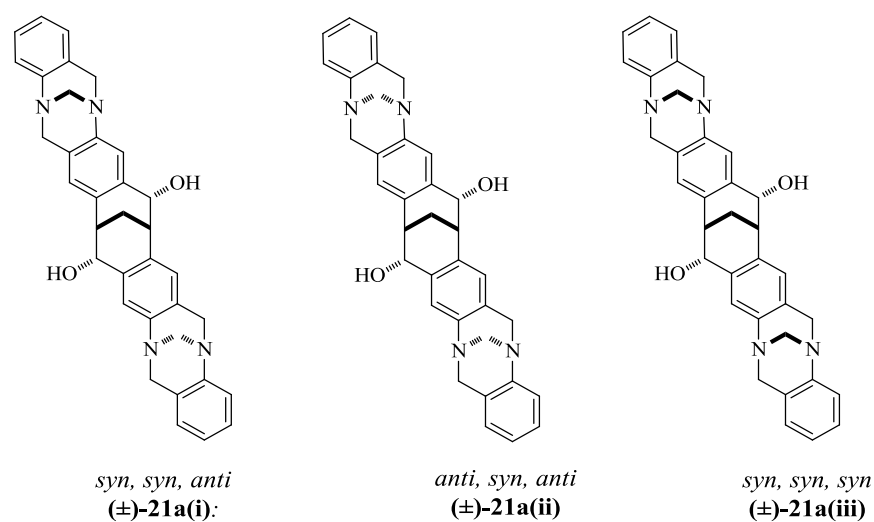
Figure 69: Possible regioisomers of the fused cleft (±)-21a.

Each of the potential rigid cleft products from this reacton pathway possess unique 3-dimensional topology ideal for chiral molecular recognition. In publications detailing the synthesis of fused TB derivatives, stereoisomers were seperated by chromatography and NMR analysis was used to identiy the diastereoselectivity of the reaction. In addition, X-Ray crystaollgraphy was used to determine the *syn/anti* stereochemical outcome.

4.3   Preliminary Experiments

As mentioned in Chapter 1, Wilcox and co-workers reported a step-by-step methodology for the synthesis of unsymmetrical TB derivatives starting from substituted anilines.[83] In an attempt to evaluate this procedure before the same reaction conditions were applied to our molecular cleft for the synthesis of the mixed fused cleft system, a series of preliminary reactions were performed. The aim was to synthesise the novel TB analogue **199** using a synthetic pathway derived from the Wilcox procedure. Literature procedures were followed exactly, and where necessary modified to improve yield and accessibility (Scheme 75).
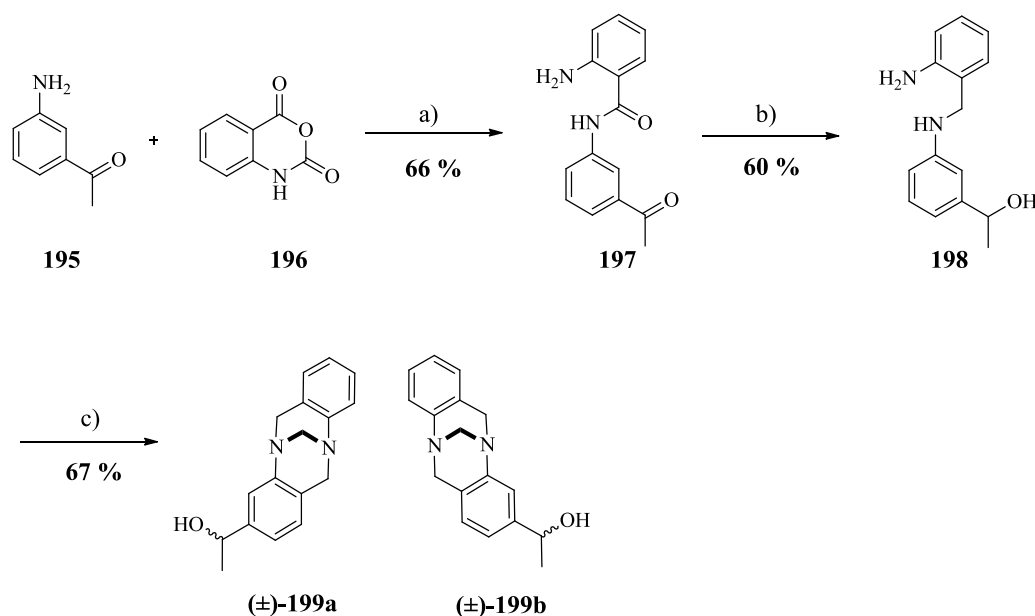
Reagents and conditions: a) DMF, reflux, 24 h; b) LiAlH$_4$, THF, reflux, 18 h; c) 95 % EtOH, 37 % CH$_2$O, 36 % HCl, 90 $^{\circ}$C, 48 h.

Scheme 75: Preliminary experiments aimed at synthesising the novel unsymmetrical TB derivative 199 using Wilcox and co-workers step-by-step approach.

When a solution of 3'-aminoacetophenone **195** and isatoic anhydride **196** in dry ethanol was refluxed for 24 h, in accordance to Wilcox's protocol no reaction was observed.

Condensation under these reaction conditions repeatedly led to the isolation of unreacted starting materials. Isatoic anhydride **196** was insoluble in ethanol which may account for the lack of reaction therefore, a range of other polar solvents were screened for reactivity. Anhydrous solvents including; tetrahydrofuran (THF), dimethylformamide (DMF), dimethyl sulfoxide (DMSO) and dimethylacetamide (DMA) were all used in the condensation step between **195** and **196**. All reactions were heated at the solvent boiling point for 24 h and reactions monitored by TLC. Table 25 summarises the reaction conditions and outcomes of solvent screening in the condensation reaction between **195** and **196**.

Table 25: Summary of results obtained from the condensation step between 196 and 196 in different solvents.
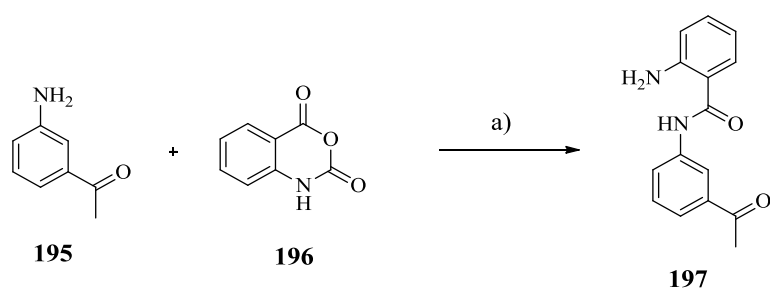
Reagents and Conditions: a) **196** (4.0 eq), solvent, reflux, 24 h.

Entry	Solvent (Anhydrous)	Solvent boiling point (^{o}C)	Reaction outcome Yield (%)
1	EtOH	79	No reaction
2	THF	66	No reaction
3	DMSO	189	No reaction
4	DMF	153	36
5	DMF[a]	153	66
6	DMA	165	29

[a] Reaction conditions: **196** (8.0 eq), 48 h.

Isatoic anhydride **196** was either insoluble or partially soluble in EtOH, THF and DMSO. Heating the reaction under reflux aided the solubility of reagents however, no reaction was observed when these solvents were used (Table 25, entries 1-3). Isatoic anhydride **196** was soluble in both DMF and DMA and led to the synthesis of the desired condensation product **197** which was isolated in 36 and 29 % yields respectively (Table 25, entries 4 and 6). Increasing the reaction time and number of equivalents of **196** almost doubled the yield of

197 to 66 % (Table 25, entry 5). Excess unreacted **196** was removed with relative ease during extraction by washing the organic phase repeatedly with water.

Reduction of **197** to the cyclisation precursor **198** under the standard reaction conditions of refluxing BH$_3$.THF gave no reaction however, treatment of **197** with four equivalents of lithium aluminium hydride in refluxing THF for 48 h gave the reduced product **198** in 60 % yield following chromatographic separation of the crude product. ^{1}H and ^{13}C NMR spectral analysis was used to confirm the structure of the reduction product **198.**

A sharp singlet at δ 4.26 ppm absent from the ^{1}H NMR spectrum of the condensation product **197** corresponds to the amine CH$_2$ protons in **198** therefore, confirming reduction of the amide all the way to the respective amine. Similarly a quartet at δ 4.86 ppm (J = 6.4 Hz) represents the single proton of the secondary alcohol, indicating partial reduction of the acetophenone functionality by lithium aluminium hydride. The intermediate **198** was converted to the unsymmetrical TB derivative **199** according to Wilcox's procedure, thus treatment of **198** with formaldehyde and hydrochloric acid in ethanol at 90 ℃ for 24 h gave (±)-**199** as a mixture of diastereomers, (±)-**199a** and (±)-**199b** (Scheme 75).

Formation of (±)-**199** was confirmed by ^{1}H and ^{13}C NMR spectral analysis. Successful cyclisation to form the TB ring system is evidenced by three peaks corresponding to the bridgehead and core methylene groups at positions 1, 2 and 3 respectively (Figure 70).
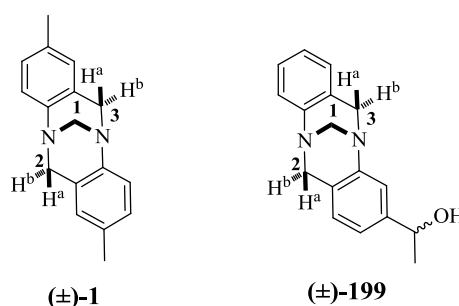
Figure 70: Structure and proton labelling of TB (±)-1 and the synthesised TB derivative (±)-199.

A doublet peak in the ^{1}H NMR spectrum at δ 4.38 ppm (J = 1.6 Hz) corresponds to the bridgehead methylene CH$_2$ protons at position 1. Similarly mulitplets at δ 4.74 and 4.23 ppm are characteristic of the methylene groups at positions 2 and 3, respectively. The assigned methylene protons and carbon chemical shifts in the NMR spectra of **199** are

consistent with those reported in the literature for **1**. Table 26 summarises the chemical shifts in the carbon and proton spectra for (±)-**199** in comparison to (±)-**1**.

Table 26: A comparison of the ^{1}H and ^{13}C chemical shifts reported in the literature for (±)-1 and the experimental values observed in the spectra of the TB derivative (±)-199.

		(±)-1		(±)-199	
Entry	Position	Proton (δ ppm)[87]	C–H carbon (δ ppm)[87]	Proton (δ ppm)	C–H carbon (δ ppm)
1	1	4.32	67.05	4.31	65.76
2	2	4.67(a), 4,12 (b)	58.68	4.66 (a), 4.17(b)	57.48
3	3	-	58.66	4.73(a), 4.21(b)	57.37

As with the fused ring system **21**, the product distribution from this cyclisation is quite complex and may produce up to four distinct product stereoisomers, not including enantiomers. Firstly, cyclisation can occur at both position flanking the amine potentially yielding two isomers (±)-**199a** (*para*) and (±)-**199b** (*ortho*) In addition, each of these diastereomers will potentially yield to two products either *syn* (i) or *anti* (ii) (Scheme 76).
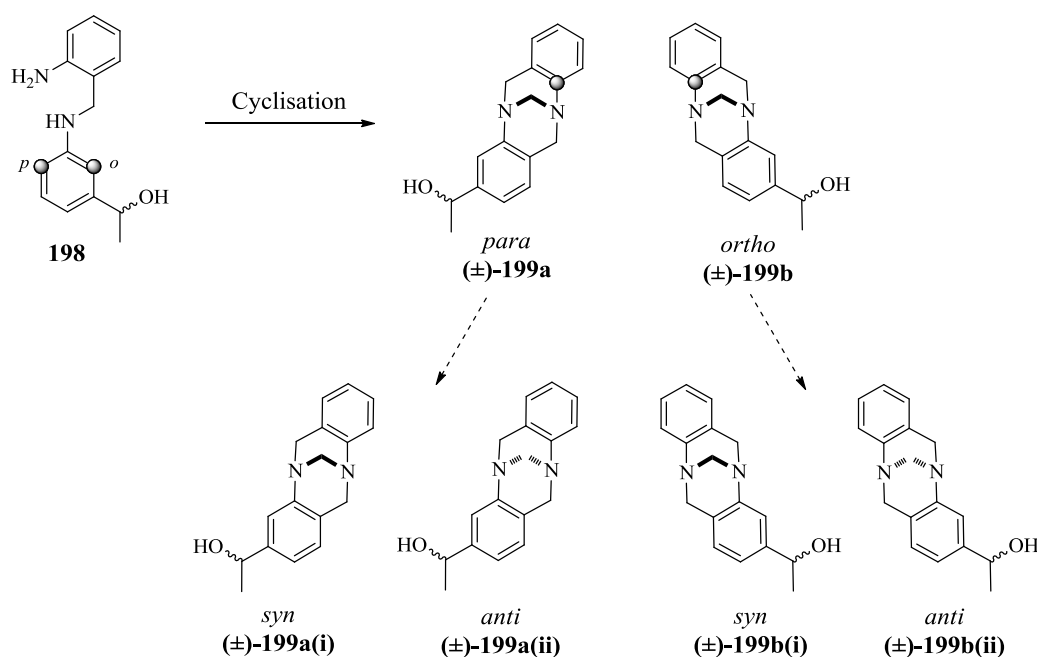
Scheme 76: Potential products following cyclisation of 198 to form the TB derivative (±)-199.

The expected dipole moment of the *para-syn*, *para-anti*, *ortho-syn* and *ortho-anti* should be very similar therefore, it is likely that all of the possible reaction products would

135

co-elute in the same spot during purification by column chromatography. The ^{1}H NMR spectrum of the isolated product supports this idea as it contains two different CH_3 (doublet) signals at δ 1.40 ppm and two separate CH (quartet) signals at δ 4.78 ppm, which is indicative of diastereomers. Moreover the ^{13}C NMR spectrum contains four different signals at δ 58.5 ppm and at least two signals at δ 25 ppm. With the existing NMR data it is not possible to differentiate or identify the diastereomers, better signal to noise and more in-depth NMR experiments are required. Alternatively, in order to determine if the isolated diastereomer was the *ortho/para - syn/anti* product X-Ray crystallographic analysis of the compound could be used, unfortunately it was not possible to isolate crystals suitable for X-Ray analysis.

4.4 Attempted Synthesis of the Mixed Fused Cleft

In an attempt to access the novel mixed fused molecular cleft **21**, the optimised reaction conditions identified from the preliminary reactions were applied to the carbocyclic molecular cleft. The precursor diamine cleft **(±)-86** was synthesised with ease using the original procedure reported by Harding and co-workers (Scheme 77).[8]

Reagents and conditions: a). H_2SO_4, KNO_3, 0 °C, 30 min, rt, 18 h; b). Fe, AcOH, EtOH, N_2, reflux, 48 h.

Scheme 77: Synthesis of (±)-86.

Treatment of **(±)-2** with concentrated sulphuric acid and potassium nitrate at room temperature for 18 h led to regioselective nitration of the aromatic rings. Repeated recrystallization from hot DMF yielded the dinitro cleft **(±)-85** in 60 % yield. Subsequent selective reduction of **(±)-85** with refluxing iron acetic acid in ethanol for 48 h gave **(±)-86** without the need for further purification in 52 % yield. Spectral data was consistent with reported literature values. The next step in this synthetic pathway involved the condensation of **(±)-86** with isatoic anhydride **196** to give the amine **(±)-193** (Scheme 78).

Reagents and conditions: a) Isatoic anhydride **196** (8.0 eq), DMA, reflux, 48 h.

Scheme 78: Condensation reaction between (±)-86 and isatoic anhydride 196 to give (±)-193.

The solubility of **(±)-86** and **196** had a large influence on the accessibility of **(±)-193** and its yield. Based on observations made during the preliminary reactions, a solution of **(±)-86** and an excess of **196** (8.0 eq) in DMF was heated at its boiling point for 24 h. At room temperature, **(±)-86** was insoluble in DMF however, when the reaction was heated to the boiling point of DMF its solubility increased. TLC of the reaction mixture indicated a new product spot however, following work-up, the NMR spectrum of the isolated product revealed negotiable amounts of the target compound with the major product being unreacted starting materials. Following this disappointing result the reaction was repeated in DMA. The higher boiling point of DMA allowed the reaction to be heated at higher temperatures moreover, both **(±)-86** and **196** were soluble in DMA at room temperature. Treatment of **(±)-86** with an excess of **196** (8.0 eq) in DMA at reflux for 48 h afforded the target compound. Excess unreacted **196** was removed primarily by washing the organic layers during work-up, multiple times with water. Purification by chromatography gave the disubstituted amide **(±)-193** in 6 % yield (Scheme 78).

The structure of **(±)-193** was confirmed by ^{1}H NMR analysis. The bridgehead methylene CH$_2$ protons (a) as well as the C–H protons at positions 4 and 8 (Figure 71) were used as reference points to confirm the structure of the central carbocyclic cleft whilst, distinct splitting patterns in the aromatic region provided evidence to support condensation with isatoic anhydride to give the target compound **(±)-193**. Broad singlet peaks at δ 10.16

137

and δ 5.76 ppm representing the amide and primary amine protons respectively provided additional evidence to support formation of the condensation product.
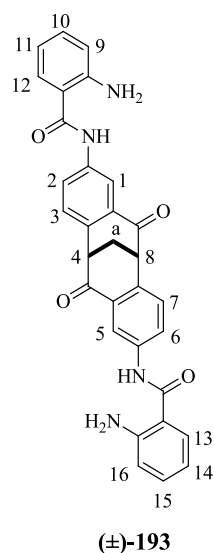
Figure 71: Structure and proton labelling of (±)-193.

A triplet at δ 4.00 ppm and a broad singlet peak at δ 2.98 ppm both integrating to two protons represent the C–H proton at positions 4 and 8 and the methylene bridgehead CH_2 protons (a), respectively. These peaks are consistent with the starting material (±)-**86** and are characteristic of the carbocyclic cleft **2**. Table 27 summarises the chemical shifts and coupling constants for these characteristic protons in both, the starting material (±)-**86** and the condensation product (±)-**193**.

Table 27: Comparison of the chemical shifts of the methylene CH_2 protons and C–H protons in the ^{1}H NMR spectrum of the starting material cleft (±)-86 and the condensation product (±)-193.

		(±)-86		(±)-193	
Entry	Protons	Chemical shift, δ (ppm)	Coupling constant, J (Hz)	Chemical shift, δ (ppm)	Coupling constant, J (Hz)
1	CH_2	2.74	2.8	2.98	Singlet
2	C–H	3.63	2.8	4.00	2.8

Unique splitting patterns in the aromatic region enabled full characterisation of the isolated compound thus confirming the formation of the desired condensation product (±)-**193**. Table 28 summarises the splitting patterns and coupling constants of aromatic protons in (±)-**193**.

Table 28: Chemical shifts, splitting patterns and coupling constants (J) of the protons in the ^{1}H spectrum of (±)-193.

Entry	Proton(s)^{a}	Chemical shift, δ (ppm)	Coupling constant, *J* (Hz)	Splitting pattern
1	NH	10.16	-	s
2	1, 5	8.26	2.4	d
3	2, 6	7.93	6.4, 2.4	dd
4	12, 13	7.61	6.4, 1.6	dd
5	3, 7	7.43	8.4	d
6	11, 14	7.20	1.2	t
7	9, 16	6.75	8.4, 1.2	dd
8	10, 15	6.57	1.2	t
9	NH$_2$	6.35	-	s

^{a} Proton labelling is based on Figure 71.

Attempts to optimise these reaction conditions and improve the yield of the condensation product (±)-**193** were met with little to no success. In fact when the reaction was performed on a gram scale the yield of (±)-**193** was reduced to 3 %.

4.4.1 Attempted Microwave Assisted Synthesis of (±)-193

In 2006 Bakavoli and co-workers reported the highly efficient synthesis of 2-amino-N-substituted-benzamides by the condensation of isatoic anhydride **196** with a range of amines in solvent-free conditions under microwave irradiation (Table 29).[88] Based on the group's observations these reaction conditions were applied to (±)-**86** in an attempt to access the condensation product (±)-**193** in improved yields. As a result, a neat mixture of isatoic anhydride **196** and amine (±)-**86** were mixed thoroughly and then subjected to microwave irradiation (210 W) interruptedly at 4 min intervals to control and monitor the reaction. However, after three cycles at 210 W for 4 min no reaction was observed, as monitored by TLC. It was decided at this stage, given time limitations that the procedure outline in Scheme 78 would be repeated multiple times on half a gram scale in order to access enough material for the reduction step.

Table 29: Bakavoli and co-workers synthesis of the 2-substituted aminobenzamide 200 under microwave irradiation.
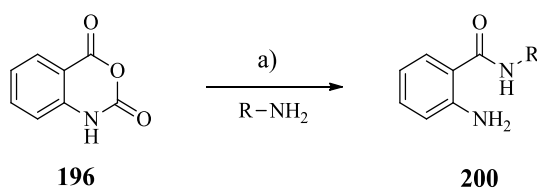
Reagents and conditions: a) microwave 210 W

Entry	R	Time(min)	Isolated yield of 200 (%)
1	Ph	4	85
2	CH₃Ph	3	85
3	*p*-Me-Ph	3	85
4	*p*-Et-Ph	3	88

Although isatoic anhydride **196** is a convenient reagent its usefulness in synthesis is limited because its chemistry has only partially been studied.[89] The literature was explored to find a viable explanation for the low yields obtained from the condensation reaction between isatoic anhydride **196** and (±)-**86** in an attempt to optimise this step in the overall synthesis of the mixed fused molecular cleft system (±)-**21.**

It has been reported that whilst interactions of **196** with primary amines proceeds readily, some reacts to liberate carbon dioxide subsequently yielding the expected amides in small amounts or not at all. In general strongly basic amines react readily with **196** at low to moderate temperatures (rt to 130°C), and some even in water, whilst aromatic primary amines are reported to react less readily and in very low yields. The probable course of these low yields becomes obvious when it is noted that the product formed from the reaction of a primary amine with **196** (Reaction 1, Scheme 79) contains a free amino group, and is therefore capable of reaction with **196** (Reaction 2, Scheme 79).[89]
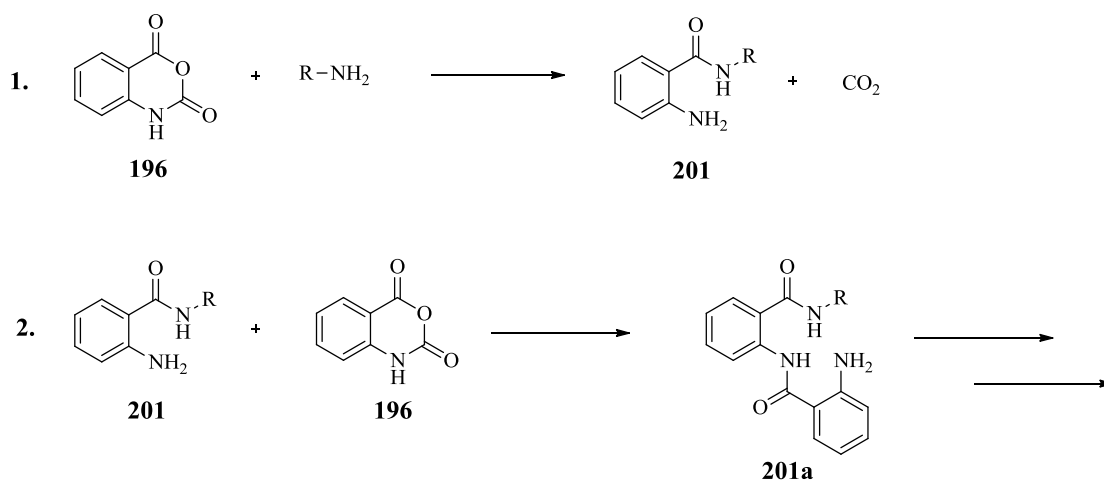
Scheme 79: Reaction of 196 with primary amines.

If the reactivity of the amino-hydrogen of compound **201** approaches or exceeds that of the amino-hydrogen of the substrate amine (R-NH$_2$), then some or all of **201** will react with isatoic anhydride to form **201a**. This product likewise contains a free amino group, and if the reactivity of the primary amine (R-NH$_2$) is for any reason low the condensation may continue.[89] It is unlikely in most cases that reactions prevail beyond 2 or 3 consecutive condensations however; it is possible that mixtures of products result. There are no examples in the literature that report the isolation of these side products however they have been made accountable for low yielding condensation reactions between primary amines and **196**.

It is unlikely that this polymerisation type reaction occurred during the condensation reaction between (±)-**86** and **196** primarily due to the dimensions of the cleft and arrangement of functional groups however, it cannot be ruled out. In theory this hypothesis could be tested by reacting stoichiometric amounts of (±)-**86** and **196**, in this instance we would expect little or none of the product (±)-**193**. Whereas if a large excess of (±)-**86** was used, it may be anticipated that the excess of amine would in part overcome the disadvantage inherent in a relatively high rate for 'reaction 2' (Scheme 79) compared with 'reaction 1' (Scheme 79) thus giving the desired condensation product in improved yields.

4.4.2   An Alternative Approach to the Synthesis of the Fused Cleft System

The direct condensation between (±)-**86** and **196** was met with low yields and poor reproducibility therefore, we sought to device an alternative preparative route to access the fused cleft system (±)-**21**. A search of the literature led us to consider a protocol involving the

reductive amination of (±)-86 with sodium triacetoxyborohydride (NaBH(OAc)$_3$) and the aromatic aldehyde 2-nitrobenzaldehyde 202 (Scheme 80).[90]
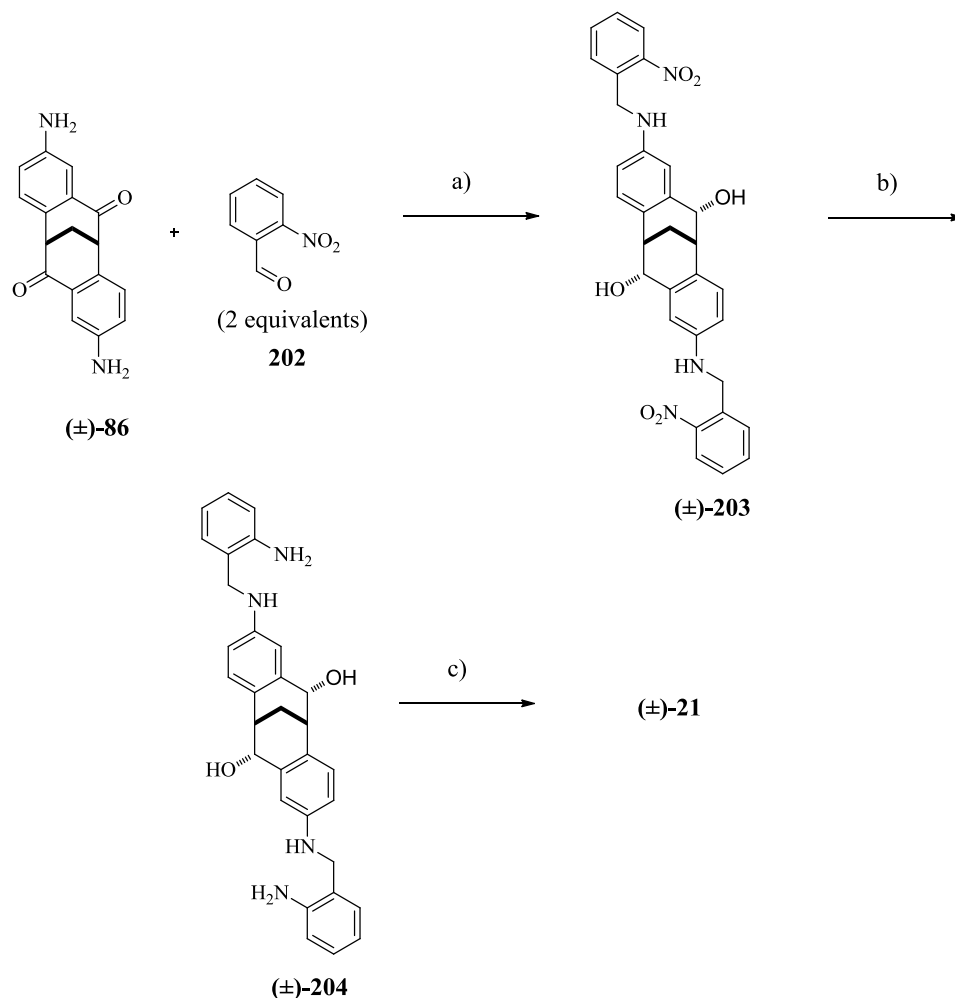
Reagents and Conditions: a) NaBH(OAc)$_3$, DCE, AcOH, rt; b) Fe, AcOH, EtOH, reflux; c) H$_2$CO, TFA.

Scheme 80: Alternative procedure for the synthesis of (±)-21.

Sodium triacetoxyborohydride (NaBH(OAc)$_3$) has been reported as a general reducing agent for the reductive amination of aldehydes and ketones. In comparison to other reductive amination procedures NaBH(OAc)$_3$ gives consistently higher yields and fewer side reactions.[90] This approach is similar to the Wilcox and co-workers alternative procedure for the synthesis of unsymmetrical TB analogues (Scheme 81).[18,91]
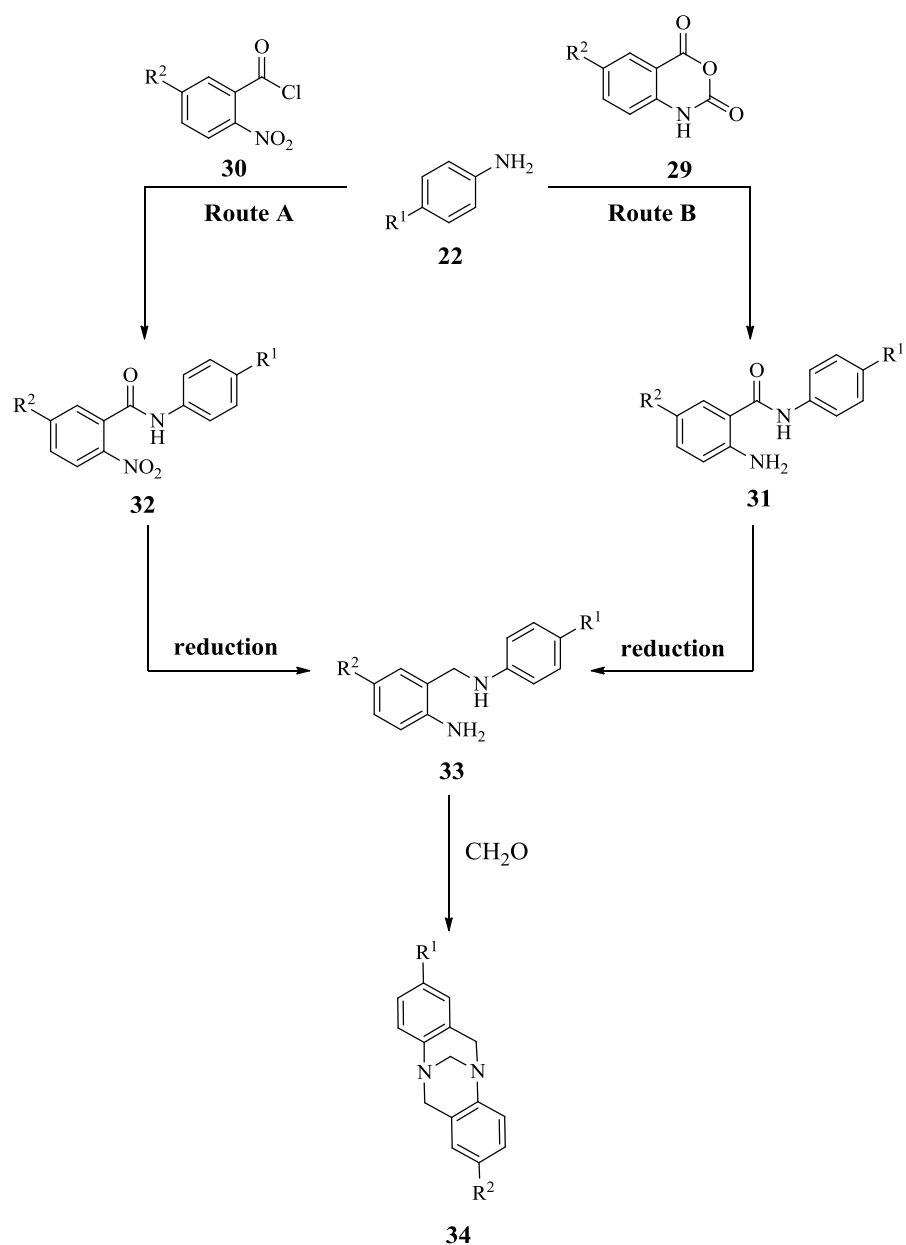
Scheme 81: Wilcox and co-workers approaches for the synthesis of unsymmetrical TB analogues.

A variety of substituents (R^1 = Me, MeO, R^2 = Me, Cl Br, NO_2) were shown to tolerate these reaction conditions to give a range of unsymmetrical TB analogues (See Chapter 1 for more detail). As previously, mentioned application of the synthetic Route B to (±)-**86** resulted in poor yields of the fused cleft intermediate (±)-**193**, thus we proposed that a procedure similar to Route A could potentially allow for the more reliable synthesis of the target fused cleft system (±)-**21**.

1,2-Dichloroethane (DCE) is reported as the preferred reaction solvent for reductive amination reactions with $NaBH(OAc)_3$, however reactions can also be carried out in THF and AcCN.[90] Due to the poor solubility of (±)-86 the reaction was performed in DCE only. A solution of (±)-86 in DCE was treated with two equivalents of 2-nitrobenzaldehyde 202 in the presence of acetic acid. Acetic acid acts as a catalyst to the reductive amination reaction. The reaction was stirred at room temperature for 24 h and gave the intermediate (±)-203 in 62 % yield (Scheme 82).
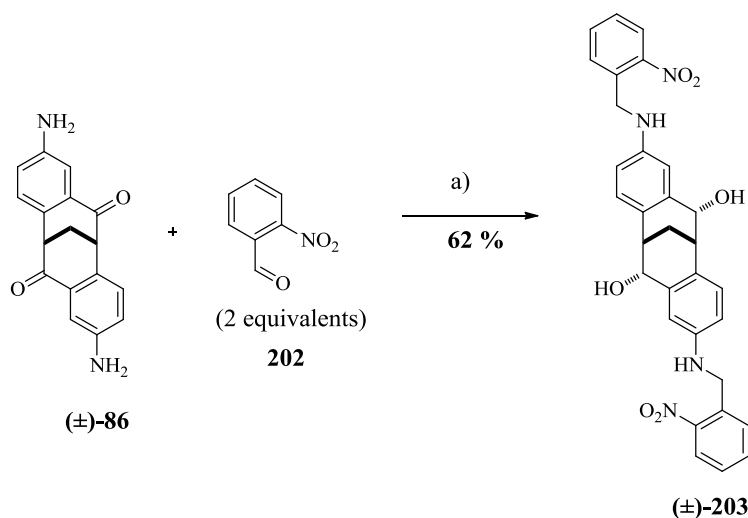
Reagents and Conditions: a) $NaBH(OAc)_3$, DCE, AcOH, rt 24 h.

Scheme 82: Reductive amination of (±)-86 and 202 with sodium triacetoxyborohydride to give intermediate (±)-203.

Unlike in the condensation reaction between (±)-86 and isatoic anhydride 196 this reduction amination step also resulted in the reduction of the carbonyl groups on (±)-86. This was evidenced by a multiplet peak in the ^1H NMR spectrum of (±)-203 at δ 4.98 ppm which integrated to two protons representing the C–H protons next to the hydroxyl groups.

The next step involved the chemoselective reduction of the nitro groups on (±)-203, which was achieved using the same Fe / AcOH reaction system used for the reduction of the nitro groups on (±)-85 in the synthesis of (±)-86 (Scheme 83).
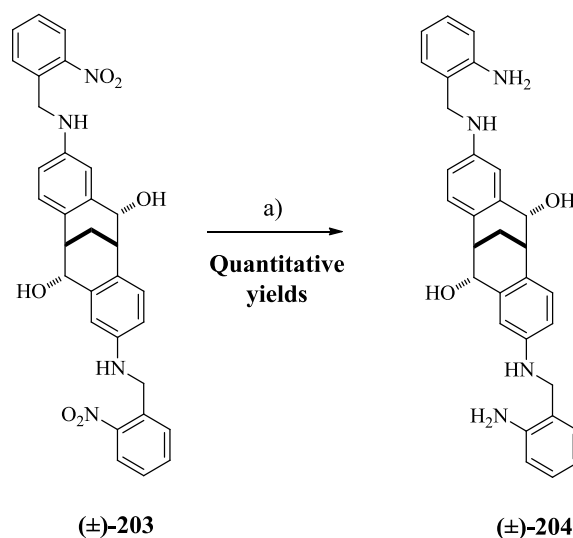
Reagents and Conditions: a) Fe, AcOH, EtOH, reflux, 48 h.

Scheme 83: Chemoselective reduction of nitro groups in (±)-203 to give the cyclisation precursor (±)-204.

Following isolation and NMR spectral analysis of (±)-204 as a crude mixture, it was then treated under the cyclisation reaction conditions reported by Wilcox. Thus a solution of (±)-204 (crude), paraformaldehyde and trifluoroacetic acid (TFA) in ethanol was stirred at 90 $^{\circ}$C for 24 h in attempt to form the target fused ring system (±)-21 (Scheme 84).
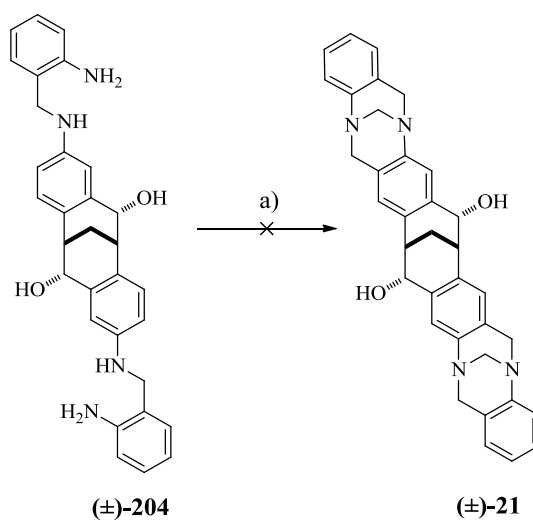
Reagent and Conditions: a) CH$_2$O, TFA, EtOH, 90 $^{\circ}$C, 24 h.

Scheme 84: Attempted cyclisation of (±)-204 to give the fused cleft system (±)-21.

Unfortunately treatment of (±)-204 under these reaction conditions led to its decomposition. At this stage the reason for this outcome is not fully understood, in addition the identities of

145

the decomposition products are also unknown due to the pure quality of NMR spectra obtained for the isolated compounds. Impurities and potentially a multitude of decomposition products may have contributed to poor spectra. It is reasonable to suggest that the hydroxyl groups attached to the carbocyclic cleft core may have impaired the cyclisation step however without further evidence to support this it is not possible to make any reliable conclusions.

4.5 Conclusions

During this research project a range of cleft molecules derived from the carbocyclic molecular cleft **2** have been synthesised. Literature procedures were followed to give access to racemic and enantiopure **2** which formed the core framework for further derivatisation. Similarly, the previously reported molecular clefts **3**, **(±)-73** and the halogen functionalised cleft **(±)-114** were synthesised, all of which can be expected to be further elaborated into complex molecular architectures. Exploration into the derivatisation of **2** with the aim of synthesising molecules presenting versatile functional groups capable of molecular recognition and binding process led us to synthesise the novel mono-hydroxylated cleft **(±)-123**. An interesting X-Ray crystal structure of the diphenyl molecular cleft **(±)-102** bound to a molecule of 3-bromopyridine **121** via H-bond interactions (Figure 16) provided important information with regards to the potential binding and uptake of target molecules by functionalised clefts presenting groups capable of H-bond donation. Although attempts to access the pyridine functionalised molecular clefts were met with little success it allowed us to redirect our research and reconsider the design of our molecular cleft systems.

Consideration of how compounds derived from this molecular cleft framework can be manipulated as asymmetric catalysts, coupled with an in-depth search of the literature for functionalities capable of H-bond donation and substrate activation led us to synthesise a family of novel amino-thiocarbamate functionalised clefts **(±)-4 – 9** (Scheme.46). Whilst these clefts were synthesised with relative ease over one-step from the reduced cleft **(±)-3** and commercially available isothiocyanates these structures proved to be incredibly complex and difficult to characterise. Sophisticated NMR studies were performed and supported the notion that these molecules exist as a complex mixture of rotamers. In some examples, spectral data was supported by X-Ray crystal structures of the novel cleft compounds. These crystal structures provided a vast amount of information about the cleft structures including the functional group orientation, cleft dimensions, packing patterns and binding interactions both to other cleft molecules and also to solvate molecules. As anticipated, cleft dimensions were influenced by the nature and position of the functional groups. This demonstrating the ability to fine-tune the structural properties and hence recognition and binding characteristics of these clefts which could potentially be manipulated for the specific up-take of target compounds. Of particular interest to this study was the X-Ray crystal structure of **(±)-4** which showed an acetonitrile solvate molecule bound within the cleft cavity via a pair of C−H⋯π

interactions (Figure 39). This result was encouraging as it demonstrated the potential of these clefts to up-take and bind molecules within a chiral pocket. Complexing of these cleft structures, targeted towards the specific uptake of substrate molecules is yet to be explored but can be expected to provide valuable information about the possible modes of binding and hence provide an insight to how these clefts can be applied as asymmetric controllers in organic reactions. The range of commercially available isothiocyanates as coupling partners to **3** is large and varied moreover; the ease in which the amino-thiocarbamate functional group can be installed onto the carbocyclic molecular cleft framework suggests that it would be possible to generate an extensive library of compounds containing this functional group. Furthermore, the ability to synthesise both the mono- and disubstituted clefts as well as the enantiopure variants lends these molecular clefts to be a potentially very versatile family of asymmetric organocatalysts.

These novel amino-thiocarbamate clefts were evaluated for catalytic activity in the HDA reaction of Rawel diene **10** and benzaldehyde **11**, and bromolactonisation reaction of **18** with NBS **19**. Whilst these clefts gave only moderate to poor yields and *ee* values in these reactions (without any optimisation) the ability of these clefts to be used as efficient organocatalysts in other asymmetric transformations is within the realms of possibility. Overall, the carbocyclic cleft offers a versatile chiral framework for the introduction of a range of functional groups capable of H-bond donation. A more comprehensive understanding of the mechanism in which these molecules bind to substrates is required. X-Ray analysis of inclusion complexes of the clefts and a range of substrate molecules would help identify a more suitable reaction for their use as asymmetric catalysts. In general it is reasonable to assume that these molecular clefts do interact with substrate molecules via H-bond interaction however, these interactions appear to result in no facial discrimination resulting in poor or no stereocontrol in the organic transformations.

The synthesis of a mixed chiral cleft containing both **1** and **2** was also investigated with a view towards the assembly of a unique family of rigid chiral cleft molecules with exceptional topology. Preliminary experiments allowed us to identify a viable route to these fused cleft systems and led to the synthesis of the novel TB derivative **199**. Applications of these conditions using the carbocyclic cleft however were met with some challenges. Overall, a stepwise approach for the synthesis of precursors which could potentially allow the

incorporation of the chiral cleft nucleus **2** into a fused system with TB **1** is reported and provides an excellent starting point for subsequent research.

This research is of significant adventure as we have established a new class of organocatalysts for asymmetric reactions which, could in the future following optimisation, achieve a low level of environmental impact in comparison to related transition-metal catalysts used for asymmetric synthesis. Coupled with the current lack of successful reagents for asymmetric carbon-carbon, carbon-heteroatom forming reactions, reactions which are of great importance to the academic and industrial world, further development of these systems will provide a much needed powerful weapon for the synthetic chemist. Our approach has shown proof of principle even though we have yet to optimise these methodologies and systems to determine how they can be perfected for natural product and large-scale synthesis. The potential rewards of further research in this area are potentially very large since to date there remains a lack of easily prepared, generally applicable chiral organocatalysts that are capable of high activity and enantioselectivity.

4.6 Future Work

The novelty of this cleft system lies in the ability to access enantiomerically pure antipodes of the core carbocyclic cleft with relative ease coupled with the ability to introduce functional groups at almost any position on the ring system. The results presented in this research project offer several areas of potential development and optimisation. Cleft derivatisation, characterisation, and optimisation studies are still expected to lead to the development of a range of functionalised clefts displaying a high level of chirality therefore, these areas will continue to form the focus of future work.

4.6.1 Derivatisation of the Carbocyclic Cleft Framework

Expanding on the scope of these cleft molecules as asymmetric catalysts by installing a range of different functional groups capable of complementary binding and activation modes, may bring their reactivity into line with that observed for other asymmetric H-bond organocatalysts. Therefore, the synthesis of clefts incorporating two different functional groups presenting bifunctional activity could serve as a starting point for subsequent research projects. In addition, the ease in which functional groups can be introduced onto the aromatic rings of the carbocyclic cleft framework offers additional opportunities for catalyst derivatisation. We have shown that the cleft dimensions in terms of interplanar 'cleft' angle (θ) can be modified through the installation of different functional groups at the aromatic ring positions. Comparison of the 'cleft' angles in a range of functionalised cleft derivatives showed that the electron density of the aromatic substituents has a greater influence on the cleft dimensions than substituents introduced at the carbonyl positions. Therefore, it is reasonable to assume that derivatisation of the cleft through functionalisation of the aromatic rings would offer a greater opportunity to fine-tune the cleft system for the binding of specific substrates.

Further elaboration of the isothiocyanate moiety onto the cleft system at these positions on the cleft leads to the proposed synthesis of a novel family of disubstituted thiourea cleft derivatives, starting from the accessible diamine cleft (±)-86 (Scheme 85) .

(±)-86 → a) → R = aryl, allyl, EWG, EDG etc

(±)-205
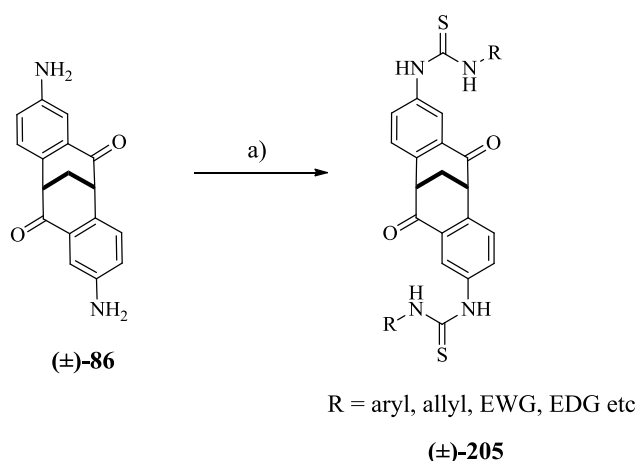
Reagents and Conditions: a) Base, substituted isothiocyanate

Scheme 85: Proposed synthesis of a novel family of disubstituted thiourea cleft catalysts.

The cleft **86** can be synthesised both as a racemic mixture and as its pure enantiomers with relative ease over two-steps starting from the carbocyclic cleft **2**. Treatment of **86** with a suitable base in the presence of substituted isothiocyanates should in theory yield the proposed disubstituted thiourea derivatives.

In recent years, several research groups worldwide have realised the potential of thiourea derivatives as H-bond organocatalysts, the scope of which covers both non-stereoselective and stereoselective applications in organic synthesis. A broad range of mono-functional and bifunctional chiral double H-bonding thiourea organocatalyst derivatives incorporating the electron deficient 3,5-bis(trifluoromethyl)phenyl substrate functionality have been developed. These catalysts have been used to accelerate various synthetically useful organic transformations employing H-bond accepting substrates such as carbonyl compounds, imines and nitroalkenes as the starting materials. Consequently it may be beneficial to explore the synthesis of cleft derivatives incorporating the 3,5-bis(trifluoromethyl) phenyl derived thiourea group (Figure 72).
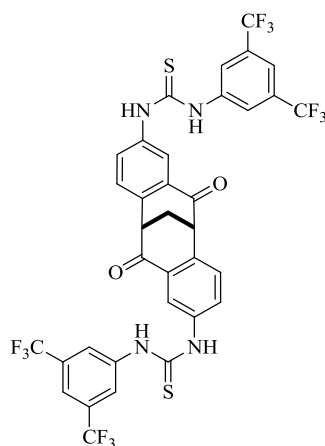
206

Figure 72: Proposed structure of the potentially useful double H-bonding disubstituted thiourea cleft 206.

These disubstituted thiourea clefts not only offer the potential to alter the cleft dimensions, but they also present two functional groups capable of double H-bond activation. Moreover as they are attached to the aromatic rings of the cleft framework they will be directed 'downwards' towards the cleft cavity thus optimising the 'chiral pocket' for substrate binding and transition state organisation (Figure 73).
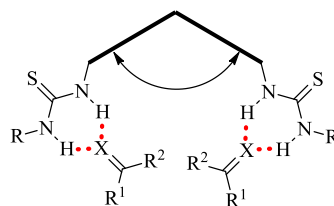
207

Figure 73: Model of potential double H-bond activation by the disubstituted thiourea cleft derivatives and how functionalisation of the aromatic rings many affect the cleft dimensions

4.6.2 Asymmetric Organocatalysis

The full potential of the amino-thiocarbamate functionalised clefts still remain elusive primarily due to the challenge in synthesising the enantiomerically pure carbocyclic cleft framework in multi-gram quantities. Systematically looking at different reaction parameters including solvent systems, reaction time and temperature in addition to the potential use of additives may lead to improved enantioselectivites.

It is possible that these cleft derivatives may interact more efficiently with different substrates and therefore, be more applicable to other organic transformations. Using these catalysts in an array of asymmetric reactions could produce interesting results and allow for an optimum transition state structure between catalyst and substrate to be identified. Screening of these catalysts in a range of organic transformations which employ H-bond accepting substrates such as carbonyl compounds, imines and nitroalkenes as the starting materials serves as a point of future interest.

4.6.3 Development of the Proposed Mixed Cleft System

4.6.3.1 Asymmetric Synthesis

Once a repeatable synthetic methodology for the synthesis of racemic fused mixed cleft system (±)-**21** is established and full characterisation of the cyclisation product is reliably determined, the next step in this research project would be for the asymmetric synthesis of **21** (Figure 74).
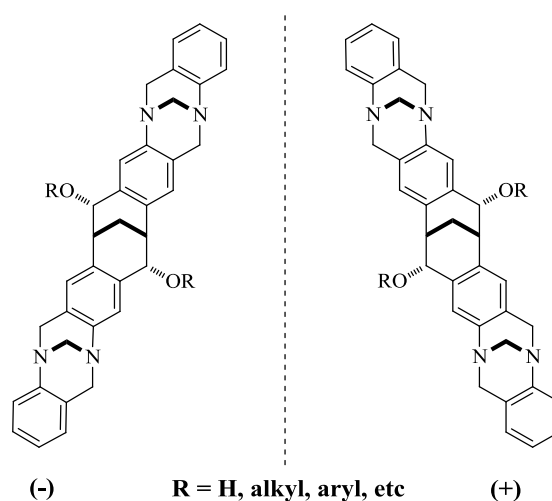
Figure 74: Proposed structures of the enantiopure fused cleft systems.

As previously reported both antipodes of the starting carbocyclic cleft **2** are readily available in gram quantities and with excellent *ee* values via the chiral resolution of the intermediate racemic diacid encountered within its synthesis. This will in theory allow access to the desired chiral analogues.

4.6.3.2 Synthesis of Analogues

The ability to use substituted isatoic anhydride presents an opportunity to further functionalise the periphery of the cleft (Scheme 86).
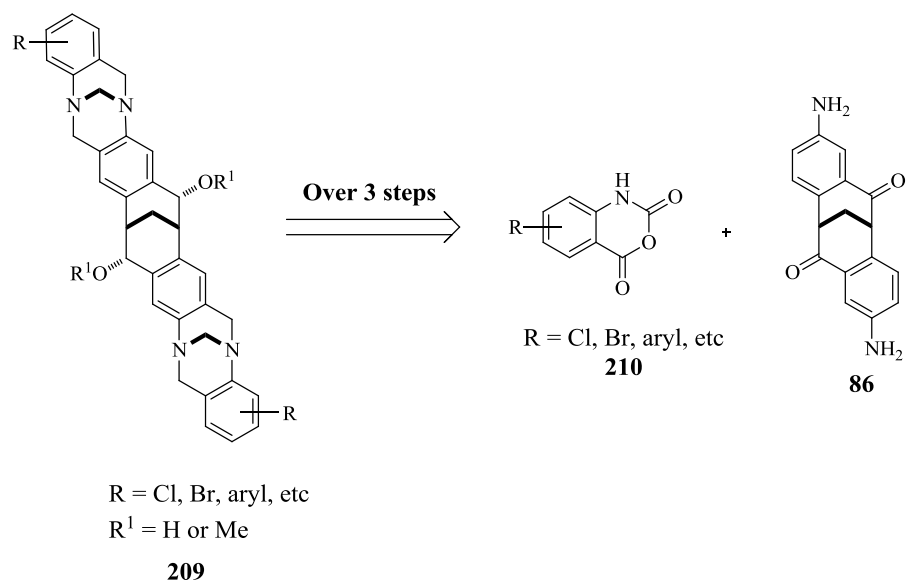
Scheme 86: Possible retrosynthetic pathway to functionalised analogues of the fused molecular cleft system, starting from substituted isatoic anhydride derivatives and the symmetrical carbocyclic cleft 86.

Similarly, using substituted aromatic aldehydes related to 2-nitrobenzaldehye **202** in the reductive amination step may also offer opportunities for the synthesis of functionalised analogues of the fused cleft. Moreover, the pyridyl isatoic anhydride **212** would allow an opportunity to develop chiral DMAP equivalents which, alone presents a whole new area of catalysis (Scheme 87).

R = H or Me
211
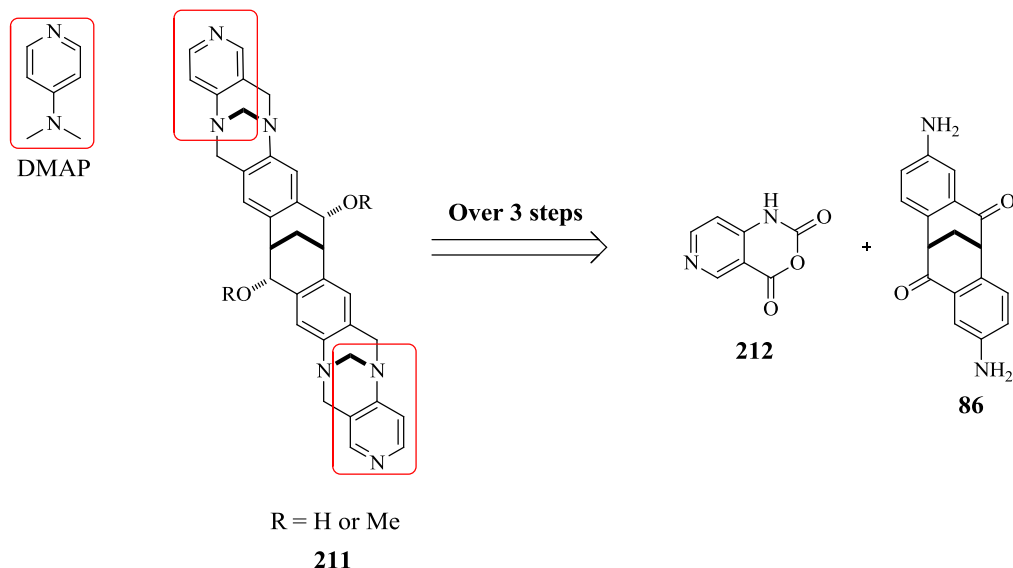
Scheme 87: Proposed structure of fused molecular cleft systems incorporating the DMAP functionality and the possible substrates required for its synthesis.

4.6.3.3 Application as H-bonding Catalysts

The rigid chiral structure of **1** coupled with the presence of transition metal binding sites (the nitrogen atoms) make **1** and its analogues good candidates as ligands in asymmetric catalysis. In recent years TB-embedded materials have been employed in different heterogeneous catalytic processes with encouraging results. Similarly, Friberg and co-workers have shown that functionalised derivatives of the carbocyclic molecular cleft **2** presenting H-bond donor groups can be effective H-bond catalysts for the HDA reaction.

In theory the fused cleft molecules, as well as the proposed functionalised analogues, are ideal surrogates as they combine all of the above features into one system. Moreover, these fused cleft systems not only supply H-bond donor groups vital for binding and catalysis but the extended concave aromatic cleft also presents a more structurally ordered chiral pocket for the binding and organisation of the reagents within the transition state.

Chapter 5

5.0 Experimental

5.1 General Considerations

All infrared spectra were obtained using a Perkin-Elmer, spectrum 65 FT-IR spectrophotometer; spectra for liquids were acquired as a thin film using sodium chloride plates or in the case of solids, as a KBr disc.

All ^{1}H and ^{13}C NMR spectra were measured at 400 and 100 MHz respectively using a Bruker DPX 400 MHz spectrometer. The solvent used for NMR spectroscopy was chloroform-d_1 (δ 7.26, ^{1}H; δ 77.0, ^{13}C) using TMS (tetramethylsilane) as the internal reference, unless stated otherwise. Chemical shifts are given in parts per million (ppm) and J values are given in Hertz (Hz). Various 2D-techniques and DEPT experiments were used to establish the structures and to assign the signals.

The mass spectra were recorded using a Thermoscientific exactive (Orbi) ESI (Ethanol) via nanomate (Advion) and by the EPSRC national mass spectrometry service at the University of Wales, Swansea, utilising electrospray (ES).

Crystal data was collected on either; a Burker APEX 2 CCD difractometer ω rotation with narrow frames using a synchrotron source (0.7749 Å), at the Advanced Light Source, U.S Department of Energy or a Burker APEX 2 CCD difractometer using Burker SAINT programs(s) to solve structure, SHELXS97 (Sheldrick, 2008) program(s) to refine structure, SHELXL2012 (Sheldrick, 2012), molecular graphics: Burker SHELXTL, software to prepare material for publication, at Loughborough University.

Melting points were recorded using an Electrothermal-IA 9100 melting point instrument and are uncorrected.

All chromatographic manipulations used silica gel as the adsorbent. Reactions were monitored using thin layer chromatography (TLC) on aluminium backed plates with Merck TLC 60 F_{254} silica gel. TLC visualised by UV radiation at a wavelength of 254 nm, or stained by exposure to an ethanolic solution of vanillin (acidified with concentrated sulphuric acid) or an ethanolic solution of Phosphomolybdic acid, followed by charring where

appropriate. Purification by column chromatography using Apollo ZEOprep 60/ 40-63 micron silica gel.

Purification by column chromatography used Merck Kiesel 60 H silica adsorbent.

Enantiomeric excess (ee) was determined by chiral HPLC. A Eurocel 01 (manufactured by Knauer, Chiracel OD equivalent) column was used for the determination of enantiomeric excess on a Gilson HPLC instrument, with the ultraviolet absorption detector set at 254 nm, attached to a Clarity data station.

The reactions requiring anhydrous conditions were carried out using flame dried glassware, under a nitrogen atmosphere unless otherwise stated. Reaction solvents were used as obtained commercially. Tetrahydrofuran (THF) was distilled under an argon atmosphere from the sodium/benzophenone ketyl radical.

5.2   Experimental Data

5.2.1   Synthesis of Carbocyclic Molecular Cleft Framework (2)

5.2.1.1   Racemic and *meso*-2,4-Diphenylpentanedinitrile (67)[30,34]

$(\pm)$-**67**   *meso*-**67**
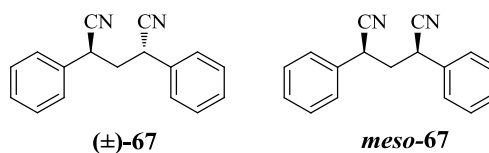
Finely powdered sodium hydroxide (20.00 g, 0.5 M) was added to a mixture of phenylacetonitrile (58.80 g, 0.50 M) and diiodomethane (67.90 g, 0.25 M). The reaction mixture was stirred at 140 $^{\circ}$C for 2 h, cooled to ambient temperature and then a 1:1 mixture of water / diethyl ether (100 mL) was added. The mixture was poured onto water (250 mL) and extracted with diethyl ether (3 x 150 mL). Combined organic layers were dried over $MgSO_4$, filtered and the solvent removed under vacuum to give crude racemic and *meso*-2,4-diphenylpentanedinitrile **67** as a dark red / brown residue (47.50 g, 79 %).

IR CH_2Cl_2 max/cm^{-1}: 3055 (aromatics), 2245 (CN); compound isolated as a mixture of diastereomers (1:1 dr); **^{1}H NMR** (400 MHz, CDCl$_3$): δ 7.52-7.30 (m, 20H), 4.09 (t, *J* = 8.0 Hz, 2H), 3.78 (t, *J* = 8.0 Hz, 2H) 2.69 (m, 1H), 2.45 (t, *J* = 7.6 Hz, 2H), 2.38 (m. 1H); **^{13}C NMR** (100 MHz, CDCl$_3$): δ 133.93, 133.57, 129.99, 129.65, 129.54, 129.16, 129.05, 128.90, 128.04, 127.96, 127.43, 127.32, 119.38, 119.34, 41.78, 40.94, 35.71, 34.90, 23.62; **MS** *m/z* found 269.1046 $C_{17}H_{14}N_2$ (M$^+$ Na) expected 269.1049 (M$^+$ Na).

5.1.2.2 Racemic 2,4-Diphenylpentanedioic acid (±)-68[30,34]

(±)-68
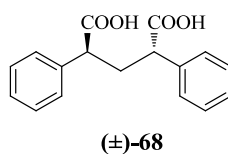
To a solution of (±, *meso*)- 2,4-diphenylpentanedinitrile **67** (1:1 dr) (57.13 g, 0.23 M) in ethanol (350 mL) was added to a solution of potassium hydroxide (195.17 g, 5.4 M) in water (400 mL). The resulting reaction mixture was stirred under reflux for 18 h. After this time the reaction was cooled to ambient temperature and the ethanol was removed under vacuum. The aqueous phase was washed with diethyl ether (3 x 200 mL) and then acidified with concentrated hydrochloric acid; the acidified solution was then extracted into ethyl acetate (3 x 250 mL). The combined organic layers were washed with water (2 x 150 mL), dried over MgSO$_4$, filtered and the solvent removed under vacuum to give crude (±, *meso*)-2,4-diphenylpentanedioic acids **68** as an orange / brown residue. Crude (±, *meso*) - **68** were recrystallized from hot toluene three times to give the pure racemate **(±)-68** as a slightly off white solid (29.84 g, 45 %).

Mp.127.5 – 130.6 ^{o}C (*Lit Mp. 147.5 – 163.0 ^{o}C a mixture of meso and rac isomers*)[30]; **IR** CH$_2$Cl$_2$ max/cm^{-1}: 3030 (b, O–H), 2661 (aromatics), 1705 (s, C=O); **^{1}H NMR** (400 MHz, CDCl$_3$): δ 7.38 – 7.19 (m, 10H), 3.46 (t, *J* = 7.6 Hz, 2H), 2.61 (t, *J* = 7.6 Hz, 2H); **^{13}C NMR** (100 MHz, CDCl$_3$): δ 178.84, 136.94, 129.05, 128.92, 128.24, 127.94, 125.31, 48.58, 21.47; **MS** *m/z* found 307.0939 C$_{17}$H$_{16}$O$_4$ (M$^+$ Na) expected 307.0941 (M$^+$ Na).

5.1.2.3 Optical Resolution of Racemic 2,4-Diphenylpentanedioic acids (68)[30]

(+)-68   (-)-68
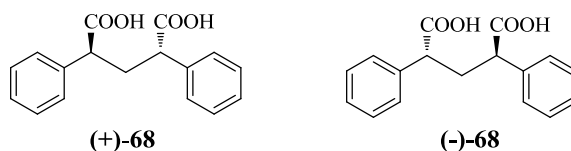
(2*S*, 4*S*)-2, 4-Diphenylpentanedioic acid (+)-68. A solution of (±)-2,4-diphenylpentanedioic acid (±)-67 (11.54 g, 0.04 M) in 99 % ethanol (150 mL) was added to a mixture of quinine (13.66 g, 0.04 M) in 99 % ethanol (200 mL). The reaction mixture was stirred at room temperature for 18 h. The resulting quinine salt was removed by filtration and washed with ethanol. The quinine salt was added to 4 M hydrochloric acid and the aqueous phase was extracted with diethyl ether (3 x 100 mL). The organic phases were combined, dried over $MgSO_4$, filtered and solvent removed under vacuum to give (+)-68 as a colourless solid (4.08 g, 35 %).

Mp 176.3 – 180.4 ^{o}C (*Lit* Mp 197.0 – 198.5 ^{o}C);[30] $[\alpha]_D$ +78.0 (*c* 0.32, $CHCl_3$) (*Lit*. $[\alpha]_D$ +70.0 (*c* 0.30, EtOH);[34] **IR** CH_2Cl_2 max/cm^{-1}: 3055 (s, O–H), 2987 (aromatics), 1710 (s, C=O); **¹H NMR** (400 MHz, $CDCl_3$): δ 7.38 – 7.23 (m, 10H), 3.45 (t, *J* = 7.6 Hz, 2H), 2.60 (t, *J* = 7.6 Hz, 2H); **¹³C NMR** (100 MHz, $CDCl_3$): δ 179.04, 136.95, 128.91, 128.25, 127.94, 48.62, 35.44; **MS** *m/z* found 307.0939 $C_{17}H_{16}O_4$ (M$^+$ Na) expected 307.0941 (M$^+$ Na).

(2*R*, 4*R*)-2,4-Diphenylpentanedioic acid (-)-68. The ethanol filtrate removed from the quinine salt above was concentrated to dryness under vacuum to give a pale yellow solid. This was dissolved in diethyl ether (100 mL) and acidified with 4 M hydrochloric acid. The aqueous phase was extracted with diethyl ether (3 x 100 mL) and the combined organic phases were dried over $MgSO_4$, filtered and concentrated to dryness under vacuum to give (-)-68 as a colourless foamy solid (3.69 g, 32 %).

Mp 187.5 – 191.6 ^{o}C (*Lit*. 197.0 – 198.5 ^{o}C (For (+) enantiomer, no data for (-))[30]; $[\alpha]_D$ -83.2 (*c* 0.31, EtOH) (*Lit*. $[\alpha]_D$ -82.1 (*c* 0.28, EtOH);[34] **IR** CH_2Cl_2 max/cm^{-1}: 3054 (s, O–H), 2987 (aromatics), 1708 (s, C=O); **¹H NMR** (400 MHz, $CDCl_3$): δ 7.38 – 7.20 (m, 10H), 3.44 (t, *J* = 7.6 Hz, 2H), 2.60 (t, *J* = 7.6 Hz, 2H); **¹³C NMR** (100 MHz, $CDCl_3$): δ 179.70, 136.91, 128.93, 128.27, 127.97, 48.74, 35.35; **MS** *m/z* found 307.0941 $C_{17}H_{16}O_4$ (M$^+$ Na) expected 307.0941 (M$^+$ Na).

5.1.2.4 Racemic, (+) and (-) 5, 11-Methanodibenzo[*a*,*e*][8]annulene-6,12(5*H*,11*H*)-dione (2)[30]
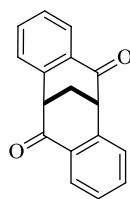
2

Racemic (±)-2 (*from (±) and meso - 2,4-Diphenylpentanedioic acid 68*). Racemic and *meso* - 2, 4-diphenylpentanedioic acids **68** (54.71 g, 0.19 M) were dissolved in an excess of concentrated sulphuric acid (550 mL) and heated under reflux for 2 h. After this time the hot black mixture was poured onto ice and extracted with toluene (3 x 200 mL). The combined organic layers were washed with *sat.*NaHCO$_3$ (2 x 100 mL) followed by water (2 x 100 mL). The organic layer was dried over MgSO$_4$, filtered and the solvent removed under vacuum to give crude (±)-2 as a fine white solid, which was recrystallized from hot methanol to give (±)-2 as colourless needle like crystals (9.56 g, 20 %).

Mp 146.1 – 146.6 ^{o}C (*Lit.* 147.7 -148.8 ^{o}C)[30]; **IR** CH$_2$Cl$_2$ max/cm^{-1}: 3054 (s, C–C, aromatics), 1685 (s, C=O); **^{1}H NMR** (400 MHz, CDCl$_3$): δ 7.99 (dd, *J* = 6.8, 1.2 Hz, 2H), 7.56 – 7.48 (m, 4H), 7.41(td, *J* = 6.8, 1.6 Hz, 2H), 4.04 (t, *J* = 2.8 Hz, 2H), 3.03 (t, *J* = 2.8 Hz, 2H); **^{13}C NMR** (100 MHz, CDCl$_3$): δ 194.44, 140.06, 134.53, 128.85, 128.83, 128.80, 48.82, 32.33; **MS** *m/z* found 271.0729 C$_{17}$H$_{12}$O$_2$ (M$^+$ Na) expected 271.0730 (M$^+$ Na); chiral HPLC (Chiralcel ID column, hexane: 2-propanol = 98:2 0.6 mL min^{-1}) showed < 5% *ee* (t_1= 31.35 min, t_2 = 32.30 min). See Appendix 7.10 for HPLC data.

(+)-2 (*from (2R, 4R)-2,4-Diphenylpentanedioic acid (-)-68*); colourless crystalline solid (0.38 g, 42 %); **Mp** 189.7 – 194.1 ^{o}C (*Lit.* 194.0 – 194.5 ^{o}C)[30]; [α]$_D$ + 120.3 (*c* 1.0, CHCl$_3$) (*Lit.* [α]$_D$ +139.5 (*c* 0.02, 99 % EtOH); **IR** CH$_2$Cl$_2$ max/cm^{-1}: 1683 (s, C=O); **^{1}H NMR** (400 MHz, CDCl$_3$): δ 7.89 (dd, *J* = 6.4, 1.2 Hz, 2H), 7.46 – 7.28 (m, 4H), 7.30 (td, *J* = 5.6, 1.6 Hz, 2H); 3.95 (t, *J* = 2.8 Hz, 2H), 2.93 (t, *J* = 2.8 Hz, 2H); **^{13}C NMR** (100 MHz, CDCl$_3$): δ 194.43, 140.06, 134.53, 128.85, 128.83, 128.80, 48.82, 32.33; **MS** *m/z* found 271.0727 C$_{17}$H$_{12}$O$_2$ (M$^+$ Na) expected 271.0730 (M$^+$ Na); chiral HPLC (Chiralcel ID column, hexane: 2-propanol = 98:2 0.6 mL min^{-1}) showed > 99 % *ee* (t_1= 32.30 min (major), t_2 = 38.56 min (minor)).See Appendix 7.11 for HPLC data.

(-)-2 (*from (2S, 4S)-2,4-Diphenylpentanedioic acid (+)-68*); colourless crystalline solid (0.66 g, 58 %); **Mp** 191.6 – 193.3 $^{\mathrm{o}}$C (*Lit.* 194.0 – 194.5 $^{\mathrm{o}}$C (For (+) Dione no data for (-))[30]; $[\alpha]_D$ − 142.6 (*c* 1.0, CHCl$_3$); **IR** CH$_2$Cl$_2$ max/cm^{-1}: 3055, 2986, 2945 (aromatics), 1685 (s, C=O); **^{1}H NMR** (400 MHz, CDCl$_3$): δ 7.99 (dd, *J* = 6.8, 1.2 Hz, 2H), 7.56 – 7.48 (m, 4H), 7.39 (td, *J* = 5.6, 1.6 Hz, 2H); 4.04 (t, *J* = 2.8 Hz, 2H), 3.03 (t, *J* = 2.8 Hz, 2H); **^{13}C NMR** (100 MHz, CDCl$_3$): δ 194.46, 140.05, 134.56, 128.84, 128.81, 128.31, 48.81, 32.32; **MS** *m/z* found 271.0723 C$_{17}$H$_{12}$O$_2$ (M$^+$ Na) expected 271.0730 (M$^+$ Na); chiral HPLC (Chiralcel ID column, hexane: 2-propanol = 98:2 0.6 mL min^{-1}) showed > 99 % *ee* (t_1= 33.07 min (minor), t_2 = 36.55 min (major)).See Appendix 7.12 for HPLC data.

5.2.2 Preparation of Reduced Carbocyclic Molecular Cleft (3)

5.2.2.1 Racemic, (+) and (-)-5, 6, 11, 12-tetrahydro-5,11-methanodibenzo [a,e][8]annulene-6,12 diol (3)

3
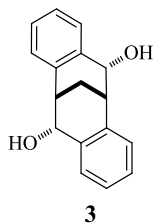
Racemic (±)-3; A solution of **(±)-2** (0.36 g, 1.45 mmol) and sodium borohydride (0.27 g, 7.22 mmol) in THF (12 mL) and methanol (12 mL) was stirred at room temperature for 48 h. After this time the solvent was removed under vacuum and ethyl acetate (25 mL) and water (20 mL) were added. The organic layer was washed with water (3 x 20 mL), dried over MgSO₄, filtered and the solvent removed under vacuum to give **(±)-3** as a colourless solid (0.29 g, 79 %).

Mp 236.6 – 238.6 $^{\circ}$C (*Lit. 225.0 $^{\circ}$C, with sublimation*)[30]; **IR** CH₂Cl₂ max/cm⁻¹: 3247 (O–H), 2922, 2858 (Aromatics); **¹H NMR** (400 MHz, CDCl₃): δ 7.49 (d, J = 7.2 Hz, 2H), 7.24 – 7.12 (m, 6H), 4.99 (dd, J = 12.0, 5.6 Hz, 2H), 3.27 (dt, J = 6.0, 2.8 Hz, 2H), 2.36 (t, J = 3.2 Hz, 2H), 1.47 (m, 2H); **¹³C NMR** (100 MHz, CDCl₃): δ 139.68, 133.93, 130.01, 127.82, 127.61, 127.12, 72.65, 39.39, 29.35; **MS** *m/z* found 275.1039 C₁₇H₁₆O₂ (M⁺ Na) expected 275.1043 (M⁺ Na); chiral HPLC (Chiralcel IB column, hexane: 2 - propanol = 95:5, 0.6 mL min⁻¹) showed < 5 % *ee* (t_1= 17.59 min, t_2 = 20.42 min).See Appendix 7.13 for HPLC data.

(+)-3 (*from (+)-2*); colourless solid (0.42 g, 81 %); **Mp** 186.2 – 188.2 $^{\circ}$C (*Lit.* 179.7 – 189.4 $^{\circ}$C)[30]; [α]$_D$ + 193.6 (*c* 1.0, CHCl₃); **IR** CH₂Cl₂ max/cm⁻¹: 3391 (b, O–H); **¹H NMR** (400 MHz, CDCl₃): δ 7.59 (d, J = 7.2 Hz, 2H), 7.31 – 7.21 (m, 6H), 5.09 (dd, J = 12.0, 5.6 Hz, 2H), 3.37 (m, 2H), 2.46 (t, J = 3.2 Hz, 2H), 1.59 (m, 2H); **¹³C NMR** (100 MHz, CDCl₃): δ 139.67, 133.94, 130.02, 127.82, 127.60, 127.12, 72.65, 39.39, 29.35; **MS** *m/z* found 275.1039 C₁₇H₁₆O₂ (M⁺ Na) expected 275.1043 (M⁺ Na); chiral HPLC (Chiralcel IB column, hexane: 2-propanol = 95:5, 0.6 mL min⁻¹) showed > 99 % *ee* (t_1= 17.96 min (major), t_2 = 21.16 min (minor)).See Appendix 7.14 for HPLC data.

(-)-3 (from (-)-2); colourless solid (0.26 g, 72 %); **Mp** 184.3 − 185.8 $^{\circ}$C (*Lit.* 187.9 − 188.3 $^{\circ}$C)[30]; $[\alpha]_D$ − 153.6 (*c* 1.0, CHCl$_3$) (*Lit.* $[\alpha]_D$ −388.5 (*c* 0.02, 99% EtOH))[30]; **IR** CH$_2$Cl$_2$ max/cm^{-1}: 3386 (b, O–H); **^{1}H NMR** (400 MHz, CDCl$_3$): δ 7.49 (d, *J* = 7.2 Hz, 2H), 7.22 − 7.12 (m, 6H), 4.99 (dd, *J* = 6.4, 5.6 Hz, 2H), 3.27 (dt, *J* = 6.4, 3.6 Hz, 2H), 2.36 (t, *J* = 3.2 Hz, 2H), 1.47 (m, 2H); **^{13}C NMR** (100 MHz, CDCl$_3$): δ 139.68, 133.93, 130.02, 127.82, 127.60, 127.12, 72.65, 39.39, 29.35; **MS** *m/z* found 275.1039 C$_{17}$H$_{16}$O$_2$ (M$^+$ Na) expected 275.1043 (M$^+$ Na); chiral HPLC (Chiralcel IB column, hexane: 2-propanol = 95:5, 0.6 mL min^{-1}) showed > 99 % *ee* (t_1= 16.68 min (minor), t_2 = 18.54 min (major)).See Appendix 7.15 for HPLC data.

5.2.3 Functionalisation of the Carbocyclic Molecular Cleft

5.2.3.1 Preparation of Racemic 2,8-Dimethyl-5,11-methanodibenzo [*a,e*][8]annulene-6,12(5*H*,11*H*)-dione (Dimethyl cleft) ((±)-73)[33]
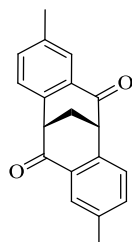
(±)-**73**

A solution of methylphenylacetonitrile (8.00 g, 0.061 M) and powdered sodium hydroxide (2.41 g, 0.061 M) in diiodomethane (8.30 g, 0.031 M) was stirred at 165 $^{\circ}$C for 45 min. The reaction mixture was cooled followed by the addition of water and dichloromethane. The aqueous layer was repeatedly washed with dichloromethane (3 x 150 mL), the combined organic layers were washed with brine, dried over anhydrous $MgSO_4$, and the solvent removed under vacuum to give a crude mixture of (±)-and *meso*-phenylpentanedinitrile (6.53 g, 39 %), which was hydrolysed by heating at 80 $^{\circ}$C for 18 h in a solution of potassium hydroxide (13.43 g, 0.37 M) in ethanol (75 mL) and water (80 mL). After this time the ethanol was removed under vacuum and the residue was diluted with water and repeatedly washed with dichloromethane. The aqueous phase was acidified to pH < 1 by the addition of hydrochloric acid (3 M) and extracted with ethyl acetate. The combined organic layers were dried over anhydrous $MgSO_4$, filtered and the solvent removed under vacuum to give a crude mixture of (±) and *meso*-phenylpentanedioic acids (4.79 g, 65 %). The crude acids were dissolved in *conc*.H_2SO_4 (250 mL) and heated at 100 $^{\circ}$C for 45 min. After this time the reaction was poured onto ice and extracted with diethyl ether, combined organic layers were washed with potassium hydroxide solution, dried over anhydrous $MgSO_4$, filtered and evaporated to dryness under vacuum. The crude compound was purified by column chromatography (R*f* = 0.53, L.Pet /EtOAc, 7:3) to give the title compound (±)-**73** as a colourless solid (0.57 g, 14 %).

Mp 186.2 – 188.6 $^{\circ}$C (*Lit*.183.0 – 186.0 $^{\circ}$C)[8]; **IR** CH_2Cl_2 max/cm^{-1}: 2939, 2868 (aromatics), 1684 (s, C=O); **^{1}H NMR** (400 MHz, $CDCl_3$): δ 7.78 (s, 2H), 7.38 – 7.32 (m, 4H), 3.98 (t, *J* = 3.2 Hz, 2H), 2.98 (t, *J* = 2.8 Hz, 2H), 2.33 (s, 6H); **^{13}C NMR** (100 MHz, $CDCl_3$): δ 194.98, 138.76, 137.23, 135.36, 128.70, 128.62, 128.44, 48.48, 32.54, 21.03; **MS** *m/z* found 299.1033 $C_{19}H_{16}O_2$ (M$^+$ Na) expected 299.1043 (M$^+$ Na).

5.2.3.2 Preparation of Racemic 6,12-Dichloro-5,6,11,12-tetrahydro-5,11-methanodibenzo[*a,e*][8]annulene (Dichloride Cleft) ((±)-144)[30]
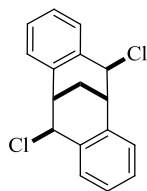
(±)-144

A neat solution of **(±)-3** (80.00 mg, 0.32 mmol) and thionyl chloride (2 mL, 14.50 mmol) was heated at 150 $^{\circ}$C for 24 h to give a dark brown solution. After this time the reaction was cooled to ambient temperature and quenched by the careful addition of water (25 ml). The reaction was extracted with diethyl ether (3 x 25 mL) and combined organic layers were dried over Na_2SO_4, filtered and solvent removed under vacuum to give the title compound **(±)144** as an off-white solid (0.072 g, 83 %).

Mp 132.7 – 133.2 $^{\circ}$C (*Lit.* 130.4 – 132.1 $^{\circ}$C, for (-) enantiomer)[30]; **¹H NMR** (400 MHz, CDCl₃): δ 7.20 – 7.17 (m, 4H), 7.13 – 7.11 (m, 4H), 5.01 (d, *J* = 2.4 Hz, 2H), 3.49 (q, *J* = 2.8 Hz, 2H), 2.60 (t, *J* = 2.8 Hz, 2H); **¹³C NMR** (100 MHz, CDCl₃): δ 136.54, 134.03, 131.27, 129.51, 129.07, 128.20, 61.91, 41.23, 18.40; **MS** *m/z* found 311.0381 $C_{17}H_{14}Cl_2$ (M^+ Na) expected 311.0365 (M^+ Na). See Appendix 7.1 for X-Ray data.

5.2.3.3 Preparation of Racemic 6,12-Diphenyl-5,6,11,12-tetrahydro-5,11-methanodibenzo[*a,e*][8]annulene-6,12-diol (Diphenyl-diol cleft) ((±)-102) via in-situ Grignard Reagent
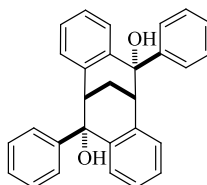
(±)-102

To a solution of 3-bromopyridine (1.64 g, 10.38 mmol) in dry THF (15 mL) under an N_2 atmosphere at -40 $^{\circ}$C was added phenylmagnesium bromide (1.0 M in THF, 0.01 mL, 10.0 mmol) over a period of 10 min. The resulting reaction mixture was stirred at –40 $^{\circ}$C for a further 30 min to give a bright orange solution. Br/Mg exchange was assumed complete after this time. The solution of prepared Grignard reagent was added to a solution of **(±)-2** (0.69 g, 2.78 mmol) in dry THF (10 mL) at -40 $^{\circ}$C via a cannula under an N_2 atmosphere. The reaction was stirred at -40 $^{\circ}$C for 1 h and then at room temperature for 1 h to give an opaque pale yellow solution. After this time the reaction was quenched by the careful addition of *sat.*NH_4Cl (10 mL) and then poured onto water (25 mL). The aqueous phase was extracted ethyl acetate (3 x 50 mL) and combined organic layers were washed with brine (50 mL), dried over anhydrous $MgSO_4$ and the solvent removed under vacuum. The crude product was purified by column chromatography (Rf = 0.3, light petroleum / EtOAc, 4:1) to give the title compound **(±)-102** as a white crystalline solid (1.19 g, 99 %).

Mp 220.7 – 221.3 $^{\circ}$C (*Lit* Mp 218 – 219 $^{\circ}$C (For (-) enantiomer)[6]; **IR** CH_2Cl_2 max/cm^{-1}: 3559 (s, OH), 3054 (Aromatics); **^{1}H NMR** (400 MHz, $CDCl_3$): δ 8.67 (d, *J* = 2.4 Hz, 1H), 8.52 (dd, *J* = 7.6, 1.2 Hz, 1H), 7.82 (dq, *J* = 4.4, 1.6 Hz, 1H), 7.61 (dd, *J* = 7.6, 1.2 Hz, 2H), 7.45 (dd, *J* = 7.6, 1.2 Hz, 2H), 7.40 (td, *J* = 7.6, 1.6 Hz, 2H), 7.31 – 7.24 (m, 12H), 3.28 (t, *J* = 3.2 Hz, 2H), 2.26 (s, 2H), 2.07 (t, *J* = 3.2 Hz, 2H); **^{13}C NMR** (100 MHz, $CDCl_3$): δ 151.60, 148.30, 147.87, 141.62, 138.68, 135.73, 130.90, 129.90, 128.42, 127.62, 127.60, 127.54, 127.11, 120.97, 78.53, 46.59, 25.40; **MS** *m/z* found 427.1660 $C_{29}H_{24}O_2$ (M$^+$ Na) expected 427.1669 (M$^+$ Na). See Appendix 7.3 for X-Ray data.

5.2.3.4 Preparation of Racemic 6,12-Diphenyl-5,6,11,12-tetrahydro-5,11-methanodibenzo[*a,e*][8]annulene-6,12-diol (Diphenyl-diol cleft) ((±)-102) via Grignard Addition[6]
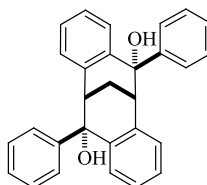
(±)-102

To a solution of **(±)-2** (0.28 g, 1.13 mmol) in dry THF (5 mL) was added PhMgBr (1.0 M in THF, 0.96 mL, 6.00 mmol) at room temperature under an N_2 atmosphere. The resulting reaction mixture was stirred at room temperature for 2 h. After this time the reaction was quenched by the careful addition of *sat*.NH_4Cl (3 mL) and the aqueous phase was extracted with ethyl acetate (3 x 10 mL). Combined organic layers were washed with *sat*.$NaHCO_3$, filtered and solvent removed under vacuum. The crude product was purified by column chromatography (R*f* = 0.47, light petroleum / EtOAc, 7:3) to give the title compound **(±)-102** as a white crystalline solid (0.42 g, 96 %).

Mp 213.9 – 217.3 $^{\circ}$C (*Lit* Mp 218 – 219 $^{\circ}$C (For (-) enantiomer)[6]; **IR** CH_2Cl_2 max/cm^{-1}: 3558 (s, OH), 3058, 3025, 2945, 2913 (Aromatics); **^{1}H NMR** (400 MHz, CDCl$_3$): δ 7.64 (dd, *J* = 7.6, 1.2 Hz, 2H), 7.45 (dd, *J* = 8.0, 1.6 Hz, 2H), 7.40 (td, *J* = 7.6, 1.2 Hz, 2H), 7.35 – 7.24 (m, 8H), 7.23 – 7.18 (m, 4H), 3.30 (t, *J* = 3.2 Hz, 2H), 2.57 (s, 2H), 2.10 (t, *J* = 3.6 Hz, 2H); **^{13}C (100 MHz, CDCl$_3$):** δ 147.24, 140.59, 134.68, 129.86, 128.89, 127.42, 126.61, 126.58, 126.55, 126.10, 77.51, 45.46, 24.38; **MS** *m/z* found 427.1664 $C_{29}H_{24}O_2$ (M$^+$ Na) expected 427.1669 (M$^+$ Na).

5.2.3.5 Preparation of Racemic 12-Hydroxy-11,12-dihydro-5,11-methanodibenzo[*a,e*][8]annulen-6(*5H*)-one (Mono-hydroxylated carbocyclic cleft) ((±) - 123)
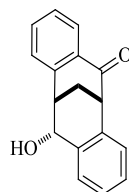
(±)-123

To a dry round-bottomed flask flushed with nitrogen, 3-bromopyridine (0.96 mL, 10.00 mmol) was dissolved in anhydrous THF (6 mL) and cooled to 0 °C. In a separate dry Schlenk tube flushed with nitrogen, isopropylmagnesium chloride (1.0 M in THF, 0.01 mL, 11.00 mmol) and lithium chloride (0.48 g, 11.00 mmol) were dissolved in anhydrous THF (16 mL) and cooled to 0 °C. The resulting reaction mixture was stirred at 0 °C until all the lithium chloride had dissolved. The *i*-PrMgCl.LiCl solution was added slowly over a period of 30 min to the stirred solution of 3-bromopyridine under an N_2 atmosphere via a cannula needle and the resulting reaction mixture was stirred at room temperature for 1 h. Formation of the Grignard reagent was assumed complete upon colour change. The solution containing the prepared Grignard reagent was added via cannula to a stirred solution of (±)-2 (0.71 g, 2.86 mmol) in THF (6 mL) at 0 °C. The resulting reaction mixture was allowed to reach room temperature and then stirred for a further 18 h. After this time the reaction was quenched by the careful addition of *sat*.NH₄Cl (10 mL) and extracted into ethyl acetate (3 x 50 mL). Combined organic layers were dried over anhydrous $MgSO_4$, filtered and solvent removed under vacuum. The crude compound was purified by column chromatography (R*f* = 0.5, L.Pet / EtOAc, 4:1) to the title compound (±)-123 as a fine white solid (0.10 g, 13 %).

Mp 154.9 – 1.56.9 °C; **IR** CH_2Cl_2 max/cm⁻¹: 3220 (b, O–H), 1685 (s, C=O); **¹H NMR** (400 MHz, CDCl₃): δ 7.54 (q, *J* = 1.2 Hz, 2H), 7.43 (d, *J* = 7.6 Hz, 1H), 7.33 (t, *J* = 7.2 Hz, 2H), 7.26 (td, *J* = 8.4, 1.6 Hz, 2H), 7.19 (t, *J* = 7.6 Hz, 1H), 5.17 (q, *J* = 5.6 Hz, 1H), 3.84 (s, 1H), 3.62 (s, 1H), 2.76 (dt, *J* = 6.8, 2.8 Hz, 1H), 2.52 (dt, *J* = 8.0, 2.8 Hz, 1H); **¹³C NMR** (100 MHz, CDCl₃): δ 197.26, 140.64, 138.09, 133.40, 132.90, 130.79, 130.74, 128.72, 128.55, 128.15, 128.09, 127.61, 70.09, 48.62, 39.88, 30.47; **MS** *m/z* found 273.0878 $C_{17}H_{14}O_2$ (M⁺ Na) expected 273.0886 (M⁺ Na). See Appendix 1.2 for X-Ray data.

5.2.3.6 Preparation of Racemic 12-(Prop-2-yn-1-yloxy)-5,6,11,12-tetrahydro-5,11-methanodibenzo[*a,e*][8]annulen-6-ol (Mono-Allyl-alcohol Cleft) ((±)-183)
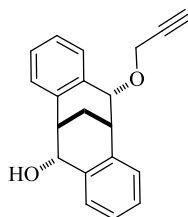
(±)-183

Sodium hydride (60 % mineral oil, 0.061 g, 1.52 mmol) was washed with hexane (3 x 10 mL) and dried under vacuum. To this DMF (10 mL) was added and the suspension was cooled to 0 °C. A solution of (±)-3 (0.38 g, 1.51 mmol) in DMF (10 mL) and added to the sodium hydride suspension via a cannula, under an N_2 atmosphere and the reaction was stirred at 0 °C for 25 min. After this time propargyl bromide (0.14 mL, 1.59 mmol) was carefully added to the reaction mixture and the solution was allowed to warm to room temperature and then stirred for 18 h. After this time the solution was quenched by the careful addition of water (25 mL) and extracted with dichloromethane (3 x 50 mL). Combined organic layers were washed with brine (25 mL), dried over $MgSO_4$, filtered and solvent removed under vacuum. The crude pale yellow residue was purified by column chromatography (R*f* = 0.67, L.Pet / EtOAc, 8:2) to give the title compound (±)-183 as a-white solid (0.09 g, 20 %).

Mp 144.9 – 147.5 °C; **IR** CH_2Cl_2 max/cm^{-1}: 3301 (s, CH, alkyne), 3054 (s, OH), 2930, 2869 (aromatics); **^{1}H NMR** (400 MHz, CDCl$_3$): δ 7.44 – 7.41 (m, 2H), 7.21 – 7.09 (m, 6H), 4.96 – 4.95 (m, 2H), 4.54 (d, *J* = 2.4 Hz, 2H), 3.44 (dt, *J* = 5.6, 3.2 Hz, 1H), 3.26 (dt, *J* = 6.0, 3.6 Hz, 1H), 2.45 (t, *J* = 2.4 Hz, 1H), 2.35 (t, *J* = 3.2 Hz, 2H), 1.45 (m, 2H); **^{13}C NMR** (100 MHz, CDCl$_3$): δ 138.96, 137.43, 134.62, 133.78, 130.86, 129.90, 127.77, 127.64, 127.37, 126.98, 126.76, 126.74, 80.17, 80.03, 74.77, 72.76, 57.34, 39.28, 35.12, 29.25; **MS** *m/z* found 313.1196 $C_{20}H_{18}O_2$ (M$^+$ Na) expected 313.1199 (M$^+$ Na).

5.2.4 Preparation of Amino-thiocarbamate Clefts

Sodium hydride (60 % mineral oil, 4.00 mmol) was washed with hexane (3 x 10 mL) and dried under vacuum, to this THF (10 mL) was added and the suspension was cooled to 0 $^{\circ}$C. A solution of (±)-**3** (1.00 mmol) in THF (5 mL) and added to the sodium hydride suspension via a cannula under an N_2 atmosphere and the resulting reaction mixture was stirred at 0 $^{\circ}$C for 25 min. After this time a solution of substituted isothiocyanate (3.00 mmol) in THF (5 mL) was added drop-wise to the reaction mixture. The solution was allowed to warm to room temperature and then stirred for a further 18 h, reactions were monitored by TLC. After this time the reaction was quenched by the careful addition of water (20 mL) and extracted with dichloromethane (3 x 25 mL). The combined organic layers were washed with brine (25 mL), dried over $MgSO_4$, filtered and solvent removed under vacuum. The crude compound was purified by chromatography.

5.2.4.1 5,6,11,12-Tetrahydro-5,11-methanodibenzo[*a,e*][8]annulene-6,12-diyll- bis(*p*-tolylcarbamothioate) (*p*-tolyl Amino-thiocarbamate Cleft) (4)

4
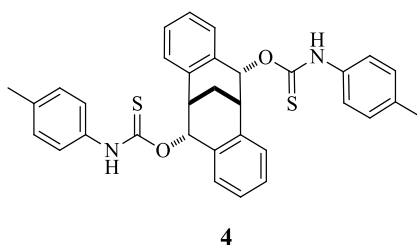
(±)-**4** fine white solid (0.40 g, 70 %); **Mp** 209.9 – 211.2 $^{\circ}$C; **IR** CH_2Cl_2 max/cm^{-1}: 3944, 3689 (s, N–H), 2986 (aromatics), 2305, 1520, 1265, 739, 704; (the compound existed as a mixture of rotamers and the major rotamer was assigned) **^{1}H NMR** (400 MHz, CDCl$_3$): δ 7.58 (d, *J* = 8.4 Hz, 2H), 7.29 – 7.15 (m, 7H), 7.09 (d, *J* = 7.2 Hz, 2H), 7.04 – 6.84 (m, 7H), 3.89 (m, 2H), 2.58 (m, 2H), 2.41 (s, 3H), 2.28 (s, 3H); **^{13}C NMR** (100 MHz, CDCl$_3$): δ 188.30, 136.32, 135.36, 134.92, 134.83, 133.85, 131.05, 129.72, 129.54, 127.39, 127.11, 126.55, 123.59, 121.47, 83.37, 79.45, 46.00, 35.36, 20.93; **MS** *m/z* found 573.1639 $C_{33}H_{30}O_2N_2S_2$ (M$^+$ Na) expected 573.1641 (M$^+$ Na), **Elemental analysis** found C 71.55; H 5.46; N 5.13 %; $C_{33}H_{30}N_2O_2S_2$ requires C 71.97; H 5.49; S 5.09 %. See Appendix 7.6 for X-Ray data.

(+)-4 fine white solid (0.28 g, 24 %); **Mp** 116.2 – 124.7 °C; $[\alpha]_D$ + 174.3 (*c* 1.0, CHCl$_3$); **IR** CH$_2$Cl$_2$ max/cm^{-1}: 3944, 3054 (N–H), 2986 (aromatics), 2305, 1522, 1265, 1171, 1034, 739, 704; (the compound existed as a mixture of rotamers and the major rotamer was assigned) **^{1}H NMR** (400 MHz, CDCl$_3$): δ 7.47 (d, *J* = 7.6 Hz, 2H), 7.17 – 7.08 (m, 7H), 6.95 (d, *J* = 5.2 Hz, 2H), 6.89 – 6.75 (m, 7H), 3.79 (m, 2H), 2.46 (m, 2H), 2.30 (s, 3H), 2.14 (s, 3H); **^{13}C NMR** (100 MHz, CDCl$_3$): δ 188.21, 136.36, 134.84, 134.30, 131.08, 129.61, 129.54, 127.14, 126.56, 123.63, 121.52, 83.34, 79.44, 35.42, 28.82, 20.99; **MS** *m/z* found 573.1642 C$_{33}$H$_{30}$O$_2$N$_2$S$_2$ (M$^+$ Na) expected 573.1641 (M$^+$ Na); **Elemental analysis** found C 71.79; H 5.57; N 5.16 %; C$_{33}$H$_{30}$N$_2$O$_2$S$_2$ requires C 71.97; H 5.49; N 5.09 %. See Appendix 7.5 for X-Ray data.

(-)-4 (0.20 g, 45 %), fine white solid; **Mp** 116.6 – 123.2 °C; $[\alpha]_D$ – 152.8 (*c* 1.0, CHCl$_3$); **IR** CH$_2$Cl$_2$ max/cm^{-1}: 3944, 3363 (N–H), 3057, 2986 (aromatics), 2306, 1521, 1263, 1171, 1034, 704; (the compound existed as a mixture of rotamers and the major rotamer was assigned) **^{1}H NMR** (400 MHz, CDCl$_3$): 7.24 (d, *J* = 7.2 Hz, 2H), 7.17 – 7.09 (m, 14H), 6.91 (d, *J* = 5.2 Hz, 2H), 3.72 (m, 2H), 3.26 (m, 2H), 2.26 (s, 3H), 2.13 (s, 3H); **^{13}C NMR** (100 MHz, CDCl$_3$): δ 188.21, 134.73, 134.53, 134.23, 134.06, 133.85, 130.84, 130.66, 130.19,129.53 127.64, 127.45, 126.85, 125.57, 123.83, 121.59, 83.51, 79.56, 39.20, 35.63, 21.12; **MS** *m/z* found 573.1629 C$_{33}$H$_{30}$O$_2$N$_2$S$_2$ (M$^+$ Na) expected 573.1641 (M$^+$ Na); **Elemental analysis** found C 71.39; H 5.47; N 5.24 %; C$_{33}$H$_{30}$N$_2$O$_2$S$_2$ requires C 71.97; H 5.49; N 5.09 %.

5.2.4.2   5,6,11,12-Tetrahydro-5,11-methanodibenzo[*a,e*][8]annulene-6,12-diyl) bis(phenylcarbamothioate) (Phenyl Amino-thiocarbamate Cleft) (5)

5
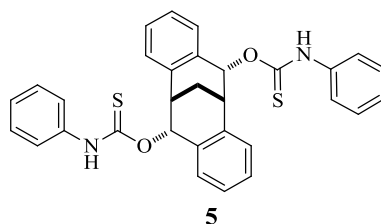
(±)-**5** fine white solid (0.29 g, 57 %); **Mp** 111.6 – 114.7 ^{o}C; **IR** CH$_2$Cl$_2$ max/cm^{-1}: 3943, 3584, 3361 (N–H), 3054, 2986 (aromatics), 2305, 1526, 1265, 1160, 1034, 743, 705; (the compound existed as a mixture of rotamers and the major rotamer was assigned) **^{1}H NMR** (400 MHz, CDCl$_3$): δ 7.74 – 7.00 (m, 20 H), 3.91 – 3.88 (m, 2H), 2.60 –2.58 (m, 2H); **MS** *m/z* found 545.1327 C$_{31}$H$_{26}$O$_2$N$_2$S$_2$ (M$^+$ Na) expected 545.1328 (M$^+$ Na), **Elemental Analysis** found C 71.06; H 4.98; N 5.41 % C$_{31}$H$_{26}$N$_2$O$_2$S$_2$ requires C 71.24; H 5.01; N 5.36 %. See Appendix 7.7 for X-Ray data.

(+)-**5** foamy colourless solid (0.30 g, 50 %); **Mp** 116.8 – 125.6 ^{o}C; [α]$_D$ + 156.8 (*c* 1.0, CHCl$_3$); **IR** CH$_2$Cl$_2$ max/cm^{-1}: 3944, 3342 (N–H), 3055, 2987 (aromatics), 2306, 1524, 1265, 739, 704; (the compound existed as a mixture of rotamers and the major rotamer was assigned) **^{1}H NMR** (400 MHz, CDCl$_3$): δ 7.65 – 6.89 (m, 20 H), 3.80 – 3.79 (m, 2H), 2.49 (s, 2H); 1.45 (s, 2H); **^{13}C NMR** (100 MHz, CDCl$_3$): δ 188.41, 136.86, 136.65, 134.61, 133.96, 130.67, 130.48, 129.04, 127.66, 127.47, 126.77, 125.26, 121.42, 83.74, 72.59, 39.22, 35.62, 29.08; **MS** *m/z* found 545.1312 C$_{31}$H$_{26}$O$_2$N$_2$S$_2$ (M$^+$ Na) expected 545.1328 (M$^+$ Na), **Elemental Analysis** found C 71.03; H 5.15; N 5.35 % C$_{31}$H$_{26}$N$_2$O$_2$S$_2$ requires C 71.24; H 5.01; N 5.36 %.

(-)-**5** off-white solid (0.61 g, 56 %); **Mp** 110.2 – 115.7 ^{o}C; [α]$_D$ – 156.0 (*c* 1.0, CHCl$_3$); **IR** CH$_2$Cl$_2$ max/cm^{-1}: 3584, 3234 (N–H), 2242, 1595, 1541, 1181, 1034, 732; (the compound existed as a mixture of rotamers and the major rotamer was assigned) **^{1}H NMR** (400 MHz, CDCl$_3$): δ 7.74 – 6.99 (m, 20 H), 3.90 – 3.89 (m, 2H), 2.59 (s, 2H); **^{13}C NMR** (100 MHz, CDCl$_3$): δ 188.47, 136.73, 134.84, 131.17, 129.10, 127.25, 126.58, 125.31, 123.26, 121.46, 83.56, 79.45, 35.45, 28.94; **MS** *m/z* found 545.1324 C$_{31}$H$_{26}$O$_2$N$_2$S$_2$ (M$^+$ Na) expected 545.1328 (M$^+$ Na).

5.2.4.3 5,6,11,12-Tetrahydro-5,11-methanodibenzo[*a,e*][8]annulene-6,12-diyl) bis((3,5-bis(trifluoromethyl)phenyl)carbamothioate) (3,5-Bis(trifluoromethyl)phenyl Amino-thiocarbamate Cleft) (6)
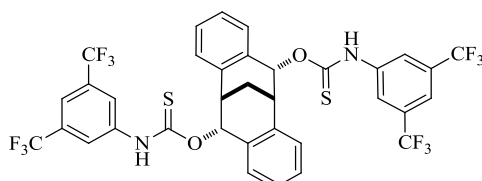
6

(±)-**6** off-white solid (0.72 g, 44 %); **Mp** 120.1 – 127.4 $^{\circ}$C; **IR** CH$_2$Cl$_2$ max/cm^{-1}: 3204, 3055 (N–H), 2987 (aromatics), 2306, 1551, 1139, 1265, 1031, 738, 703; (the compound existed as a mixture of rotamers and the major rotamer was assigned) **^{1}H NMR** (400 MHz, CDCl$_3$): δ 7.67-6.74 (m, 14H), 3.75 (s, 2H), 2.52-2.51 (m, 2H); **MS** *m/z* found 817.0777 C$_{35}$H$_{22}$O$_2$N$_2$S$_2$F$_{12}$ (M$^+$ Na) expected 817.0823 (M$^+$ Na); **Elemental analysis** found C 52.34; H 2.77; N 3.72 % C$_{35}$H$_{22}$F$_{12}$N$_2$O$_2$S$_2$ requires C 52.90; H 2.79; N 3.53 %. See Appendix 7.8 for X-Ray data.

5.2.4.4 5,6,11,12-Tetrahydro-5,11-methanodibenzo[*a,e*][8]annulene-6,12-diyl) bis(methylcarbamothioate) (Methyl Amino-thiocarbamate Cleft) (7)
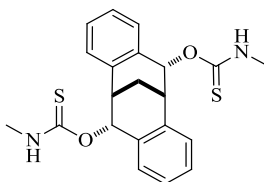
7

(±)-**7** (0.64 g, 75 %), colourless solid; **Mp** 212.1 – 218.2 $^{\circ}$C; **IR** CH$_2$Cl$_2$ max/cm^{-1}: 3399, 3052 (aromatics),1528, 1265, 1068, 737, 703; (the compound existed as a mixture of rotamers and the major rotamer was assigned) **^{1}H NMR** (400 MHz, CDCl$_3$): δ 7.24 – 7.13 (m, 6H), 7.09 – 7.04 (m, 2H), 6.96 – 6.89 (m, 2H), 3.23 – 3.21 (m, 6H), 2.65 (d, *J* = 5.2 Hz, 1H), 2.53 (d, *J* = 5.2 Hz, 1H), 2.44 – 2.39 (m, 2H); **^{13}C NMR** (100 MHz, CDCl$_3$): δ 190.90, 135.51, 135.23, 134.86, 134.61, 131.08, 130.98, 127.37, 127.33, 127.22, 126.30, 126.78, 126.70, 81.53, 79.73, 35.33, 32.07, 28.78; **MS** *m/z* found 421.1013 C$_{21}$H$_{22}$O$_2$N$_2$S$_2$ (M$^+$ Na) expected 421.1015 (M$^+$ Na); **Elemental analysis** found C 63.07; H 5.58; N 6.99 % C$_{21}$H$_{22}$N$_2$O$_2$S$_2$ requires C 63.29; H 5.56; N 7.03 %. See Appendix for 7.9 for crystal data.

(+)-7 colourless solid, (0.42 g, 56 %); **Mp** 220.7 – 225.1 ^{o}C; $[\alpha]_D$ + 10.4 (*c* 1.0, CHCl$_3$); **IR** CH$_2$Cl$_2$ max/cm^{-1}: 3396, 3256 (N–H), 2936 (Aromatics),1538, 1210, 1123, 737; **^{1}H NMR** (400 MHz, CDCl$_3$): 7.26 – 7.13 (m, 6H), 7.08 – 7.01 (m, 2H), 6.91 – 6.80 (m, 2H), 3.24 – 3.20 (m, 6H), 2.74 (d, *J* = 5.2 Hz, 1H), 2.71 (d, *J* = 4.8 Hz, 1H), 2.44 – 2.38 (m, 2H); **^{13}C NMR** (100 MHz, CDCl$_3$): δ 191.08, 135.59, 135.51, 134.94, 134.59, 131.05; 130.72, 127.57, 127.36, 127.26, 126.83, 126.74, 126.65, 81.60, 79.79,35.64, 32.10, 28.79; **MS** *m/z* found 421.1011 C$_{21}$H$_{22}$O$_2$N$_2$S$_2$ (M$^+$ Na) expected 421.1015 (M$^+$ Na); **Elemental analysis** found C 62.85; H 5.45; N 6.95 % C$_{21}$H$_{22}$N$_2$O$_2$S$_2$ expected C 63.29; H 5.56; N 7.03 %.

5.2.4.5 5,6,11,12-Tetrahydro-5,11-methanodibenzo[*a,e*][8]annulene-6,12-diyl) bis(butylcarbamothioate) (Butyl Amino-thiocarbamate Cleft (8)
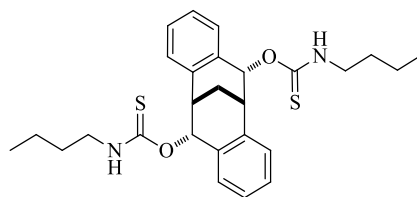
8

(±)-8 colourless solid (0.22 g, 20 %); **Mp** 213.3 – 214.4 ^{o}C; **IR** CH$_2$Cl$_2$ max/cm^{-1}: 3257, 2957, 2931 (aromatics), 1519, 1179, 1038, 752; the compound existed as a mixture of rotamers and the major rotamer was assigned) **^{1}H NMR** (400 MHz, CDCl$_3$): δ 7.22 – 7.15 (m, 8H), 6.93-6.88 (m, 2H), 3.67-3.64 (m, 2H), 3.24-3.12 (m, 2H), 2.53-2.49 (m, 2H), 1.70 (m, 2H), 1.52-1.45 (m, 4H), 1.03 (t, *J* = 7.2 Hz, 6H), 0.91-0.86 (m, 4H);**^{13}C NMR** (100 MHz, CDCl$_3$): δ 189.88, 135.56, 135.21, 134.76, 134.57, 131.01, 130.95, 127.33, 127.31, 127.18, 126.97, 126.85, 126.67, 81.84, 79.44, 45.10, 42.85, 35.42, 31.15, 30.69, 28.73, 20.08, 13.80; **MS** *m/z* found 505.1954 C$_{27}$H$_{34}$O$_2$N$_2$S$_2$ (M$^+$ Na) expected 505.1954 (M$^+$ Na); **Elemental analysis** found C 66.96; H 7.02; N 5.73 % C$_{27}$H$_{34}$O$_2$N$_2$S$_2$ requires C 67.18; H 7.10; N 5.80 %.

5.2.4.6 5,6,11,12-Tetrahydro-5,11-methanodibenzo[*a,e*][8]annulene-6,12-diyl) bis(allylcarbamothioate) (Allyl Amino-thiocarbamate Cleft) (9)
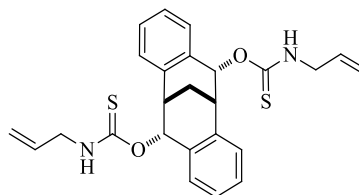
9

(±)-9 off-white solid (0.15 g, 68 %); **Mp** 173.1 – 176.9 $^{\circ}$C; **IR** CH_2Cl_2 max/cm^{-1}: 3944, 3687, 3387 (N–H), 3054, 2987 (aromatics), 2305, 1391,1012, 1044, 739, 704; (the compound existed as a mixture of rotamers and the major rotamer was assigned) ^{1}**H NMR** (400 MHz, CDCl$_3$): δ 7.11-7.06 (m, 8H), 6.82 (d, *J* = 6Hz, 2H), 5.95-5.85 (m, 1H), 5.74-5.60 (m, 1H), 5.27-5.16 (m, 2H), 5.14-5.08 (m, 2H), 4.36-4.29 (m, 2H), 4.26-4.19 (m, 2H), 3.77-3.76 (m, 2H), 2.42-2.41 (m, 2H); ^{13}**C NMR** (100 MHz, CDCl$_3$): δ 190.23, 189.55, 135.48, 135.28, 134.76, 134.39, 132.65, 131.04, 127.37, 127.31, 127.24, 126.93, 126.91, 126.79, 126.74, 126.65, 117.58, 117.45, 81.75, 79.79, 47.62, 45.27, 35.32, 35.21, 28.76; **MS** *m/z* found 473.1319 $C_{25}H_{26}O_2N_2S_2$ (M$^+$ Na) expected 473.1328 (M$^+$ Na); **Elemental analysis** found C 66.03; H 5.75; N 6.23 % $C_{25}H_{26}N_2O_2S_2$ requires C 66.63; H 5.82; N 6.22 % .

5.2.4.6 Preparation of 12-Hydroxy-5,6,11,12-tetrahydro-5,11-methanodibenzo[*a,e*][8]annulen-6-yl) p-tolylcarbamothioate ((±)-128)

(±)-128

Sodium hydride (60 % mineral oil, 0.071 g, 1.93 mmol) was washed with hexane (3 x 10 mL) and dried under vacuum. THF (10 mL) was added and the suspension was cooled to 0 °C. (±)-3 (0.54 g, 2.14 mmol) was dissolved in THF (10 mL) and added to the sodium hydride suspension via a cannula under nitrogen. The reaction was stirred at 0 °C for 25 min. After this time a solution of *p*-tolyl isothiocyanate (0.29 g, 1.94 mmol) in THF (10 mL) was carefully added to the reaction mixture. The solution was allowed to reach room temperature and then stirred for a further 18 h. After this time the solution was quenched by the careful addition of water (25 mL) and extracted with dichloromethane (3 x 50 mL). Combined organic layers were washed with brine (25 mL), dried over MgSO$_4$, filtered and the solvent removed under vacuum. The pale yellow foamy solid was purified by silca column chromatography (R*f* = 0.67, L.Pet / EtOAc, 7:3) to give the title compound (±)-128 as a white solid (0.58 g, 68 %).

Mp 109.4 – 114.4 °C; **IR** CH$_2$Cl$_2$ max/cm^{-1}: 3563 (s, N–H), 3392, 3365 (b, OH), 3053, 2985, 2927 (aromatics), 1520, 1264, 1034; **^{1}H NMR** (400 MHz, CDCl$_3$): δ 7.48 – 7.43 (m, 2H), 7.27 (d, *J* = 7.6 Hz, 1H), 7.17 – 7.10 (m, 5H), 6.93 – 6.92 (m, 1H), 6.81 (s, 4H), 5.00 (m, 1H), 3.74 (s, 1H), 3.31 (s, 1H), 2.46 – 2.36 (m, 2H), 2.16 (s, 3H), 1.56 (m, 1H); **^{13}C NMR** (100 MHz, CDCl$_3$): δ 188.38, 139.73, 138.95, 135.19, 134.78, 134.20, 134.01, 130.87, 130.67, 130.11, 129.62, 127.89, 127.71, 127.51, 127.42, 127.19, 126.81, 123.83, 121.57, 83.67, 72.72, 39.29, 35.68, 29.15, 20.88; **MS** *m/z* found 424.1338 C$_{25}$H$_{23}$NO$_2$S (M$^+$ Na) expected 424.1342 (M$^+$ Na); **Elemental analysis** found C 72.22; H 5.68; N 3.15 % C$_{25}$H$_{23}$NO$_2$S requires C 74.78; H 5.77; N 3.49 %.

5.2.5 Preparation of Amino-thiocarbamate Cinchonine Alkaloid Catalysts

Sodium hydride (60 % mineral oil, 6.80 mmol) was washed with hexane (3 x 15 mL) and dried under vacuum, THF (10 mL) was added under an N_2 atmosphere and the resulting suspension was cooled to 0 °C. To this a solution of (+)-cinchonine (3.40 mmol) in THF (15 mL) was added and the resulting reaction mixture was stirred at 0 °C for 25 min. After this time substituted isothiocyanate (6.80 mmol) was carefully added and the reaction mixture was allowed to reach room temperature and then stirred for a further 18 h. The reaction was quenched by the careful addition of water (25 mL) and extracted with dichloromethane (3 x 50 mL). The combined organic layers were washed with brine (15 mL), dried over $MgSO_4$, filtered and solvent removed under vacuum. The crude product was purified by silica column chromatography.

5.2.5.1 *O*-((*S*)-Quinolin-4-yl((1*S*,2*R*,4*S*,5*R*)-5-vinylquinuclidin-2-yl)methyl) (3,5-dimethoxyphenyl) carbamothioate (2,4-Dimethoxyphenyl Amino-thiocarbamate Cinchona Alkaloid) ((+)-13)

(+)-13

(+)-13[43] colourless solid (1.11 g, 71 %); **Mp** 80.7 – 84.6 °C (*Lit.* 82.0 – 84.0 °C)[43]; $[\alpha]_D$ – 92.1 (*c* 1.0, CHCl$_3$) (*Lit.* $[\alpha]_D$ – 93.7 (*c* 1.0, CHCl$_3$)[43]; **IR** CH$_2$Cl$_2$ max/cm^{-1}: 2936 (aromatics), 1605, 1460, 1378, 1264, 1156, 1037, 741, 704; (the compound existed as a mixture of rotamers and the major rotamer was assigned according to literature values) **^{1}H NMR** (400 MHz, CDCl$_3$): δ 8.85 (d, *J* = 4.4 Hz, 1H), 8.22 (m, 1H), 8.09 (d, *J* = 8.8 Hz, 1H), 7.70-7.66 (m, 1H), 7.55-7.51 (m, 2H), 7.38-7.34 (m, 2H), 6.39-6.33 (m, 2H), 6.01-5.84 (m, 1H), 5.11-5.03 (m, 2H), 3.73-3.71 (m, 6H), 3.41-3.37 (m, 1H), 2.87-2.64 (m, 4H), 2.25-2.21 (m, 1H), 1.93-1.91 (m, 1H), 1.77-1.39 (m, 4H); **^{13}C NMR** (100 MHz, CDCl$_3$): δ 161.09, 150.28, 149.96, 148.63, 145.23, 140.15, 130.35, 129.29, 126.83, 126.43, 124.13, 119.56, 114.99, 68.07, 60.61, 49.67, 49.57, 40.17, 39.84, 28.22, 26.13; **MS** *m/z* found 512.1995 C$_{28}$H$_{31}$O$_3$N$_3$S (M$^+$ Na) expected 512.1978 (M$^+$ H); **Elemental analysis** found C 68.64; H 6.60; N 8.42 %; C$_{28}$H$_{31}$O$_3$N$_3$S requires C 68.68; H 6.63; N 8.58 %.

5.2.5.2 *O*-((*S*)-Quinolin-4-yl((1*S*,2*R*,4*S*,5*R*)-5-vinylquinuclidin-2-yl)methyl) phenylcarbamothioate (Phenyl Amino-thiocarbamate Cinchona Alkaloid) ((+)-14)[43]

(+)-14

(+)-14[43] (1.03 g, 57 %), colourless solid; **Mp** 143.7 − 144.2 $^{\circ}$C (*Lit.* 149.0 − 150.0 $^{\circ}$C);[43] $[\alpha]_D$ − 94.6 (*c* 1.0, CHCl$_3$) (*Lit.* $[\alpha]_D$ − 95.0 (*c* 1.0, CHCl$_3$);[43] **IR** CH$_2$Cl$_2$ max/cm^{-1}: 2934(aromatics), 1594, 1539, 1376, 1180, 1026, 746, 732; (the compound existed as a mixture of rotamers and the major rotamer was assigned according to literature values) **^{1}H NMR** (400 MHz, CDCl$_3$): δ 8.82 (d, *J* = 4.4 Hz, 1H), 8.20 − 8.17 (m, 1H), 8.05 (d, *J* = 8.4 Hz, 1H), 7.33 − 7.17 (m, 9H), 5.85 − 5.76 (m, 1H), 5.03 − 4.99 (m, 2H), 3.35 − 3.29 (m, 1H), 2.84 − 2.19 (m, 4H), 1.86 − 1.56 (m, 2H), 1.52 − 1.46 (m, 4H); **^{13}C NMR** (100 MHz, CDCl$_3$): δ 185.84, 149.59, 147.18, 129.09, 128.70, 127.98, 126.06, 125.37, 124.95, 122.45, 119.03, 114.34, 78.71, 59.27, 47.67, 26.79, 25.12, 23.81; **MS** *m/z* found 452.1758 C$_{26}$H$_{27}$ON$_3$S (M$^+$ Na) expected 452.1767 (M$^+$ Na); **Elemental analysis** found C 71.09; H 6.44; N 9.16 %; C$_{26}$H$_{27}$ON$_3$S requires C 72.69; H 6.34; N 9.78 %.

5.2.5.3 *O*-((*S*)-Quinolin-4-yl(1*S*,2*R*,4*S*,5*R*)-5-vinylquinuclidin-2-yl)methyl) p-tolylcarbamothioate (*p*-Tolyl Amino-thiocarbamate Cinchona Alkaloid) ((+)-15)

(+)-15
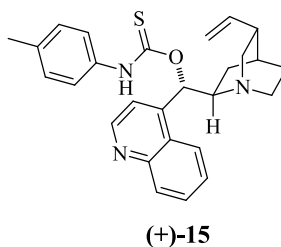
(+)-**15** (0.60 g, 40 %), white flaky solid; **Mp** 103.7 − 104.1 $^{\circ}$C; $[\alpha]_D$ − 97.3 (*c* 1.0, CHCl$_3$); **IR** CH$_2$Cl$_2$ max/cm^{-1}: 2938 (aromatics), 1592, 1512, 1385, 1181, 1040, 758, 735; (the compound existed as a mixture of rotamers and the major rotamer was assigned) **^{1}H NMR** (400 MHz, CDCl$_3$): δ 8.89 (d, *J* = 4.4 Hz, 1H), 8.13 (d, *J* = 8.4 Hz, 1H), 7.72 (t, *J* = 7.6 Hz, 1H), 7.56 − 7.54 (m, 1H), 7.39 − 7.36 (m, 2H), 7.22 − 7.15 (m, 4H), 6.02 − 5.83 (m, 1H), 5.11 − 5.06 (m, 2H), 3.38 − 3.36 (m, 1H), 2.90 − 2.66 (m, 4H), 2.35 (m, 3H), 1.94 − 1.79 (m, 4H), 1.54 − 1.53 (m, 3H); **^{13}C NMR** (100 MHz, CDCl$_3$): δ 187.97, 150.16, 149.84, 148.04, 140.26, 136.31, 130.10, 129.75, 126.30, 124.20, 119.61, 115.05, 81.04, 68.00, 60.50, 50.75, 28.17, 26.30, 25.63, 21.09; **MS** *m/z* found 444.2102 C$_{27}$H$_{29}$ON$_3$S (M$^+$ H) expected 444.2104 (M$^+$ H); **Elemental analysis** found C 72.91; H 6.64; N 9.36 %; C$_{27}$H$_{29}$ON$_3$S requires C 73.10; H 6.59; N 9.47 %.

5.2.5.4 *O*-((*S*)-Quinolin-4-yl(1*S*,2*R*,4*S*,5*R*)-5-vinylquinuclidin-2-yl)methyl) (3,5-bis(trifluoromethyl)phenyl)carbamothioate (3, 5-Bis(trifluoromethyl)phenyl Amino-thiocarbamate Cinchona Alkaloid) ((+)-16)
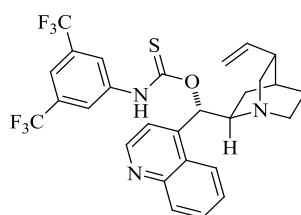
(+)-16

(+)-16[43] (0.73 g, 76 %), colourless solid; **Mp** 102.6 – 107.4 ^{o}C (*Lit.* 103.0 – 105.0 ^{o}C)[43]; [α]$_D$ – 82.3 (*c* 1.0, CHCl$_3$) (*Lit.* [α]$_D$ – 80.1 (*c* 1.0, CHCl$_3$)[43]; **IR** CH$_2$Cl$_2$ max/cm^{-1}: 2934 (aromatics), 1575, 1379, 1278, 1135, 756, 736; (the compound existed as a mixture of rotamers and the major rotamer was assigned according to literature values) **^{1}H NMR** (400 MHz, CDCl$_3$): δ 8.81 (d, *J* = 8.4 Hz, 1H), 8.04 (d, *J* = 7.6 Hz, 1H), 7.91 – 7.87 (m, 2H), 7.66 – 7.61 (m, 2H), 7.50 (t, *J* = 7.2 Hz, 1H), 7.28 (d, *J* = 2.4 Hz, 2H), 5.91 (m, 1H), 5.04 – 5.00 (m, 2H), 3.42 – 3.35 (m, 1H), 2.82 (d, *J* = 8.8 Hz, 1H), 2.67 – 2.57 (m, 1H), 2.24 – 2.17 (m, 1H), 1.89 – 1.81 (m, 1H), 1.77 (s, 1H), 1.61 – 1.50 (m, 3H); **^{13}C NMR** (100 MHz, CDCl$_3$): δ 187.53, 149.73, 148.15, 145.45, 140.13, 132.77, 132.44, 132.10, 129.77, 127.08, 126.52, 124.32, 123.98, 121.61, 119.68, 115.13, 60.52, 50.92, 49.44, 49.10, 39.82, 29.39, 27.70, 24.81; **MS** *m/z* found 566.1683 C$_{28}$H$_{25}$F$_6$ON$_3$S (M$^+$ H) expected 566.1695 (M$^+$ H); **Elemental analysis** found C 59.08; H 4.63; N 7.00 %; C$_{28}$H$_{25}$F$_6$ON$_3$S requires C 59.46; H 4.46; N 7.43 %.

5.2.6 Hetero Diels-Alder Reactions

5.2.6.1 Procedure for the Synthesis of (*E*)-3-((*tert*-butyldimethylsilyl)oxy)-*N*,*N*-dimethylbuta-1,3-dien-1-amine (Rawel Diene) (10)[68]
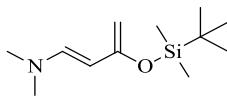
10

A dry, 500 mL three-necked round-bottomed flask equipped with a pressure equalising addition funnel, a large egg-shaped magnetic stirrer bar, and a nitrogen / vacuum adaptor was evacuated and flushed with nitrogen three times. To this NaHMDS in THF (100 mL, 0.10 mol) was added and the flask was cooled to -78 °C in a dry ice-acetone bath, giving a viscous yellow / white suspension. To this, a solution of *trans*-4-(dimethyl) amino-3-buten-2-one (11.30 g, 0.099 mol) in dry THF (50 mL) was added slowly over a period of 30 min via the addition funnel. The resulting solution was stirred at -78 °C for 1 h. After this time a solution of tert-butylchlorodimethylsilane (15.80 g, 0.15 mol) in THF (50 mL) was added over a period of 5 min, via the addition funnel. The reaction was removed from the ice-bath and stirred for 1.5 h until it reached reach room temperature. Once the reaction had reached ambient temperature it was poured into anhydrous diethyl ether (600 mL) and the resulting suspension was allowed to stand for 30 min. After this time the solution was filtered through a pad of Celite and washed with anhydrous diethyl ether (3 x 50 mL). The resulting filtrate was concentrated to dryness under vacuum resulting in a dark red / brown oil which was purified by bulb-to-bulb distillation (150.3 °C, 11.0 mbar) giving the title compound **10** as a pale yellow oil (19.82 g, 87 %).

¹H NMR (400 MHz, CDCl₃): δ 6.52 (d, *J* = 13.2 Hz, 1H), 4.73 (d, *J* = 13.2 Hz, 1H), 3.87 (s, 1H), 3.78 (s, 1H), 2.65(s, 6H), 0.87 (s, 9H), 0.14 (s, 6H); **¹³C NMR** (100 MHz, CDCl₃): δ 154.01, 138.49, 93.44, 83.41, 38.82, 38.11, 23.46, 23.19, 23.07, 15.85, -0.03, -7.04.

5.2.6.2 Procedure for the Uncatalysed Hetero Diels-Alder Reaction[69]

To a solution of freshly distilled diene **10** (0.23 g, 1.01 mmol) in chloroform (3 mL), benzaldehyde (0.15 mL, 1.50 mmol) was added under a N_2 atmosphere. The reaction was stirred at room temperature for 1 h before the temperature was decreased to -78 °C. The reaction diluted by the addition of CH_2Cl_2 (2 mL) followed by the drop-wise addition of acetyl chloride (0.14 mL, 2.0 mmol). The resultant reaction mixture was stirred for a further 30 min. After this time *sat*.NaHCO$_3$ (2 mL) and water (2 mL) were added, aqueous phase was extracted with dichloromethane (3 x 15 mL). The organic layers were combined and dried over MgSO$_4$, filtered and the solvent removed under vacuum. The crude residue was purified by prep-plate chromatography (EtOAc / L.Pet, 5:1) to give 2-Phenyl-2,3-dihydro-pyran-4-one **12a** (0.14 g, 82 %).

5.2.6.3 General Procedure for the Asymmetric HDA Reaction [6]

To a 25 mL oven dried round-bottom flask under nitrogen freshly distilled diene **10** (0.50 mmol) and 20 mol % catalyst (1.00 mmol) were dissolved in toluene (2 mL). The reaction mixture was cooled to -40 ^{o}C and benzaldehyde (1.00 mmol) was added. The reaction mixture was stirred at -40 ^{o}C for 48 h. After this period the reaction was cooled to -78 ^{o}C and the diluted with CH_2Cl_2 (2 mL) followed by the addition of acetyl chloride (1.00 mmol). The resulting reaction mixture was stirred for at room temperature for approximately 15 min. After this time *sat*.NaHCO$_3$ (2 mL) and water (2 mL) were added, the aqueous phase was extracted with dichloromethane (3 x 15 mL). The organic layers were combined and dried over MgSO$_4$, filtered and the solvent removed under vacuum. The crude residues were purified by prep-plate chromatography (EtOAc / L.Pet, 5:1) and the structure of the isolated products established by ^{1}H NMR spectroscopy. Enantiomeric excesses were determined by enantioselective HPLC.

2-Phenyl-2,3-dihydro-pyran-4-one (12a).
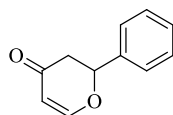
12a

IR CH_2Cl_2 max/cm^{-1}: 1664 (C=O); **^{1}H NMR** (400 MHz, CDCl$_3$): δ 7.51 (d, J = 5.6 Hz, 1H), 7.48 − 7.39 (m, 5H), 5.56 (dd, *J* = 4.6, 1.2 Hz, 1H), 5.46 (dd, *J* = 14.4, 3.2 Hz, 1H), 2.94 (dd, *J* = 16.8, 14.4 Hz, 1H), 2.67 (ddd, *J* = 16.8, 3.6, 1.2 Hz, 1H); **^{13}C NMR** (100 MHz, CDCl$_3$): δ 191.45, 162.24, 136.82, 128.76, 128.01, 127.25, 106.37, 80.10, 42.39; **MS** *m/z* found 197.0572 $C_{11}H_{10}O_2$ (M$^+$ Na) expected 197.0573 (M$^+$ Na); chiral HPLC (Chiralcel IB column, hexane: 2-propanol = 85:15, 0.5 mL min^{-1}) showed < 5 % *ee* (*t$_1$*= 47.93 min, *t$_2$* = 51.36 min).See Appendix 7.17 for HPLC data.

5.2.7 Bromolactonisation Reactions

5.2.7.1 Synthesis of Dimethyl 2-(2-bromoallyl) malonate (177)[3]

177
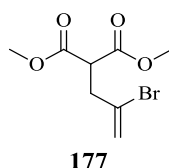
Sodium hydride (2.30 g, 60 % mineral oil, 57.52 mmol) was washed with hexane (2 x 50 mL) and dried under vacuum, anhydrous THF (200 mL) was added and the suspension was cooled to 0 °C. Dimethylmalonate (6.4 mL, 56.00 mmol) was added over a period of 5 min and the reaction mixture was stirred at 0 °C for 25 min. After this time 2,3-dibromopropene (5.08 mL, 50.00 mmol) and TBAI (5.58 g, 15.11 mmol) were added and the reaction was heated under reflux for 18 h. After this time the reaction was cooled to room temperature and quenched with *sat.*NH_4Cl (50 mL). The aqueous layer was extracted with diethyl ether (3 x 50 mL), combined organic layers were washed with brine (100 mL), dried over $MgSO_4$, filtered and the solvent removed under vacuum to give the title compound **177** as a brown liquid (13.66 g, 99 %). The crude oil was used without further purification in the next step.

IR CH_2Cl_2 max/cm^{-1}: 1744 (C=O); **^{1}H NMR** (400 MHz, $CDCl_3$): δ 4.76 (s, 1H), 4.69 (s, 1H), 3.72 − 3.70 (m, 6H), 3.59 (t, *J* = 7.6 Hz, 1H), 2.58 (d, *J* = 7.6 Hz, 2H), 1.71 (s, 3H); **^{13}C NMR** (100 MHz, $CDCl_3$): δ 171.15, 131.63, 122.61, 52.79, 50.67, 42.78.

5.2.7.2 Synthesis of Methyl 4-bromopent-4-enoate (178)[3]
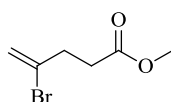
178

A mixture of **177** (6.40 g, 25.60 mmol) and lithium chloride (2.57 g, 60.63 mmol) in anhydrous DMSO (200 mL) was stirred at 140 $^{\circ}$C for 48 h to give a dark purple / black solution. After this time the solution was diluted with water (100 mL) and extracted with diethyl ether (3 x 100 mL). Combined organic layers were washed with brine (100 mL) and solvent removed under vacuum to give an orange / brown residue. The crude residue was purified by column chromatography (Rf = 0.86, L.Pet / EtOAc, 9:1) to give the title compound **178** as a pale yellow residue (1.38 g, 28 %).

IR CH$_2$Cl$_2$ max/cm^{-1}: 1630 (C=O); **^{1}H NMR** (400 MHz, CDCl$_3$): δ 5.65 (q, J = 1.6 Hz, 1H), 5.46 (dd, J = 18.8, 1.6 Hz, 1H), 3.68 (s, 3H), 2.81 − 2.74 (m, 2H), 2.60 − 2.56 (m, 2H); **^{13}C NMR** (100 MHz, CDCl$_3$): δ 171.73, 128.00, 117.90, 51.04, 35.60, 30.21; **MS** m/z found 214.9680 C$_6$H$_9$O$_2$Br (M$^+$ Na) expected 214.9678 (M$^+$ Na).

5.2.7.3 Synthesis of Methyl-4-phenylpent-4-enoate (179)
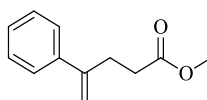
179

A mixture of **178** (0.21 g, 1.98 mmol), phenyl boronic acid (0.15 g, 1.23 mmol), Pd(Ph$_3$)$_4$ (0.061 g, 0.053 mmol) and Na$_2$CO$_3$ (0.24 g, 2,26 mmol) in dioxane / water (7:1 v/v) (8 mL) was stirred at 100 $^{\circ}$C for 16 h under an N$_2$ atmosphere. After this time the solvent was removed under reduced vacuum and the residue was diluted with water (20 mL) and extracted with ethyl acetate (3 x 25 mL). Combined organic layers were washed with brine (25 mL), dried over MgSO$_4$, filtered and the solvent removed under vacuum to give a brown residue. The crude residue was purified by prep-plate TLC (Rf = 0.5, L.Pet / EtOAc, 9:1) to the title compound **179** as a colourless oil (0.031 g, 15 %).

IR CH$_2$Cl$_2$ max/cm^{-1}: 1737 (C=O); **^{1}H NMR** (400 MHz, CDCl$_3$): δ 7.44 − 7.29 (m, 5H), 5.34 (s, 1H), 5.12 (m, 1H), 3.70 (s, 3H), 2.78 (td, J = 6.8, 1.2 Hz, 2H), 2.52 (t, J = 6.0 Hz, 2H).

5.2.7.4   Synthesis of 4-Phenyl-4-pentenoic Acid (18)
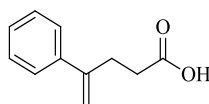
18

To a solution of **179** (0.034 g, 0.18 mmol) in THF (0.5 mL) and water (0.5 mL), lithium hydroxide monohydrate (0.069 g, 1.64 mmol) was added. The reaction was stirred at room temperature for 18 h and then diluted with water (2 mL). The aqueous fraction was washed with diethyl ether (3 x 20 mL) and acidified with 2 M HCl to pH 2. The aqueous phase was washed with ethyl acetate (3 x 15 mL) and combined organic layers were washed with brine (15 mL), dried over $MgSO_4$, filtered and the solvent removed under vacuum to give the title compound **18** as a colourless solid (0.012 g, 39 %).

IR CH_2Cl_2 max/cm^{-1}: 3415 (O–H), 1705 (C=O); **^{1}H NMR** (400 MHz, CDCl$_3$): δ 7.42 – 7.05 (m, 5H), 5.25 (s, 1H), 4.98 (s, 1H), 2.78 (t, *J* = 8.0 Hz, 2H), 2.47 (t, *J* = 7.6 Hz, 2H); **^{13}C NMR** (100 MHz, CDCl$_3$): δ 178.23, 146.55, 140.42, 128.44, 127.69, 126.09, 113.00, 32.76, 30.16; **MS** *m/z* found 177.1123 $C_{11}H_{12}O_2$ (M$^+$ H) expected 177.0910 (M$^+$ H).

5.2.7.5 General Procedure for the Asymmetric Bromolactonisation Reactions[43]

To a solution of 4-phenylpent-4-enoic acid **18** (0.10 mmol) and catalyst (0.010 mmol) in chloroform (1 mL) and toluene (2 mL) under nitrogen, N-bromosuccinimide (0.12 mmol) was added. The resulting reaction mixture was stirred at -78 °C for 4 h. After this time the reaction was quenched with *sat*.Na$_2$SO$_3$ (2 mL) and then warmed to room temperature. The solution was diluted with water (3 mL) and extracted with dichloromethane (3 x 5 mL). The combined extracts were washed with brine (5 mL), dried over MgSO$_4$, filtered and solvent removed under vacuum. The crude residue was purified by prep-plate TLC (L.Pet / EtOAc, 2:1) to give the bromo-lactone **20**.

5-Benzyl-5-bromodihydrofuran-2(3H)-one (Bromo-lactone 20)[43]
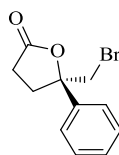
20

Colourless oil; **¹H NMR** (400 MHz, CDCl$_3$): δ 7.63 – 7.58 (m, 5H), 3.68 (d, *J* = 11.6 Hz, 1H), 3.62 (d, *J* = 11.2 Hz, 1H), 2.80 – 2.73 (m, 2H) 2.53 – 2.43 (m, 2H); **¹³C NMR** (100 MHz, CDCl$_3$): δ 175.55, 140.75, 132.07, 128.71,124.93, 86.45, 41.05, 32.40, 29.10; chiral HPLC (Chiralcel IB column, hexane: 2-propanol = 85:15, 0.6 mL min^{-1}) showed < 5 % *ee* (*t$_1$*= 29.5 min, *t$_2$* = 34.73 min).See Appendix 7.16 for HPLC data.

5.2.8 Preliminary Reaction – Fused Cleft Synthesis

5.2.8.1 Preparation of *N*-(3-acetylphenyl)-2-aminobenzamide (197)

197
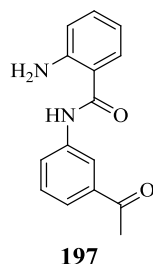
Isatoic anhydride (4.80 g, 29.42 mmol) and 3'aminoacetophenone (1.00 g, 7.40 mmol) were dissolved in DMA (59 mL) and heated at under reflux for 24 h. After this time the reaction was cooled to room temperature, poured onto water (50 mL) and extracted into dichloromethane (3 x 50 mL). Combined organic layers were repeatedly washed with water until no more insoluble isatoic anhydride precipitated from the organic layer. The combined organic layers were dried, filtered and solvent removed under vacuum. The crude compound was recrystallized from a minimum amount of chloroform to the target compound **197** as an off-white solid (0.55 g, 29 %).

Mp 134.2 – 137.6 $^{\circ}$C; **IR** CH_2Cl_2 max/cm^{-1}: 3468, 3371 (N–H), 2960, 2923 (aromatics), 1669 (C=O); **^{1}H NMR** (400 MHz, CDCl$_3$): δ 10.12 (s, 1H), 8.34 (t, *J* = 1.6 Hz, 1H), 8.00 (dd, *J* = 7.2, 1.8 Hz, 1H), 7.68 (t, *J* =1.6 Hz, 2H), 7.49 (t, *J* = 8.0 Hz, 1H), 7.22 (t, *J* = 1.2 Hz, 1H), 6.77 (dd, *J* = 7.6, 0.8 Hz, 1H), 6.60 (t, *J* = 1.2 Hz, 1H), 6.38 (s, 2H), 2.59 (s, 3H); **^{13}C NMR** (100 MHz, CDCl$_3$): δ 197.7, 168.0, 149.9, 139.7, 137.2, 136.9, 132.3, 128.9, 128.7, 124.9, 123.3, 119.8, 116.4, 114.7, 26.7; **MS** *m/z* found 277.0945 $C_{15}H_{14}N_2O_2$ (M$^+$ Na) expected 277.0947 (M$^+$ Na).

5.2.8.2 Attempted Preparation of 1-(3-((2-aminobenzyl)amino)phenyl)ethanol (198)

198
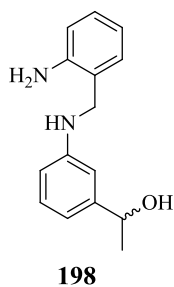
To a solution of **197** (104.90 mg, 0.41 mmol) in anhydrous THF (1 mL) at 0 $^{\circ}$C under an N_2 atmosphere was added a 1.0 M solution of BH_3.THF (0.04 mL, 4.00 mmol). The resultant reaction mixture was heated under reflux for 1 h and then cooled to room temperature. 6M HCl was added and the reaction mixture was stirred at room temperature for 1 h. After this period the reaction was basified with 6M NaOH (pH 9), poured onto water and extracted with dichloromethane (3 x 25 mL). The organic layers were combined, dried and the solvent removed under vacuum. Target product was not isolated.

5.2.8.3 Preparation of 1-(3-((2-aminobenzyl)amino)phenyl)ethanol (198)

198
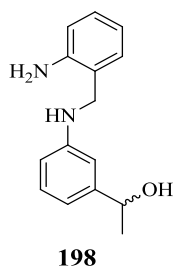
A solution of **197** (0.10 g, 0.39 mmol) in THF (5 mL) was added via cannula under nitrogen to a stirred solution of lithium aluminium hydride (0.079 g, 2.08 mmol) in THF (5 mL). The reaction was refluxed for 18 h and monitored by TLC. After this time the reaction was quenched by the careful addition of *sat.*NH$_4$Cl and extracted into diethyl ether (3 x 25 mL). Combined organic layers were dried over anhydrous MgSO$_4$, filtered and solvent removed under vacuum. The crude compound was purified by gradient column chromatography (R*f* = 0.65, L.Pet / EtOAc; 3:1 to 1:1) to give **198** as a pale orange / brown solid (0.057 g, 60 %).

Mp 109.4 – 114.4 $^{\circ}$C; **IR** CH$_2$Cl$_2$ max/cm^{-1}: 3380 (b, O–H), 2970, 2925 (aromatics); **^{1}H NMR** (400 MHz, CDCl$_3$): δ 7.25 – 7.16 (m, 3H), 6.82 – 6.74 (m, 5H), 6.65 (dd, *J* = 2.4, 1.2 Hz, 1H), 4.86 (m, 1H), 4.26 (s, 2H), 1.50 (d, *J* = 6.4 Hz, 3H); **^{13}C NMR** (100 MHz, CDCl$_3$): δ 147.60, 146.19, 144.76, 129.12, 128.49, 128.00, 120.46, 118.53, 117.43, 114.36, 111.64, 109.45, 69.55, 46.08, 24.06; **MS** *m/z* found 241.1348 C$_{15}$H$_{18}$ON$_2$ (M$^-$ H) expected 241.1346 (M$^-$ H).

5.2.8.4 Preparation of Unsymmetrical TB derivative 1-(6,12-dihydro-5,11-methanodibenzo[*b,f*][1,5]diazocin-3-yl)ethanol (199)

199
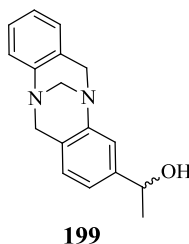
To a stirred suspension of amine **198** (0.10 g, 0.41 mmol) in 95 % ethanol (0.94 mL), under nitrogen at room temperature, 35 − 40 % aqueous formaldehyde (0.24 mL, 2.4 mmol) and 36 % hydrochloric acid (0.23 mL, 2.40 mmol) were added. The resulting reaction mixture was stirred at 90 $^\circ$C for 48 h. After this time the reaction was cooled to room temperature and basified with concentrated ammonium solution (pH 9). The alkaline solution was extracted with dichloromethane (3 x 5 mL), combined organic layers were washed with *sat.*NaHCO$_3$ (10 mL) and *sat.* NaCl (10 mL), dried over MgSO$_4$, filtered and solvent removed under vacuum. The crude product was purified by silca column chromatography (R*f* = 0.71, EtOAc / MeOH; 5:1) to give **199** as a mixture of diastereomers (0.22 g, 67 %).

IR CH$_2$Cl$_2$ max/cm^{-1}: 3391 (O–H, b), 2972 (aromatics); **^{1}H NMR** (400 MHz, CDCl$_3$): δ 7.20 − 7.13 (m, 3H), 7.03 − 7.01 (m, 2H), 6.93 − 6.89 (m, 2H), 4.83 (q, *J* = 3.2 Hz, 1H), 4.70 (dd, *J* = 16.8, 9.6 Hz, 2H), 4.31 (s, 2H), 4.20 (dd, *J* = 16.8, 8.4 Hz, 2H), 1.48 (dd, *J* = 6.4, 1.6 Hz, 3H); **^{13}C NMR** (100 MHz, CDCl$_3$): δ 126.55, 126.20, 126.13, 126.01, 124.04, 123.96, 123.42, 120.93, 120.83, 69.09, 69.01, 65.76, 57.48, 57.37, 24.12, 24.08, 14.20; **MS** *m/z* found 266.1487 C$_{17}$H$_{18}$N$_2$O (M$^+$) expected 266.1414 (M$^+$).

5.2.9 Procedure for the Preparation of Fused Cleft Systems

5.2.9.1 Preparation of Racemic 2,8-Dinitro-5,11-methanodibenzo[*a,e*][8]annulene-6,12(5*H*,11*H*)-dione (Dinitro cleft) ((±)-85)
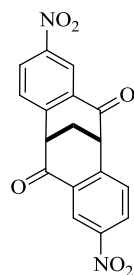
(±)-85

Racemic **(±)-2** (9.65 g, 0.039 M) was dissolved in concentrated sulphuric acid (500 mL) and stirred at 0 $^{\circ}$C while potassium nitrate (23.49 g, 0.23 M) was added in portions over 30 min. The solution was stirred at room temperature for 18 h. The mixture was poured onto ice and the white precipitate was collected by filtration and washed successively with cold water and diethyl ether, Recrystallization from hot DMF afforded the target compound **(±)-85** as slightly off-white solid (7.89 g, 60 %).

Mp 310.0 – 312.3 $^{\circ}$C (*Lit.* > 300 $^{\circ}$C)[8]; **IR** CH$_2$Cl$_2$ max/cm^{-1}: 1693 (C=O), 1523, 1342 (NO); **^{1}H NMR** (400 MHz, d$_6$-DMSO): δ 8.84 (d, *J* = 2.4 Hz, 2H), 8.41 (dd, *J* = 6.0, 2.4 Hz, 2H), 7.74 (d, *J* = 8.4 Hz, 2H), 4.29 (m, 2H), 3.16 (m, 2H); **MS** *m/z* found 361.0423 C$_{17}$H$_{10}$O$_6$N$_2$ (M$^+$ Na) expected 361.0431 (M$^+$ Na).

5.2.9.2 Preparation of Racemic 2,8-Diamino-5,11-methanodibenzo[*a,e*][8]annulene-6,12(5*H*,11*H*)-dione (Diamine cleft) ((±)-86)
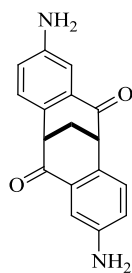
(±)-86

Racemic **(±)-85** (3.42 g, 0.010 M), iron powder (6.21 g, 0.11 M), acetic acid (13.15 mL, 0.23 M), and ethanol (300 mL) were refluxed under a nitrogen atmosphere for 48 h. The reaction was poured onto water and the aqueous layer was extracted with dichloromethane (3 x 150 mL). The combined organic layers were washed with *sat*.NaHCO$_3$, dried over anhydrous MgSO$_4$, filtered and the solvent removed under vacuum to give the title compound **(±)-86** as a bright yellow solid (1.46 g, 52 %).

Mp 295.7 – 299.1 ^{o}C (*Lit.* 288 – 291 ^{o}C)[8]; **IR** (Nujol) max/cm^{-1}: 3446, 3349 (N–H), 2725, 2670 (aromatics), 1672 (C=O); **^{1}H NMR** (400 MHz, CDCl$_3$): δ 6.99 (d, *J* = 8.4 Hz, 2H), 6.93 (d, *J* = 2.4 Hz, 2H), 6.71 (dd, *J* = 8.0, 2.4 Hz, 2H), 5.33 (s, 4H), 3.63 (t, *J* = 2.8 Hz, 2H), 2.74 (t, *J* = 2.8 Hz, 2H); **^{13}C NMR** (100 MHz, CDCl$_3$): δ 195.60, 149.69, 129.83, 129.68, 127.65, 120.48, 111.38, 47.72, 32.74; **MS** *m/z* found 301.0942 C$_{17}$H$_{14}$O$_2$N$_2$ (M^{+} Na) expected 301.0958 (M^{+} Na).

5.2.9.3 Preparation of *N,N'*-((5*S*,11*S*)-6,12-Dioxo-5,6,11,12-tetrahydro-5,11-methanodibenzo[*a,e*][8]annulene-2,8-diyl)bis(2-aminobenzamide) (Di-amide cleft) ((±)-193)

(±)-193
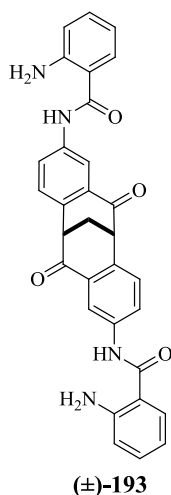
Isatoic anhydride (2.80 g, 17.16 mmol) and (±)-**86** (0.60 g, 2.16 mmol) were dissolved in dimethylacetamide (17 mL) and heated at reflux for 44 h. After this time the reaction was cooled to room temperature, poured onto water (50 mL) and extracted into dichloromethane (3 x 50 mL). Combined organic layers were repeatedly washed with water until no more insoluble isatoic anhydride precipitated from the organic layer. The resulting organic layer was dried over anhydrous MgSO$_4$, filtered and the solvent removed under vacuum. The crude product was purified by column chromatography (R$_f$ = 0.76, EtOAc / Petroleum; 5:1) and the isolated compound recrystallized slowly from a minimum amount of dichloromethane to give the target compound (±)-**193** as an off-white solid (0.067 g, 6 %).

Mp 272.5 – 276.3 $^{\circ}$C; **IR** CH$_2$Cl$_2$ max/cm^{-1}: 3584, 3449, 3341 (N–H), 1673, 1656 (C=O); **^{1}H NMR** (400 MHz, d$_6$-DMSO): δ 10.15 (s, 2H), 8.27 (d, *J* = 2.4 Hz, 2H), 7.93 (dd, *J* = 6.4, 2.0 Hz, 2H), 7.61 (dd, *J* = 6.4, 1.6 Hz, 2H), 7.43 (d, *J* = 8.4 Hz, 2H), 7.20 (td, *J* = 5.6, 1.6 Hz, 2H), 6.72 (dd, *J* = 7.2, 1.2 Hz, 2H), 6.55 (t, *J* = 7.2 Hz, 2H), 6.35 (s, 4H), 3.99 (t, *J* = 2.8 Hz, 2Hz), 2.98 (s, 2H); **^{13}C NMR** (100 MHz, CDCl$_3$): δ 193.51, 167.35, 149.36, 139.34, 134.17, 131.80, 128.60, 128.12, 125.83, 118.12, 115.87, 114.06, 46.91, 20.03; **MS** *m/z* found 539.1693 C$_{31}$H$_{24}$N$_4$O$_4$ (M$^+$ Na) expected 539.1695 (M$^+$ Na); **Elemental analysis** found C 71.98; H 4.78; N 10.01 %; C$_{31}$H$_{24}$O$_4$N$_4$ requires C 72.08; H 4.68; N 10.85 %.

5.2.9.4 Attempted Preparation of *N,N'*-((5*S*,11*S*)-6,12-Dioxo-5,6,11,12-tetrahydro-5,11-methanodibenzo[*a,e*][8]annulene-2,8-diyl)bis(2-aminobenzamide) (±)-193 –Microwave Assisted Reaction

(±)-193
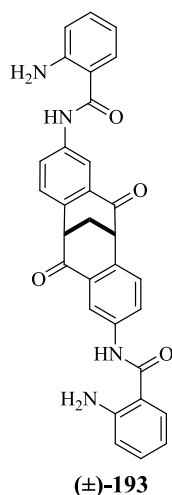
A neat mixture of isatoic anhydride (0.67 g, 4.11 mmol) and **(±)-86** (0.24 g, 0.86 mmol) were mixed thoroughly and then subjected to microwave irradiation (210 W) interruptedly at 4 min intervals to control and monitor the reaction. The reaction mixture was subject to three cycles at 210 W for 4 min and monitored by TLC. No reaction was observed.

5.2.11.5 Attempted Synthesis of 2,8-Bis((2-aminobenzyl)amino)-5,11-methanodibenzo[*a,e*][8]annulene-6,12(5*H*,11*H*)-dione ((±)-194)

(±)-194
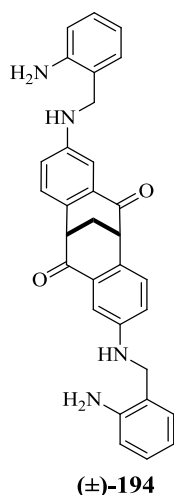
To a solution of **(±)-193** (16 mg, 0.031 mmol) in anhydrous THF (5 mL) at 0 $^{\circ}$C under an N_2 atmosphere, was added a 1.0 M solution of BH_3.THF (0.03 mL, 0.30 mmol). The resultant reaction mixture was heated under reflux for 1 h. After this period the reaction was cooled to room temperature and 6M HCl added. The reaction was stirred at room temperature for 1 h, poured onto water and extracted with dichloromethane (3 x 25 mL). The combined organic layers were dried, filtered and the solvent removed under vacuum. The crude solid was purified by chromatography but the target compound was not isolated.

5.2.9.6 Attempted Synthesis of 2,8-Bis((2-aminobenzyl)amino)-5,11-methanodibenzo[*a,e*][8]annulene-6,12(5*H*,11*H*)-dione (±)-194

(±)-194
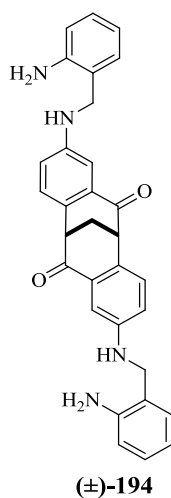
To a solution of **(±)-193** (19.99 mg, 0.039 mmol) in THF (5 mL) was added solution of LiAlH$_4$ (12.00 mg, 0.32 mmol) in THF (2 mL) under an N$_2$ atmosphere. The resultant reaction mixture was heated under reflux for 6 h. After this period the reaction was quenched with NH$_4$Cl and extracted with diethyl ether (3 x 15 mL). The combined organic layers were dried, filtered and the solvent removed under vacuum. The crude compound was purified by chromatography but ^{1}H NMR analysis revealed the target compound was not isolated.

5.2.9.7 Preparation of 2,8-Bis((2-nitrobenzyl)amino)-5,6,11,12-tetrahydro-5,11-methanodibenzo[*a,e*][8]annulene-6,12-diol ((±)-203) via Reductive Amination

(±)-203
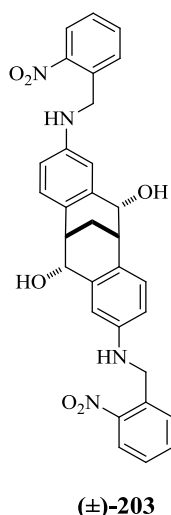
To a solution of the **(±)-86** (100.00 mg, 0.36 mmol) and 2-nitrobenzaldehyde (109.00 mg, 0.72 mmol) in DCE (5.00 mL) was added acetic acid (0.05 mL, 0.72 mmol) followed by NaBH(OAc)$_3$ (214.00 mg, 1.00 mmol) and the resultant reaction mixture stirred for 16 h under an N$_2$ atmosphere at room temperature. After this period the reaction was diluted with H$_2$O (20mL) and extracted with ethyl acetate (3 x 20 mL). The combined organic extracts were then dried, filtered and the solvent removed under vacuum. The crude oil was then purified by chromatography to give the title compound as yellow oil (123.00 mg, 62%).

^{1}H NMR (400 MHz, CDCl$_3$): δ 8.04 (dd, *J* = 8.0, 1.6 Hz, 2H), 7.59-7.57 (m, 2H), 7.50 (td, *J* = 7.6, 1.2 Hz, 2H), 7.40 (td, *J* = 8.0, 1.6 Hz, 2H), 7.02 (d, *J* = 8.0 Hz, 2H), 7.22 (d, *J* = 2.0 Hz, 2H), 6.33 (dd, *J* = 8.0, 2.4 Hz, 2H), 4.56 (s, 4H), 3.13 (q, *J* = 5.2 Hz, 2H), 2.27 (m, 2H); **^{13}C NMR** (100 MHz, CDCl$_3$): δ 148.15, 147.14, 140.92, 135.62, 133.69, 130.92, 129.85, 128.01, 125.20, 123.42, 111.83, 111.38, 72.74, 60.44, 45.73, 38.57.

5.2.9.8 Preparation of 2,8-Bis((2-aminobenzyl)amino)-5,6,11,12-tetrahydro-5,11-methanodibenzo[*a,e*][8]annulene-6,12-diol ((±)-204)
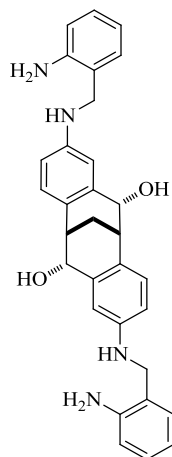
(±)-204

The di-nitro cleft (60.00 mg, 0.11 mmol), ion powder (86.01 mg, 1.52 mmol) was suspended in ethanol (10 mL) and acetic acid added (0.18 mL, 3.05 mmol). The reaction mixture was then refluxed for 16h under an N_2 atmosphere, after which the mixture was cooled, and poured into H_2O (50 mL), and extracted with ethyl acetate (3 x 50 mL). The crude organic extracts were then washed with $NaHCO_3$ (80 mL), dried, filtered and the solvent removed under reduced pressure. The crude oil was used without further purification in the next step.

5.2.9.9 Attempted Cyclisation of di-amine cleft
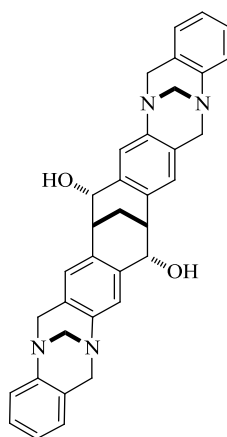
(±)-21

To a solution of di-amine **(±)-204** (50 mg, 0.11 mmol) in 95 % ethanol (0.5 mL) was added 37 % aqueous formaldehyde (0.02 mL, 0.66 mmol) and 36 % hydrochloric acid (0.02 mL, 0.66 mmol) at room temperature under an N_2 atmosphere. The resulting reaction mixture was stirred at 90 ^{o}C for 48 h. After this time the reaction was cooled to room temperature and basified with concentrated ammonium solution (pH 9) and extracted with dichloromethane (3 x 5 mL). The combined organic layers were washed with *sat.*NaHCO$_3$ (5 mL) followed by NaCl (5 mL), dried, filtered and the solvent removed under vacuum. The target compound was not isolated. Reaction led to decomposition of the intermediate di-amine cleft.

6.0   References

1.   M. J. Gaunt, C. C. C. Johansson, A. McNally, and N. T. Vo, *Drug Discov. Today*, 2007, **12**, 8–27.

2.   P. I. Dalko, *Asymmetric Organocatalysis : A New Stream in Organic Synthesis*, 2007.

3.   Ö. V. Rúnarsson, J. Artacho, and K. Wärnmark, *European J. Org. Chem.*, 2012, **2012**, 7015–7041.

4.   J. J. Turner and M. M. Harding, in *Supramolecular Chemistry*, 2005, vol. 17, pp. 369–375.

5.   S. Goswami and K. Ghosh, *Tetrahedron Lett.*, 1997, **38**, 4503–4506.

6.   A. Friberg, C. Olsson, F. Ek, U. Berg, and T. Frejd, *Tetrahedron: Asymmetry*, 2007, **18**, 885–891.

7.   B. Baldeyrou, C. Tardy, C. Bailly, P. Colson, C. Houssier, F. Charmantray, and M. Demeunynck, *Eur. J. Med. Chem.*, 2002, **37**, 315–322.

8.   M. C. Kimber, A. C. Try, L. Painter, M. M. Harding, and P. Turner, *J. Org. Chem.*, 2000, **65**, 3042–3046.

9.   C. Pardo, E. Sesmilo, E. Gutiérrez-Puebla, A. Monge, J. Elguero, and A. Fruchier, *J. Org. Chem.*, 2001, **66**, 1607–1611.

10.   J. Troger and J. Prakt, *J. Prakt. Chem*, 1887, **36**, 225–245.

11.   A. Spielman, *J. Am. Chem. Soc.*, 1935, **57**, 583–585.

12.   P. Prelog and P. Wieland, *Helv. Chim. Acta*, 1944, **27**, 1127 – 1134.

13.   C. S. Wilcox, *Tetrahedron Lett.*, 1985, **26**, 5749–5752.

14.   D. P. Becker, P. M. Finnegan, and P. W. Collins, *Tetrahedron Lett.*, 1993, **34**, 1889–1892.

15.   S. Satishkumar and M. Periasamy, *Tetrahedron: Asymmetry*, 2009, **20**, 2257–2262.

16.   S. Satishkumar and M. Periasamy, *Tetrahedron: Asymmetry*, 2006, **17**, 1116–1119.

17.   A. Hansson, J. Jensen, O. F. Wendt, and K. Wärnmark, *European J. Org. Chem.*, 2003, 3179–3188.

18.   T. . Webb and C. . Wilcox, *J. Org. Chem.*, 1990, **55**, 363–365.

19.   J. Jenson and K. Warnmark, *Synthesis (Stuttg).*, 2001, 1873–1877.

20.   J. Jenson, M. Strozyk, and K. Warnmark, *Synthesis (Stuttg).*, 2002, **18**, 2761 – 2765.

21.   U. Kiehne and A. Lutzen, *Synthesis (Stuttg).*, 2004, **10**, 1687–1695.

22.   D. Didier and S. Sergeyev, *Tetrahedron*, 2007, **63**, 3864–3869.

23.   C. Solano, D. Svensson, Z. Olomi, J. Jensen, O. F. Wendt, and K. Wärnmark, *European J. Org. Chem.*, 2005, **2005**, 3510–3517.

24.   F. Hof, M. Sch, D. M. Scofield, F. Fischer, and F. Diederich, *h*, 2005, **88**, 2333–2344.

25.   J. Artacho and K. Warnmark, *Synthesis (Stuttg).*, 2009, **18**, 3120–3126.

26.   J. Šturala and R. Cibulka, *European J. Org. Chem.*, 2012, **2012**, 7066–7074.

27.   D. Didier and S. Sergeyev, *European J. Org. Chem.*, 2007, 3905–3910.

28.   E. Yashima, M. Akashi, and N. Miyauchi, *Chem Lett*, 1991, 1017 – 1020.

29.   S. Goswami and K. Ghosh, *J. Org. Chem.*, 2000, **65**, 1907 – 1914.

30.   H. Tatemitsu, F. Ogura, Y. Nakagawa, M. Nakagawa, K. Naemura, and M. Nakazaki, *Chem. Soc. Japan*, 1975, **48**, 2473 – 2483.

31.   P. Molina, A. Arques, T. Alberto, and M. R. Obn, *Tetrahedron*, 1998, **54**, 997–1004.

32.   K. Mitra, M. . Pohl, L. . MacGillivray, C. . Barnes, and K. . Gates, *J. Org. Chem.*, 1997, **62**, 9361 – 9364.

33.   A. Try, L. Painter, and M. Harding, *Tetrahedron Lett.*, 1998, **39**, 9809–9812.

34.   L. Thunberg, S. Allenmark, A. Friberg, F. Ek, and T. Frejd, *Chirality*, 2004, **16**, 614–624.

35.   K. Naemura, R. Fukunaga, and M. Yamanaka, *Chem. Soc. Japan*, 1985, 1560 – 1561.

36.   A. Reischl and H. Setter, *Chem. Soc. Japan*, 1960, **93**, 791–795.

37.   C. . K. . Lee, J. . Groneman, P. Turner, L. . Rendina, and M. . Harding, *Tetrahedron*, 2006, **62**, 4870 – 4878.

38.   K. Naemura and M. Yamanaka, *Chem. Commun.*, 1985, **20**, 1560–1561.

39.   P. Jilka, C. Millington, M. R. J. Elsegood, J. W. a. Frese, S. Teat, and M. C. Kimber, *Tetrahedron*, 2010, **66**, 9327–9331.

40.   J. D. Field, P. Turner, M. M. Harding, T. Hatzikominos, and L. Kim, *New J. Chem.*, 2002, **26**, 720–725.

41.   H. Heaney and S. . Ley, *J. Chem.Soc., Perkin Trans*, 1973, **1**, 499–500.

42.   M. C. Kimber, *Unpubl. result*, 2014.

43.   L. Zhou, C. K. Tan, X. Jiang, F. Chen, and Y.-Y. Yeung, *J. Am. Chem. Soc.*, 2010, **132**, 15474–15476.

44. P. Knochel, W. Dohle, N. Gommermann, F. F. Kneisel, F. Kopp, T. Korn, I. Sapountzis, and V. A. Vu, *Angew. Chem. Int. Ed. Engl.*, 2003, **42**, 4302–4320.

45. A. Krasovskiy and P. Knochel, *Angew. Chem. Int. Ed. Engl.*, 2004, **43**, 3333–3336.

46. M. S. Taylor and E. N. Jacobsen, *Angew. Chem. Int. Ed. Engl.*, 2006, **45**, 1520–1543.

47. E. M. O. Yeboah, S. O. Yeboah, and G. S. Singh, *Tetrahedron*, 2011, **67**, 1725–1762.

48. J. Halpern and B. . Trost, *Proc. Natl. Acad. Sci. U. S. A.*, 2004, **101**, 5347.

49. L. Zhou, J. Chen, C. . Tan, and Y. . Yeung, *J. Am. ...*, 2011, 9164–9167.

50. C. K. Tan, L. Zhou, and Y.-Y. Yeung, *Org. Lett.*, 2011, **13**, 2738–2741.

51. S. E. Denmark and W. R. Collins, *Org. Lett.*, 2007, **9**, 3801–3804.

52. S. . Larson and C. . Wilcox, *Acta Crystallogr. Sect, C Cryst.Struct.Commun.*, 1986, 224 – 227.

53. N. Agra-, *J. Biomed. Sci. Res. Res.*, 2010, **2**, 29–45.

54. P. I. Dalko and L. Moisan, *Angew. Chem. Int. Ed. Engl.*, 2001, **40**, 3726–3748.

55. R. Noyori, *Asymmetric Catalysis in Organic Synthesis*, 1994.

56. E. N. Jacobsen, A. Pfaltz, and H. Yamamoto, *Comprehensive Asymmetric Catalysis*, 1999.

57. D. W. C. MacMillan, *Nature*, 2008, **455**, 304–8.

58. S. . Connon, *Chem. Commun.*, 2008, 2499 – 2510.

59. M. Rueping, A. P. Antonchick, and T. Theissmann, *Angew. Chem. Int. Ed. Engl.*, 2006, **45**, 3683–3686.

60. A. N. Thadani, A. R. Stankovic, and V. H. Rawal, *Proc. Natl. Acad. Sci. U. S. A.*, 2004, **101**, 5846–5850.

61. C. Uyeda and E. N. Jacobsen, *J. Am. Chem. Soc.*, 2008, **130**, 9228–9229.

62. M. S. Sigman and E. N. Jacobsen, *J. Am. Chem. Soc.*, 1998, **7863**, 4901–4902.

63. P. Vachal and E. N. Jacobsen, *Org. Lett.*, 2000, **2**, 867–870.

64. A. K. Unni, N. Takenaka, H. Yamamoto, and V. H. Rawal, *J. Am. Chem. Soc.*, 2005, **127**, 1336–1337.

65. P. M. Pihko, *Angew. Chem. Int. Ed. Engl.*, 2004, **43**, 2062–2064.

66. S. Danishefsky, J. . Kerwin, and S. Kobayashi, *J. Am. Chem. Soc.*, 1982, **104**, 358–359.

67. T. Schuster, M. Bauch, G. Durner, and M. Gobel, *Org. Lett.*, 2000, **2**, 179–181.

68. S. . Kozmin, J. . Janey, and V. H. Rawel, *J. Org. Chem.*, 1999, 3039 – 3052.

69. Y. Huang and V. H. Rawel, *Org. Lett.*, 2000, **2**, 3321 – 3323.

70. Y. Huang and V. H. Rawal, *J. Am. Chem. Soc.*, 2002, **124**, 9662–9663.

71. Y. Huang, K. Unni, A, N. Thadani, A, and V. H. Rawel, *Nature*, 2003, 146.

72. H. Du, D. Zhao, and K. Ding, *Chemistry*, 2004, **10**, 5964–5970.

73. X. Zhang, H. Du, Z. Wang, Y.-D. Wu, and K. Ding, *J. Org. Chem.*, 2006, **71**, 2862–2869.

74. R. Gordillo, T. Dudding, C. D. Anderson, and K. N. Houk, *Org. Lett.*, 2007, **9**, 501–503.

75. S. C. Hawkins, R. Bishop, D. C. Craig, S. Kim, and M. L. Scudder, *J. Chem. Soc. Chem. Commun.*, 1990, 1683–1984.

76. S. He, V. H. Rawal, and S. . Kozmin, *Org. Synth.*, 2004, **10**, 301–304.

77. C. S. Cucinotta, M. Kosa, P. Melchiorre, A. Cavalli, and F. L. Gervasio, *Chemistry*, 2009, **15**, 7913–7921.

78. S. E. Denmark and M. T. Burk, *Proc. Natl. Acad. Sci. U. S. A.*, 2010, **107**, 20655–20660.

79. A. A. Neverov and R. S. Brown, *J. Org. Chem.*, 1996, 962–968.

80. W. Zhang, S. Zheng, N. Liu, J. Werness, L. Guzei, and W. Tang, *J. Am. Chem. Soc.*, 2010, 3664–3665.

81. K. Murai, T. Matsushita, A. Nakamura, S. Fukushima, M. Shimura, and H. Fujioka, *Angew. Chem. Int. Ed. Engl.*, 2010, **49**, 9174–9177.

82. J. . Lehn, *Supramolecular Chemistry, Concepts and Persepectives*, 1995.

83. T. . Webb and C. . Wilcox, *J. Org. Chem.*, 1990, **55**, 363–365.

84. T. Mas, C. Pardo, and J. Elguero, *Mendeleev Commun.*, 2004, **14**, 235–237.

85. A. Hansson, T. Wixe, K.-E. Bergquist, and K. Warnmark, *Org. Lett.*, 2005, **7**, 2019 – 2022.

86. B. Dolensky, M. Valik, D. Sykora, and V. Kral, *Org. Lett.*, 2005, **7**, 67 –70.

87. F. Salort, C. Pardo, and J. Elguero, *Magn. Reson. Chem.*, 2002, **40**, 743–746.

88. M. Bakavoli, O. Sabzevari, and M. Rahimizadeh, *Chinese Chem. Lett.*, 2007, **18**, 533–535.

89. R. H. Clark and E. . Wagner, 1943, 55–67.

90. A. F. Abdel-Magid, K. G. Carson, B. D. Harris, C. a. Maryanoff, and R. D. Shah, *J. Org. Chem.*, 1996, **61**, 3849–3862.

91.	S. Sergeyev, *Helv. Chim. Acta*, 2009, **92**, 415–444.

7.0 Appendix

7.1 Crystal Data for (±)-114

Chemical formula	$C_{17}H_{14}Cl_2$
Formula weight	289.18
Temperature	150(2) K
Radiation, wavelength	MoKα, 0.71073 Å
Crystal system, space group	triclinic, P $\bar{1}$
Unit cell parameters	a = 8.2607(12) Å $\quad\quad$ α = 78.121(2)°
	b = 10.3800(15) Å $\quad\quad$ β = 79.597(2)°
	c = 16.780(2) Å $\quad\quad$ γ = 76.209(2)°
Cell volume	1354.3(3) Å^3
Z	4
Calculated density	1.418 g/cm^3
Absorption coefficient μ	0.461 mm^{-1}
F(000)	600
Crystal colour and size	colourless, $1.46 \times 0.27 \times 0.04$ mm^3
Reflections for cell refinement	5098 (θ range 2.51 to 28.32°)
Data collection method	Bruker APEX 2 CCD diffractometer
	ω rotation with narrow frames
θ range for data collection	2.05 to 28.37°
Index ranges	h −11 to 11, k −13 to 13, l −22 to 22
Completeness to θ = 28.37°	98.3 %
Intensity decay	0%
Reflections collected	13769
Independent reflections	6654 (R$_{int}$ = 0.0242)
Reflections with F^2>2σ	5311
Absorption correction	semi-empirical from equivalents
Min. and max. transmission	0.553 and 0.982
Structure solution	direct methods
Refinement method	Full-matrix least-squares on F^2
Weighting parameters a, b	0.0540, 0.3480
Data / restraints / parameters	6654 / 0 / 343
Final R indices [F^2>2σ]	R1 = 0.0380, wR2 = 0.0945
R indices (all data)	R1 = 0.0512, wR2 = 0.1032
Goodness-of-fit on F^2	1.020
Largest and mean shift/su	0.001 and 0.000
Largest diff. peak and hole	0.467 and −0.278 e Å^{-3}

Computing details

Data collection: Bruker *APEX* 2; cell refinement: Bruker *SAINT*; data reduction: Bruker *SAINT*; program(s) used to solve structure: *SHELXS97* (Sheldrick, 2008); program(s) used to refine structure: *SHELXL2012* (Sheldrick, 2012); molecular graphics: Bruker *SHELXTL*; software used to prepare material for publication: Bruker *SHELXTL*.

7.2 Crystal Data for (±)-123

Chemical formula	$C_{17}H_{14}O_2$
Formula weight	250.28
Temperature	150(2) K
Radiation, wavelength	MoKα, 0.71073 Å
Crystal system, space group	rhombohedral on hexagonal axes, R $\overline{3}$
Unit cell parameters	a = 24.834(2) Å $\quad\quad$ α = 90°
	b = 24.834(2) Å $\quad\quad$ β = 90°
	c = 10.4685(9) Å $\quad\quad$ γ = 120°
Cell volume	5591.2(12) Å^3
Z	18
Calculated density	1.338 g/cm^3
Absorption coefficient μ	0.087 mm^{-1}
F(000)	2376
Crystal colour and size	colourless, $0.82 \times 0.64 \times 0.21$ mm^3
Reflections for cell refinement	5575 (θ range 2.16 to 28.41°)
Data collection method	Bruker APEX 2 CCD diffractometer
	ω rotation with narrow frames
θ range for data collection	1.64 to 30.58°
Index ranges	h −35 to 35, k −35 to 35, l −14 to 14
Completeness to θ = 30.58°	99.6 %
Intensity decay	0%
Reflections collected	21770
Independent reflections	3808 (R_{int} = 0.0276)
Reflections with $F^2 > 2\sigma$	2775
Absorption correction	semi-empirical from equivalents
Min. and max. transmission	0.932 and 0.982
Structure solution	direct methods
Refinement method	Full-matrix least-squares on F^2
Weighting parameters a, b	0.0712, 6.7552
Data / restraints / parameters	3808 / 0 / 174
Final R indices [$F^2 > 2\sigma$]	R1 = 0.0608, wR2 = 0.1565
R indices (all data)	R1 = 0.0837, wR2 = 0.1736
Goodness-of-fit on F^2	1.062
Largest and mean shift/su	0.000 and 0.000
Largest diff. peak and hole	0.394 and −0.421 e Å^{-3}

Hydrogen-bond geometry (Å and º)

D–H...A	d(D–H)	d(H...A)	d(D...A)	<(DHA)
O(1)–H(1)...O(1')	0.84	1.80	2.6401(12)	175.5

Symmetry operations for equivalent atoms
' y−1/3,−x+y+1/3,−z+1/3

7.3 Crystal Data for (±)-102 – H-Bonded complex with 3-bromopyridine

Chemical formula	$C_{34}H_{28}BrNO_2$
Formula weight	562.48
Temperature	150(2) K
Radiation, wavelength	MoKα, 0.71073 Å
Crystal system, space group	triclinic, P $\bar{1}$
Unit cell parameters	a = 7.542(3) Å α = 95.065(5)°
	b = 11.206(4) Å β = 96.632(6)°
	c = 16.167(6) Å γ = 99.148(6)°
Cell volume	1332.0(9) Å^3
Z	2
Calculated density	1.402 g/cm^3
Absorption coefficient μ	1.576 mm^{-1}
F(000)	580
Crystal colour and size	colourless, 0.32 × 0.25 × 0.03 mm^3
Reflections for cell refinement	3203 (θ range 2.36 to 23.75°)
Data collection method	Bruker APEX 2 CCD diffractometer
	ω rotation with narrow frames
θ range for data collection	1.85 to 26.33°
Index ranges	h −9 to 9, k −13 to 13, l −20 to 20
Completeness to θ = 26.33°	99.4 %
Intensity decay	0%
Reflections collected	15196
Independent reflections	5388 (R_{int} = 0.0588)
Reflections with $F^2 > 2σ$	3661
Absorption correction	semi-empirical from equivalents
Min. and max. transmission	0.633 and 0.954
Structure solution	Patterson synthesis
Refinement method	Full-matrix least-squares on F^2
Weighting parameters a, b	0.0502, 0.0376

Data / restraints / parameters	5388 / 0 / 345
Final R indices [$F^2 > 2\sigma$]	R1 = 0.0425, wR2 = 0.0944
R indices (all data)	R1 = 0.0772, wR2 = 0.1075
Goodness-of-fit on F^2	1.006
Largest and mean shift/su	0.000 and 0.000
Largest diff. peak and hole	0.489 and −0.575 e Å^{-3}

Hydrogen-bond geometry (Å and º)

D–H...A	d(D–H)	d(H...A)	d(D...A)	<(DHA)
O(2)–H(2)...N(1)	0.84	2.07	2.905(3)	174.7

7.4 Crystal Data for (±)-102

Chemical formula	$C_{29}H_{24}O_2$
Formula weight	404.48
Temperature	150(2) K
Radiation, wavelength	MoKα, 0.71073 Å
Crystal system, space group	monoclinic, C2/c
Unit cell parameters	a = 19.1343(10) Å $\quad$ α = 90°
	b = 11.3871(6) Å $\quad$ β = 94.6835(8)°
	c = 19.2660(10) Å $\quad$ γ = 90°
Cell volume	4183.7(4) Å^3
Z	8
Calculated density	1.284 g/cm^3
Absorption coefficient μ	0.079 mm^{-1}
F(000)	1712
Crystal colour and size	colourless, 0.33 × 0.25 × 0.20 mm^3
Reflections for cell refinement	5457 (θ range 2.30 to 30.47°)
Data collection method	Bruker APEX 2 CCD diffractometer
	ω rotation with narrow frames
θ range for data collection	2.08 to 30.57°
Index ranges	h −26 to 27, k −16 to 16, l −27 to 27
Completeness to θ = 30.00°	100.0 %
Intensity decay	0%
Reflections collected	23965
Independent reflections	6350 (R_{int} = 0.0330)
Reflections with $F^2>2\sigma$	4906
Absorption correction	semi-empirical from equivalents
Min. and max. transmission	0.974 and 0.984
Structure solution	direct methods
Refinement method	Full-matrix least-squares on F^2
Weighting parameters a, b	0.0554, 2.3334
Data / restraints / parameters	6350 / 0 / 286
Final R indices [$F^2>2\sigma$]	R1 = 0.0458, wR2 = 0.1139
R indices (all data)	R1 = 0.0617, wR2 = 0.1237
Goodness-of-fit on F^2	1.053
Largest and mean shift/su	0.000 and 0.000
Largest diff. peak and hole	0.424 and −0.208 e Å^{-3}

Hydrogen-bond geometry (Å and º)

D–H...A	d(D–H)	d(H...A)	d(D...A)	<(DHA)
O(1)–H(1)...O(2')	0.827(17)	2.149(17)	2.8340(12)	140.1(15)

Symmetry operations for equivalent atoms
'   −x+1/2,y−1/2,−z+1/2

7.5   Crystal Data for (+)-4

Crystal Data

$C_{33}H_{30}N_2O_2S_2$	$Z = 2$
$M_r = 550.71$	$F(000) = 580$
Triclinic, $P\bar{1}$	$D_x = 1.193$ Mg m^{-3}
$a = 8.800$ (3) Å	Synchrotron radiation, $\lambda = 0.8856$ Å
$b = 11.513$ (3) Å	Cell parameters from 3400 reflections
$c = 15.976$ (5) Å	$\theta = 3.2$–$31.3°$
$\alpha = 106.418$ (4)°	$\mu = 0.37$ mm^{-1}
$\beta = 96.339$ (4)°	$T = 150$ K
$\gamma = 94.583$ (4)°	Block, colourless
$V = 1532.6$ (8) Å^3	$0.06 \times 0.05 \times 0.04$ mm

Data Collection

Bruker APEX 2 CCD diffractometer	5123 independent reflections
Radiation source: ALS Station 11.1.1	3405 reflections with $I > 2\sigma(I)$
silicon 111	$R_{int} = 0.052$
ω rotation with narrow frames scans	$\theta_{max} = 31.4°$, $\theta_{min} = 2.9°$
Absorption correction: multi-scan *SADABS* v2009/1, Sheldrick, G.M., (2009)	$h = ? \rightarrow ?$
$T_{min} = 0.978$, $T_{max} = 0.986$	$k = ? \rightarrow ?$
18076 measured reflections	$l = ? \rightarrow ?$

Refinement

Refinement on F^2	Secondary atom site location: difference Fourier map
Least-squares matrix: full	Hydrogen site location: mixed
$R[F^2 > 2\sigma(F^2)] = 0.051$	H atoms treated by a mixture of independent and constrained refinement
$wR(F^2) = 0.136$	$w = 1/[\sigma^2(F_o^2) + (0.0796P)^2]$ where $P = (F_o^2 + 2F_c^2)/3$
$S = 0.99$	$(\Delta/\sigma)_{max} < 0.001$
5123 reflections	$\Delta\rangle_{max} = 0.24$ e Å^{-3}
364 parameters	$\Delta\rangle_{min} = -0.27$ e Å^{-3}
57 restraints	Extinction correction: *SHELXL*, Fc*=kFc[1+0.001xFc$^2\lambda^3$/sin(2θ)]$^{-1/4}$
Primary atom site location: structure-invariant direct methods	Extinction coefficient: 0.011 (2)

Hydrogen-bond geometry (Å and º)

D—H$\cdots A$	D—H	H$\cdots A$	$D\cdots A$	D—H$\cdots A$
N1—H1$\cdots$S1[i]	0.94 (4)	2.40 (4)	3.319 (4)	166 (3)
N2—H2$\cdots$S2[ii]	0.83 (4)	2.54 (4)	3.338 (4)	162 (3)

Symmetry codes: (i) -x+2, -y, -z; (ii) -x, -y, -z+1.

Computing details

Data collection: Bruker *APEX* 2; cell refinement: Bruker *SAINT*; data reduction: Bruker *SAINT*; program(s) used to solve structure: *SHELXS97* (Sheldrick, 2008); program(s) used to refine structure: *SHELXL2012* (Sheldrick, 2012); molecular graphics: Bruker *SHELXTL*; software used to prepare material for publication: Bruker *SHELXTL*.

Special details

Geometry. All esds (except the esd in the dihedral angle between two l.s. planes) are estimated using the full covariance matrix. The cell esds are taken into account individually in the estimation of esds in distances, angles and torsion angles; correlations between esds in cell parameters are only used when they are defined by crystal symmetry. An approximate (isotropic) treatment of cell esds is used for estimating esds involving l.s. planes.

Refinement. Refined as a 2-component twin with components related about reciprocal axis 0 1 0 with major component = 51.22(19) %.

7.6 Crystal Data for (±)-4 – H-Bonded complex with acetonitrile

Chemical formula	$C_{36}H_{37}N_3O_3S_2$
Formula weight	623.81
Temperature	150(2) K
Radiation, wavelength	MoKα, 0.71073 Å
Crystal system, space group	monoclinic, I2/a
Unit cell parameters	a = 8.6163(6) Å α = 90°
	b = 22.5734(15) Å β = 95.5620(9)°
	c = 17.2003(12) Å γ = 90°
Cell volume	3329.7(4) Å^3
Z	4
Calculated density	1.244 g/cm^3
Absorption coefficient μ	0.199 mm^{-1}
F(000)	1320
Crystal colour and size	colourless, $0.75 \times 0.41 \times 0.28$ mm^3
Reflections for cell refinement	7726 (θ range 2.38 to 30.34°)
Data collection method	Bruker APEX 2 CCD diffractometer
	ω rotation with narrow frames
θ range for data collection	1.80 to 30.54°
Index ranges	h −12 to 12, k −31 to 32, l −24 to 24
Completeness to θ = 29.00°	99.9 %
Intensity decay	0%
Reflections collected	18935
Independent reflections	5034 (R_{int} = 0.0231)
Reflections with $F^2 > 2\sigma$	4203
Absorption correction	semi-empirical from equivalents
Min. and max. transmission	0.865 and 0.946
Structure solution	direct methods
Refinement method	Full-matrix least-squares on F^2
Weighting parameters a, b	0.0705, 2.1231
Data / restraints / parameters	5034 / 0 / 216
Final R indices [$F^2 > 2\sigma$]	R1 = 0.0423, wR2 = 0.1198
R indices (all data)	R1 = 0.0514, wR2 = 0.1268
Goodness-of-fit on F^2	1.038
Largest and mean shift/su	0.000 and 0.000
Largest diff. peak and hole	0.537 and −0.217 e Å^{-3}

Hydrogen-bond geometry (Å and º)

D–H...A	d(D–H)	d(H...A)	d(D...A)	<(DHA)
N(1)–H(1)...S(1")	0.816(18)	2.602(18)	3.3611(10)	155.4(15)

Symmetry operations for equivalent atoms
"   −x+5/2,−y+1/2,−z−1/2

7.7 Crystal Data for (±)-5

Crystal Data

$C_{31}H_{26}N_2O_2S_2 \cdot CHCl_3$	$Z = 2$
$M_r = 642.02$	$F(000) = 664$
Triclinic, $P\bar{1}$	$D_x = 1.377$ Mg m^{-3}
$a = 10.9583\,(6)$ Å	Mo $K\alpha$ radiation, $\lambda = 0.71073$ Å
$b = 12.3033\,(7)$ Å	Cell parameters from 12139 reflections
$c = 12.8962\,(7)$ Å	$\theta = 2.2$–$30.6°$
$\alpha = 109.9319\,(7)°$	$\mu = 0.46$ mm^{-1}
$\beta = 105.3809\,(8)°$	$T = 150$ K
$\gamma = 94.4415\,(8)°$	Block, colourless
$V = 1548.75\,(15)$ Å^3	$0.84 \times 0.73 \times 0.37$ mm

Data Collection

Bruker APEX 2 CCD diffractometer	9328 independent reflections
Radiation source: fine-focus sealed tube	7720 reflections with $I > 2\sigma(I)$
graphite	$R_{int} = 0.017$
ω rotation with narrow frames scans	$\theta_{max} = 30.6°$, $\theta_{min} = 1.8°$
Absorption correction: multi-scan *SADABS* v2009/1, Sheldrick, G.M., (2009)	$h = -15 \rightarrow 15$
$T_{min} = 0.697$, $T_{max} = 0.847$	$k = -17 \rightarrow 17$
24178 measured reflections	$l = -18 \rightarrow 18$

Refinement

Refinement on F^2	Primary atom site location: structure-invariant direct methods
Least-squares matrix: full	Secondary atom site location: difference Fourier map
$R[F^2 > 2\sigma(F^2)] = 0.045$	Hydrogen site location: mixed
$wR(F^2) = 0.126$	H atoms treated by a mixture of independent and constrained refinement
$S = 1.03$	$w = 1/[\sigma^2(F_o^2) + (0.063P)^2 + 0.6834P]$ where $P = (F_o^2 + 2F_c^2)/3$
9328 reflections	$(\Delta/\sigma)_{max} < 0.001$
511 parameters	$\Delta\rangle_{max} = 0.88$ e Å^{-3}
116 restraints	$\Delta\rangle_{min} = -0.59$ e Å^{-3}

Hydrogen-bond geometry (Å and º)

D—H⋯A	D—H	H⋯A	D⋯A	D—H⋯A
N1—H1⋯S1[i]	0.88 (2)	2.50 (2)	3.3623 (14)	167 (2)
N2—H2⋯S2[ii]	0.82 (2)	2.55 (2)	3.3610 (12)	170 (2)

Symmetry codes: (i) -*x*+1, -*y*+1, -*z*; (ii) -*x*, -*y*, -*z*+1.

Computing details

Data collection: Bruker *APEX* 2; cell refinement: Bruker *SAINT*; data reduction: Bruker *SAINT*; program(s) used to solve structure: *SHELXS97* (Sheldrick, 2008); program(s) used to refine structure: *SHELXL2012* (Sheldrick, 2012); molecular graphics: Bruker *SHELXTL*; software used to prepare material for publication: Bruker *SHELXTL*.

Special details

Geometry. All esds (except the esd in the dihedral angle between two l.s. planes) are estimated using the full covariance matrix. The cell esds are taken into account individually in the estimation of esds in distances, angles and torsion angles; correlations between esds in cell parameters are only used when they are defined by crystal symmetry. An approximate (isotropic) treatment of cell esds is used for estimating esds involving l.s. planes.

7.8 Crystal Data for (±)-6

Crystal Data

$C_{35}H_{21}F_{12}N_2O_2S_2 \cdot 0.25(C_5H_{12})$	$F(000) = 3300$
$M_r = 812.70$	$D_x = 1.328$ Mg m^{-3}
Monoclinic, $P2_1/n$	Synchrotron radiation, $\lambda = 0.8856$ Å
$a = 15.9043$ (18) Å	Cell parameters from 8243 reflections
$b = 13.0965$ (15) Å	$\theta = 2.9$–$26.5°$
$c = 39.167$ (4) Å	$\mu = 0.39$ mm^{-1}
$\beta = 94.944$ (2)°	$T = 150$ K
$V = 8127.8$ (15) Å^3	Plate, colourless
$Z = 8$	$0.16 \times 0.09 \times 0.03$ mm

Data Collection

Bruker APEX 2 CCD diffractometer	9361 independent reflections
Radiation source: ALS Station 11.3.1	7202 reflections with $I > 2\sigma(I)$
silicon 111	$R_{int} = 0.075$
ω rotation with narrow frames scans	$\theta_{max} = 27.2°$, $\theta_{min} = 2.9°$
Absorption correction: multi-scan *SADABS* v2008/1, Sheldrick, G.M., (2008)	$h = -16 \rightarrow 16$
$T_{min} = 0.940$, $T_{max} = 0.988$	$k = -13 \rightarrow 13$
51498 measured reflections	$l = -40 \rightarrow 40$

Refinement

Refinement on F^2	Secondary atom site location: difference Fourier map
Least-squares matrix: full	Hydrogen site location: mixed
$R[F^2 > 2\sigma(F^2)] = 0.095$	H atoms treated by a mixture of independent and constrained refinement
$wR(F^2) = 0.276$	$w = 1/[\sigma^2(F_o^2) + (0.1508P)^2 + 19.4351P]$ where $P = (F_o^2 + 2F_c^2)/3$
$S = 1.06$	$(\Delta/\sigma)_{max} = 0.001$
9361 reflections	$\Delta\rangle_{max} = 0.65$ e Å^{-3}
1178 parameters	$\Delta\rangle_{min} = -0.47$ e Å^{-3}
1430 restraints	Extinction correction: *SHELXL*, Fc*=kFc[1+0.001xFc$^2\lambda^3$/sin(2θ)]$^{-1/4}$
Primary atom site location: structure-invariant direct methods	Extinction coefficient: 0.0013 (3)

Hydrogen-bond geometry (Å and º)

D—H···A	D—H	H···A	D···A	D—H···A
N1—H1···S3^{i}	0.84 (2)	2.61 (4)	3.369 (5)	151 (6)
N2—H2···S2^{ii}	0.85 (2)	2.96 (6)	3.560 (6)	130 (6)
N3—H3X···S1^{iii}	0.88	2.51	3.351 (6)	160
N4—H4···S3^{iv}	0.83 (2)	2.65 (4)	3.436 (6)	157 (7)

Symmetry codes: (i) x, y+1, z; (ii) -x+1, -y+1, -z+2; (iii) x, y-1, z; (iv) -x+1/2, y+1/2, -z+3/2.

Computing details

Data collection: Bruker *APEX* 2; cell refinement: Bruker *SAINT*; data reduction: Bruker *SAINT*; program(s) used to solve structure: *SHELXS97* (Sheldrick, 2008); program(s) used to refine structure: *SHELXL2012* (Sheldrick, 2012); molecular graphics: Bruker *SHELXTL*; software used to prepare material for publication: Bruker *SHELXTL*.

Special details

Geometry. All esds (except the esd in the dihedral angle between two l.s. planes) are estimated using the full covariance matrix. The cell esds are taken into account individually in the estimation of esds in distances, angles and torsion angles; correlations between esds in cell parameters are only used when they are defined by crystal symmetry. An approximate (isotropic) treatment of cell esds is used for estimating esds involving l.s. planes.

7.9 Crystal Data for (±)-7

Crystal Data

$C_{21}H_{22}N_2O_2S_2$	$F(000) = 2520$
$M_r = 398.52$	$D_x = 1.326$ Mg m^{-3}
Monoclinic, $P2_1/c$	Synchrotron radiation, $\lambda = 0.7749$ Å
$a = 12.246$ (2) Å	Cell parameters from 9946 reflections
$b = 20.733$ (4) Å	$\theta = 2.9$–$33.5°$
$c = 23.948$ (4) Å	$\mu = 0.36$ mm^{-1}
$\beta = 99.900$ (2)°	$T = 100$ K
$V = 5989.8$ (18) Å^3	Tablet, colourless
$Z = 12$	$0.20 \times 0.15 \times 0.02$ mm

Data Collection

Bruker APEX 2 CCD diffractometer	14919 reflections with $I > 2\sigma(I)$
Radiation source: ALS Station 11.3.1	$R_{int} = 0.073$
ω rotation with narrow frames scans	$\theta_{max} = 33.6°$, $\theta_{min} = 2.8°$
Absorption correction: multi-scan *SADABS* v20012/1, Sheldrick, G.M., (2012)	$h = -17 \rightarrow 17$
$T_{min} = 0.932$, $T_{max} = 0.993$	$k = -29 \rightarrow 29$
86661 measured reflections	$l = -34 \rightarrow 34$
18216 independent reflections	

Refinement

Refinement on F^2	Primary atom site location: structure-invariant direct methods
Least-squares matrix: full	Secondary atom site location: difference Fourier map
$R[F^2 > 2\sigma(F^2)] = 0.056$	Hydrogen site location: difference Fourier map
$wR(F^2) = 0.157$	All H-atom parameters refined
$S = 1.02$	$w = 1/[\sigma^2(F_o^2) + (0.0755P)^2 + 3.2158P]$ where $P = (F_o^2 + 2F_c^2)/3$
18216 reflections	$(\Delta/\sigma)_{max} = 0.001$
994 parameters	$\Delta\rangle_{max} = 1.40$ e Å^{-3}
1 restraint	$\Delta\rangle_{min} = -0.63$ e Å^{-3}

Hydrogen-bond geometry (Å and º)

D—H⋯*A*	*D*—H	H⋯*A*	*D*⋯*A*	*D*—H⋯*A*
N1—H1⋯S3	0.84 (3)	2.58 (3)	3.310 (2)	145 (3)
N2—H2⋯S4	0.80 (3)	2.74 (3)	3.457 (2)	151 (2)
N3—H3⋯S5	0.80 (2)	2.70 (2)	3.4072 (18)	148 (2)
N4—H4⋯S6	0.90 (3)	2.62 (3)	3.3255 (19)	135 (2)
N5—H5⋯S2[i]	0.82 (3)	2.61 (3)	3.3221 (17)	147 (2)
N6—H6⋯S1[i]	0.82 (3)	2.73 (3)	3.457 (2)	149 (2)

Symmetry code: (i) *x*+1, -*y*+1/2, *z*+1/2.

Computing details

Data collection: Bruker *APEX* 2; cell refinement: Bruker *SAINT*; data reduction: Bruker *SAINT*; program(s) used to solve structure: *SHELXS97* (Sheldrick, 2008); program(s) used to refine structure: *SHELXL2012* (Sheldrick, 2012); molecular graphics: Bruker *SHELXTL*; software used to prepare material for publication: Bruker *SHELXTL*.

Special details

Geometry. All esds (except the esd in the dihedral angle between two l.s. planes) are estimated using the full covariance matrix. The cell esds are taken into account individually in the estimation of esds in distances, angles and torsion angles; correlations between esds in cell parameters are only used when they are defined by crystal symmetry. An approximate (isotropic) treatment of cell esds is used for estimating esds involving l.s. planes.

7.10 Chiral HPLC Analysis (±)-2

HPLC; Chiracel ID column, 98:2 hexane: propan-2-ol, 0.6 mL min^{-1}, 220nm detector, retention time = 31.35 min, 35.78 min.
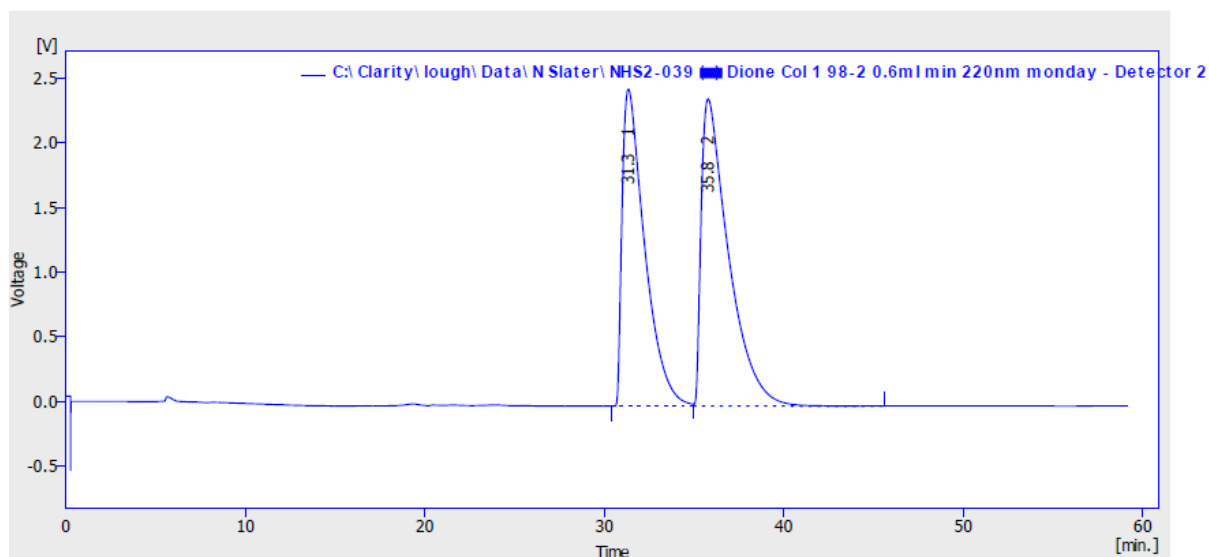
Result Table (Uncal - C:\Clarity\lough\Data\N Slater\NHS2-039 (-) Dione Col 1 98-2 0.6ml min 220nm monday - Detector 2)

	Reten. Time [min]	Start Time [min]	End Time [min]	Area [mV.s]	Height [mV]	Area [%]	Height [%]	W05 [min]
1	31.348	30.388	34.972	214008.060	2451.846	45.9	50.8	1.32
2	35.780	34.972	45.612	251805.401	2376.953	54.1	49.2	1.57
	Total	Total	Total	465813.460	4828.799	100.0	100.0	

7.11 Chiral HPLC Analysis (+)-2

HPLC; Chiracel ID column, 98:2 hexane: propan-2-ol, 0.6 mL min^{-1}, 220nm detector, retention time = 32.30 min, 38.56 min.
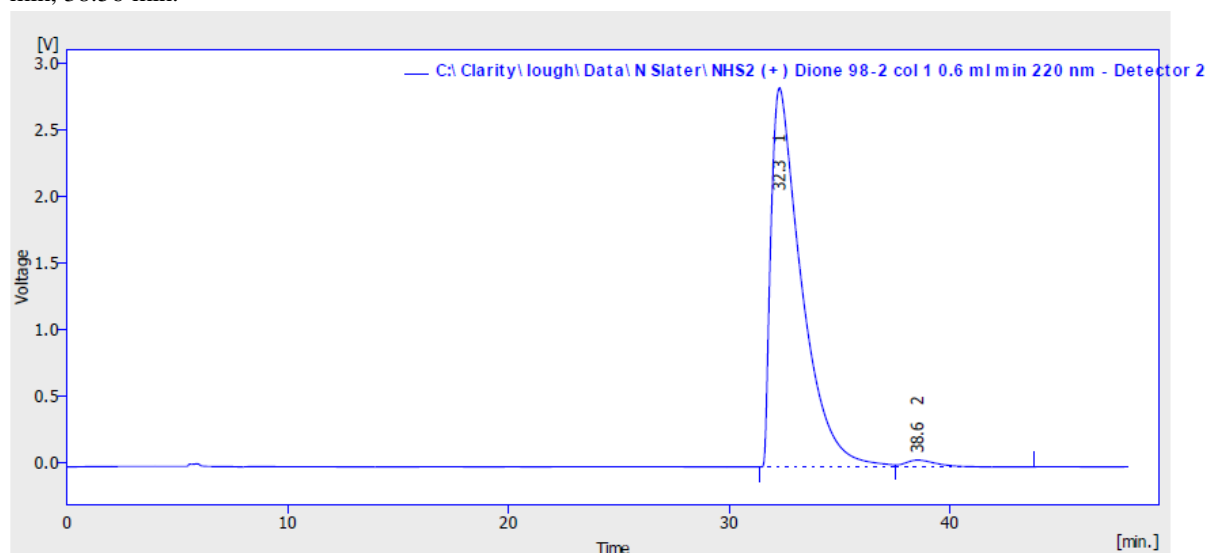
Result Table (Uncal - C:\Clarity\lough\Data\N Slater\NHS2 (+) Dione 98-2 col 1 0.6 ml min 220 nm - Detector 2)

	Reten. Time [min]	Start Time [min]	End Time [min]	Area [mV.s]	Height [mV]	Area [%]	Height [%]	W05 [min]
1	32.296	31.360	37.572	273695.505	2853.639	98.2	98.2	1.42
2	38.556	37.572	43.792	5097.809	51.282	1.8	1.8	1.50
	Total	Total	Total	278793.314	2904.921	100.0	100.0	

7.12   Chiral HPLC Analysis (-)-2

HPLC; Chiracel ID column, 98:2 hexane: propan-2-ol, 0.6mL min^{-1}, 220nm detector, retention time = 33.07 min, 36.55 min.

Result Table (Uncal - C:|Clarity|lough|Data|N Slater|NHS2-039 (-) Dione (3) 98-2 0.6 ml min 220nm - Detector 2)

	Reten. Time [min]	Start Time [min]	End Time [min]	Area [mV.s]	Height [mV]	Area [%]	Height [%]	W05 [min]
1	33.072	31.884	35.412	447.149	6.408	0.3	0.4	1.08
2	36.552	35.560	45.796	148538.093	1435.126	99.7	99.6	1.54
	Total	Total	Total	148985.243	1441.534	100.0	100.0	

7.13   Chiral HPLC Analysis (±)-3

HPLC; Chiracel ID column, 95:5 hexane: propan-2-ol, 0.6 mL min^{-1}, 220nm detector, retention time = 17.59 min, 20.42 min.
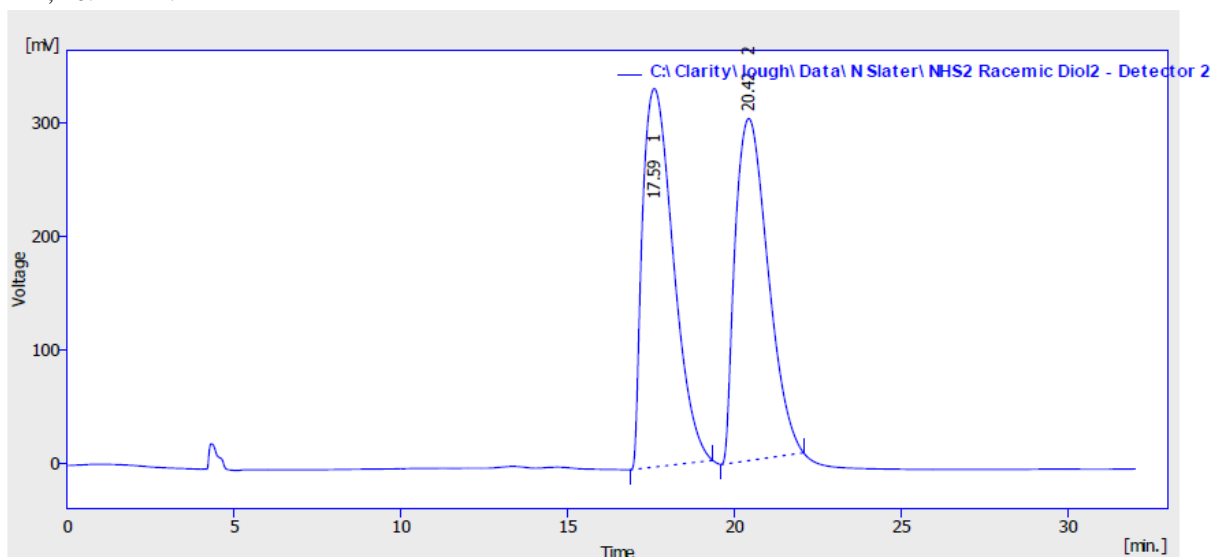
Result Table (Uncal - C:|Clarity|lough|Data|N Slater|NHS2 Racemic Diol2 - Detector 2)

	Reten. Time [min]	Start Time [min]	End Time [min]	Area [mV.s]	Height [mV]	Area [%]	Height [%]	W05 [min]
1	17.592	16.868	19.344	21453.735	333.357	51.0	52.5	1.04
2	20.420	19.596	22.068	20598.640	301.277	49.0	47.5	1.12
	Total	Total	Total	42052.374	634.634	100.0	100.0	

227

7.14 Chiral HPLC Analysis (+)-3

HPLC; Chiracel ID column, 95:5 hexane: propan-2-ol, 0.6 mL min^{-1}, 220nm detector, retention time = 17.96 min, 21.16 min.
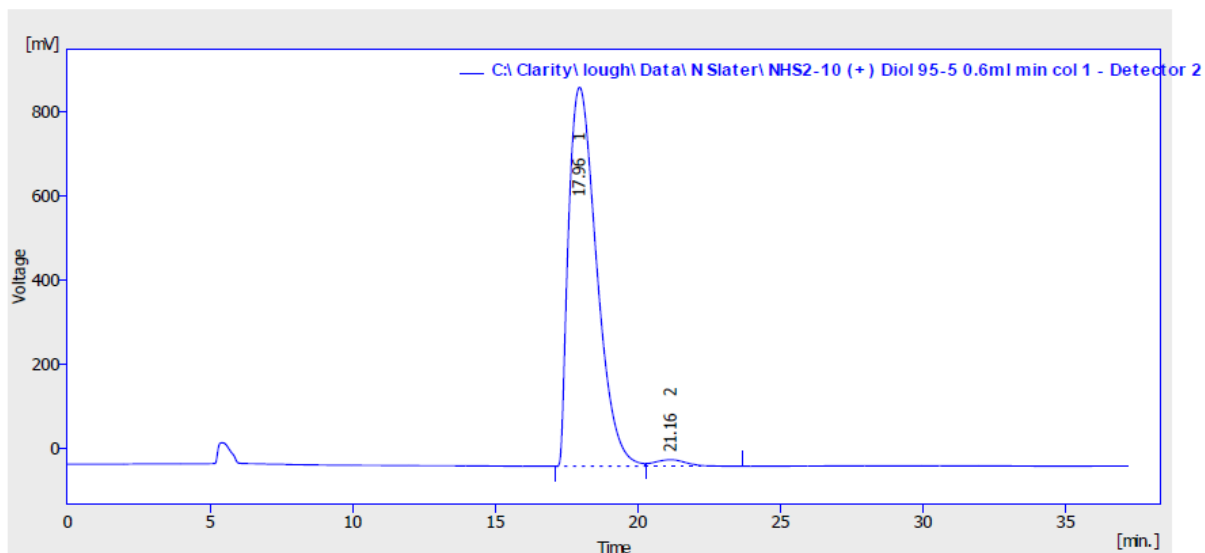
Result Table (Uncal - C:|Clarity|lough|Data|N Slater|NHS2-10 (+) Diol 95-5 0.6ml min col 1 - Detector 2)

	Reten. Time [min]	Start Time [min]	End Time [min]	Area [mV.s]	Height [mV]	Area [%]	Height [%]	W05 [min]
1	17.960	17.124	20.272	61487.555	903.072	98.1	98.3	1.08
2	21.156	20.272	23.668	1202.004	15.587	1.9	1.7	1.26
	Total	Total	Total	62689.558	918.660	100.0	100.0	

7.15 Chiral HPLC Analysis (-)-3

HPLC; Chiracel ID column, 95:5 hexane: propan-2-ol, 0.6 mL min^{-1}, 220nm detector, retention time = 16.68 min, 18.54 min.
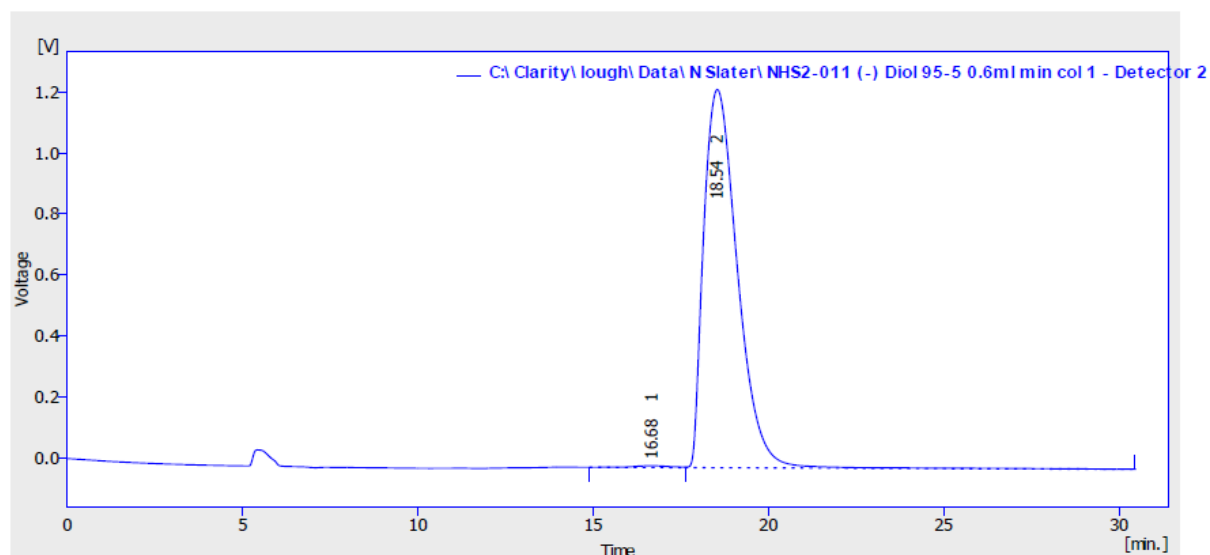
Result Table (Uncal - C:|Clarity|lough|Data|N Slater|NHS2-011 (-) Diol 95-5 0.6ml min col 1 - Detector 2)

	Reten. Time [min]	Start Time [min]	End Time [min]	Area [mV.s]	Height [mV]	Area [%]	Height [%]	W05 [min]
1	16.676	14.900	17.624	438.928	5.889	0.5	0.5	1.12
2	18.544	17.624	30.444	83283.440	1239.247	99.5	99.5	1.05
	Total	Total	Total	83722.368	1245.135	100.0	100.0	

7.16 Racemic Bromolactonisation (±)-20

HPLC; Chiracel ID column, 85:15 hexane: propan-2-ol, 0.6m L min^{-1}, 214 nm detector, retention time = 29.50 min, 34.74 min.
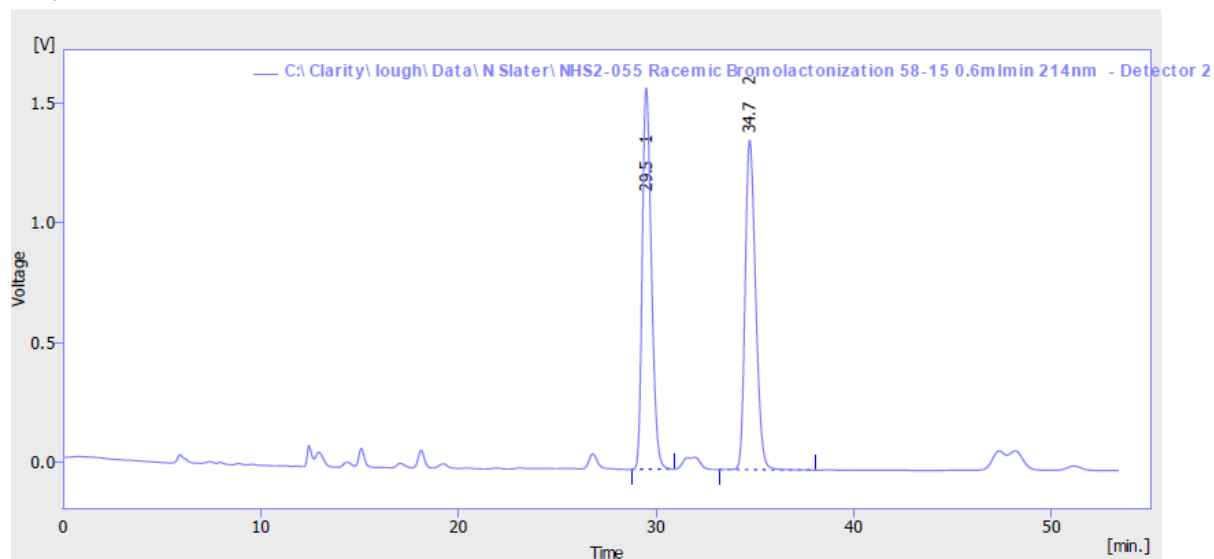
Result Table (Uncal - C:|Clarity|lough|Data|N Slater|NHS2-055 Racemic Bromolactonization 58-15 0.6mlmin 214nm - Detector 2)

	Reten. Time [min]	Start Time [min]	End Time [min]	Area [mV.s]	Height [mV]	Area [%]	Height [%]	W05 [min]
1	29.500	28.764	30.916	51051.994	1593.709	50.2	53.7	0.50
2	34.736	33.192	38.032	50663.003	1376.161	49.8	46.3	0.57
	Total	Total	Total	101714.997	2969.870	100.0	100.0	

7.17 Hetero Diels Alder Reaction (±)-12a

HPLC; Chiracel ID column, 85:15 hexane: propan-2-ol, 0. 5 mL min^{-1}, 254 nm detector, retention time = 49.10 min, 52.64 min.
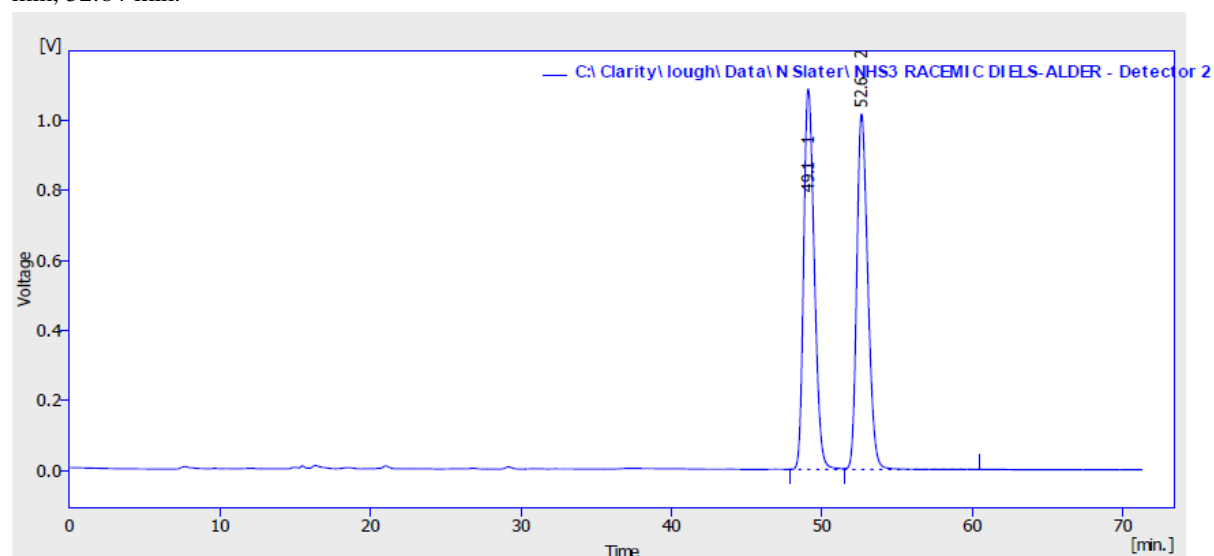
Result Table (Uncal - C:|Clarity|lough|Data|N Slater|NHS3 RACEMIC DIELS-ALDER - Detector 2)

	Reten. Time [min]	Start Time [min]	End Time [min]	Area [mV.s]	Height [mV]	Area [%]	Height [%]	W05 [min]
1	49.104	47.876	51.472	53404.223	1087.911	50.7	51.7	0.76
2	52.644	51.472	60.512	51835.447	1016.252	49.3	48.3	0.79
	Total	Total	Total	105239.670	2104.163	100.0	100.0	

7.18 Asymmetric Hetero Diels Alder Reaction 12a
(+)-13 catalysed reaction (Table 23, entry 5)

HPLC; Chiracel ID column, 85:15 hexane: propan-2-ol, 0.5 mL min^{-1}, 254 nm detector, retention time = 47.93 min, 51.36 min.
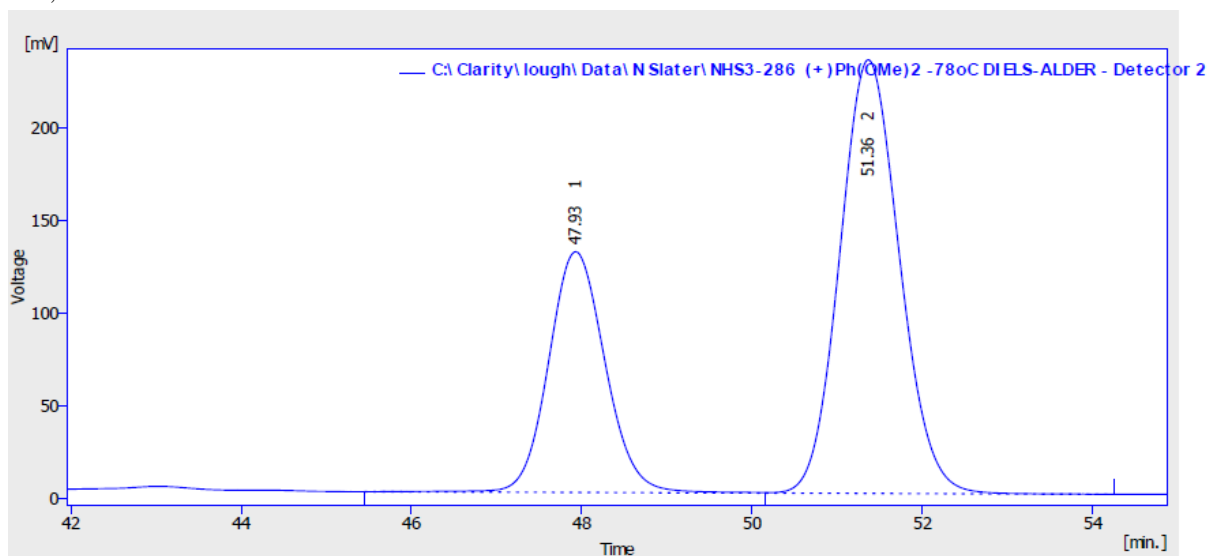
Result Table (Uncal - C:|Clarity|lough|Data|N Slater|NHS3-286 (+)Ph(OMe)2 -78oC DIELS-ALDER - Detector 2)

	Reten. Time [min]	Start Time [min]	End Time [min]	Area [mV.s]	Height [mV]	Area [%]	Height [%]	W05 [min]
1	47.928	45.452	50.160	6014.675	130.104	34.5	35.7	0.71
2	51.364	50.160	54.248	11422.900	234.383	65.5	64.3	0.76
	Total	Total	Total	17437.574	364.488	100.0	100.0	

7.19 ^{1}H-^{1}H COSY Spectra for (±)-123

NHS3-033 Racemic Mono p-Tolyl Amino Thiocarbamate Cleft (VERY WEAK SAMPLE Multiple scans PLEASE)
(Kimber) Natasha Slater